Jem Pearson
Hertford College

Hydrogen-Bonding Motifs for Non-Covalent Synthesis

University of Oxford

Department of Chemistry

September 2013

Supervisor: Dr E. A. Anderson

Abstract

This work describes the design and synthesis of a set of four organic molecules that are intended to hydrogen-bond to each other in a pairwise manner. The four hydrogen-bonding units, termed 'A', 'B', 'C' and 'D', when placed in solution together, are designed so that A binds only to B, and C binds only to D. Each unit does not bind to itself, nor to either of the other two units to which binding is not intended. For example, A binds to B, but not to A, C, or D. Each unit contains an array of four hydrogen-bonds for strong binding to its partner, is designed to be as rigid as possible, as non-tautomeric as possible, and utilises a staggered non-symmetrical architecture.

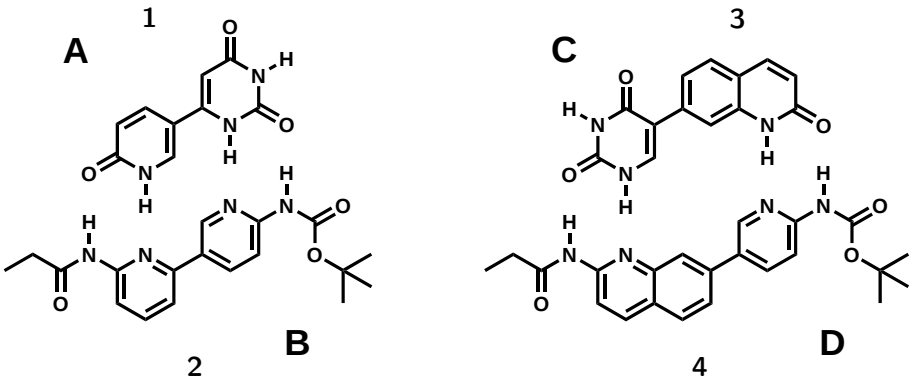

Fig. 1 The four original hydrogen-bonding units.

The original designs are shown in Fig. 1. Of these four compounds, three were successfully synthesised (A, B and D). Units B and D were soluble in $CDCl_3$, but Unit A was not. Therefore, the design and synthesis of Unit A was amended, and two variants of Unit A that are both soluble in $CDCl_3$ were successfully synthesised (Fig. 2).

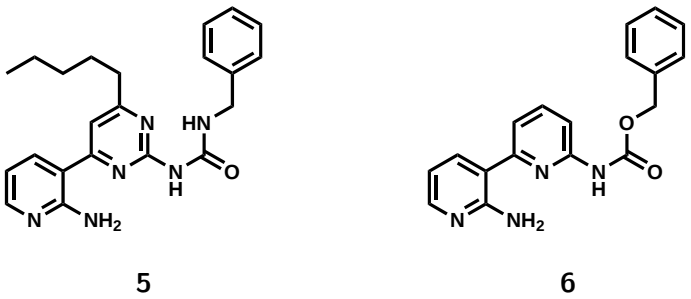

Fig. 2 Variants of Unit A.

^{1}H NMR binding experiments were performed between Unit B **2** and each of the two variants of Unit A, **5** and **6**. Their binding behaviour was described. A binding constant could not be calculated because the units did not bind in a 1:1 fashion.

Acknowledgements

To Ed Anderson, for all his help and support for over four years, and the many stimulating discussions about hydrogen-bonding construction sets.
To the EAA Group, past and present, for all their help in the lab and fun and games out of it.
To Hertford College, for their pastoral and financial support.
To Barbara Odell, for much assistance with NMR binding experiments.
To Ivanhoe Leung, for helping with the calculation of binding constants.
To Dan Pantoş, for valuable advice regarding hydrogen-bonding and binding experiments.
To Sonia Bracegirdle, for so much entertainment and making long days in the lab bearable.
To my parents, for all their support.

Abbreviations and Symbols

[A]	concentration of species A
$[A]_0$	known total concentration of guest
AIBN	azoisobutyronitrile
^{13}C	carbon 13
CDI	carbonyldiimidazole
conc.	concentration
COSY	correlation spectroscopy
Da	Daltons
dba	dibenzylideneacetone
DBU	1,8-diazabicycloundec-7-ene
DCC	N,N′-dicyclohexylcarbodiimide
DCM	dichloromethane
$\Delta\delta_X$	change in chemical shift of proton X
DIBAL	diisobutylaluminium hydride
DIPEA	N,N-diisopropylethylamine
DMAP	4-dimethylaminopyridine
DMF	dimethylformamide
DMF·DMA	dimethylformamide dimethyl acetal
DMP	Dess-Martin periodinane
DMSO	dimethylsulfoxide
DMU	dimethylurea
dppf	1,1′-bis(diphenylphosphino)ferrocene
E	*E* alkene configuration
EDC	1-ethyl-3-(3-dimethylaminopropyl)carbodiimide
eq.	equivalents
^1H	proton
HMBC	heteronuclear multiple-bond correlation spectroscopy
HRMS	high resolution mass spectrometry
HSQC	heteronuclear single quantum correlation spectroscopy
Hz	Hertz
i-	iso
IBX	2-iodoxybenzoic acid
IR	infra-red
J	coupling constant
K_a	association constant/binding constant
LHMDS	lithium hexamethyldisilazide
M	molar

mg	milligram
MHz	megahertz
mL	millilitre
mmol	millimole
NaHMDS	sodium hexamethyldisilazide
NBS	N-bromosuccinamide
NMP	N-methyl-2-pyrrolidone
NMR	nuclear magnetic resonance
PCC	pyridinium chlorochromate
P.E.	petroleum ether
ppm	parts per million
R	unspecified substituent
RCM	ring-closing metathesis
R_f	thin layer chromatography retention factor
r.t.	room temperature
s-	sec
t-	tertiary
TBDPS	*tert*-butyldiphenylsilyl
TBAF	tetrabutylammonium fluoride
TBS	*tert*-butyldimethylsilyl
THF	tetrahydrofuran
TLC	thin layer chromatography
TMS	trimethylsilyl
tol	toluene
X_A	mole fraction of species A
Z	*Z* alkene configuration

Contents

1 Introduction

1.1 Summary

Macromolecular synthesis *via* the controlled non-covalent assembly of molecular building-blocks remains an elusive but desirable aim. Access to precisely-designed supramolecular architectures would unlock potential applications in many areas, including supramolecular catalysis, enzyme mimetics, molecular recognition, biosensors, materials, and synthetic biology. To date, there are many known supramolecular self-assembling systems. However, many efforts in the field of non-covalent synthesis involving hydrogen-bonding units have found most success in polymer formation *via* processes of uncontrolled oligomerisation. The currently-known organic building-blocks of such 'macromolecular construction kits' are quite primitive and possess a range of undesirable properties. There is clearly scope for harnessing the benefits of non-covalent self-assembly in a more controlled and specific manner, with the aim of constructing smaller but well-defined macromolecules of similar scale to proteins.

1.2 Non-Covalent Synthesis

Nowadays we have control over a vast range of chemical transformations, rendering the synthesis of very complex molecules, such as taxol or brevetoxin, possible.[1,2] However, the covalent synthesis of molecules with molecular weights exceeding 1000 Da is limited by time and yield constraints. To go beyond this point arguably requires us to enter the non-covalent realm.

Non-covalent synthesis encompasses five types of molecular interaction: hydrogen-bonding, Van der Waals, hydrophobic (strictly an effect of solvent rather than an interaction), metal coordination and ionic. The first three, the 'weak interactions', are of strengths typically in the range of 0.1–5 kcal mol^{-1}, whereas metal coordination and ionic forces can be as high as 20 kcal mol^{-1}, compared to around 35–135 kcal mol^{-1} for covalent bonds.[3] Weak interactions between molecules containing hydroxyl groups were noted in 1892 by Nernst.[4] Werner described the phenomenon of the hydrogen-

bond ten years later, although it did not have a name at the time.[5] Latimer and Rodebush in 1920 were the first to suggest that the hydrogen atom was involved,[6] but it wasn't until 1935-6 that the term 'hydrogen-bond' was proposed, by Bernal and Huggins.[7,8]

Hydrogen-bonds, abbreviated as 'H-bonds', consist of two parts. The 'proton donor' (D), is an atom more electronegative than hydrogen, such as nitrogen or oxygen, with a hydrogen atom covalently bound. The 'proton acceptor' (A) is an atom with a free lone pair, typically nitrogen, oxygen, or fluorine. The larger the dipole moment of the D and the A lone pair, the stronger the H-bond. Thus, strong H-bonds are formed when nitrogen and oxygen feature in both the donor and acceptor, although C–H bonds can act as the donor. 'π' bonds can be considered as a type of H-bond, as the partially positive hydrogen atoms bind to the electrons of unsaturated bonds in an electron-rich aromatic system. The thermodynamic stability of H-bonds is very dependent on the solvent. Generally speaking, the less polar the solvent, the stronger the H-bond. Solvents that contain either H-bond donors or acceptors can themselves H-bond to the compound, thus lowering the association constant due to competitive binding with the solvent. Unlike covalent bond formation, which involves a massive shift of electron density, H-bond formation involves more subtle changes of electron distribution; there is a small shift from the proton acceptor to the donor.

1.2.1 Cooperativity

H-bonds acting together are much stronger than the sum of their parts – as described by Reinhoudt,[3] '$1+1$ is more than 2.' There is a non-linear relationship between the number of H-bonds and the binding strength between molecules. It is not the intrinsic strength of H-bonds that makes them so powerful a tool for the purpose of non-covalent assembly, but rather the concept of *cooperativity*.[3] Indeed, DNA base-pairing and receptor-ligand binding studies showed that the contribution of H-bonding to the overall binding energy had long been overestimated, with hydrophobic interactions playing a significant role.[9,10] The average energy of an H-bond in solution is around 1.5 kcal mol^{-1}, which is rather small. This means that H-bonding alone cannot be the main driving force for self-assembly and binding processes that take place in water.[3] Rather, H-bonds come into their own when they cooperate. One H-bond alone contributes little to the overall binding energy, but a lot of H-bonds acting together can create a strongly-binding surface. Moreover, H-bonds possess specificity of binding. A donor must line up exactly opposite an acceptor in three-dimensional space, and as such H-bonds can be designed into synthetic structures at precisely-controlled positions. These qualities make H-bonds very attractive for the purposes of non-covalent synthesis.

1.2.2 Solute-Solvent Interactions

When a compound is dissolved in a solvent, there are three possible interactions: solute-solute, solvent-solvent, and solute-solvent. The nature and relative strengths of these interactions determine the properties of the system. Hunter[11] plotted the functional group interaction profile for a variety of groups and solvents (Fig. 1.1). The profiles for the two solvents of $CHCl_3$ (A) and H_2O (B) are shown. Each chart contains four important regions; two red and two blue. In both of the red quadrants, the H-bonding interactions are unfavourable, because the solute-solvent interactions are stronger than both the solute-solute interactions and the solvent-solvent interactions. In the blue quadrants, the H-bonding interactions are favourable. In the top-right blue quadrant, the solute-solute interactions are strong and therefore dominate. In the bottom-left blue quadrant, the solvent-solvent interactions are stronger than both the solute-solute and the solute-solvent interactions, and are therefore dominant. α and β are constants that relate to the H-bonding properties of the functional groups; α for the H-bond donor, and β for the acceptor.

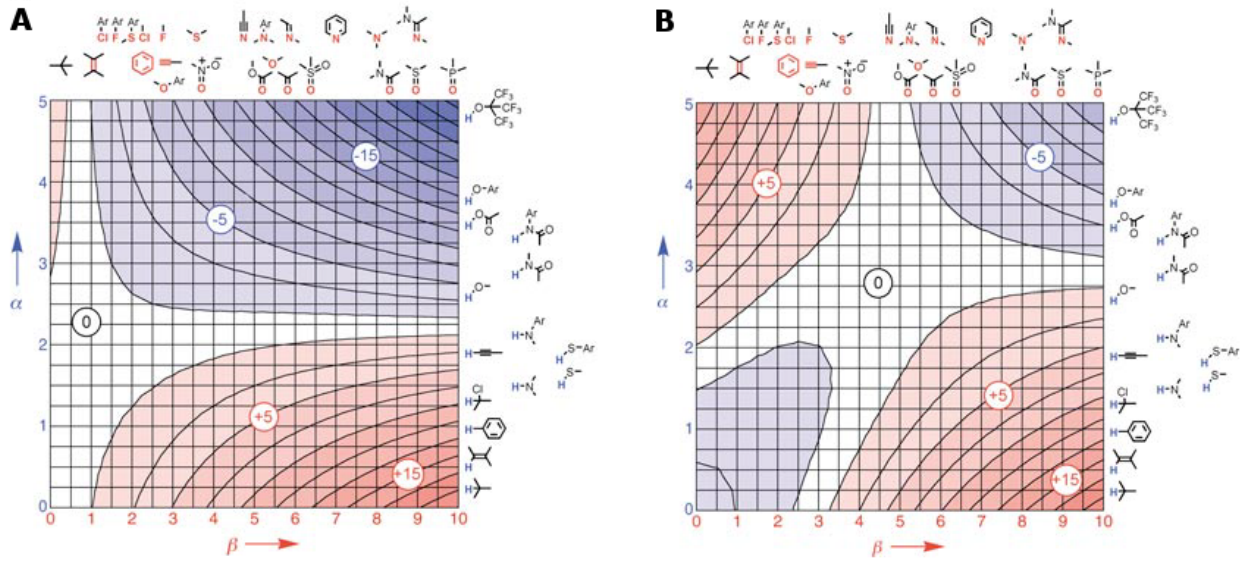

Fig. 1.1 Hunter's solute-solvent interaction profiles.[11]

The profiles for $CHCl_3$ and H_2O are quite different. For example, a simple alcohol H-bond donor forms a positive interaction with virtually all types of H-bond acceptor in $CHCl_3$, whereas in H_2O it is incapable of forming a positive interaction with any of the acceptors. In H_2O, only the strongest donors and acceptors (top-right blue region) can form a positive interaction, while in $CHCl_3$ the range of functional groups that form a positive interaction is much larger. However, in H_2O, unlike in $CHCl_3$, it is possible to take advantage of the strong solvent-solvent interaction (bottom-left blue region) to achieve a positive solute-solute donor-acceptor interaction between less

polar lipophilic-type groups, such as alkenes and butyl groups.

1.3 Hydrogen-Bonds in Non-Covalent Synthesis

Non-covalent synthesis is the assembly of large organic molecules by utilising non-covalent interaction forces between each molecular subunit; frequently H-bonds.[3,12–14] The H-bond is a particularly attractive tool for this purpose due to the fact that it can be designed and synthesised at precise locations in the molecule. The general approach is to use small-molecule motifs, each containing an array of donor and acceptor H-bonds, attached to larger structural units. Donors are usually oxygen-hydrogen and nitrogen-hydrogen moieties, and acceptors are typically oxygen and nitrogen. The binding between the arrays holds the structural subunits in place to form the complex. Fig. 1.2 shows examples of a 3-H-bond dimer **7**·**8** and a 4-H-Bond dimer **9**·**9**.[3]

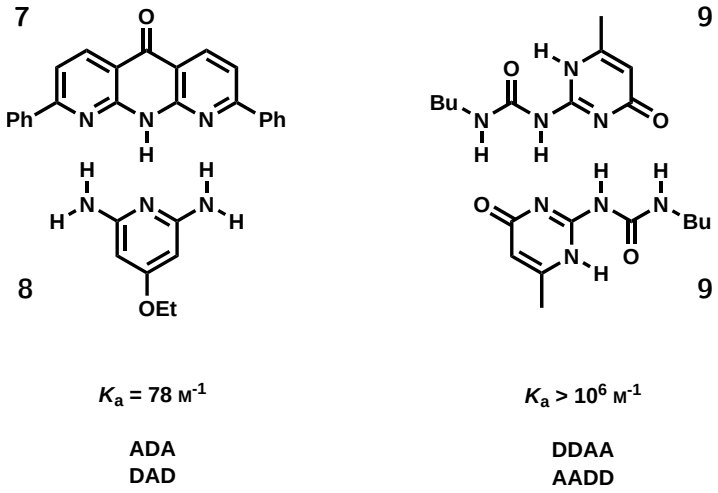

Fig. 1.2 Examples of a 3-H-Bond dimer **7**·**8** and a 4-H-Bond dimer **9**·**9**.[3]

1.3.1 Secondary Interactions

For the purpose of non-covalent synthesis, the binding strength between H-bonded motifs must be as high as possible. Generally, the more H-bonds, the stronger the binding. However, there are numerous factors which affect binding strength, and the binding constant K_a can vary considerably across two or three orders of magnitude for different molecules with the same donor/acceptor pattern. In 1967, Rich found that the binding constant for triple-H-bond dimers in $CDCl_3$ varied considerably from 10^2 to 10^5 M^{-1}.[15,16] This shows that the number of H-bonds involved is certainly not the only important stability-determining factor. Jorgensen showed in 1990[17,18] that the large differences were chiefly due to *secondary interactions* between adjacent base-pairs (Fig. 1.3).

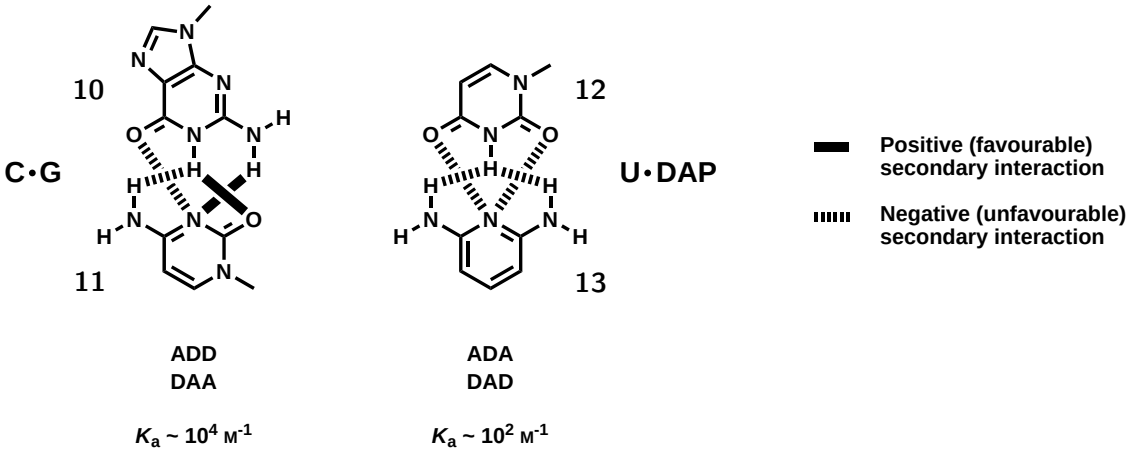

Fig. 1.3 Secondary interactions have a large effect on binding strength.

An H-bond donor has a positive attractive force towards an H-bond acceptor and a negative repulsive force towards another H-bond donor directly opposite to it. In exactly the same way, the H-bond will experience the same attractive or repulsive force to a donor or acceptor adjacent to it, although the force will be smaller because the adjacent donor/acceptor is slightly further away.

Electrostatic attraction between positively and negatively polarized atoms in adjacent H-bonds increases the binding strength, whereas electrostatic repulsion between similarly-polarized adjacent H-bonds decreases binding strength. Molecular dynamics simulations demonstrated that the 1-methylcytosine·9-methylguanine (C·G) dimer **10·11** was 10.7 kcal mol^{-1} lower in energy than the 1-methyluracil·2,6-diaminopyridine (U·DAP) dimer **12·13** (Fig. 1.3). This result agrees closely with experimental data on the binding energies.[17,18] Examination of the C·G dimer shows two negative secondary interactions and two positive ones, but in the U·DAP dimer all four secondary interactions are negative.

Schneider[19] derived an empirical rule based on various synthetic H-bonding complexes that each H-bond contributes 1.88 kcal mol^{-1} to the binding energy and each secondary interaction contributes $\pm$ 0.7 kcal mol^{-1} depending on whether it is attractive or repulsive. The predicted binding for all possible array combinations up to four-H-bond motifs is shown in Fig. 1.4.

1.3.2 2- and 3-Hydrogen-Bond Arrays

The gain in enthalpy from the binding of a DA·AD dimer, with two negative secondary interactions, is not enough to compensate for the concomitant loss in entropy. Schneider's model[19] (Fig. 1.4) predicted a K_a of 60 M^{-1} for the DA·AD dimer, which is far too low to be useful for non-covalent synthesis. Schneider predicted a much higher value for the DD·AA dimer, and this figure has been

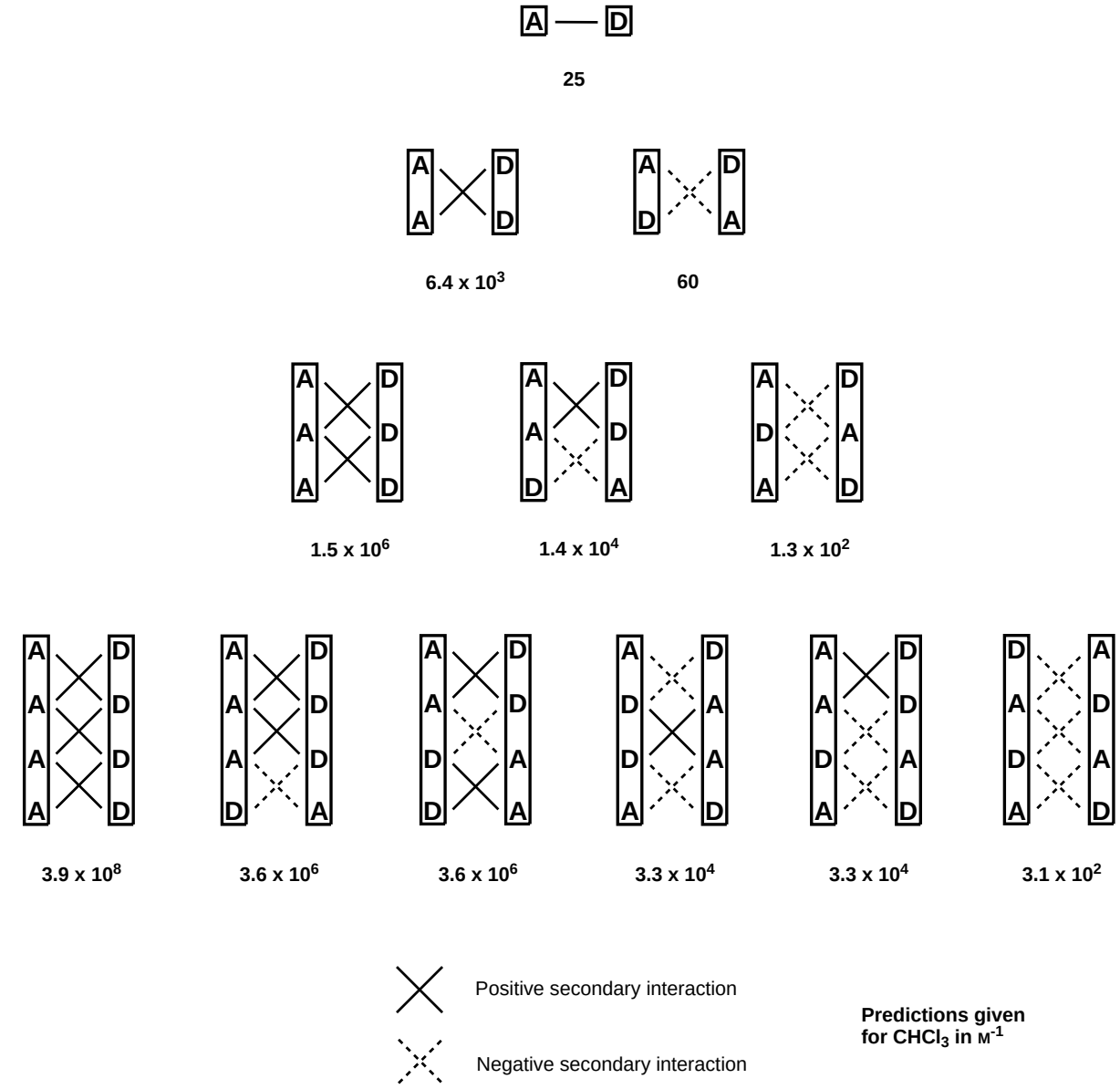

Fig. 1.4 Predicted binding between the different arrangements of 1-, 2-, 3- and 4-H-bond arrays.[19]

matched experimentally by a number of dimers. However, the DD·AA motif does demonstrate a wide range of binding constants depending on the particular compounds involved, with Zimmerman[20] observing a K_a of 260 M^{-1} for the DD·AA dimer **14·15** (Fig. 1.5). None of these values are in the range that is useful for non-covalent synthesis.

Theoretically, the most stable three-H-bond structure possible is AAA·DDD, and this was proved experimentally by Zimmerman[22] (Fig. 1.6). Zimmerman's results, as with other dimers studied in the literature, generally agree very well with Schneider's model predictions as shown in Fig. 1.4.

Due to the odd number of H-bonds, it is not possible for 3-H-bond motifs to be self-complementary (see Section 1.6.2).

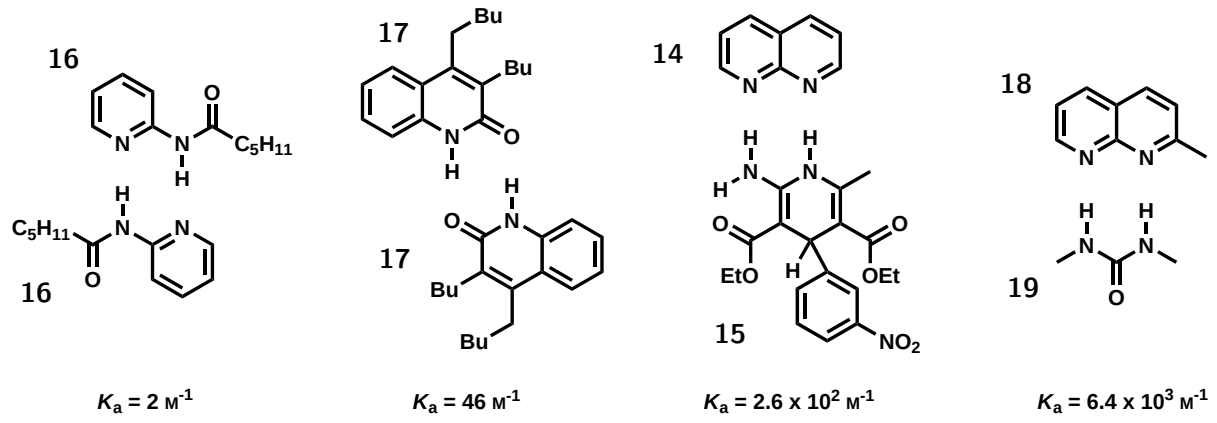

Fig. 1.5 Examples of 2-H-bond dimers.[3,21]

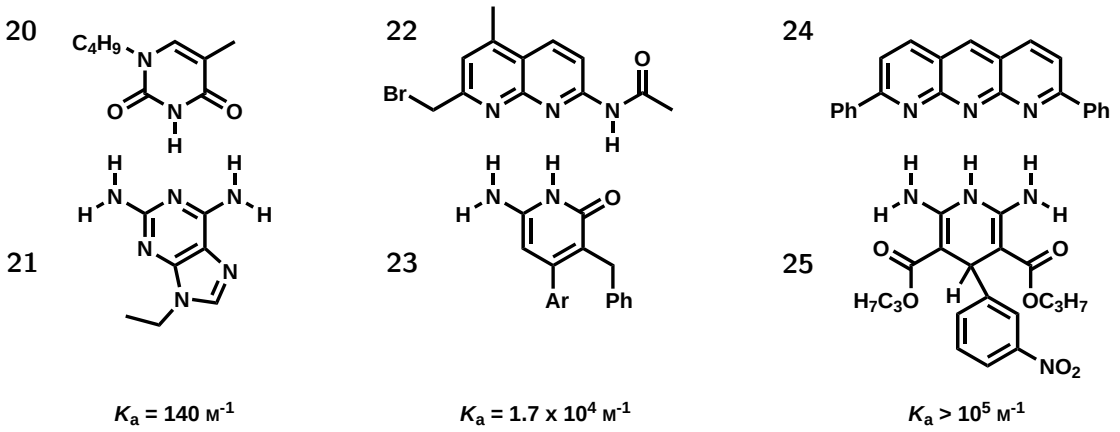

Fig. 1.6 Examples of ADA·DAD, AAD·DDA, and AAA·DDD dimers and their corresponding binding constants as measured by Zimmerman.[22]

1.3.3 4-Hydrogen-Bond Arrays

The first 4-H-bond crystal structure was recorded in 1992, but its properties were not investigated.[23] Meijer performed the first investigations into four-H-bond arrays in 1998,[24] a family of ADAD self-complementary arrays based on ureidopyrimidines. The strongest binding of these, **26**·**26**, is shown in Fig. 1.7. Around the same time, Lüning[25] published a non-self-complementary 4-H-bond dimer, **27**·**28** (Fig. 1.7).

There are a limited number of four-H-bond arrays in the literature. For four linear H-bonds, there are six possible permutations of the array pattern (Fig. 1.8). To date, five of the six dimers have been synthesised (Fig. 1.9).[24,26–30] The one remaining unexplored pattern is DDDA·AAAD.

The last example **32**·**33**, involving a cationic DDDD array (Fig. 1.9), was published by Leigh and co-workers in 2011.[29] It was the first stable four-H-bond dimer with an AAAA·DDDD array pattern, with therefore exclusively positive secondary interactions. As expected, the binding constant K_a was extraordinarily high, at greater than 3×10^{12} M^{-1} in CH_2Cl_2, corresponding to a binding free

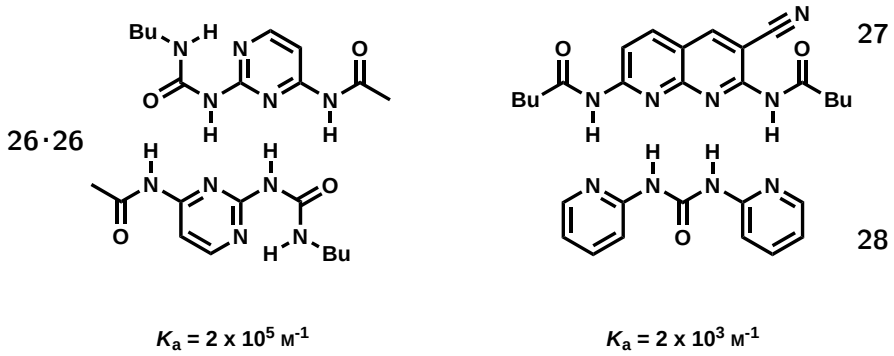

Fig. 1.7 Early 4-H-bond motifs.

Fig. 1.8 The six possible permutations of a four-H-bond array.

energy (ΔG) in excess of $-71\,\mathrm{kJ\,mol^{-1}}$. This is more than 20 % of the thermodynamic stability of a carbon–carbon covalent bond.

1.3.4 Switches

There are a number of examples of H-bonding units that can switch their bonding array pattern in response to an external signal.[29,31–38] Leigh[29,38] showed that protonation of a diaminopyridine motif with a DAD array converted it into a DDD array. This increased the binding constant K_a between it and an AAA array by more than a factor of 10^9. Hecht[37] described a photoswitchable dimer. While not actually altering the array pattern, there was a much enhanced binding affinity between ADA and DAD arrays using a photochemical reaction. Irradiation with 313 nm light caused a ring-closing covalent bond to form and the colour to change from yellow to deep red. The bond formation is reversible *via* irradiation with visible light of wavelength above 500 nm. Upon switching to the ring-closed deep-red form, the K_a value increased from $231\,\mathrm{M^{-1}}$ to $318\,\mathrm{M^{-1}}$.

Zimmerman[39] has demonstrated the reversible binding of a four-H-bond dimer *via* an oxidation-reduction chemical switch (Fig. 1.10). The oxidation of **36** converts the N–H donor into an N acceptor, creating a repulsive force between the N acceptor on **37**. This one change results in a fall in binding constant by a factor of more than 2×10^3.

1.3.5 Other Array Designs

Gong has reported more than one example of 6-H-bond dimers with very strong binding (Fig. 1.11). His unusual 'trident' design **39**·**40** comprises a central cyclohexane ring with three branches, each

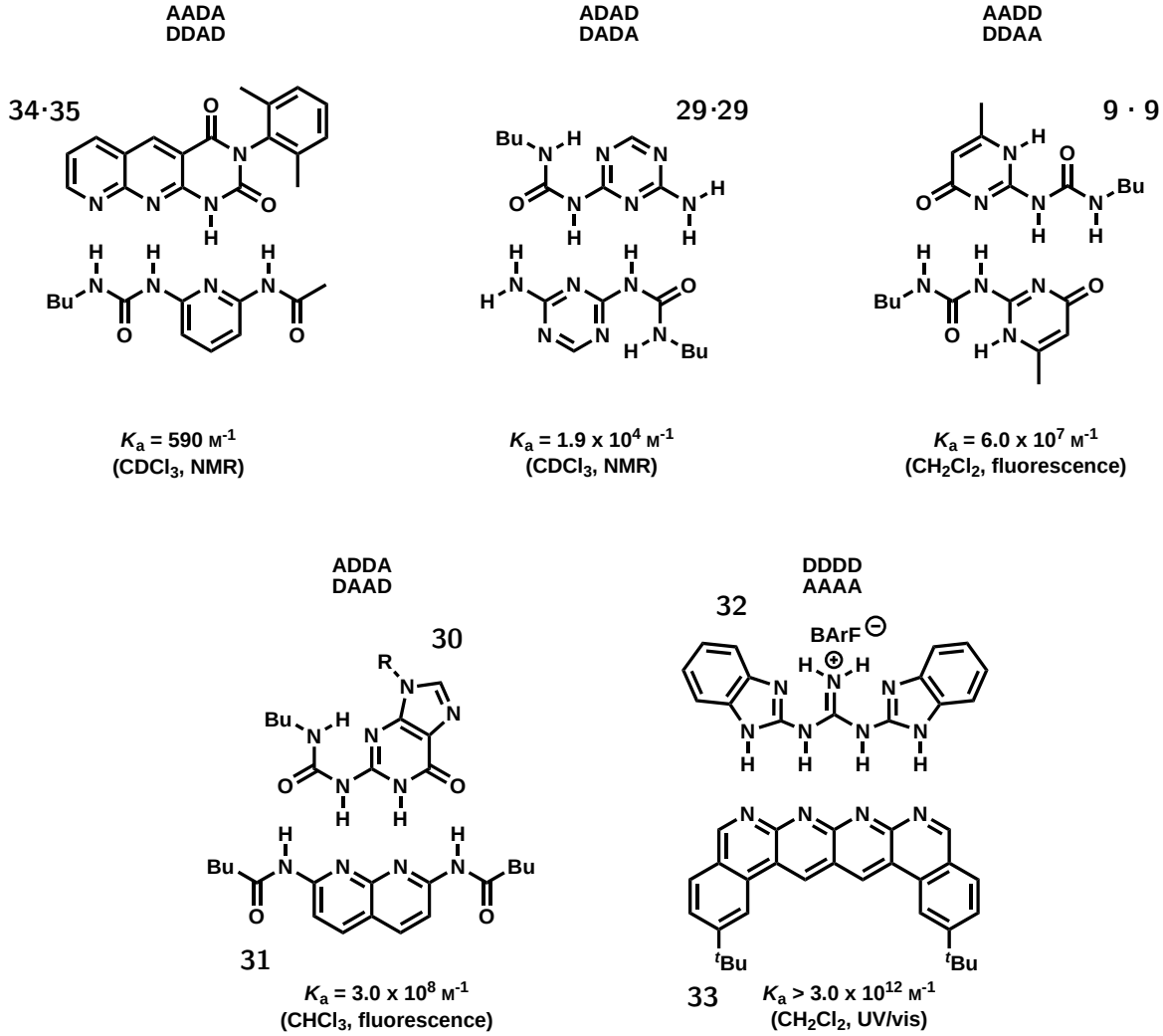

Fig. 1.9 Examples of 4-H-bond motifs.

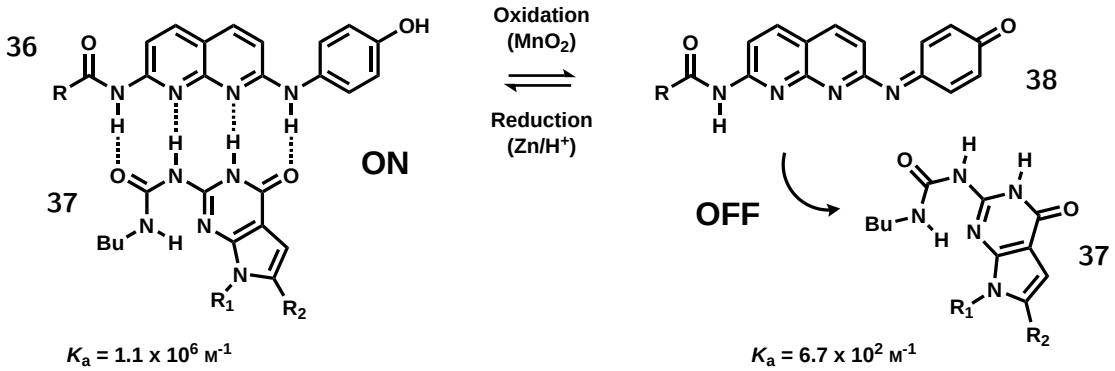

Fig. 1.10 Redox-responsive binding of a H-bonding dimer.[39]

containing two H-bonds.[40] The dimer binds very strongly with a K_a of greater than 9×10^6 м$^{-1}$. His linear dimer **41**·**42** has an even larger K_a of around 10^9 м$^{-1}$.[41] The linear design consists of six H-bonds in a DADADA·ADADAD pattern. The distance between adjacent H-bonds is larger than in the 4-H-bond examples in Fig. 1.9. This means the repulsive effects of negative secondary

interactions are diminished, resulting in the very high binding constant.

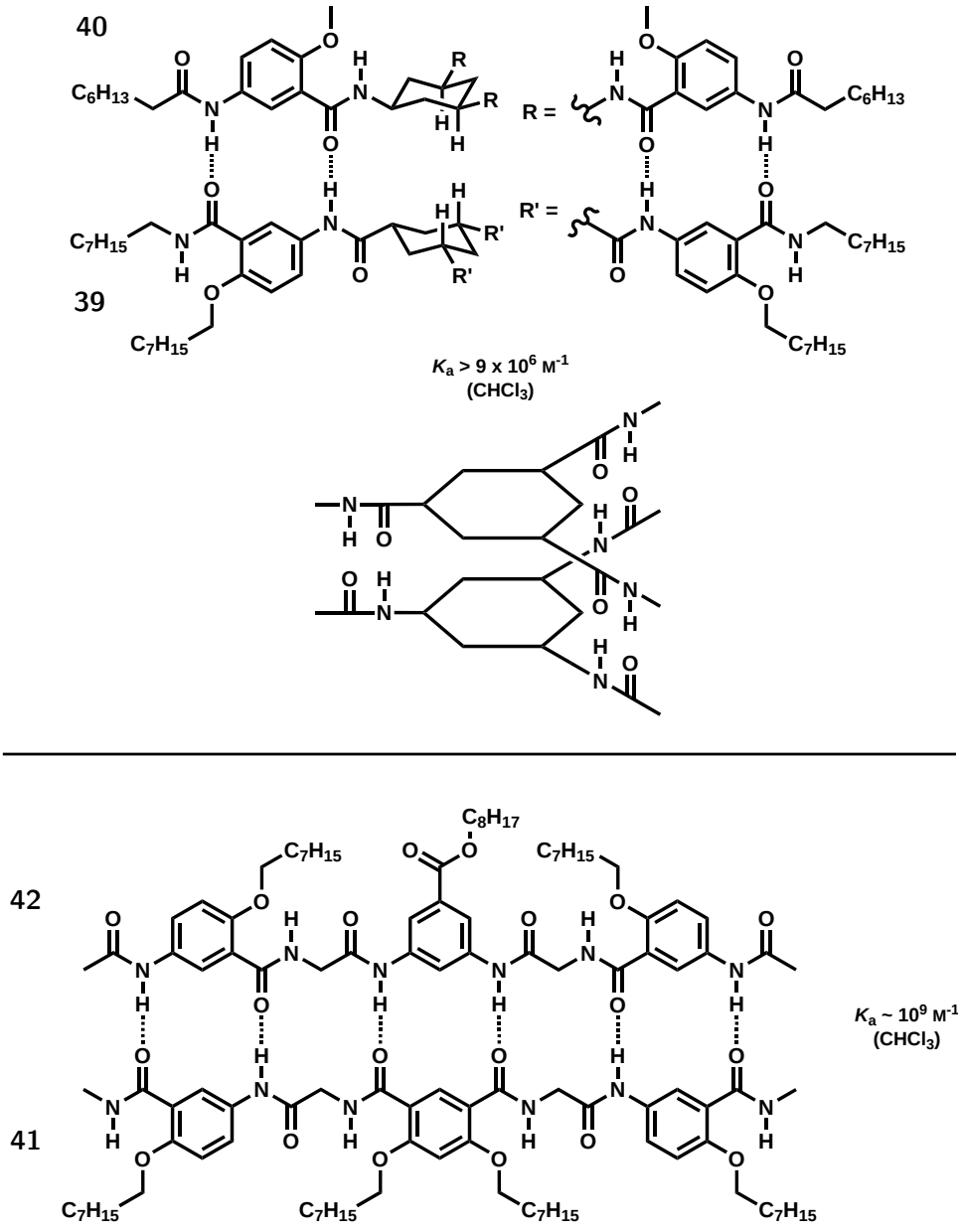

Fig. 1.11 Two different 6-H-bond dimers synthesised by Gong.[40,41]

Zimmerman[42] has published a non-self-complementary dimer **43**·**44** consisting of six H-bonds, with a K_a of 5×10^5 M^{-1} (Fig. 1.12). Hamilton[43] reported a binding constant of 2.1×10^4 M^{-1} for 6-H-bond binding between tetraamide **45** and barbiturate **46** (Fig. 1.13). This design involves several inward-facing hydrogen bonds within a cavity structure provided by the tetraamide **45**, into which slots the barbiturate **46**.

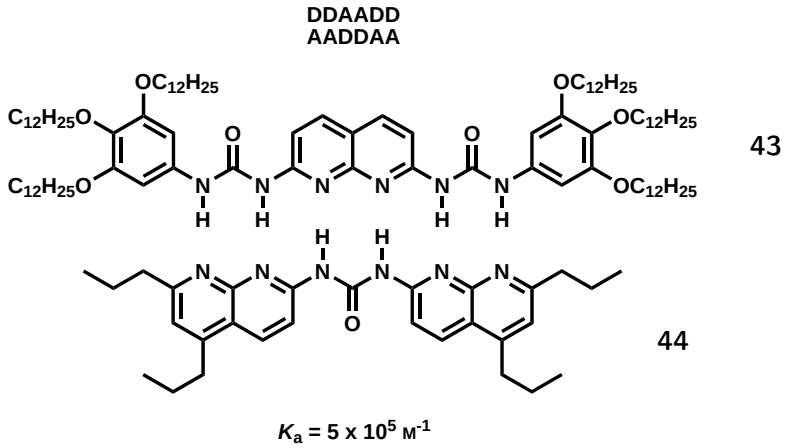

Fig. 1.12 A 6-H-bond dimer **43**·**44** synthesised by Zimmerman.[42]

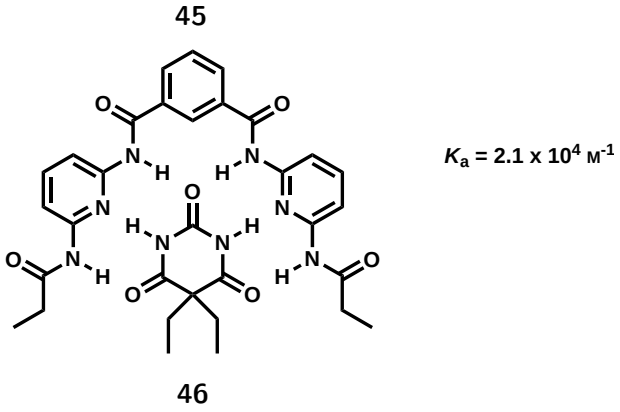

Fig. 1.13 The barbiturate·tetraamide system reported by Hamilton.[43]

1.4 Self-Sorting

'Self-sorting' describes the phenomenon of high selectivity of recognition between different molecules in complex mixtures.[44–49] The individual molecules successfully identify and bind to only their intended partner, picking them out over the many different possible binding partners present in solution. This process can be further divided into 'narcissistic self-sorting' and 'social self-sorting' (Fig. 1.14). Narcissistic self-sorting is when the different molecules bind only to themselves. Social self-sorting is when the molecules bind to other molecules in the solution. Social self-sorting can be either 'Integrative' or 'Non-integrative'.[50] Integrative social self-sorting is when all the molecules combine to form a single supramolecular structure. Non-integrative self-sorting occurs when the molecules combine to form two or more separate supramolecular structures.

The first investigations into the binding selectivity behaviour of synthetic molecules in solution were performed by Lehn in 1993.[48] He demonstrated that two different varieties of tris-bipyridine ligands, when placed in solution in the presence of nickel and copper ions, precipitated as helicates

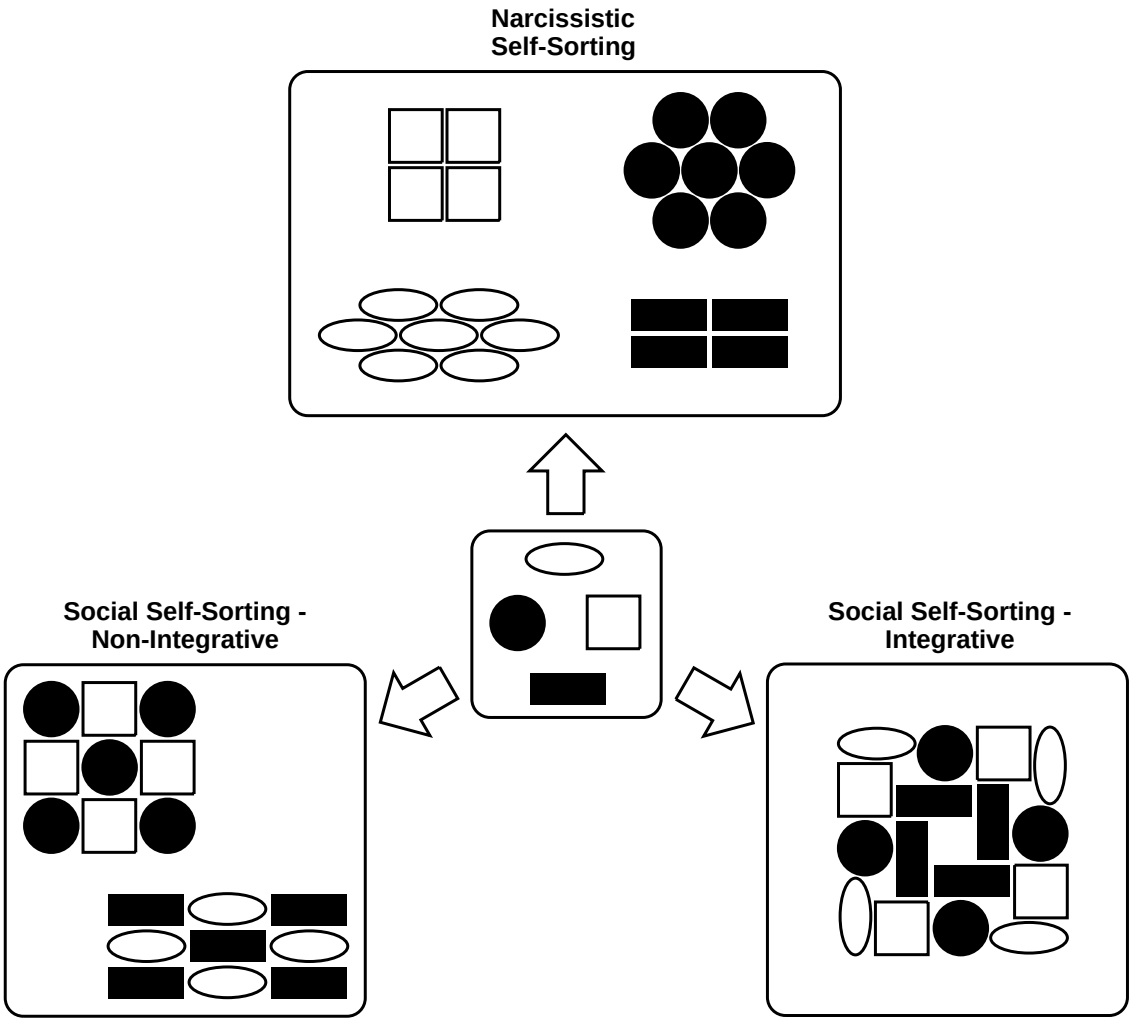

Fig. 1.14 Narcissistic, Integrative, and Non-integrative self-sorting.[51]

with one ligand exclusively bound to the nickel ions, and the other ligand bound exclusively to the copper ions.

High-fidelity self-sorting among a large number of synthetic molecules in solution was elegantly demonstrated by Issacs and co-workers in 2003.[45] The authors selected a variety of molecules from the literature, nine in all, that on their own were known to assemble into supramolecular structures. A wide variety of molecules were chosen, including ionophores, calixarenes, and linear H-bonding arrays, which utilised both narcissistic and social self-sorting processes. It was found that the ^{1}H NMR spectra of the combined molecules was almost identical to the superposition of the ^{1}H NMR spectra of the individual supramolecular architectures, demonstrating high-fidelity self-recognition among all the component molecules.

1.4.1 Molecular Codes

Würthner[44] identified five factors that endow a system with the capacity to self-sort. These factors, which are intrinsic to the molecules themselves rather than due to external factors, are termed 'molecular codes'. In decreasing order of importance they are: size and shape complementarity, H-bond complementarity, steric effects, coordination sphere interactions, and charge-transfer interactions. When molecules have been suitably 'programmed' with the appropriate codes, they can bind by forming the maximum possible number of interactions, which provides the strongest possible binding. The most important factor is size and shape. Clearly, interacting molecules must possess complementary physical shapes in order for significant recognition to occur. The next most important factor, H-bond complementarity, acts in a similar way: H-bond donors must align opposite H-bond acceptors, otherwise there will be a repulsive force between the molecules. Steric effects allow for selectivity when bulky substituents prevent interactions with sterically hindered species. Coordination sphere and charge-transfer interactions are closely related, and describe the ability of metal ions and species with opposing electron donating and accepting properties to preferentially coordinate to molecules with complementary patterns.

The importance of molecular codes was elegantly demonstrated in work by Reinhoudt,[52,53] using the following three compounds: bismelamine **47**, barbiturate **46**, and tetramelamine **48** (Fig. 1.15). Initially, the authors assembled a large box-like rosette structure stabilised by 36 hydrogen bonds, using only bismelamine **47** and barbiturate **46** (Fig. 1.16 A). Next, Reinhoudt investigated the self-sorting capacity of this system. In solution with barbiturates **46**, tetramelamines **48** assembled into tetramelamine rosettes (Fig. 1.16 B), although with a lower stability than the bismelamine rosettes. When the tetramelamines **48** were mixed in solution with the bismelamines **47** and a slight excess of barbiturates **46**, only homomeric assemblies were formed, with no trace of heteromeric assemblies (Fig. 1.16 C). This result demonstrates the power of a combination of molecular codes: size, shape, and H-bonding complementarity.

According to Würthner,[44] metal-ligand interactions are currently the best way to assemble large supramolecular architectures. Indeed, metal-ligand interactions involving a single metal ion have been demonstrated to produce a variety of structures.[54–56] However, the use of multiple different metal ions in solution for self-sorting has been relatively unexplored ever since the first investigations by Lehn in 1993.[48] That study showed how different metal ions with different coordination spheres can coordinate into different ligand geometries. However, one such investigation by Schmittel

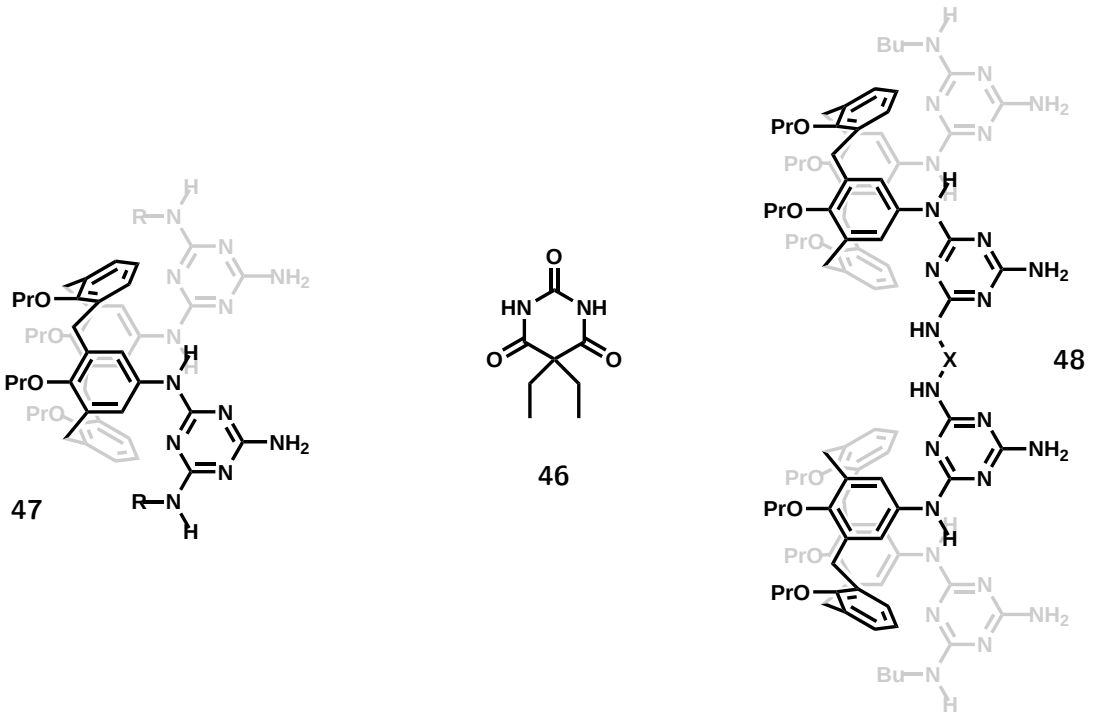

Fig. 1.15 Reinhoudt's bismelamine **47**, barbiturate **46**, and tetramelamine **48**.

and co-workers[57,58] did demonstrate a self-sorting process among four different terpyridine and phenanthroline ligands with two different metal ions, Zn(II) and Cu(I). Out of 20 possible combinations of ligand and ion, only two different complexes were formed. In further work by Schmittel,[59] the authors used compounds **49**, **50**, and **51** to construct a supramolecular triangle with either Zn(II) or Hg(II) and Cu(I) using the self-sorting properties involving the metal ions (Fig. 1.17).

Nitschke[60] has also demonstrated self-sorting behaviour with the assembly of a supramolecular cube based around two different metal ions, Pt(II) and Fe(II), consisting of 62 building blocks and the formation of 96 new bonds.

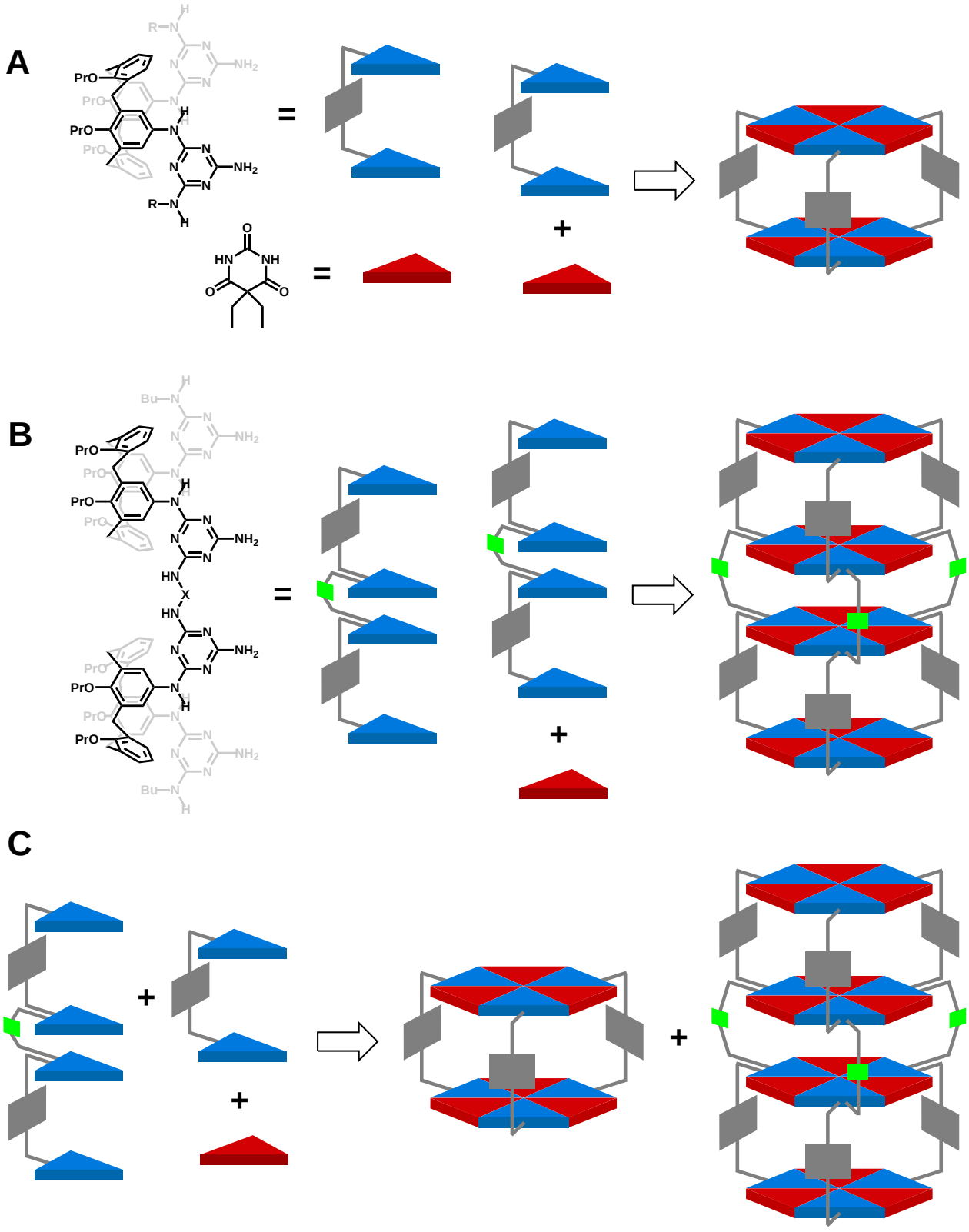

Fig. 1.16 Self-sorting into two distinct homomeric supramolecular assemblies.[52,53]

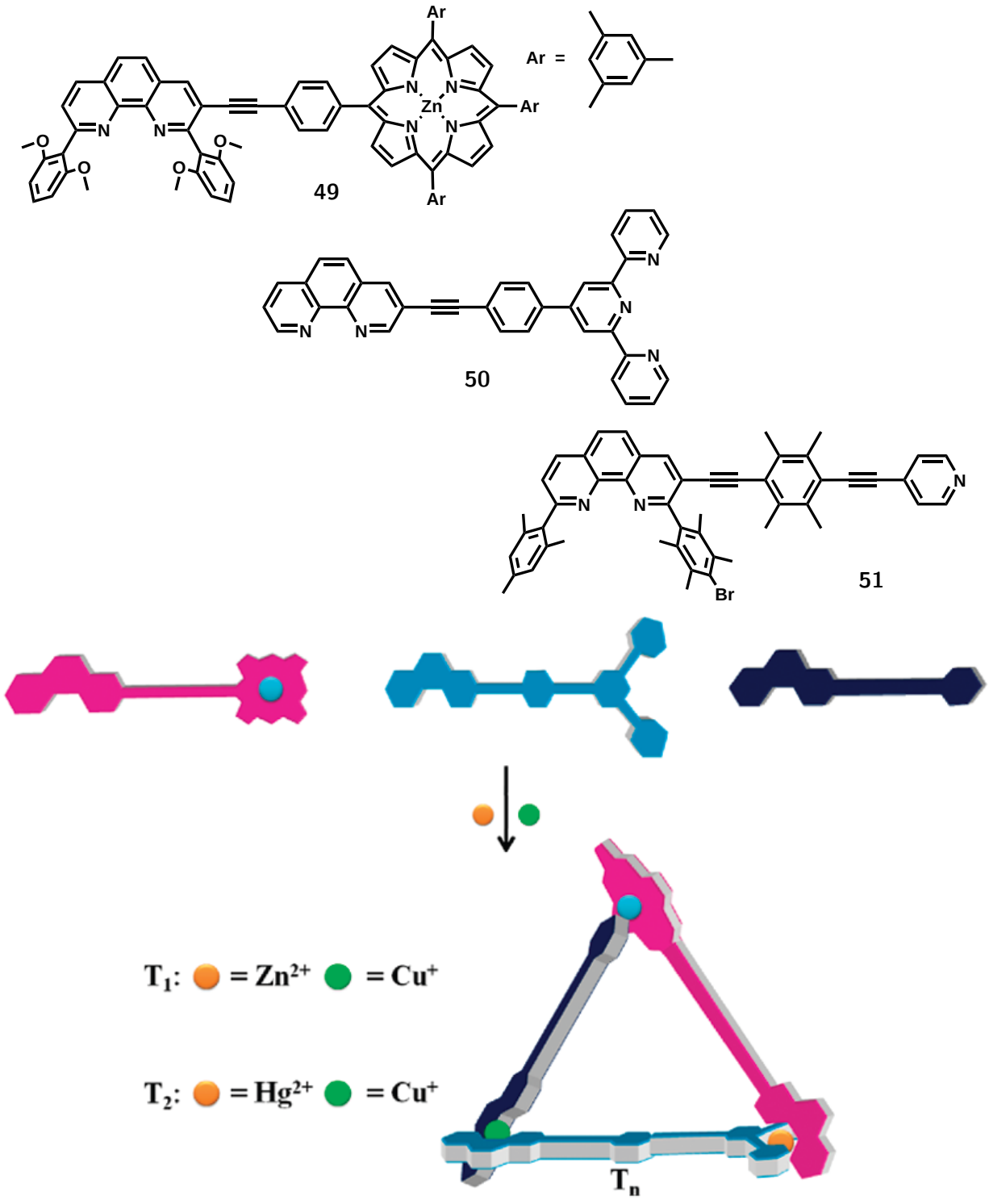

Fig. 1.17 Schmittel's supramolecular triangle built around Zn(II) and Cu(I), using ligands **49**, **50**, and **51**.[59]

1.5 Supramolecular Structures

A wide variety of supramolecular structures have been synthesised by a number of groups, including nanotubes,[61,62] cavity-forming structures,[63,64] cyclic structures (from trimers[65] to hexamers[66]), and structures made from dendrimer subunits.[67] Further, supramolecular architectures are often employed in the area of molecular machines, including oscillators/pistons,[68] macroscopic transport,[69] semiconductors,[70] sensors,[71] and motors.[72]

Shionoya of the University of Tokoyo synthesised ligand **52** (Fig. 1.18).[73] Four of these ligands plus two d^8 metal ions, either Pd^{II} or Pt^{II}, form a supramolecular coordination cage that binds a stack of three bis(anionic) guest compounds in the cavity (Fig. 1.18 A and B). The guest compounds are $[PtX_4]^{2-}$ (yellow) and $[PtY_4]^{2+}$ (blue), where X = Cl or Br, and Y = pyridine or $NH_2(CH_2)_3CH_3$. There are two external $[ClO_4]^{2-}$ counter ions (yellow/red). The crystal structure of this cage shows even higher-order structure, with a hexameric arrangement of cages around a central cavity containing $[ClO_4]^{2-}$ counter ions (Fig. 1.18 C).[74]

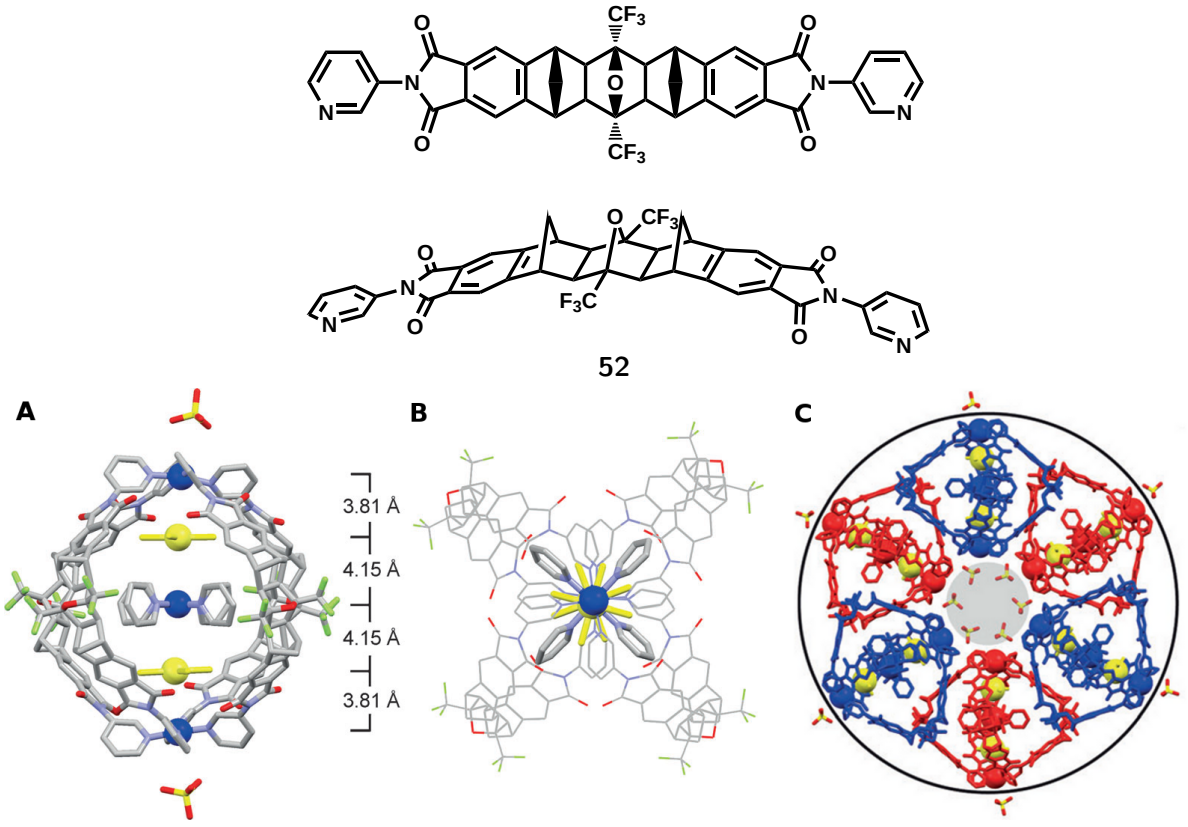

Fig. 1.18 Shionoya's ligand (top), used to form a supramolecular coordination cage, viewed from the side (A) and top (B). The cage assembles into a hexameric supramolecular structure consisting of six supramolecular cages (C).[73,74]

A wonderful geometrical supramolecular structure known as a 'cuboctahedron' has been reported

by a number of groups.[75–80] This polyhedron combines square and triangular faces with 12 vertices and 24 edges. Stang and co-workers[75] used the chemical structures shown in Fig. 1.19 to form a cuboctahedron, consisting of 12 tritopic planar units **53** and 8 ditopic angular units **54**. Fig. 1.19 shows a geometrical diagram of the cuboctahedron on the left, and a space-filled molecular model on the right. The structure is obtained as a result of coordination between the pyridine nitrogen on the tritopic unit and the platinum centre on the ditopic unit. Despite the large mass and high charge (24+), the cuboctahedron is highly soluble in organic solvents such as DCM. It has a diameter of around 5 nanometres.

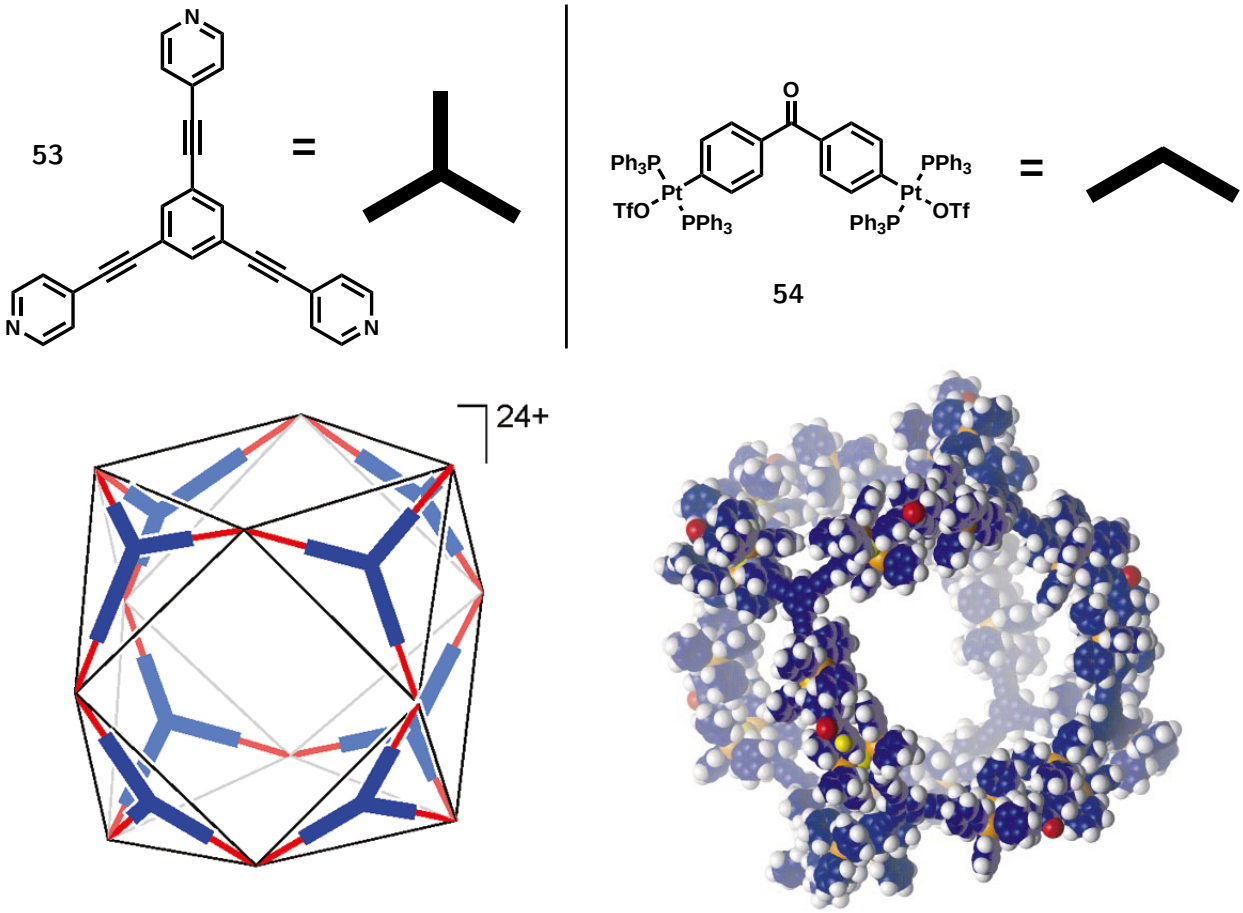

Fig. 1.19 Tritopic **53** and ditopic **54** ligands used by Stang to form a cuboctahedron, shown as geometrical (left) and space-filled (right) models.[75]

Fujita and co-workers achieved the same cuboctahedral symmetry by combining 24 equivalents of ditopic compound **55** (Fig. 1.20) with 12 equivalents of Pt(II).[79] Again, the structure is a result of coordination between the pyridine of the ligand and the platinum centre. The crystal structure of the $Pt(II)_{12}\mathbf{55}_{24}$ assembly is shown with the Pt(II) in yellow. There are two SbF_6^- counterions present, but these have been omitted for clarity.

DNA has proven to be an ideal building material, enabling the creation of precisely-defined large

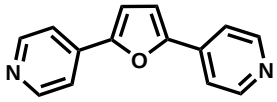

55

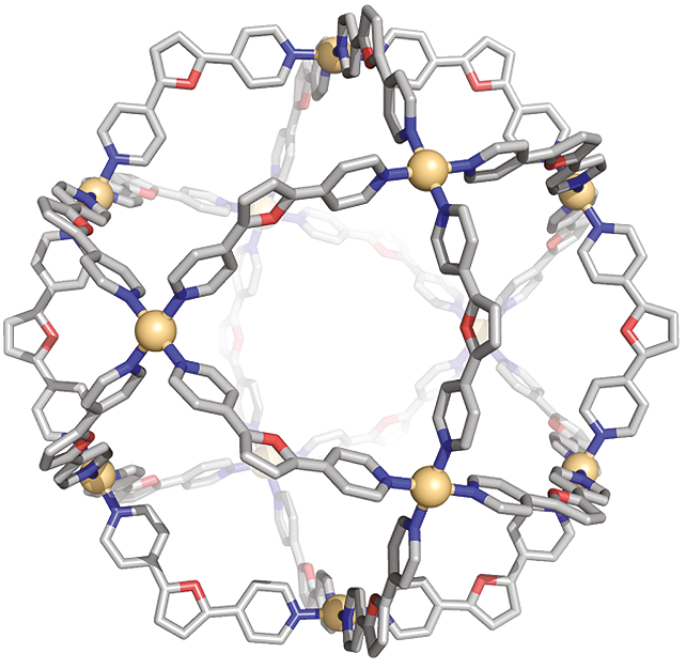

Fig. 1.20 The ditopic ligand **55** (top) used by Fujita for the construction of a cuboctahedron (bottom, crystal structure).[79] The two SbF_6^- counterions have been omitted for clarity.

three-dimensional structures.[81,82] DNA forms a stable helix, and the Watson-Crick base pairs allow the control of strand-pairing *via* the design of base-pair sequence. These qualities have enabled some extraordinary structures to be built and characterized, such as a tetrahedron and a cube (Fig. 1.21).

Rothemund of Caltech used the templating properties of long strands of DNA to assemble 2-dimensional structures on a surface, a technique he termed 'DNA origami'.[83] Using this method, very well-defined patterns could be created at the nanoscale, including letters and faces. Recently, the principles of DNA origami have been used to construct a large layered structure, larger than a prokaryotic ribosome.[84]

Foldamers are synthetic, sequence-specific oligomers similar to peptides that fold up in solution to form well-defined secondary helical structures.[85,86] They are often studied to aid our understanding of the dynamics of protein-folding. They also allow the presentation of synthetically-inserted functional groups at specific positions in space along the oligomer chain. This makes them attractive for the design and synthesis of compounds that bind in a sequence- and structure-specific manner to large 3-dimensional surfaces, such as proteins. Many foldamers are constructed from β-amino acids, which have their amino group bonded to the β carbon (instead of the α for natural amino

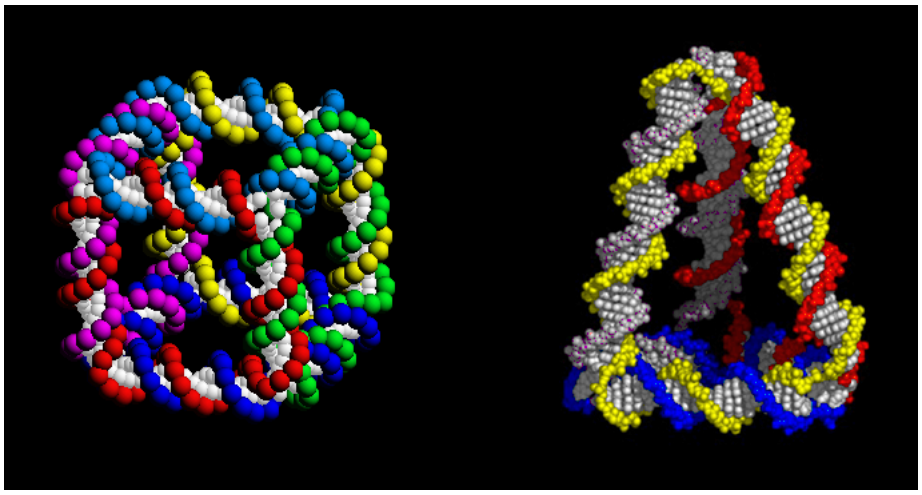

Fig. 1.21 Examples of DNA nanostructures.[81,82]

acids). Fig. 1.22 shows a foldamer as synthesised by Gellman, constructed from alternating α and β peptides.[87]

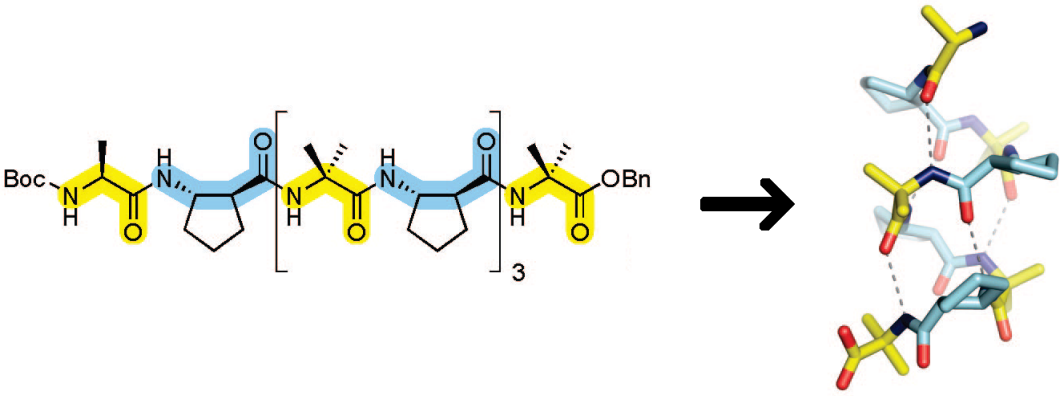

Fig. 1.22 An α/β-peptide foldamer[87] (yellow - α-peptide; blue - β-peptide).

H-bonding arrays have proven to be of high utility in the formation of supramolecular polymers.[88] The building-block **56** (Fig. 1.23) consists of Meijer's ureidopyrimidinone (UPy)[89] motif **9** joined on each end of an organic linking chain (**56** = · · ·–**9**·**9**–**9**·**9**–**9**·**9**–· · ·). In its self-complementary tautomer (with an AADD H-bonding array), the UPy motif **9** has a binding constant of 6×10^7 M^{-1} in $CDCl_3$, and has been shown to form supramolecular polymers in solution.[26,90] In its non-self-complementary tautomer (ADDA array) it can also form dimers with the non-self-complementary DAAD diamidonaphthyridine motif Napy **57**,[91] with a binding constant of 5×10^6 M^{-1}. Despite the lower binding constant of the heterodimer, when solutions of the UPy homopolymers (made of building-blocks **56**) are titrated with Napy-based building-blocks **58**, the homopolymers are efficiently replaced by the formation of heteropolymers, consisting of 1:1 equivalents of the UPy

building-block **56** and the Napy building-block **58** (Fig. 1.23 C).[92] This is due to fact that the Napy motif **57** is non-self-complementary, so in solution the Napy building-block **58** is free and the H-bond sites are not filled. However, in the 1:1 heteropolymer, all H-bond donor and acceptor sites are satisfied, so this is the lower-energy and hence preferred state of the system.

The work shown in Fig. 1.23 highlights two important points that are highly pertinent to our work in this project. Firstly, the UPy homopolymer (shown in green) demonstrates how polymerisation is inevitable in systems involving a single self-complementary array, in this case the UPy motif **9**. Secondly, even in polymers involving non-self-complementary arrays, polymerisation is also unavoidable (the red and blue polymer). Thus, non-self-complementary motifs alone are insufficient to prevent polymerisation.

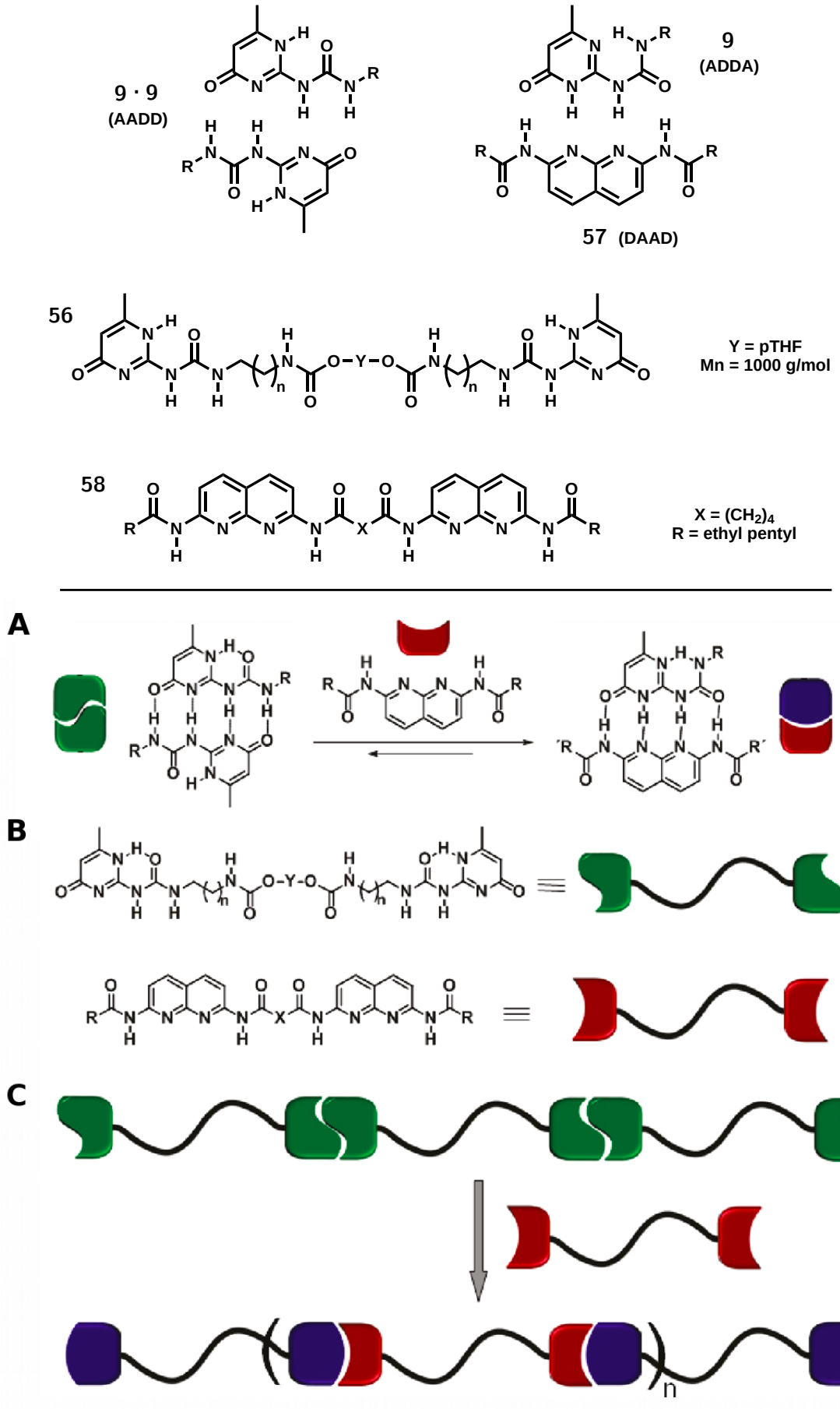

Fig. 1.23 Supramolecular polymer formation utilising 4-H-bond binding motifs.[92]

1.6 Challenges Facing Non-Covalent Synthesis

There are many difficulties which must be surmounted when attempting to assemble a macromolecule in a controlled fashion. These include binding strength, polymerisation, motif symmetry, and tautomerism.

1.6.1 Binding Strength

Entropy has a large effect on binding strength. The greater the number of possible conformations a structure can take, the greater the entropic price it must pay in order to adopt an essentially rigid H-bonded structure as part of a macromolecule, and thus the smaller the binding constant. Generally speaking, rigid motifs form stronger non-covalent bonds. In the context of this project, the literature binding constants for 4-H-bond motifs are mostly in the range 10^4–$10^7\,\mathrm{M}^{-1}$.

It is very hard to estimate the binding strength between H-bonding motifs. Meijer found that the addition of an intramolecular H-bond, rigidifying the structure and thus lowering the entropy, increased the association constant K_a by three orders of magnitude (from $530\,\mathrm{M}^{-1}$ to $2 \times 10^4\,\mathrm{M}^{-1}$ – Fig. 1.24).[93]

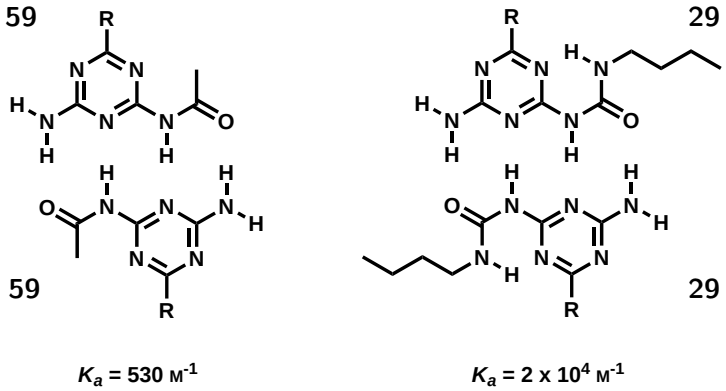

Fig. 1.24 Intramolecular H-bonds can rigidify structures and increase binding strength.

1.6.2 Self-Complementarity and Polymerisation

Motifs can be either 'Self-Complementary' or 'Non-Self-Complementary'. Self-complementary motifs can fully bind to themselves using all of the available H-bonds (**29**·**29**, Fig. 1.25). In contrast, non-self-complementary motifs cannot fully bind to themselves due to the arrangement of H-bonds, and require a complementary partner to form a fully-bound dimer (**31**·**9**, Fig. 1.25).

Non-self-complementary motifs are still capable of partially binding to themselves *via* the

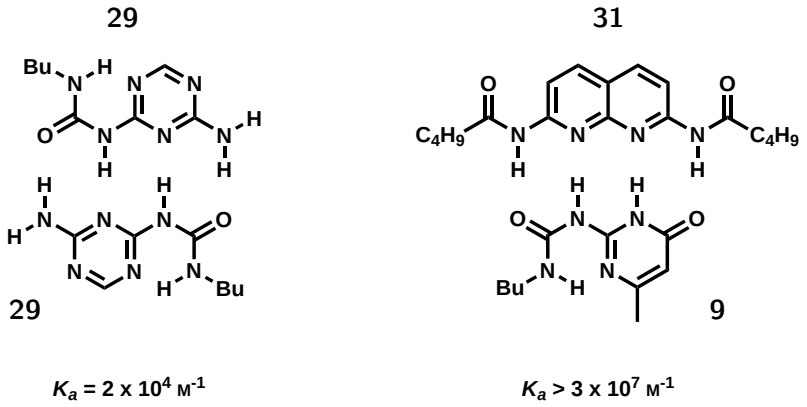

Fig. 1.25 A self-complementary motif **29**·**29** compared to non-self-complementary motifs **31**·**9**.[13]

phenomenon of 'overlapping' (Fig. 1.26). However, the binding strength of such interactions, typically involving only two H-bonds, is several orders of magnitude lower than fully-bound dimers, which involve all four H-bonds.

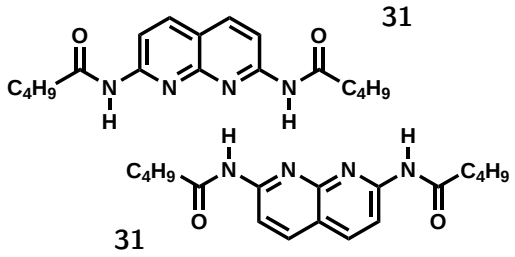

Fig. 1.26 Non-self-complementary motifs can 'overlap' and partially bind to themselves.

Self-complementary motifs have crucially different properties to non-self-complementary motifs. For the purposes of macromolecular synthesis *via* the controlled step-by-step addition of subunits, self-complementarity is an undesirable property because it can lead to uncontrolled polymerisation (Fig. 1.27). In 2002 Meijer described non-self-complementary four-H-bond arrays as being 'largely unexplored'.[93]

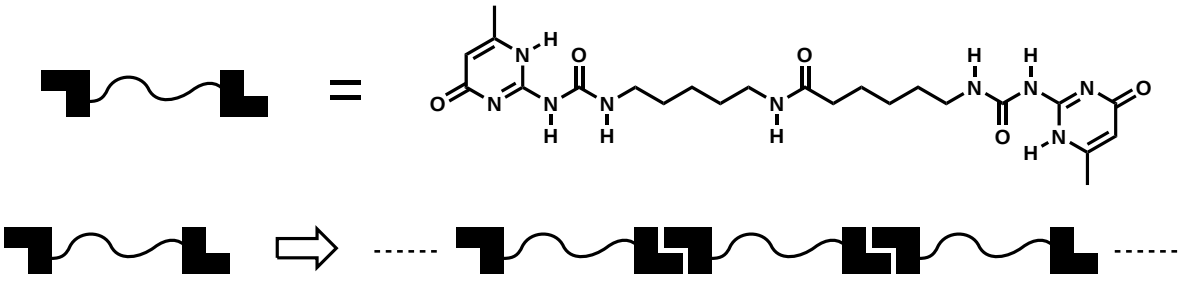

Fig. 1.27 Polymerisation as a result of motif self-complementarity.

1.6.3 Motif Symmetry

The symmetry of the motif determines the orientation of binding. Symmetrical motifs can bind in one of two orientations, whereas non-symmetrical motifs can only bind in one orientation (Fig. 1.28).

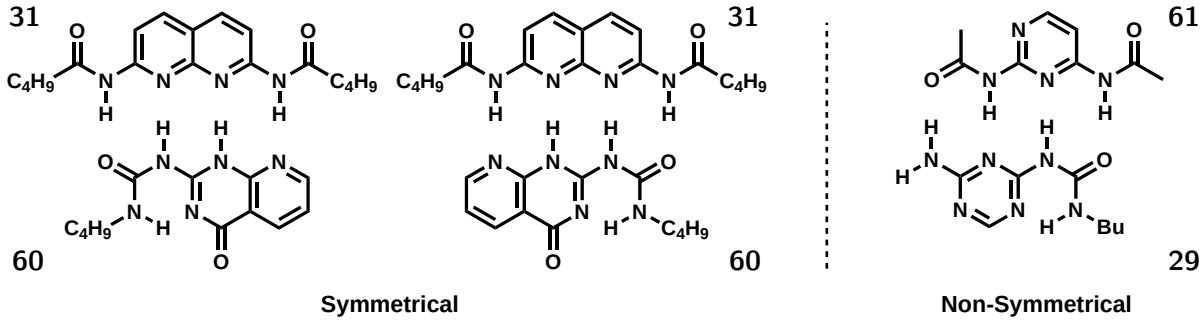

Fig. 1.28 Symmetrical motifs can bind in two orientations (left), but non-symmetrical motifs can bind in only one (right).

The orientation of the binding determines which functional groups line up opposite each other. If one is concerned with controlling the subsequent interactions between sidechain subunits to which the motifs are attached, motif symmetry becomes undesirable.

It should be noted that in the above analysis, it is assumed that the motifs do not tautomerise, and therefore retain their array pattern. The motifs in Fig. 1.28 are taken from the literature, and can in fact tautomerise. For example, pyrimidine **61** can tautomerise from an ADAD pattern to a DADA pattern, and can therefore bind to triazine **29** in either orientation. As discussed in Section 1.7, we aim to synthesise compounds with minimal tautomerism, so they can only bind with one orientation if they have a non-symmetrical motif.

1.6.4 Tautomerism and Isomerism

Many H-bonding candidates can exist in different tautomeric forms and different isomers due to rotation around single bonds. This can cause the H-bonding array pattern to change. For example, in Fig. 1.29, the array pattern shifts from ADDA, which is non-self-complementary, to DDAA, which is self-complementary. As self-complementarity can be an undesirable property, tautomerism and rotational isomerism may well also be undesirable in an H-bonding motif.

The strongest known 3-H-bond complex is the AAA·DDD dimer **24**·**25** shown in Fig. 1.6 and Fig. 1.30. However, the binding strength of even this dimer is lowered by the tautomerism of **25**, which exists as both the 1,4-dihydro form **25** and the 3,4-dihydro form **63**.[28]

Zimmerman and Wilson both described similar approaches to tackle the problem of tautomerism.

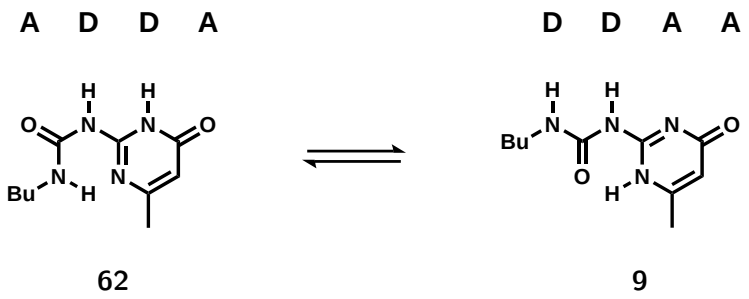

Fig. 1.29 Tautomerism can cause the binding array to shift from ADDA to DDAA.

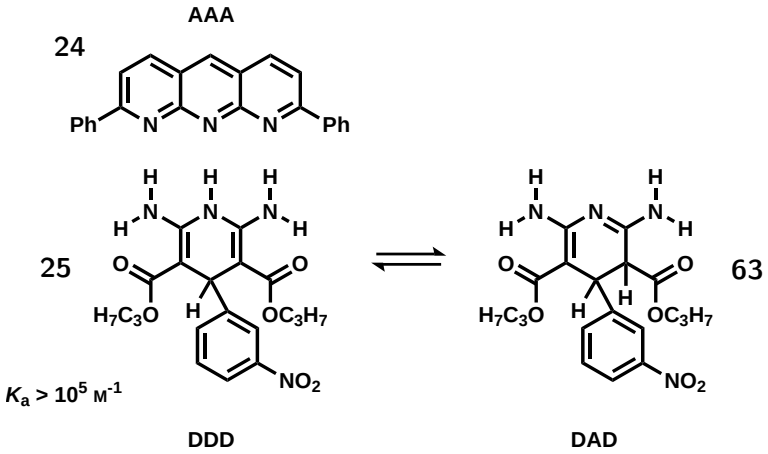

Fig. 1.30 Tautomerism lowers the binding strength.

Zimmerman[28] published an amido-urea motif **64** that mainly presents a self-complementary AADD array no matter what the tautomeric form. Fig. 1.31 shows the five tautomeric forms of **64**; two that form an ADDA array (**65** and **60**, top row); two that form an AADD array (**66** and **64**, middle row); and one that forms a DADA array (**67**, middle row). However, when **64** is in solution (in $CDCl_3$), the non-self-complementary tautomers **65** and **60** are not observed. Only the self-complementary tautomers **67**, **66**, and **64** are observed, forming dimers with relative abundances as shown on the bottom row. The minor tautomer **67**, a DADA array, constitutes only 6 % of the compound in $CDCl_3$. Therefore, 94 % of the compound, irrespective of its tautomeric form, is in the AADD array pattern. The relative abundances were found not to change over a large range of concentrations. For this reason only a lower limit of the binding constant K_a could be measured, and this was found to be 10^7 M^{-1} in $CDCl_3$, indicating very strong binding.

In 2008 Wilson[94] described a motif **68** which always presents a DDA array no matter which conformational form it adopts (Fig. 1.32). This is achieved by the combination of an imidazole and a urea.

The DDAD/AADA array **34**·**35** shown previously in Fig. 1.9 had an anomalously low binding constant of 590 M^{-1}. This is due to tautomerism in the 2-pyridylurea. The favoured tautomer **69** is

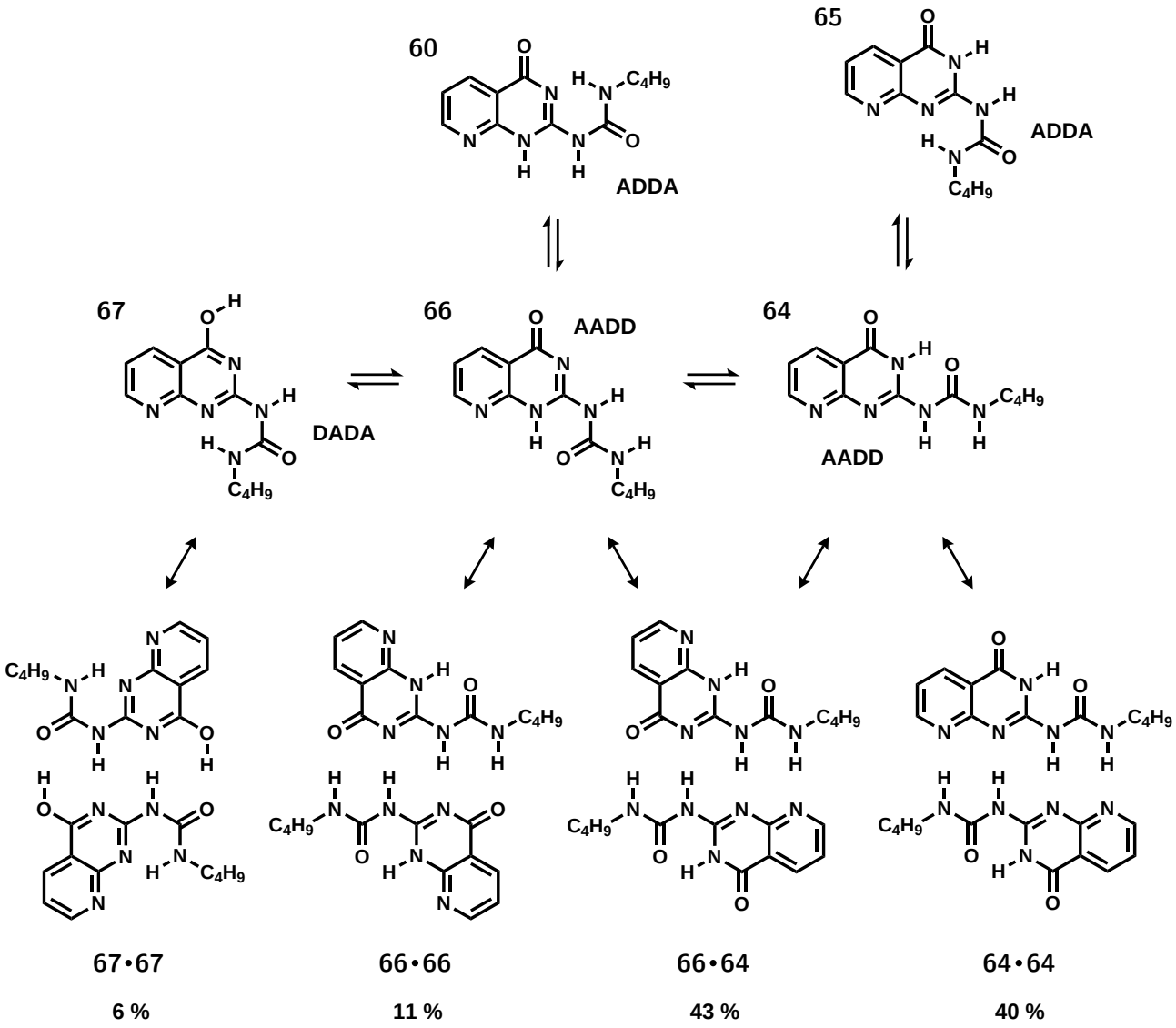

Fig. 1.31 Relative abundance of tautomers of the same compound in $CDCl_3$.[28]

the one following formation of an intramolecular H-bond (Fig. 1.33). This tautomer can go on to form a H-bonded dimer with itself *via* a DA/AD motif.

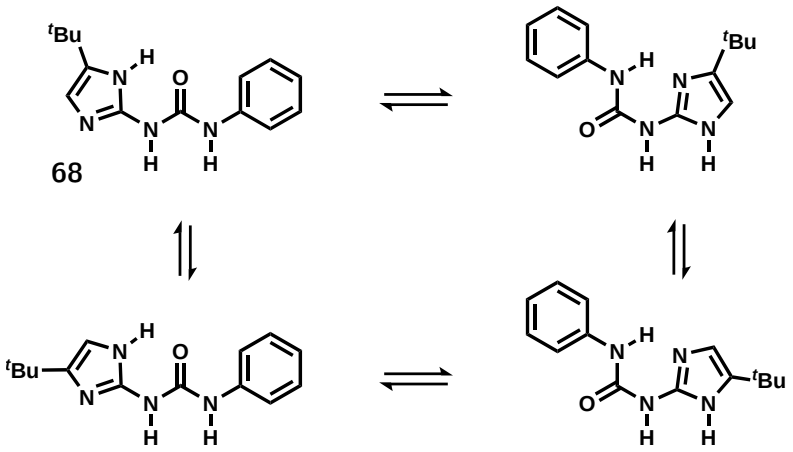

Fig. 1.32 A motif **68** that presents an ADD array no matter which conformational form it adopts.[94]

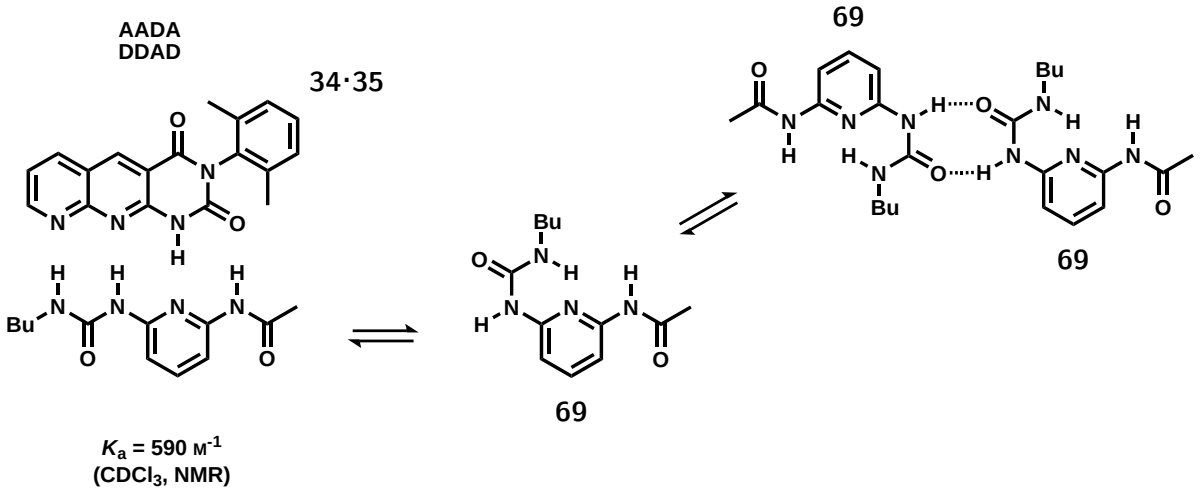

Fig. 1.33 An intramolecular H-bond disfavours the intended DDAD array.[95]

1.7 Project Aim

1.7.1 Stepwise Synthesis

Complex biological macromolecules assemble from a number of smaller subunits (Fig. 1.34). Each subunit binds selectively to the macromolecule in precisely its intended position. We therefore propose that supramolecular synthesis should ideally be performed in a controlled, step-by-step fashion. In this way, by following nature's lead, we could control the precise shape of the macromolecule, and hence its function.

We have seen that current motifs possess many undesirable properties such as self-complementarity, symmetry, and tautomerism. Motif self-complementarity leads to polymerisation, while motif symmetry provides no control over orientation. There are currently no known motifs that are both

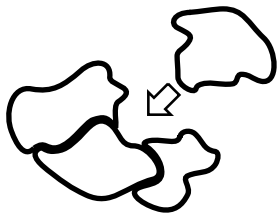

Fig. 1.34 Biological macromolecules assemble subunit by subunit in a stepwise manner.

non-self-complementary and non-symmetrical. Therefore, with current technology, it is difficult to control both the orientation of binding whilst preventing polymerisation. In terms of motif design, we therefore require our motifs to be both non-self-complementary and non-symmetrical. We also seek to reduce the potential for tautomerism to a minimum, and have as high a binding constant as possible.

1.7.2 A Four-Motif Macromolecular Construction Language

In order to assemble a construction kit that facilitates the controlled, step-by-step assembly of macromolecules, we have seen that the ideal molecular building-blocks must be all of the following:

1. Strongly-binding.
2. Non-self-complementary.
3. Non-symmetrical.
4. Non-tautomeric.

We saw in Section 1.5 that building-blocks constructed from both self-complementary and non-self-complementary motifs resulted in polymerisation (Fig. 1.23). These types of motifs are perfectly suitable and indeed desirable for polymerisation reactions and the synthesis of polymers. However, more than just non-self-complementarity is necessary. We reason that a subunit should not bind to the macromolecular structure at a position where it is not intended. A completely different design paradigm is necessary to achieve controlled stepwise synthesis. The ideal system would provide complete control over the location where each macromolecular subunit binds.

For this reason we propose an additional and essential final requirement for our macromolecular construction set: it must consist of a minimum of four binding motifs (let us call them A, B, C and D), in which A binds only to B, and C binds only to D, and no motif binds to itself or to either of the others to which binding is not intended. In other words, the motifs must bind in a

pairwise, orthogonal manner. Therefore, we would like to construct a set of motifs that observe non-integrative social self-sorting behaviour.

1.7.3 Aim

We aim to synthesise four H-bonding motifs, 'A', 'B', 'C' and 'D', which together fulfill the requirements of our macromolecular construction language: A binds to B, and C binds to D. Crucially, all four motifs must not bind to themselves, nor to either of the other two motifs to which binding is not intended. For example, motif A will bind to B, but not to A, C, or D. Each motif shall contain an array of four H-bonds for strong binding to its partner, will be as rigid as possible, as non-tautomeric as possible, will not suffer from overlapping, and will be non-symmetrical.

The four motifs that we initially proposed are depicted in Fig. 1.35. The motifs are referred to as 'Unit A' (**1**), 'Unit B' (**2**), 'Unit C' (**3**), and 'Unit D' (**4**).

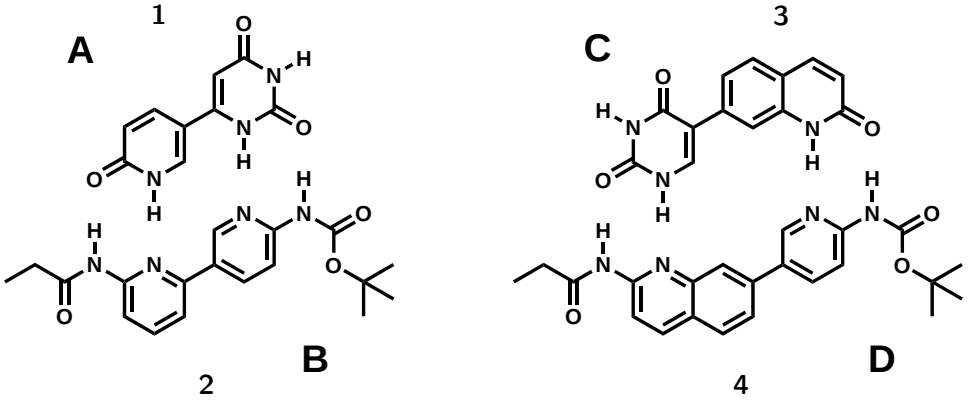

Fig. 1.35 The four originally-proposed motifs.

The design of these four motifs is intended to satisfy as many as possible of the requirements listed above of the ideal macromolecular construction kit. Each unit has four H-bonds for strong binding. While rotation can occur around the single C–C bond joining the two aryl regions, the motifs otherwise have a high degree of rigidity, which should also contribute to strong binding. The use of a 'staggered' array design is employed to force binding to take place in only one possible orientation. The binding array pattern for both pairs, AB and CD, is ADDA/DAAD. The combination of this pattern with the staggered architecture satisfies the dual requirements of non-self-complementarity and non-symmetry (note that even with a staggered motif architecture, an ADAD/DADA array pattern would create a self-complementary motif). While the 2-pyridone moiety can in principle tautomerise into a 2-hydroxypyridine, thus destroying motif non-self-complementarity, one would expect the 2-pyridone tautomer to be strongly favoured. The units cannot

overlap by more than two H-bonds, which should not be enough to interfere with the intended binding behaviour. Finally, the extra aromatic ring in Units C and D compared to Units A and B acts as a spacer, preventing undesired binding between the pairs, providing the necessary pairwise binding orthogonality (Fig. 1.36).

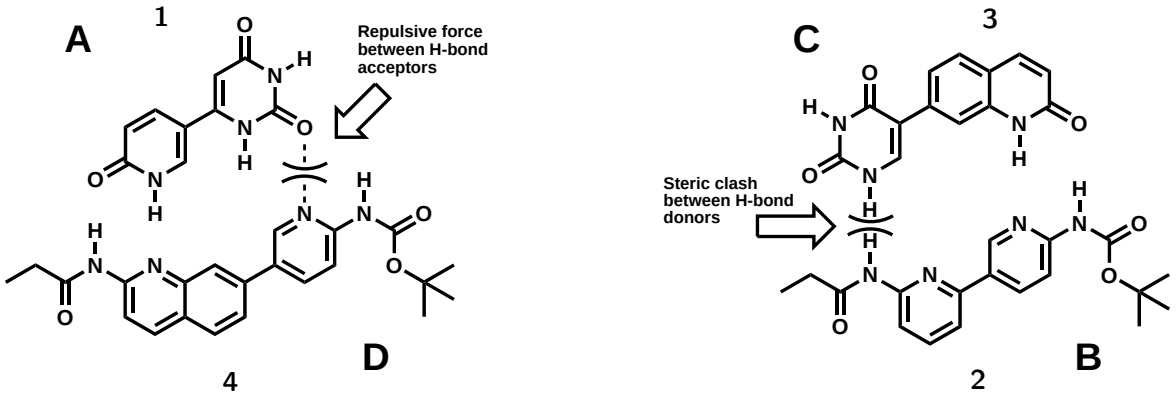

Fig. 1.36 The positioning of H-bond donors and H-bond acceptors prevents undesired binding between motifs.

The design was also motivated by the desire for ease of synthesis. The synthesis of these motifs should be readily achievable using standard cross-coupling reactions to form the C–C bond between the two heterocyclic regions of each motif. Furthermore, they possess synthetic 'handles' (for example the propionyl-functionalised amine) for the ready attachment of selected macromolecules.

No design is perfect however, and a compromise must be made between ease of synthesis and the optimal design. The single C–C bond joining the two aryl regions of each unit allows for rotation about that bond. The compounds will always choose the conformation which will minimise their energy. From the perspective of looking down the axis of the C–C bond, each unit, if alone in solution, would therefore want to sit with the heterocyclic rings at right-angles to each other. This conformation reduces the interaction between the two protons circled in Fig. 1.37 (Unit B is shown as an example, although the protons are arranged in exactly the same way on all four units).

In order for binding to take place with the complementary partner, we are asking for each of the four units to adopt a planar conformation. We hope that the lowering of energy as a result of forming four H-bonds with its complementary partner will more than compensate for the gain in energy from adopting a planar conformation. Binding could still take place even if the binding pairs do not sit in a perfectly planar conformation. A slight twist angle between the two aryl regions would alleviate steric repulsion between them, and still allow for four H-bonds to form between the two units.

Another area for concern is the area inbetween the two binding units. As shown in Fig. 1.38, this

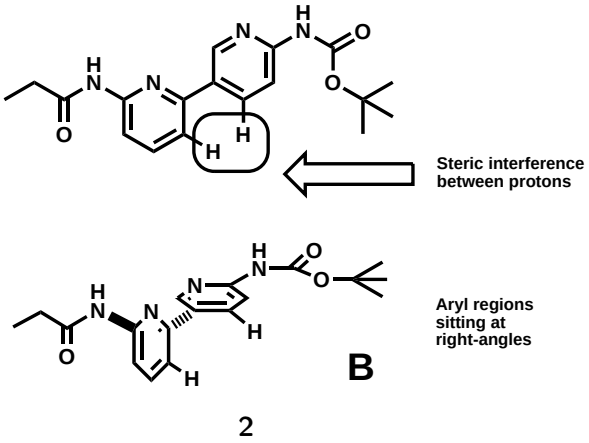

Fig. 1.37 Energy-minimising conformation as shown for Unit B **2**.

region is rather congested with protons. There is the potential for a steric clash not only between the protons on adjacent halves as discussed above, but also between the protons on both units that project into the intermolecular space. Again, this clash can be assuaged by a slight twist between the C–C bond that joins the two halves.

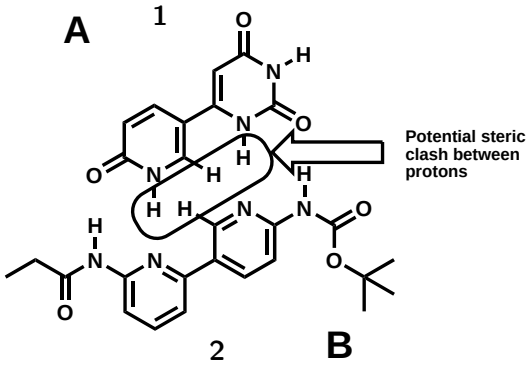

Fig. 1.38 Potential steric clash between Units A and B.

The only certain way to establish the true extent of these steric issues is to synthesise the compounds and measure the binding. So, with these concerns in mind, the synthesis was commenced with the intention of making the compounds as quickly as possible, and then to measure the binding between them. If it then became apparent that these steric concerns were indeed causing major problems with the binding, the design would be revised and the process of synthesis and binding measurement repeated.

2 Initial Synthesis

2.1 Synthesis of Original Designs

2.1.1 Retrosynthesis

The planned synthesis of the four first-generation target compounds is outlined in Scheme 2.1 and Scheme 2.2. The key step of the strategy is based on a Suzuki cross-coupling reaction to form the crucial C–C bond which links together the two aryl regions of each of the four targets. The Suzuki reaction[96] is the natural choice as it is well-known to be a reliable reaction for C–C bond formation, particularly in biaryl systems. These Suzuki reactions require a heteroaryl boronic acid and a heteroaromatic halide as the two reactants. This strategy therefore requires firstly the synthesis of the boronic acid and bromide compounds, and secondly the cross coupling reaction to form the C–C bond. The retrosynthetic strategy utilises 7-bromoquinolone **70**, which is common to the synthetic plan for both Units C and D.

The results are divided up on a unit-by-unit basis. First, the synthesis of Units B and D will be described. Both are based on 2-aminopyridines, and in the event proved the most straightforward to synthesise. Units A and C are then described; both are based on 2-pyridones, and proved by far to be the most difficult to synthesise.

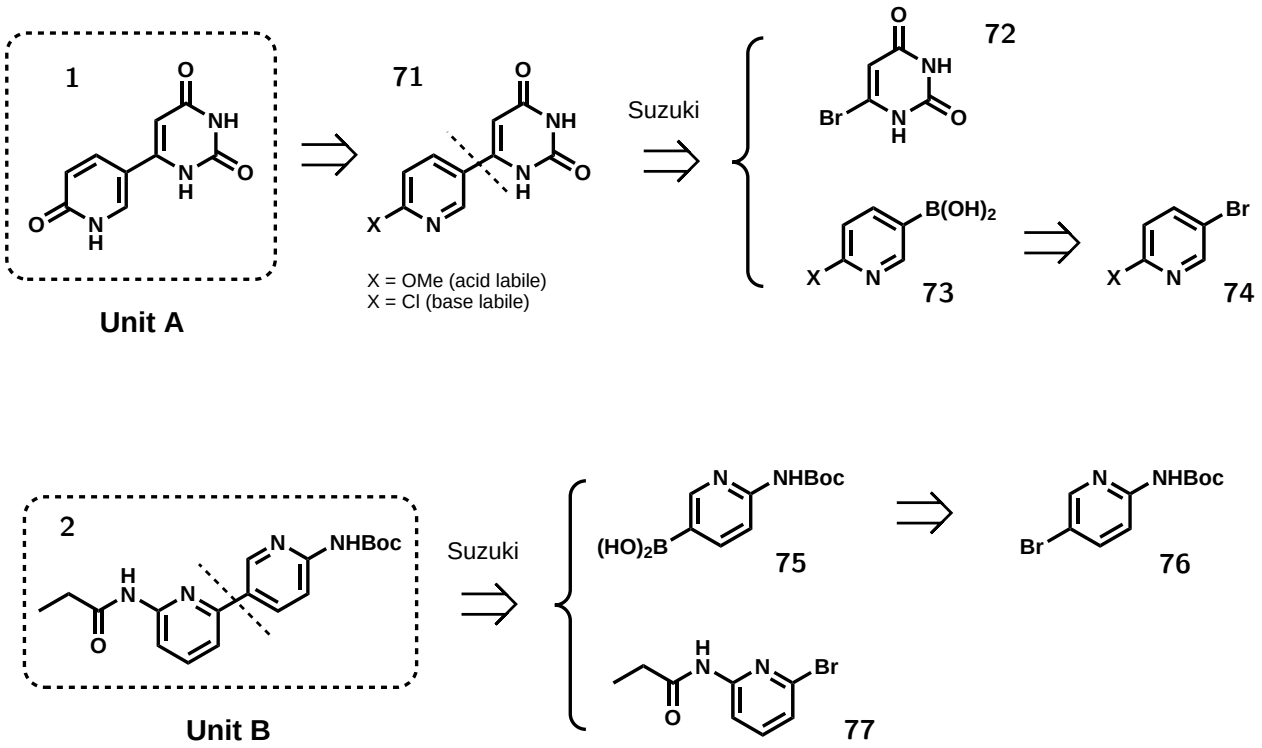

Scheme 2.1 Planned routes towards Units A **1** and B **2**.

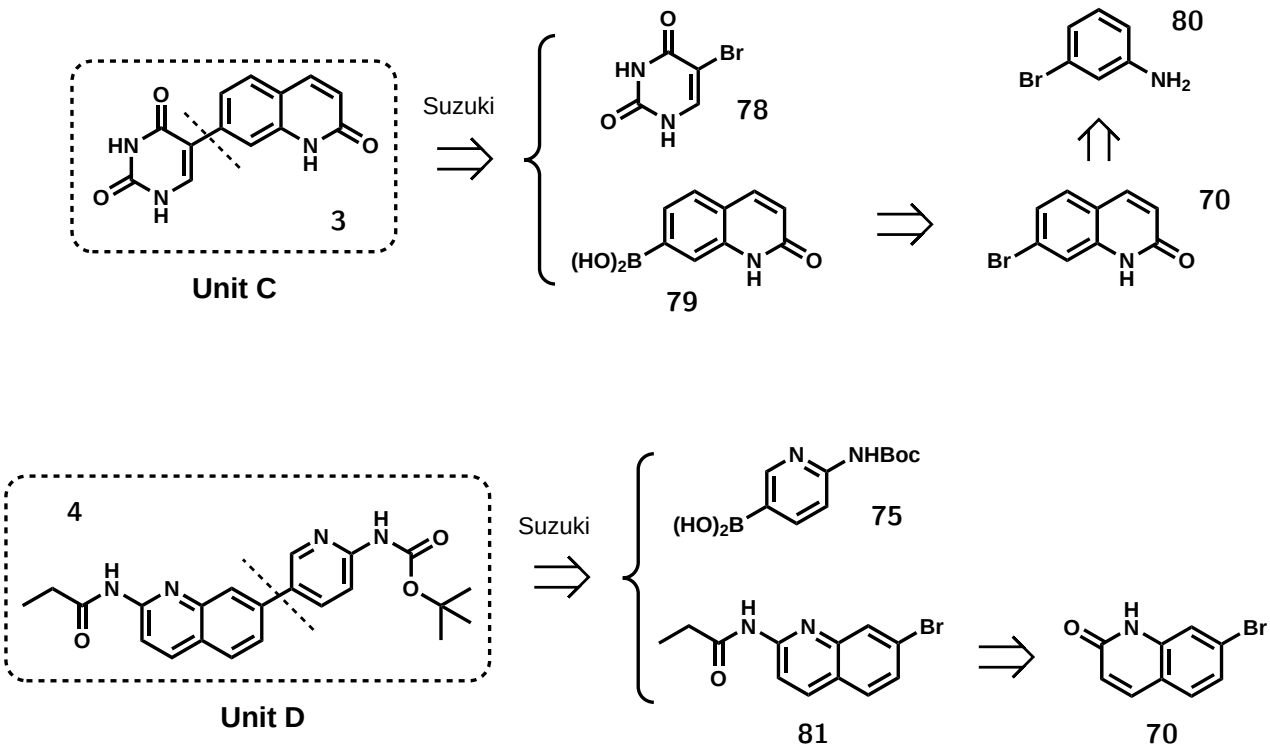

Scheme 2.2 Planned routes towards Units C **3** and D **4**.

2.2 Synthesis of Unit B

2.2.1 Bromopyridines

The synthetic strategy towards Unit B relied upon the successful preparation of bromopyridines **76** and **77** (Scheme 2.3).

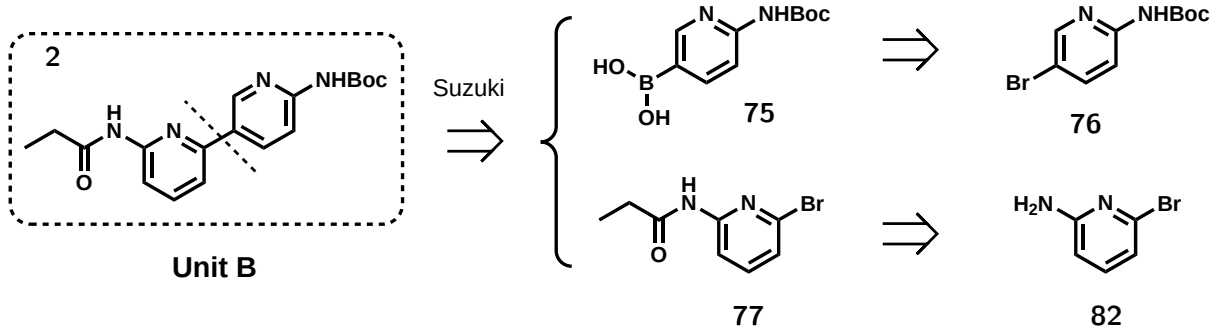

Scheme 2.3 Planned route towards Unit B **2**.

The synthesis of bromide **76** required for boronic acid **75** commenced with a selective bromination of 2-aminopyridine **83** at the 5-position (Scheme 2.4). By following a literature precedent[97] for this reaction the desired product was isolated in high yield. Substitution took place only at the 5-position, as this is the most electron-rich position in the ring, activated by the strongly electron-donating amine group in the 2-position. The product **84** was purified by simple washing with water, which removed the succinimide by-product.

Pyridine **84** was then Boc-protected[98] using NaHMDS to deprotonate the amine. The resultant sodium amide reacted selectively with the Boc_2O to deliver the protected product **76** in 92 % yield (Scheme 2.4).

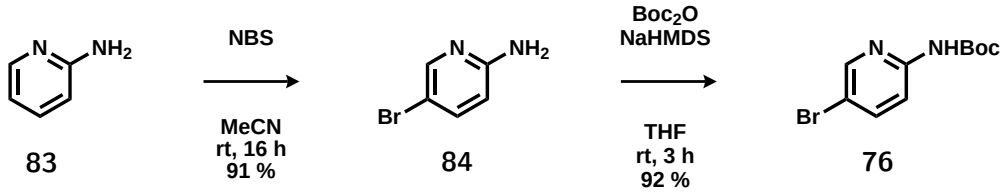

Scheme 2.4 Synthesis of tert-butyl (5-bromopyridin-2-yl)carbamate **76**.

Propionamido pyridine **77** was prepared by reacting 2-amino-6-bromopyridine **82** with propionyl chloride in DCM and pyridine[99,100] (Scheme 2.5). The pure product was isolated in 68 % yield without the need for further purification.

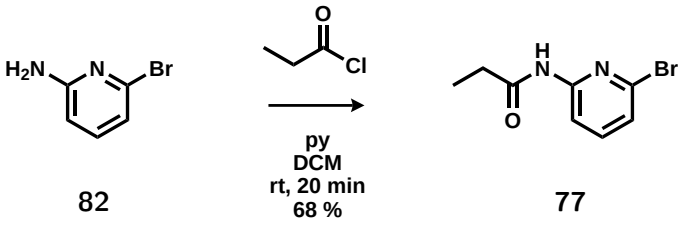

82 77

Scheme 2.5 Synthesis of N-(6-bromopyridin-2-yl)propionamide **77**.

2.2.2 Boronic Acid

It was now necessary to convert bromide **76** to the corresponding boronic acid **75**. This proved to be more challenging than the preparation of the bromides. An extended discussion is provided in the appendix (Section 11.1.1, Appendix C). The desired boronic acid **75** was eventually isolated in 32 % yield (Scheme 2.6) in sufficiently high purity that it could be subjected to the subsequent Suzuki coupling.

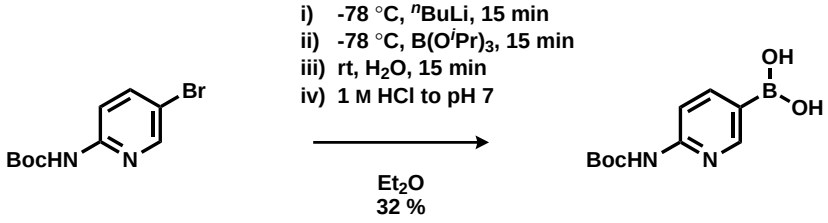

76 75

Scheme 2.6 Synthesis of boronic acid **75**.

2.2.3 Suzuki Coupling

As discussed previously, we proposed that the Suzuki cross-coupling reaction[96] be used to join the two aryl regions of not just Unit B, but of all the target compounds. The reaction relies upon palladium catalysis and proceeds through the catalytic cycle shown in Fig. 2.1.

Initially, test reactions were performed with phenylboronic acid **85** and bromide **77** (Scheme 2.7). The results were encouraging, with the desired Suzuki product **86** produced in 65 % yield following purification by flash chromatography.

Initial attempts to couple bromopyridine **77** with boronic acid **75** were only partially successful (Scheme 2.8). Following suitable literature precedent,[101] the reaction mixture was heated at 110 °C for 48 h in the presence of $Pd(PPh_3)_4$ with aqueous Na_2CO_3 as base. Subsequent purification and ^{1}H NMR analysis revealed that while the coupling had indeed taken place, the isolated product contained no Boc group.

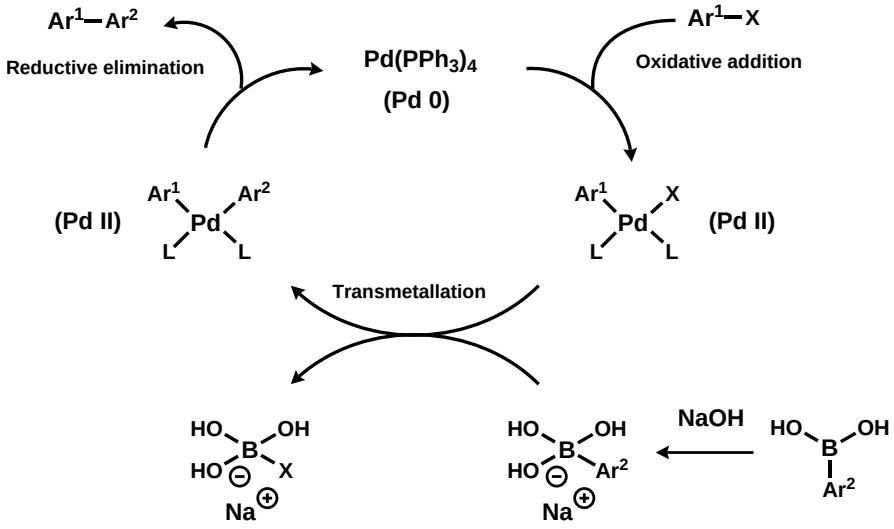

Fig. 2.1 The catalytic cycle of the Suzuki cross-coupling reactions.

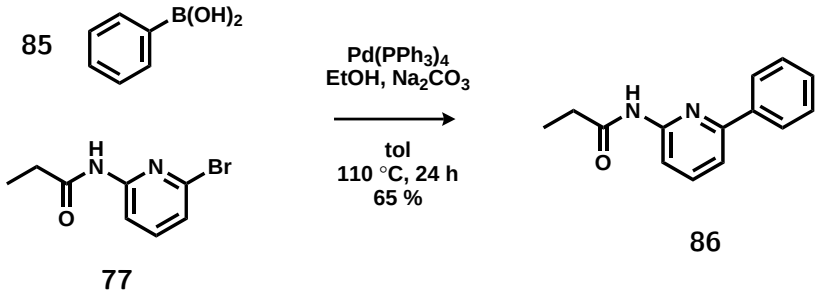

Scheme 2.7 Test Suzuki coupling with phenylboronic acid **85** and bromopyridine **77**.

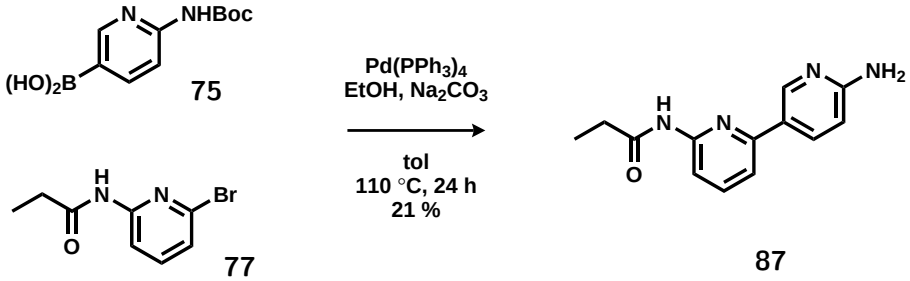

Scheme 2.8 Suzuki cross-coupling at 110 °C, resulting in loss of the Boc group.

Gratifyingly, repeating the reaction at 80 °C prevented the loss of the Boc group and afforded Unit B **2** in a satisfying 72 % yield (Scheme 2.9). We were pleased to note that Unit B **2** was perfectly soluble in $CDCl_3$.

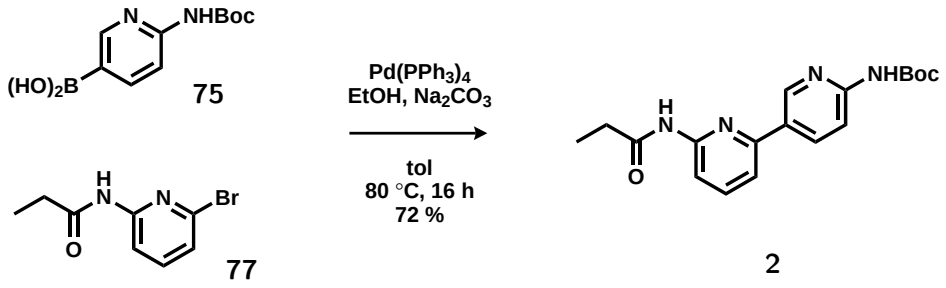

Scheme 2.9 Suzuki cross-coupling to make Unit B **2**.

2.3 Synthesis of Unit D

2.3.1 Bromopyridine Synthesis

With boronic acid **75** already in hand from the synthesis of Unit B, it only remained to synthesise the bromoquinoline coupling partner **81** (Scheme 2.10). Precursor **81** could in turn be reached in two steps *via* bromoquinolone **70**, a known compound, from 3-bromoaniline **80** using the Doebner-Miller synthesis.[102–106]

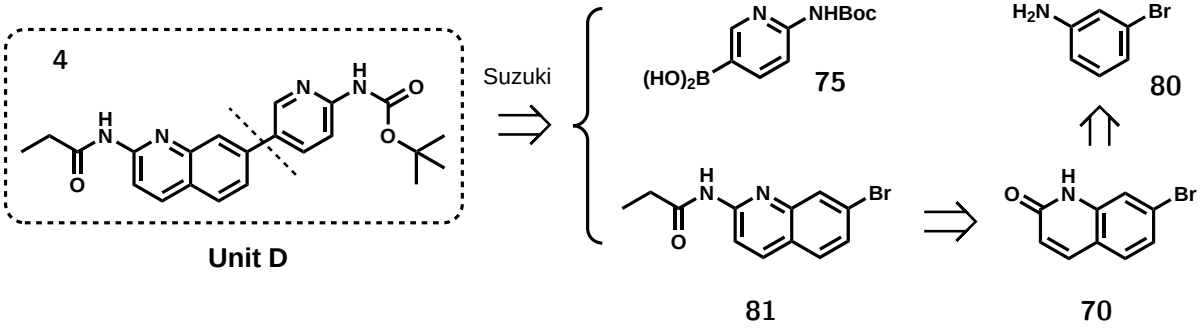

Scheme 2.10 Planned route towards Unit D **4**.

The first step in the synthesis is the formation of cinnamaniline **88** prior to the ring-closing reaction to form the quinolone (Scheme 2.11). Cinnamaniline **88** was synthesised in high yield by reacting cinnamoyl chloride **89** with 3-bromoaniline **80**.[106] The product was efficiently purified simply by a base wash followed by an acid wash, allowing the isolation following work-up in excellent purity.

Conversion of the cinnamaniline **88** to the desired bromoquinolone isomer **70** was then attempted. The desired conversion had been performed on a very similar compound, using $AlCl_3$ at 100 °C.[106] Unusually, this reaction required no solvent, with a heat-gun being employed to initiate the reaction. A 1.5:1 mix of isomers **70** and **90** occurred in repeated reactions, as determined by ^{1}H NMR spectroscopic analysis, although the combined yield was quantitative. The 7-bromo isomer **70**

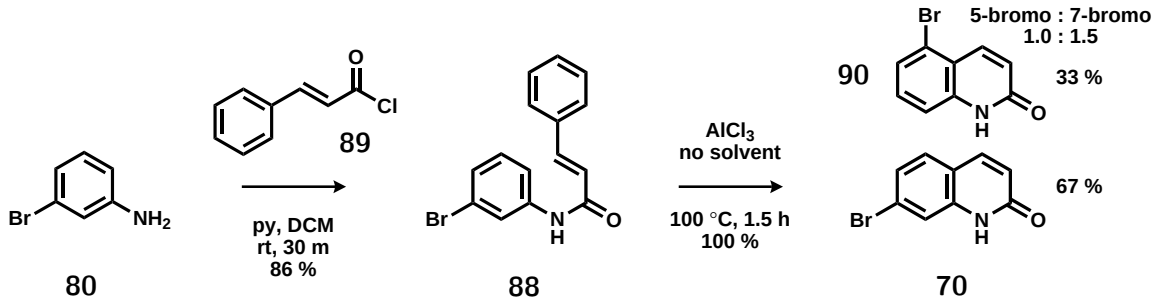

Scheme 2.11 Doebner-Miller synthesis of bromoquinolones **70** and **90**.

could be clearly distinguished from the 5-bromo isomer **90** in the NMR spectrum by the presence of a singlet corresponding to H8 of **70**, and a triplet corresponding to H7 of **90**.

A different procedure[104] was explored, which employed the same conditions except in a solvent of chlorobenzene. This also produced a 1.5:1 mix of isomers, although the product, a brown sludge, was harder to handle and purify than the solvent-free route, and so the former conditions were preferred.

The formation of two products from this reaction is easily rationalized by the reaction mechanism (Scheme 2.12).

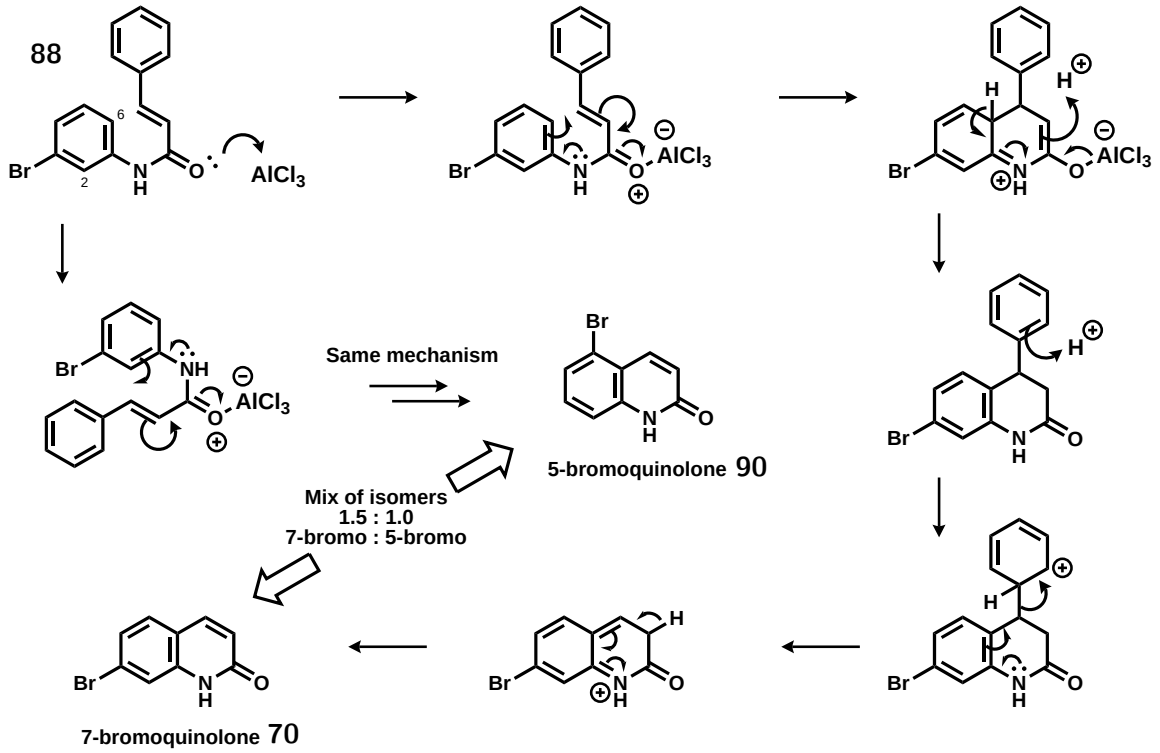

Scheme 2.12 Mechanism of the Doebner-Miller reaction.[102,103]

Activation of the amide carbonyl with $AlCl_3$ promotes a Friedel-Crafts cyclisation by the proximal benzene ring, which can occur at either C2 or C6 on compound **88**. The slight preference for

cyclisation to take place on the 6-position can be explained by the greater steric hindrance caused by the bromine when cyclisation takes place on the 2-position. The reaction is then completed by an acid-mediated loss of benzene, which leads to the observed quinolone products.

Many different solvent systems were investigated in an attempt to find a chromatography system in which the isomers could be separated. Unfortunately, analysis by TLC indicated an identical retention factor for both isomers in a range of solvent systems, so no attempt at chromatographic separation was performed at this stage. Recrystallization from EtOH did not improve the isomeric purity. The mix of isomers was therefore carried through to the next reaction.

Well-established methodologies were used to transform quinolone **70** into desired bromoquinoline **81**, ready for cross-coupling (Scheme 2.13). Treatment of the isomeric quinolones (**70** and **90**) with $POCl_3$[107,108] afforded isomeric chloroquinolines **96** and **97**. It was pleasing to discover that at this stage, unlike their quinolone predecessors, the isomers **96** and **97** could be separated by column chromatography. Interestingly, the 5-isomer **97** eluted from the column first, in the space of only a few fractions. In contrast, the desired 7-isomer **96**, despite starting to elute very soon after the 5-isomer, came off in a long streak over many fractions, nevertheless allowing it to be isolated cleanly.

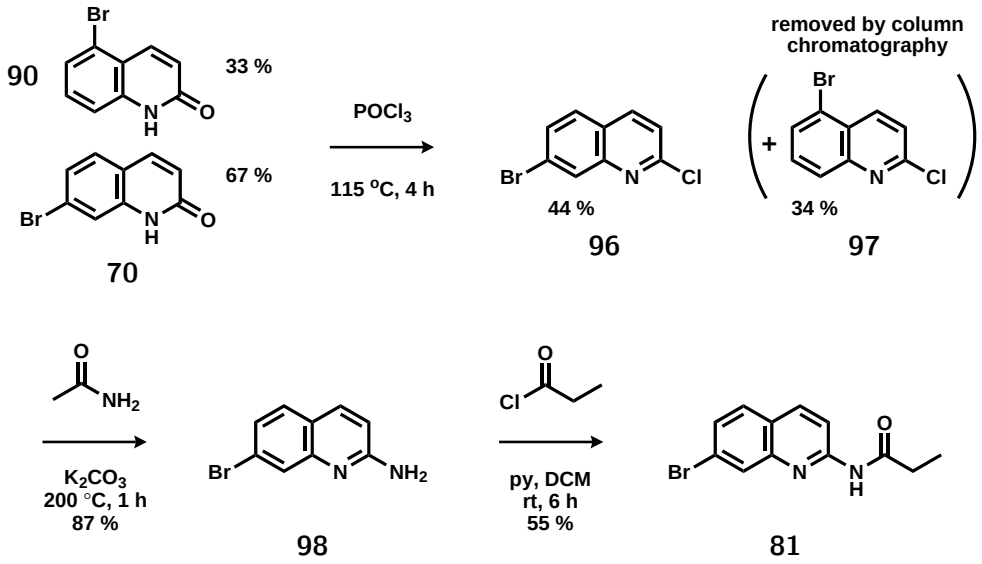

Scheme 2.13 Synthesis of bromoquinoline **81**.

Treatment of the isolated 7-bromoquinoline **96** with acetamide[109,110] provided aminoquinoline **98** in good yield. Subsequent reaction with propionyl chloride delivered the desired amide precursor **81** ready for Suzuki coupling.

2.3.2 Suzuki Coupling

Due to the presence of a Boc group on boronic acid **75**, the same conditions as for the successful Unit B Suzuki coupling were used for the synthesis of Unit D, employing $Pd(PPh_3)_4$ at 80 °C in toluene. Intriguingly, during an early attempt at this reaction, the Boc group reacted with the small amount of EtOH in the reaction. Despite many other Suzuki reactions being performed during the course of this project, this was the only time this occurred (Scheme 2.14). The unexpected modification of Unit D produced a compound, **99**, that still possesses exactly the same intended DAAD hydrogen-bonding array. It would therefore be perfectly viable for binding to Unit C.

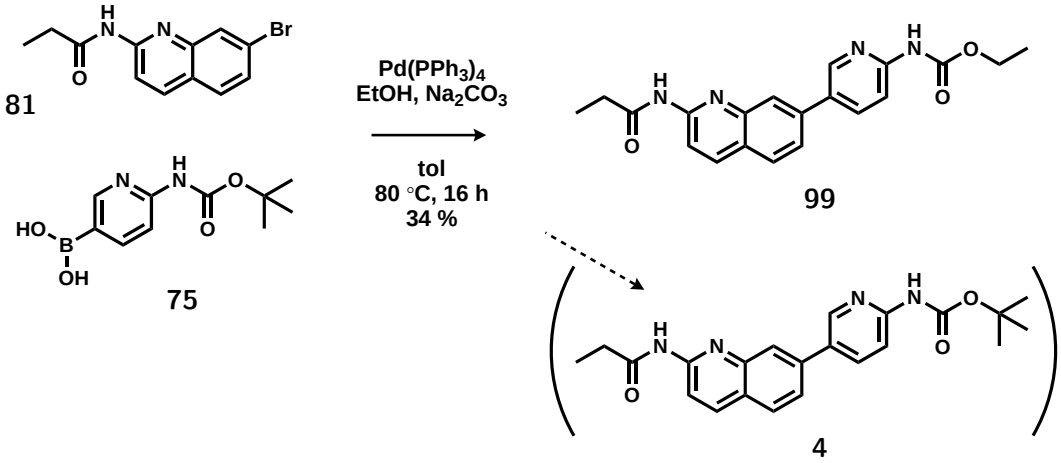

Scheme 2.14 Suzuki cross-coupling to make slight variant of Unit D, **99**.

The intended version of Unit D **4**, was successfully delivered in 57 % yield at 80 °C following further experiments (Scheme 2.15).

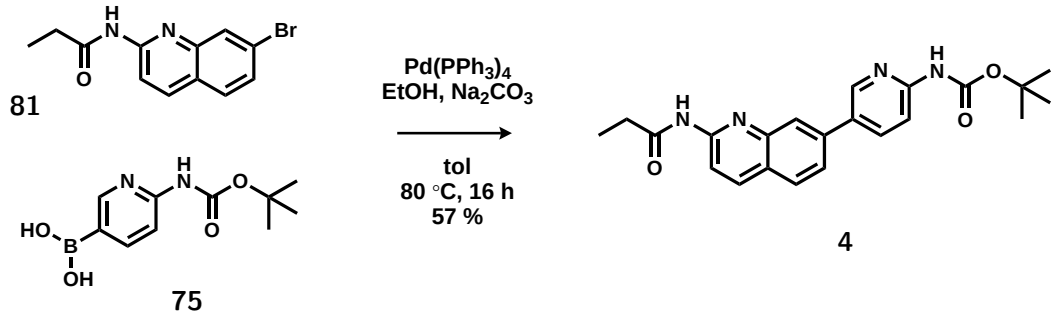

Scheme 2.15 Suzuki cross-coupling to make Unit D **4**.

2.4 Synthesis of Unit A

2.4.1 Bromopyridine Synthesis

With the aminopyridine-derived building blocks B and D now successfully synthesised, attention turned to the construction of the pyridone-derived architectures present in Units A and C. Due to a lack of literature precedent involving a direct coupling of 6-bromouracil with the corresponding boronic acid, a protecting group strategy was employed to mask the pyridone functionalities. It was proposed that brominated methoxy-protected derivative **100** and boronic acid **101** could be coupled to afford trimethoxy pyrimidine derivative **102** (Scheme 2.16). The methoxy protecting groups could then be removed from this key intermediate, thus unmasking the pyridone-uracil motif of Unit A **1**.

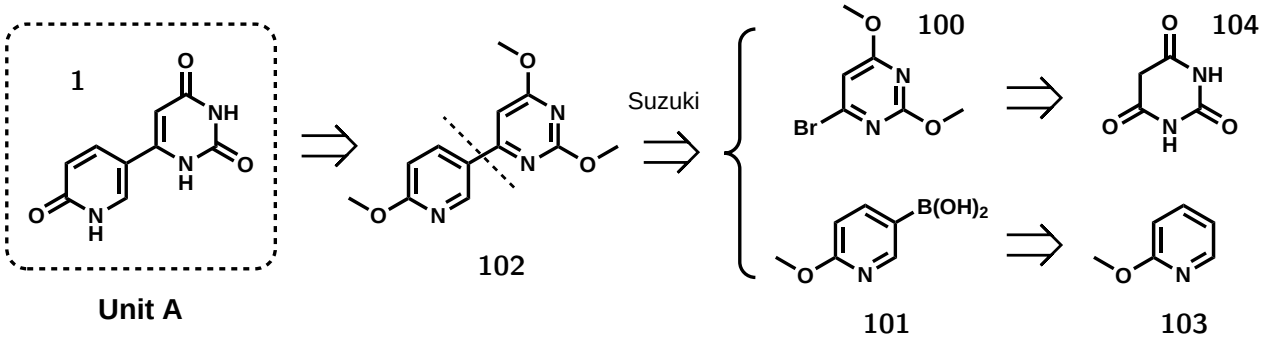

Scheme 2.16 Planned route towards Unit A **1**.

The synthesis of desired precursor 6-bromo-2,4-dimethoxypyrimidine **100** could be achieved in two steps from readily available barbituric acid **104** by following literature precedent[111] (Scheme 2.17).

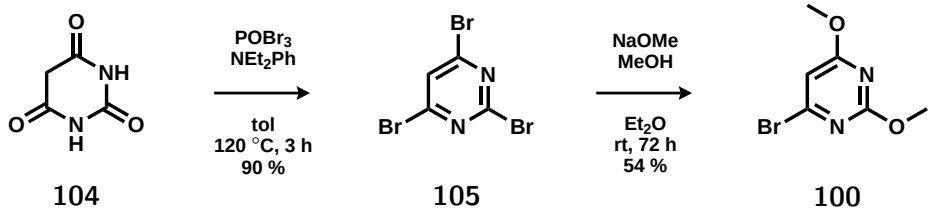

Scheme 2.17 Synthesis of bromopyrimidine coupling partner **100**.

Treatment of this commercially available starting material with $POBr_3$ in diethylaniline at 120 °C afforded tribromide **105** in a pleasing 90 % yield. Exposure of the tribromide to two equivalents of freshly prepared sodium methoxide led to the selective methanolysis of two of the bromide substituents, affording the targeted pyrimidine **100**. ^{1}H NMR spectroscopic analysis of the crude reaction mixture suggested that some mono-methoxy-substituted pyrimidine remained following this reaction, and this compound was subsequently isolated during purification by flash column

chromatography. Pleasingly, it was found that this undesired by-product could be then transformed to the desired bisubstituted pyrimidine **100** following resubmission to the reaction conditions.

2.4.2 Boronic Acid Synthesis

The desired boronic acid **101** could be reached in two steps, starting with commercially-available 2-methoxypyridine **103** (Scheme 2.18).

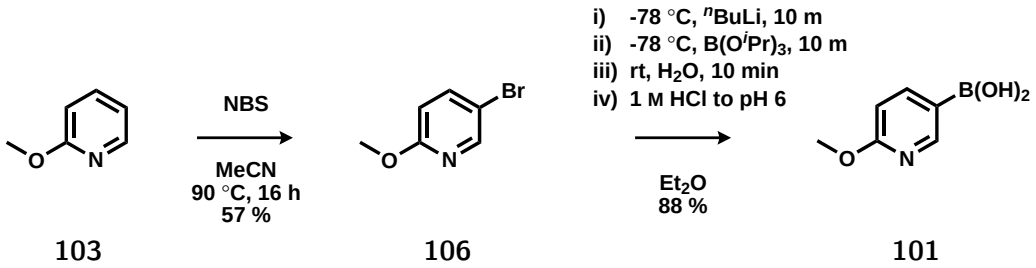

Scheme 2.18 Synthesis of boronic acid coupling partner **101**.

There was comprehensive literature precedent for the bromination of 2-methoxypyridine **103** and a procedure was chosen which produced **106** cleanly and in good yield.[97] Only the 5-substituted pyridine was formed, with the electron-donating methoxy group directing bromination to the 5-position as desired. These literature results were successfully repeated, providing **106** in 57 % yield.

As discussed earlier, we had previously developed an optimised procedure for the synthesis and isolation of pyridyl boronic acids, this methodology being employed during the synthesis of Unit B. The same conditions and aqueous precipitation procedure were employed to convert bromopyridine **106** into the desired boronic acid **101**. These conditions proved to be highly suitable here. Upon acidification of the aqueous phase, boronic acid **101** precipitated from solution as before, in an excellent 88 % yield.

We also prepared 2-chloro pyridyl boronic acid **107** following the same procedure (Scheme 2.19). This compound, once coupled with dimethoxypyrimidine **100**, would provide an alternative route to Unit A. It was proposed that the chlorine moiety could be subsequently displaced by methoxide in an S_NAr reaction, providing the trimethoxy precursor to Unit A.

2.4.3 Further Boronic Acid Studies

We now had economical access to boronic acid **101** (88 % yield) on the gram scale (Scheme 2.18). We therefore performed some experiments to determine the robustness of this boronic acid (Scheme 2.20).

The boronic acid was synthesised *via* our optimised route; quenching with water followed by stirring at room temperature, then removal of the Et_2O under reduced pressure. At this point, with

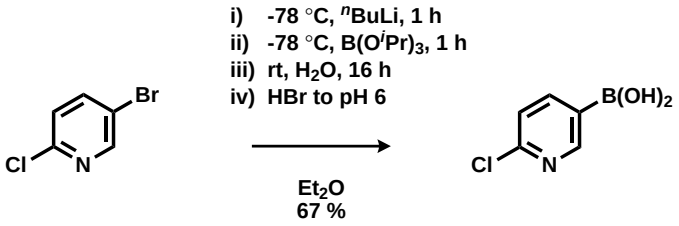

108 **107**

Scheme 2.19 Synthesis of boronic acid **107**.

an aqueous solution of high pH remaining, the solution was split into three. The first portion was acidified to pH 7 as normal, with the boronic acid **101** precipitating from the solution as before. The second portion was left at pH 14, concentrated, and then re-hydrated and acidified to pH 7. Once again, the boronic acid **101** precipitated from the solution as normal. The third and final portion was acidified to pH 2. The boronic acid **101** was observed to precipitate from the solution during this process, but completely redissolved again just before reaching pH 2. Upon re-basification to pH 7, it precipitated from the solution again and was isolated as normal.

These experiments indicated to us that the boronic acid **101** is a robust compound. It can withstand extremes of pH, but as long as it is returned to neutral pH, it can be easily isolated from aqueous solution by filtration.

We also wanted to know if the different forms of boronic acid **101** isolated at different levels of acidity could successfully perform a Suzuki coupling (Scheme 2.21). The three aqueous solutions described previously (at pH 14, 7 and 2) were directly submitted to the Suzuki coupling conditions following concentration *in vacuo*. For these investigations, bromobenzene **111** was employed as a coupling partner.

Pleasingly, all three experiments produced the desired product **112**. Notably, the highest yield obtained for this transformation was realised from the reaction in which the boronic acid derivative isolated at pH 14 was employed. In all three examples, the dimer **113** was noted to be a by-product, but the formation of this species was minimised when the aforementioned boronic acid derivative from the highly basic solution was acting as the coupling partner.

This was a very interesting result, and these experiments served to confirm that the boronic acid **101** is rather robust. This species could successfully Suzuki couple with an aryl bromide without the need for extensive prior purification. Simply concentrating the boronic acid solution in crude form under reduced pressure was sufficient, thus suggesting that a one-pot boronic acid synthesis/Suzuki coupling methodology could be developed.

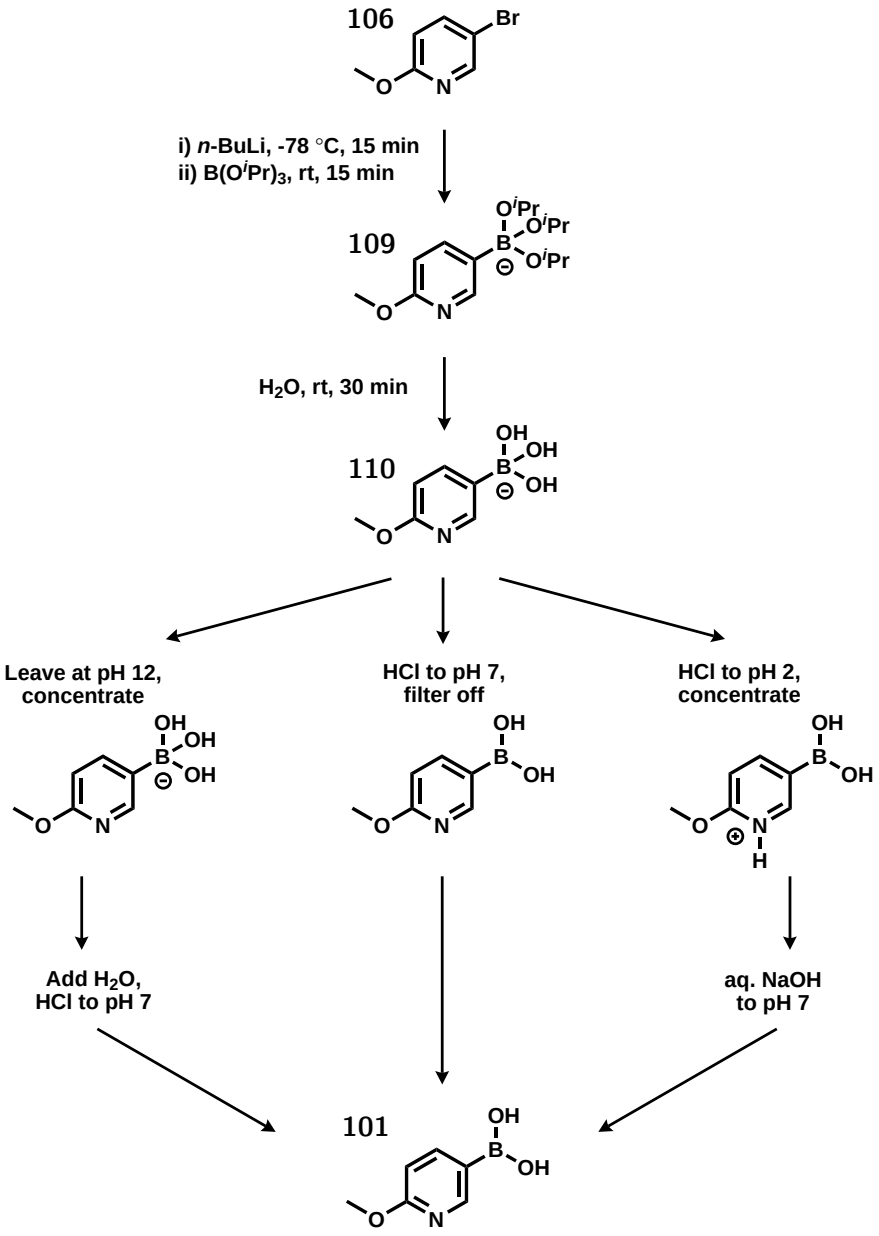

Scheme 2.20 Different routes towards boronic acid **101**.

2.4.4 Suzuki Coupling

The same conditions[101] that were used to cross-couple Units B and D also proved suitable for Unit A (Scheme 2.22). Due to the absence of a Boc protecting group, the coupling could be performed at 110 °C, affording Unit A precursor **102** in an acceptable 55 % yield following purification by flash column chromatography.

The same conditions[101] (at 80 °C) were also employed successfully to arrive at chlorodimethoxy biaryl **114** (Scheme 2.23). It was gratifying to observe that as expected, coupling took place exclusively on the bromine functionality as opposed to the chlorine. Furthermore, it was noted that palladium-catalysed dimerisation of the chloropyridine boronic acid **107** did not take place.

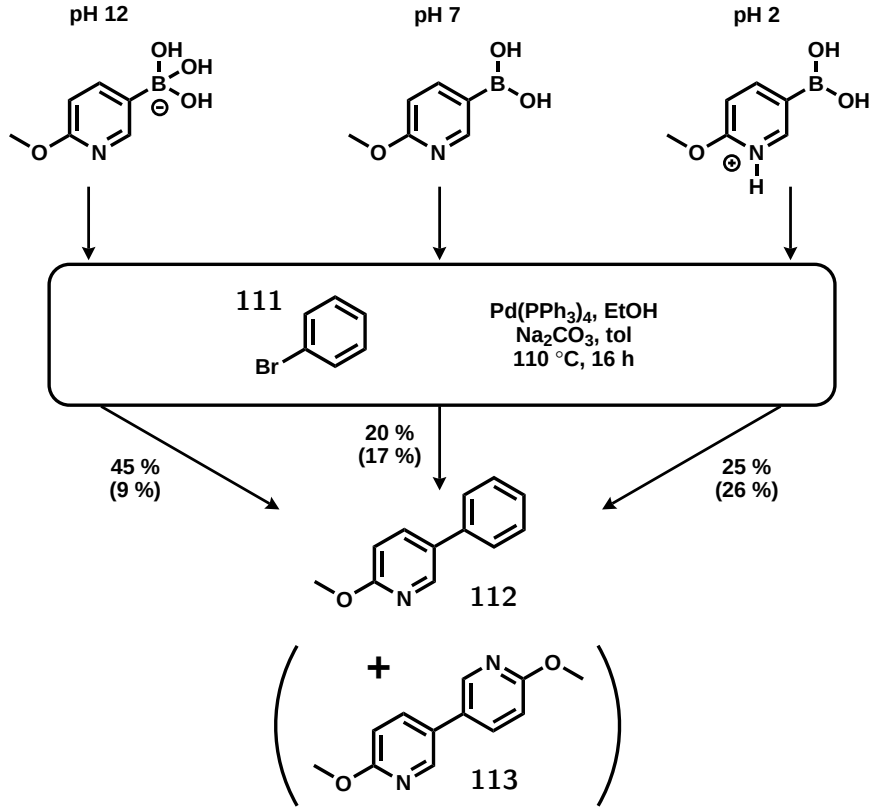

Scheme 2.21 Suzuki cross-couplings with different forms of boronic acid **101**.

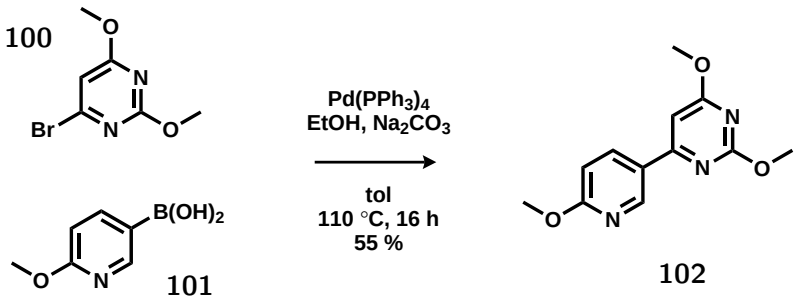

Scheme 2.22 Suzuki cross-coupling to make Unit A precursor **102**.

2.4.5 Deprotection

The final step to Unit A **1** was the deprotection of trimethoxybiaryl **102**. A wide variety of conditions to hydrolyse 2-methoxypyridines and dimethoxypyrimidines are known.[112–114] Two sets of conditions were chosen to attempt the concurrent deprotection of all three methoxy groups: aqueous concentrated hydrobromic acid in acetic acid at reflux;[115] and boron tribromide at room temperature.[112]

The hydrobromic acid-mediated conditions produced **1** in 47 % yield (Scheme 2.24). After several failed attempts, it was discovered that washing the crude reaction mixture with water and chloroform yielded the product in very high purity, as evidenced by ^{1}H NMR spectroscopic analysis (in DMSO-

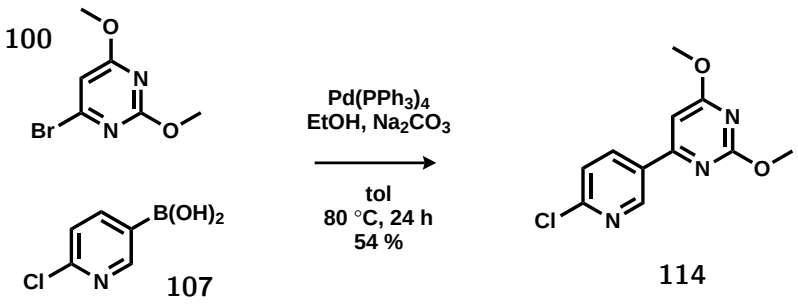

Scheme 2.23 Suzuki coupling of boronic acid **107** and bromide **100**.

d_6). In contrast, while spectroscopic analysis of the crude reaction mixture resulting from the boron tribromide conditions indicated the presence of Unit A, the desired compound was only present in very small quantities. Therefore, the hydrobromic acid-mediated deprotection methodology was preferred for the preparation of Unit A.

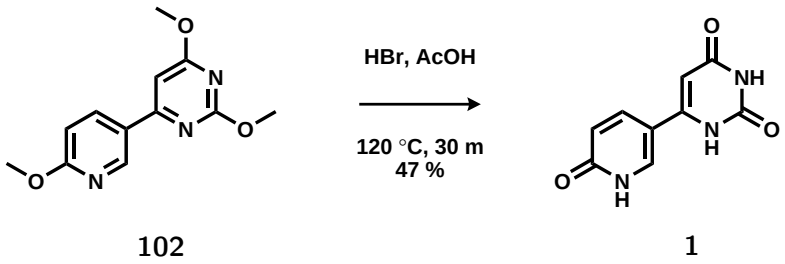

Scheme 2.24 Deprotection of trimethoxy biaryl **102** to afford Unit A **1**.

2.4.6 Binding to Unit B

It was extremely satisfying to have successfully synthesised our desired compound. However, it was equally disappointing to discover that Unit A was highly insoluble in all standard NMR solvents except DMSO-d_6. DMSO is used by biochemists to deliberately disrupt hydrogen-bonding between biomolecules, for example to denature DNA.[116,117]

At this juncture we had successfully synthesised the binding pair Units A and B, and were therefore in theory in a position to perform NMR binding experiments between them. We were however not optimistic about the success of such an experiment in DMSO, and our fears proved to be correct. Unit A was dissolved in DMSO in an NMR tube, and a total of two equivalents of Unit B was titrated in, 0.2 equivalents at a time. No change in the ^{1}H NMR chemical shift of the binding (N-H) protons of Unit A was observed, demonstrating that in DMSO at least, no interaction between Unit A and Unit B was taking place.

2.5 Synthesis of Unit C

2.5.1 Introduction

A Suzuki coupling was once again proposed as the key C–C bond-forming reaction for the synthesis of Unit C (Scheme 2.25). Fortunately, the desired bromine coupling partner, 5-bromouracil **78**, is commercially available at low cost. It was therefore only necessary to synthesise the boronic acid **79** in order to prepare for the Suzuki coupling.

2.5.2 Boronic Acid Synthesis

During the previous synthesis of Unit D, the desired bromoquinoline **70** had been successfully synthesised, albeit as a mixture of the inseparable 5- and 7-substituted isomers. From this starting point, it was proposed that the desired boronic acid **79** could be readily prepared in one step, although again as a mixture of isomers.

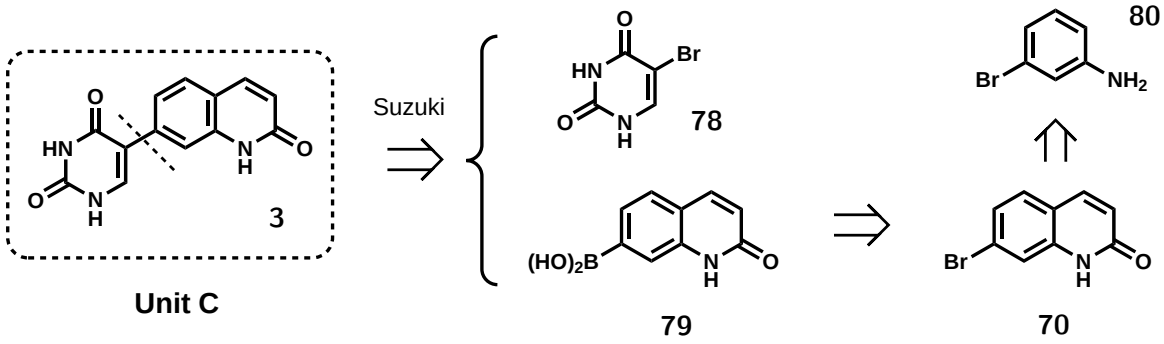

Scheme 2.25 Planned route towards Unit C **3**.

The same reaction and workup conditions, utilising the precipitation of the boronic acid from the aqueous phase as the pH was lowered to approximately 6, did indeed produce the desired boronic acid **79**, although in moderate yield of 21 % (Scheme 2.26). Despite many attempts, this reaction proved to be very difficult to repeat. Recovered material was mostly debrominated starting material, quinolone, suggesting that the bromoquinolone **70** was being lithiated, but was failing to trap the borate.

In similar fashion to quinoline isomers **96** and **97**, it was pleasing to note that the desired boronic acid 7-isomer **79** could be isolated from the undesired 5-isomer by flash column chromatography. None of the 5-substituted boronic acid isomer was isolated, suggesting the possibility that this isomer was not formed under these reaction conditions. It is proposed that the greater steric hindrance at the 5-position could have prevented the 5-lithium anion trapping the triisopropylborate.

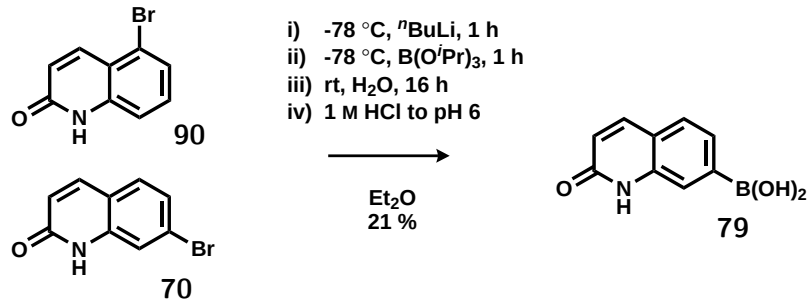

Scheme 2.26 Synthesis of quinolone boronic acid **79**.

2.5.3 Suzuki Coupling

The literature report that provided the successful Suzuki coupling conditions for the synthesis of the other three units contained a very similar transformation to that required to form Unit C **3**; the cross-coupling of a quinolone with an aryl halide.[101] As such, these conditions were again employed in an attempt to cross-couple aryl halide **78** with quinolone boronic acid **79** (Scheme 2.27).

The results were inconclusive. The crude product was extracted with EtOAc and the resulting ^{1}H NMR spectrum showed a complex product mixture. However, further spectroscopic analysis suggested the presence of a compound that did not correspond to either starting material or deborylated quinolone, suggesting that the desired product may have been present. The ^{1}H NMR spectrum was very messy and no definite conclusion could be drawn. Ultimately, however, this synthesis was not pursued further due to the solubility problems experienced with our other uracil- and pyridone-derived compounds.

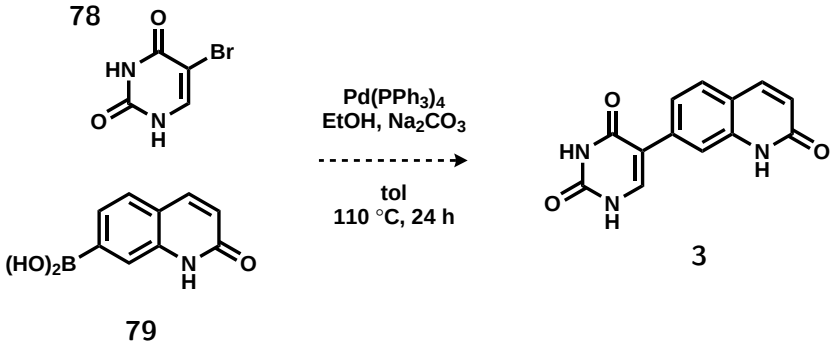

Scheme 2.27 Attempted Suzuki cross-coupling to synthesise Unit C **3**.

2.6 Bis-quinolone Modification

2.6.1 Introduction

The insolubility of Unit A in all common NMR solvents except DMSO-d_6 was a grave concern. It was of paramount importance to make a version of Unit A that dissolved readily in non-hydrogen-bonding solvents such as $CDCl_3$. In these solvents, the H-bond donor and acceptor functionalities of our proposed molecular building blocks can interact, and thus the specificity of binding between the four units can be realised. These interactions are of central importance to the entire philosophy behind the four-motif construction language. It was thus decided that the first-generation designs for Units A and C should be modified in an attempt to pursue these more desirable solubility properties.

2.6.2 Unit A – Bipyridone Architecture

The uracil motif in Unit A is especially polar and was therefore the subject of the first revision (Fig. 2.2). The uracil functionality was replaced with another 2-pyridone motif, resulting in a bipyridone design. The hope was that the removal of the highly polar uracil moiety would be enough to enable bipyridone **115** to dissolve in $CDCl_3$.

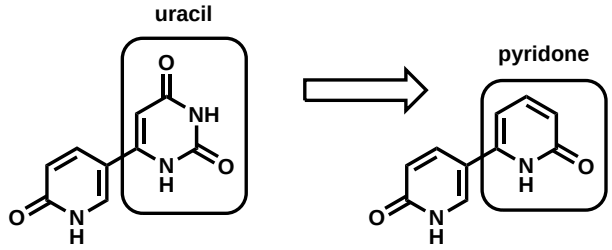

1 **115**

Fig. 2.2 Revision of old version **1** to new version **115** of Unit A.

2.6.3 Synthesis

The planned synthesis of Unit A **115** once again employed a Suzuki coupling as the key C–C bond-forming reaction (Scheme 2.28). With boronic acid **101** already in hand, this new route only required the synthesis of bromopyridine **116**.

Bromopyridine **116** was prepared in reasonable yield from readily-available 2,6-dibromopyridine **118** (Scheme 2.29).[118] A 2.8 M solution of NaOMe in MeOH was freshly prepared to limit the

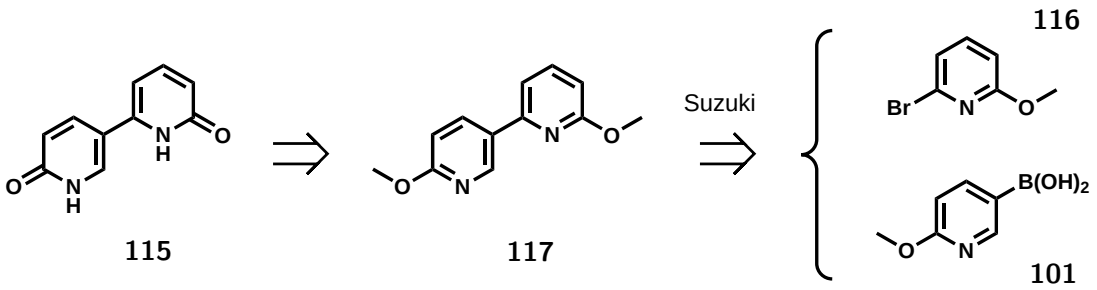

Scheme 2.28 Synthesis of Unit A **115**.

presence of water in this reagent. The product was easily isolated in good purity by extraction into Et_2O.

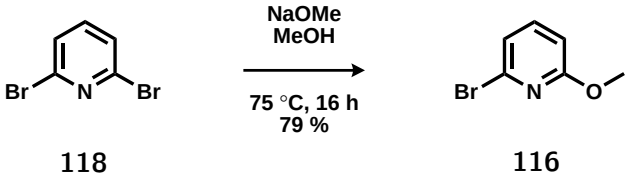

Scheme 2.29 Synthesis of 2-bromo-6-methoxypyridine **116**.

The same Suzuki coupling conditions as used before were again employed to couple bromopyridine **116** with boronic acid **101** (Scheme 2.30). The transformation proceeded in very good yield to afford the desired bipyridone **117**.

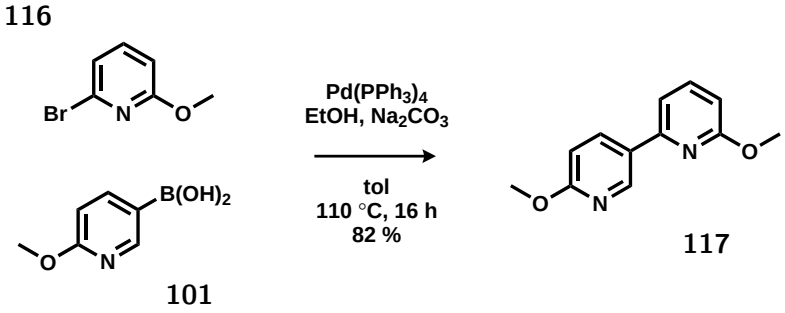

Scheme 2.30 Suzuki cross-coupling to afford bismethoxypyridine **117**.

2.6.4 Deprotection

Test deprotections on methoxypyridine **116** produced good results, using both our previously proven HBr/AcOH conditions, and the milder conditions of NaI and TMSCl in MeCN (Scheme 2.31).[112–114] The desired pyridone **119** was isolated in good purity and yield by a straightforward extraction into DCM. Strikingly, bromopyridone **119** was perfectly soluble in $CDCl_3$. This bode well for our new bipyridone design for Unit A **115**.

Thus, bismethoxypyrine **117** was successfully deprotected using the same hydrobromic acid

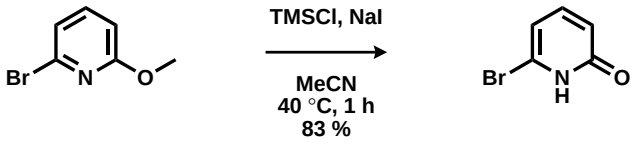

116 **119**

Scheme 2.31 Test deprotection of methoxypyridine **116**.

conditions as for the successful deprotection of trimethoxypyridine **102**. Bipyridone **115** was isolated in a reasonable yield of 65 % (Scheme 2.32).

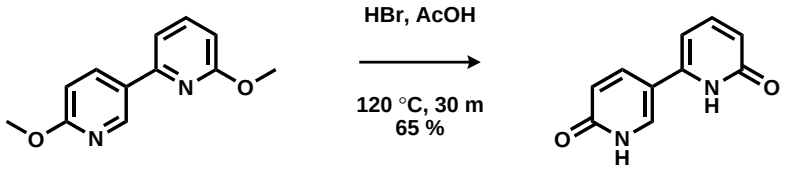

117 **115**

Scheme 2.32 Deprotection of bismethoxy biaryl **117** to afford Unit A **115**.

2.6.5 Solubility

Unfortunately, to our dismay, the newly-designed bipyridone Unit A **115** also proved to be highly insoluble in all standard NMR solvents except DMSO-d_6. This was a very disappointing result, especially given the solubility of bromopyridone **119** in $CDCl_3$. Clearly, much further work was required in order to synthesise a version of Unit A with desirable solubility properties.

2.7 Unit C – Pyridone/Quinolone

2.7.1 Redesign

As with the redesign of Unit A, the uracil motif in Unit C was replaced with a pyridone, resulting in a pyridone/quinolone design (Fig. 2.3). Again, the hope was that removal of the highly polar uracil motif would help the new Unit C design **120** to dissolve in $CDCl_3$.

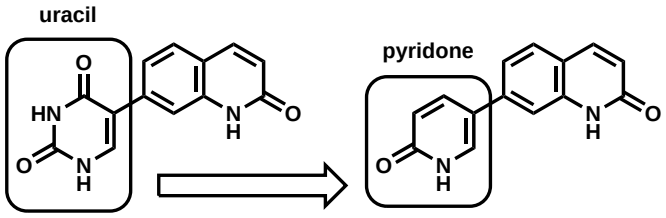

3 **120**

Fig. 2.3 Revision of old Unit C **3** to new Unit C **120**.

2.7.2 Synthesis

The precursors for the pyridone/quinolone version of Unit C were already synthesised – boronic acid **101** and bromoquinolone isomer mix **70** and **90**. It only remained to subject them to a Suzuki coupling (Scheme 2.33). Under our favoured conditions for non-Boc-protected compounds (110 °C), the coupling was successful. Luckily, the isomers **121** and **122** could be separated by flash column chromatography.

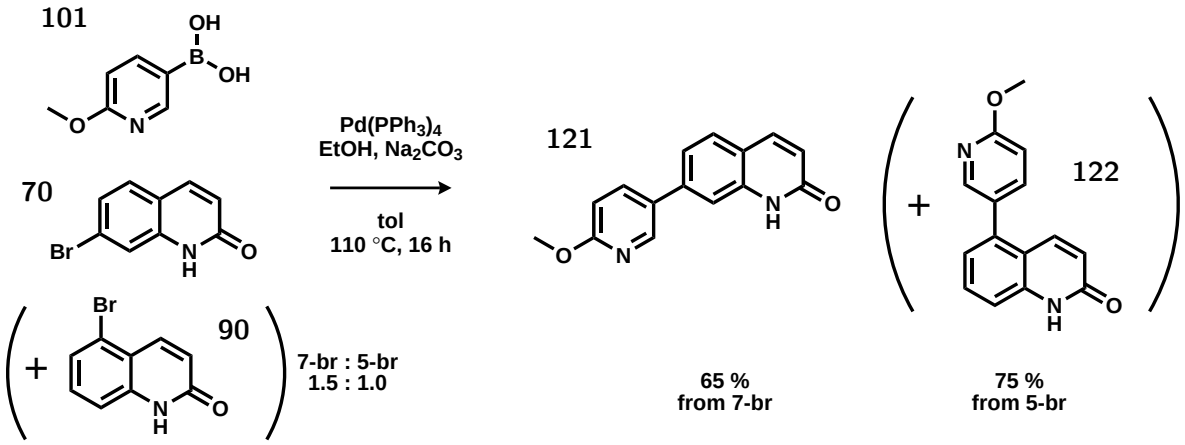

Scheme 2.33 Suzuki cross-coupling to make methoxy precursor to new Unit C **121**.

The synthesis of our target Unit C **120** now just required the deprotection of the methoxy group of **121**. Again, using the reliable acidic deprotection conditions, Unit C was isolated in 85 % yield (Scheme 2.34).

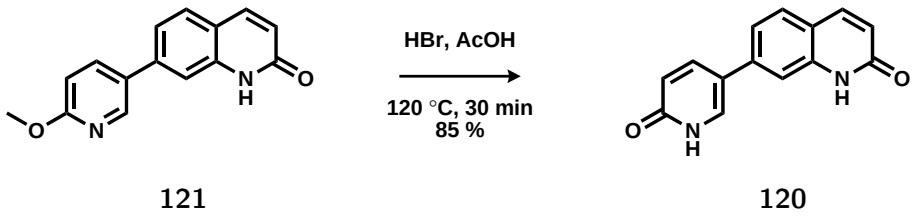

Scheme 2.34 Deprotection of methoxy **121** to yield Unit C **120**.

2.7.3 Solubility

As feared from our experiences with Unit A, this new version of Unit C was also soluble only in DMSO. So, as with Unit A, a new approach would be required to produce a version of Unit C that satisfies our solubility requirements.

2.7.4 Quinolone Single Isomer

As reported previously, 7-bromoquinolone **70** is synthesised as an inseparable isomer mix along with the 5-bromine isomer **90**. However, when treated with $POCl_3$, the resultant chloroquinoline isomer mixture of **96** and **97** could be separated on silica. Therefore, if the desired chloroquinoline isomer **96** could be hydrolyzed, it would provide an inelegant but effective method for synthesising pure quinolone isomer **70**.

We found that strong conditions were required, but the transformation was indeed possible (Scheme 2.35). Chloroquinoline **96** was stirred in a mixture of H_2SO_4 and water at reflux overnight. Pure quinolone **70** was isolated in 87 % yield on one occasion. However, the procedure proved very difficult to repeat. For this reason, and the fact that we had produced our desired units in isomerically pure form, this hydrolysis route was not pursued further.

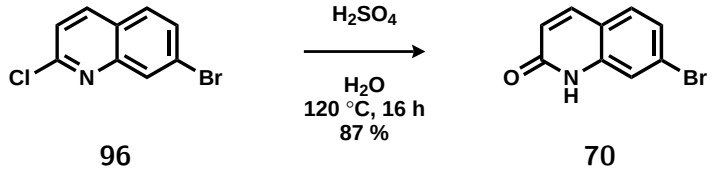

Scheme 2.35 Hydrolysis of chloroquinoline **96**.

3 Side-Chain Addition

3.1 Introduction

Replacing the uracil motif with an unsubstituted pyridone had made no difference to the solubility properties of Unit A. Our first plan to solve this problem involved the addition of a hydrocarbon side-chain to the bipyridone structure, in an attempt to increase the lipophilicity of the compound (Fig. 3.1).

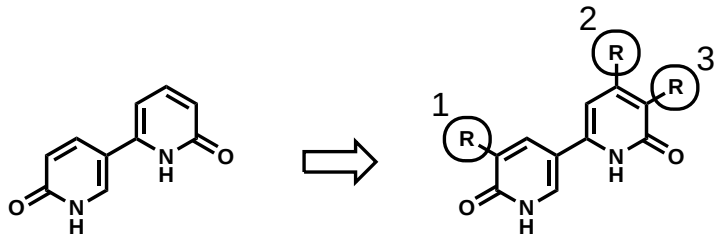

115 **123**

Fig. 3.1 Functionalisation of Unit A **115** with a hydrocarbon side-chain.

There are three positions on which a side-chain could be installed without causing significant steric interference between the two pyridine halves of the molecule, as shown on **123** in Fig. 3.1. Positions 2 and 3 would require the synthesis of either a 2,4-bromo- or a 2,5-bromo-6-methoxy pyridine. Such isomers are very synthetically challenging. Position 1 however requires the synthesis of a 3,5-bromo-2-methoxypyridine compound (Scheme 3.1), which is far more synthetically accessible. For this reason, position 1 was chosen.

3.2 Allyl Side Chain

Initial attempts were focussed on the addition of an allyl side-chain in order to improve the solubility properties of Unit A. The planned synthesis is shown in Scheme 3.1. With 6-bromo-2-aminopyridine **116** having been previously synthesised, we needed only to synthesise 3,5-dibromo-2-methoxypyridine **124**. Deprotection of **125** would afford desired bipyridone **126**.

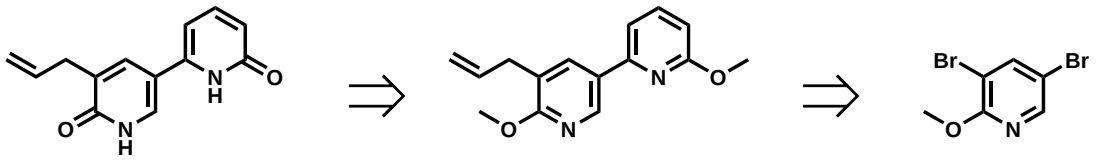

126 **125** **124**

Scheme 3.1 Synthetic strategy towards functionalised Unit A **126**.

3.2.1 Synthesis

During the synthesis of the original Unit A **1**, NBS was found to be a suitable reagent for the selective bromination of 2-methoxypyridine **103** at the 5-position (Section 2.4.2).[119] No further bromination was observed at the 3-position. In order to achieve the desired dibrominated compound **124**, the more electrophilic brominating reagent Br_2 was required.[120]

The desired transformation from **103** to **124** proceeded smoothly using an excess of Br_2 in the presence of sodium acetate in acetic acid (Scheme 3.2). A long reaction time was required, with some singly-brominated 5-bromo-2-methoxypyridine **106** still present after 40 hours. However, this undesired compound was isolated on the column and re-submitted, allowing the desired doubly-brominated product **124** to be isolated in reasonable yield.

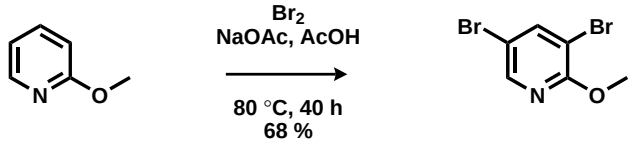

103 **124**

Scheme 3.2 Synthesis of 3,5-dibromo-2-methoxypyridine **124**.

3.2.2 Suzuki Test Reaction

Before proceeding further with the synthesis of the allylated variant of Unit A, we wanted to know how dibromopyridine **124** would behave under coupling conditions. If, for example, it demonstrated a strong preference to react at the 5-position, we could Suzuki couple at this stage without the need to perform any specific manipulations on either bromine first. We therefore performed a test coupling reaction between phenylboronic acid **85** and bromide **124** (Scheme 3.3). The reaction was performed at 115 °C and 80 °C, with slightly different results. In both cases, there was a mix of all three possible products and starting material, with coupling preferentially taking place at the 3-position. This is possibly due to the methoxy group directing insertion at the 3-position due to an inductive effect from the oxygen weakening the C-Br bond at the 3-position. At the lower

temperature the 5-position product was more favoured, but at only 21 %, certainly no way near high enough to make coupling at this stage a viable strategy.

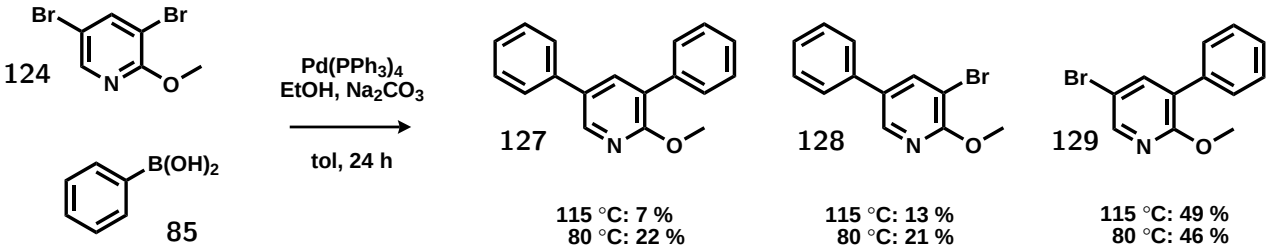

Scheme 3.3 Suzuki cross-coupling of phenylboronic acid **85** and bromide **124**.

3.2.3 Selective Lithiation

We hoped that the methoxy substituent would prove to be a good directing group for selective lithiation at the 3-position. If that were found to be the case, we could install the side chain first, and then Suzuki couple exclusively at the 5-position. Directed ortho-lithiation is a well-documented phenomenon,[121,122] but less so with methoxy directing groups.

One equivalent of *n*-BuLi was added to **124** in Et_2O at −78 °C. After stirring for a short time, an excess of allyl bromide was added. Pleasingly, these early experiments indicated that lithiation and trapping took place only at the 3-position, leaving the 5-position untouched. Utilising this simple procedure, initial experiments produced the desired allyl pyridine **130** in reasonable yields.

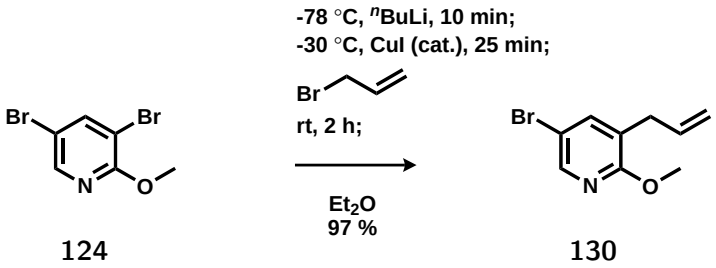

Scheme 3.4 Lithiation and trapping of bromopyridine **124** to afford allylpyridine **130**.

Further optimisation of the procedure produced **130** in nearly quantitative yields (Scheme 3.4). After the initial lithiation in diethyl ether at −78 °C, the temperature was raised to −30 °C. At this point, a catalytic amount of copper iodide was added, prior to the addition of the allyl bromide. Copper iodide is well-known to assist these types of lithiation and trapping,[123] by inserting into the C-Li bond to form a softer nucleophile, which is more reactive towards the allyl bromide electrophile. The use of catalytic copper iodide proved to be highly suitable in this case. The product **130** was isolated in high purity by quenching with water and extraction into diethyl ether, without the need

for column chromatography.

3.2.4 Boronic Acid Formation and Suzuki Coupling

Our optimised procedure for the formation of boronic acids had already worked very well for the production of precursors **75** and **101**. The same method, involving the precipitation of the product from aqueous solution upon reduction in pH, also proved ideally suited for the production of the desired boronic acid **131**. The compound was isolated in excellent yield (Scheme 3.5).

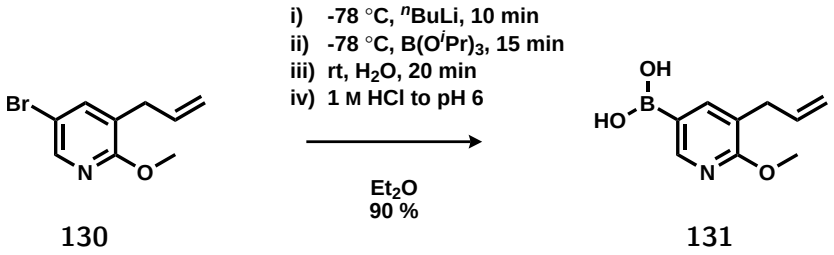

Scheme 3.5 Conversion of bromopyridine **132** into boronic acid **131**.

Gratifyingly, the subsequent Suzuki coupling proceeded smoothly under our favoured conditions to provide **125** in good yield (Scheme 3.6).

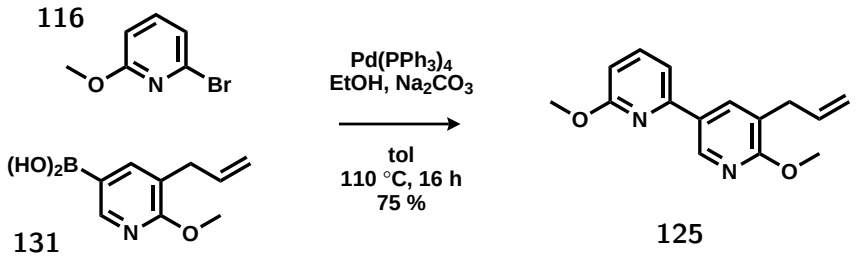

Scheme 3.6 Suzuki cross-coupling to afford bismethoxypyridine **125**.

3.2.5 Alternative Routes – Pyridone Suzuki Couplings

We performed a Suzuki coupling with boronic acid **131** and bromopyridone **119** to give methoxyallyl **132** (Scheme 3.7). This provided an alternative route towards bispyridone **126** (although the final deprotection to produce **126** was never successfully performed).

Another alternative route to the desired product was explored by converting pyridone **133** into the boronic acid **134** before coupling (Scheme 3.8). Our well-established isolation methodology proceeded well, affording boronic acid **134** in respectable yield.

The Suzuki coupling between the pyridone boronic acid **134** and pyridone **119** was less successful (Scheme 3.9). At every attempt only starting material was recovered.

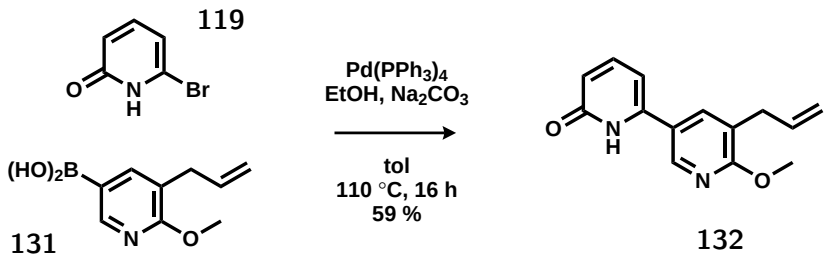

Scheme 3.7 Suzuki coupling of boronic acid **131** and bromopyridone **119** to give methoxyallyl **132**.

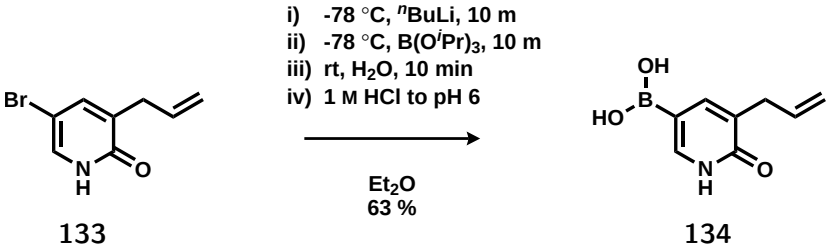

Scheme 3.8 Conversion of bromopyridone **133** into boronic acid **134**.

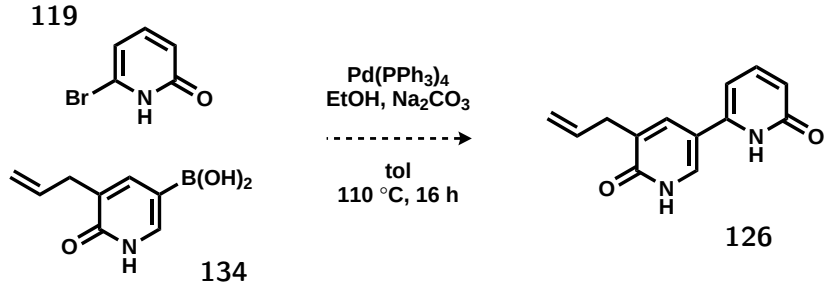

Scheme 3.9 Attempted Suzuki cross-coupling of pyridone boronic acid **134** and bromopyridone **119**.

3.2.6 Deprotection

We were now in a position to attempt deprotection of the two methoxy groups of allyl bipyridine **125**. Attempts were initially made on a small scale using both NaI/TMSCl and HBr/AcOH conditions. We were aware of potentially undesired reactivity due to the proximity of the allyl group to the pyridone.

The HBr/AcOH conditions proved to be too forcing, with none of the desired product being identified. Instead, a side-reaction had indeed taken place. ^{1}H NMR and mass spectroscopy analysis revealed the unintended product to be dihydrofuropyridine **135** (Scheme 3.10).

To our surprise, hydrofuran-forming cyclisations such as these had not previously been reported in the literature. We propose the mechanism for the formation of dihydrofuropyridine **135** in Scheme 3.11. Initially, the methoxy is hydrolysed, promoted by acid. The oxygen then cyclises onto the alkene, which attacks a proton. Loss of hydrogen from the nitrogen affords the product.

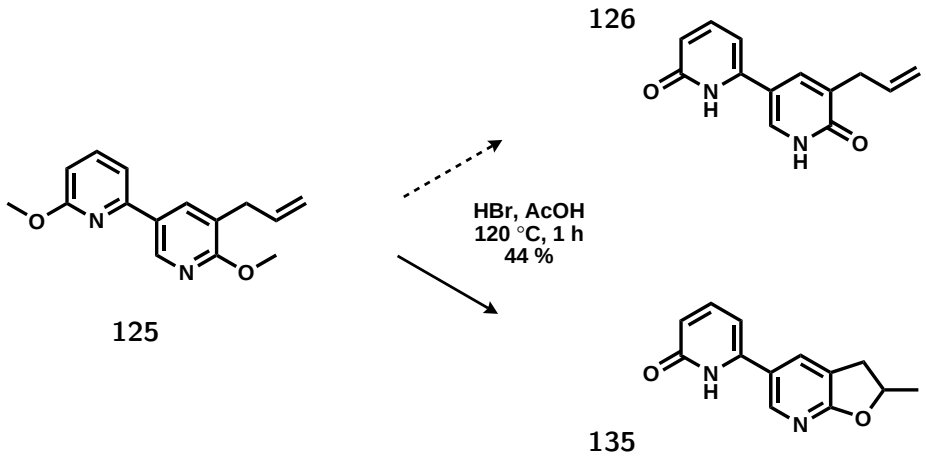

Scheme 3.10 HBr/AcOH attempted deprotection of bismethoxypyridine **125**.

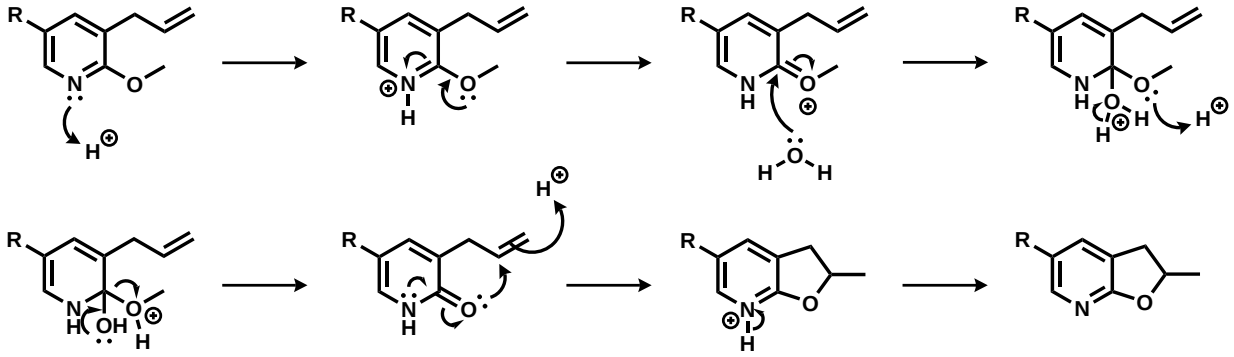

Scheme 3.11 Proposed mechanism during synthesis of hydrofuran **135**.

A number of test deprotections were therefore performed on bromopyridine **130** using the milder NaI/TMSCl conditions, at a variety of temperatures and times (Table 3.1).

The desired product **133** was isolated in 20 % yield at room temperature, 30 % at 40 °C, and 65 % at 50 °C. Pleasingly, the side-reaction observed with cyclised product **135** was not observed at these temperatures. Like bromopyridone **119**, allyl pyridone **133** was soluble in chloroform. Unlike with bromopyridone **119**, thanks to the disappointing solubility of the bipyridone variant of Unit A, this time we did not let this raise our expectations about the solubility of allyl Unit A too high.

Having established that the NaI/TMSCl conditions were able to successfully remove a methoxy group in the presence of adjacent allyl functionality, deprotection was performed on the bipyridine **125** using NaI/TMSCl at 50 °C, successfully producing the fully deprotected compound **126** (Scheme 3.12). Allylbispyridone **126** was soluble in CD_3CN and D_2O, but unfortunately not $CDCl_3$. Earlier experiments had established that performing the deprotection at room temperature produced the singly-deprotected product **138** (Scheme 3.13).

In an attempt to maximise the yield of the deprotection step and avoid complications with the allyl group, bismethoxypyridone **125** was hydrogenated to remove the terminal alkene first, and

Table 3.1 Deprotection of bromopyridine **130**.

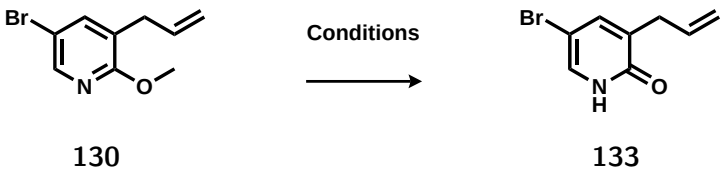

130 **133**

	Reagents	Temp.	Time	Yield	Comments
1	TMSCl, NaI	r.t.	90 min	20 %	Some SM remaining. No side-reaction observed.
2	TMSCl, NaI	40 °C	90 min	30 %	No side-reaction observed.
3	TMSCl, NaI	50 °C	60 min	65 %	No side-reaction observed.
4	TMSCl, NaI	50 °C	80 min	54 %	No side-reaction observed.

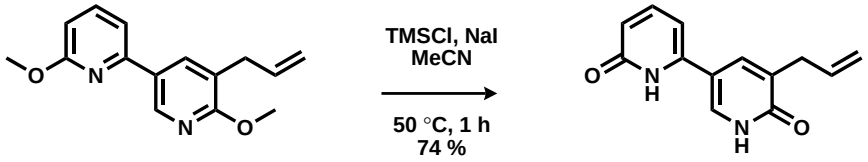

125 **126**

Scheme 3.12 Deprotection of bismethoxypyridine **125**.

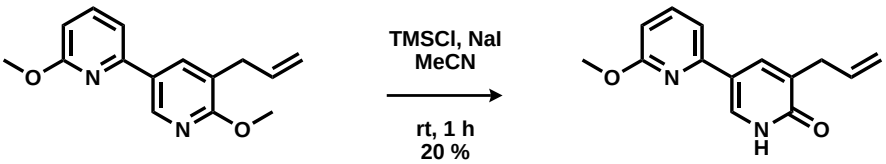

125 **138**

Scheme 3.13 Partial deprotection of bismethoxypyridine **125**.

then deprotected. Standard hydrogenation conditions of palladium on carbon in EtOAc were used, affording bismethoxypyridine **139** in 95 % yield (Scheme 3.14).

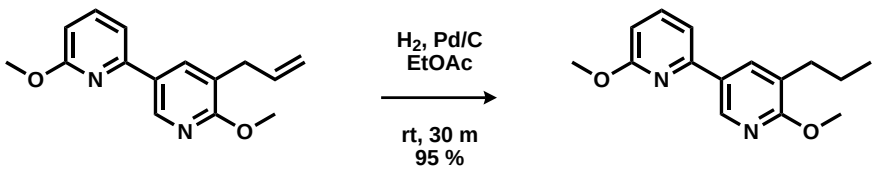

125 **139**

Scheme 3.14 Hydrogenation of bismethoxypyridine **125**.

The more forcing acidic conditions could now be used for the deprotection (Scheme 3.15). As expected, there was no side product such as **135** observed, and the product **140** was isolated in

good yield.

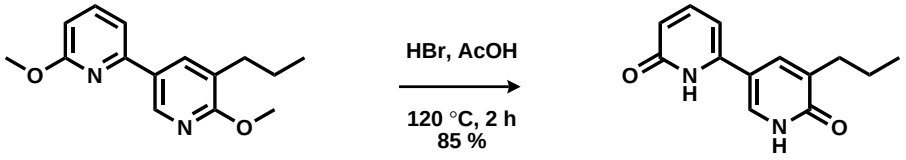

139 **140**

Scheme 3.15 HBr/AcOH deprotection of bismethoxypyridine **139**.

Like the allyl pyridone **126**, propylbispyridone **140** was soluble in D_2O. Disappointingly however, it was not soluble in $CDCl_3$.

3.2.7 Solubility

It was very disappointing that both the allyl pyridone **126** and propyl pyridone **140** variants of Unit A were both insoluble in $CDCl_3$. However, there was some consolation in the observation that allyl pyridone **126** was soluble in CD_3CN and D_2O, suggesting that some progress was being made, and thus we elected to further explore this solubilisation strategy.

3.3 Octyl Side-Chain

The addition of an allyl side-chain to bipyridone Unit A had marginally improved the solubility, allowing it to dissolve in CD_3CN and D_2O. We hoped that the addition of a longer side chain would improve the solubility further, to the point that it would dissolve in $CDCl_3$.

3.3.1 Triflate S_N2 Substitution Strategy

A more complicated strategy would be required for the addition of an octyl side chain. It was proposed that the appropriate aryl anion might be able to attack octyl triflate in an S_N2 reaction to provide direct access to an octyl-substituted derivative. With this strategy in mind, octanol **141** was triflated in an excellent yield of 96 % following a straightforward procedure[124] (Scheme 3.16). The product **142** was isolated in good purity by simple concentration of the crude reaction mixture under reduced pressure, with no need to employ chromatographic separation techniques.

Prior studies indicated that bromopyridine **124** could be selectively lithiated at the 3-position, so with dibromomethoxypyridine **124** in hand the same lithiation procedure was employed. Repeated attempts to trap the triflate **142** with the aryl anion of pyridine **124** were unsuccessful (Scheme 3.17). However, in every instance only purely quenched material, 5-bromo-2-methoxypyridine **106**, was

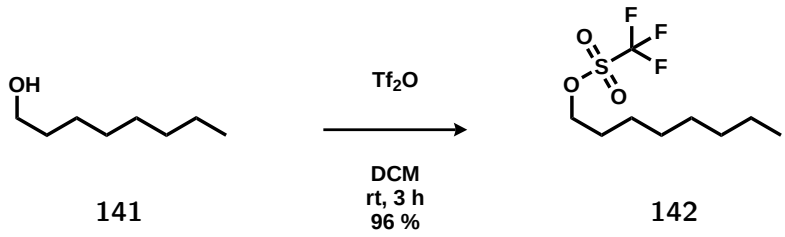

Scheme 3.16 Triflation of octanol **141**.

isolated. This result indicates that the bromopyridine **124** was lithiating successfully, but not reacting with the triflate.

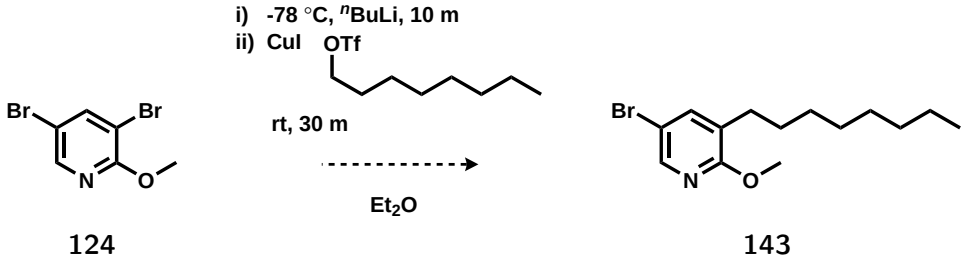

Scheme 3.17 Attempted octylation of bromopyridine **124** with triflate **142**.

3.3.2 Octanal

Following the failure of the octyl triflate to react with the lithiated derivative of bromomethoxypyridine **124**, we elected to employ an alternative electrophile, octanal (Scheme 3.18). Octanal was selected not only for its ready availability, but also for the considerations that the resulting product **144** would contain an alcohol, which could be subsequently eliminated to afford an alkene, and that further derivatisation of the alcohol would be possible. This alkene could then be hydrogenated as before to yield the desired octyl side-chain. To our delight, octanal proved to be a reliable electrophile for this reaction, with the pyridyl alcohol **144** being isolated in a reasonable 62 % yield.

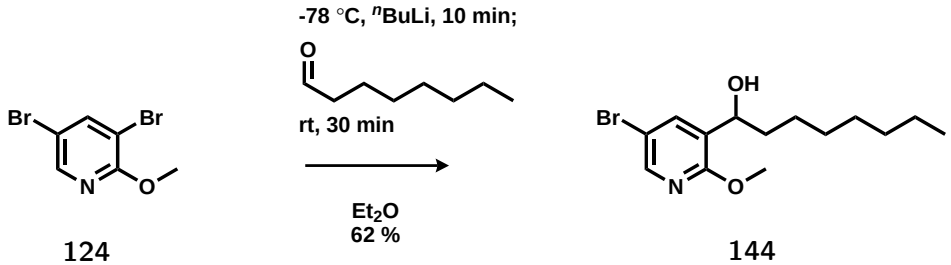

Scheme 3.18 Lithiation and trapping of **124** with octanal.

The next step was elimination of the nascent alcohol functionality to provide alkene **145**. This transformation proved to be more challenging than expected. Extremely forcing conditions were

necessary in order to achieve this transformation from the free alcohol **144**, with this precursor being subjected to treatment with H_2SO_4 and water at reflux for 90 minutes (Scheme 3.19). Using this methodology, yields better than 40 % could not be achieved.

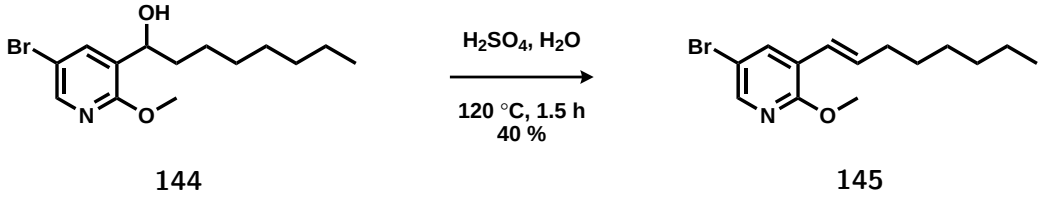

144 **145**

Scheme 3.19 Elimination of alcohol **144** by refluxing in H_2SO_4.

Given these disappointing results, it was proposed that the mesylated derivative **146** would be a better precursor for this elimination step. We were pleased to note that alcohol **144** could be successfully mesylated under standard conditions[125] (Scheme 3.20). However, the product **146** proved to be unstable, degrading to both the original alcohol and the eliminated alkene **145** during purification by flash column chromatography. It was possible that the mesylate was being hydrolysed to produce the alcohol. Despite this limitation, a yield of 42 % was achieved for the synthesis of **146** by employing a short column, but it should be noted that ^{1}H NMR analysis of the crude reaction mixture suggested that this mesylation reaction was proceeding in quantitative yield.

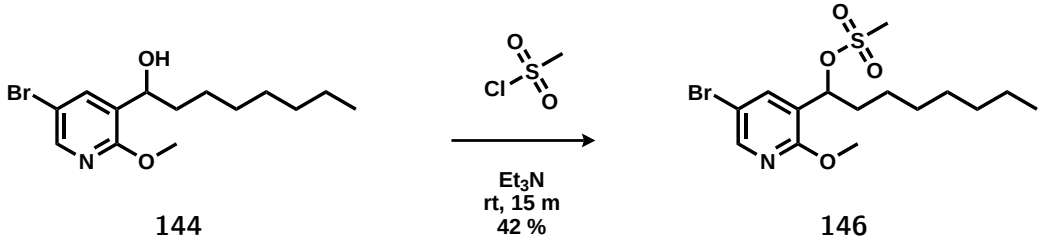

144 **146**

Scheme 3.20 Mesylation of alcohol **144**.

With mesylate **146** in hand, our investigations now focussed upon uncovering an appropriate protocol for the elimination of this precursor to the alkene **145**.[126,127] The instability of mesylate **146** on silica gel would suggest that elimination to the alkene would be straightforward, but this did not prove to be the case. The best conditions found were 100 °C in Et_3N overnight, which produced alkene **145** in only 46 % yield (Scheme 3.21). This was surprising, especially given the instability that the mesylate **146** demonstrated on silica.

Despite the disappointing yields obtained for both elimination strategies, the desired alkene **145** was successfully synthesised, and thus further optimisation of this methodology was postponed in favour of proceeding with the synthesis of our modified variant of Unit A.

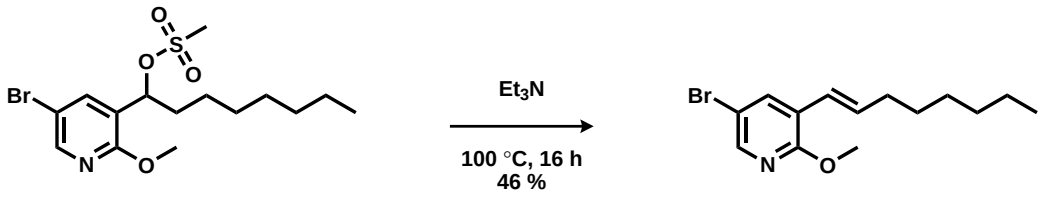

146 **145**

Scheme 3.21 Elimination of mesyl pyridine **146** by refluxing in Et_3N.

3.3.3 Hydrogenation

At this juncture, a number of appropriate synthetic strategies were apparent. The alkene could be hydrogenated at the end of the synthesis, just prior to deprotection, but equally it could also be removed prior to coupling. In order to investigate the latter approach, we subjected alkene **145** to standard hydrogenation conditions[128–130] in MeOH. Unfortunately, this hydrogenation protocol removed the bromine as well as the alkene, affording methoxypyridine **147** in excellent yield (Scheme 3.22). It was proposed that this result may have arisen due to the enhanced lability of the C-Br bond when positioned *para* to an electron-donating methoxy substituent.

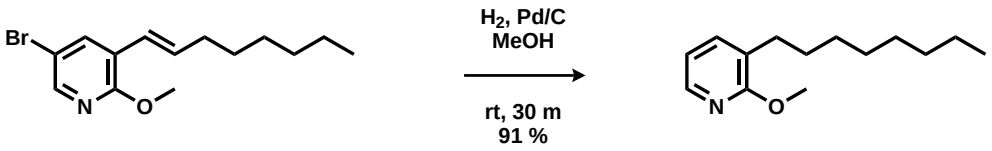

145 **147**

Scheme 3.22 'Double-hydrogenation' of alkene **145**.

3.3.4 Boronic Acid Synthesis

As a result of the observed debromination under hydrogenation conditions, it was decided to postpone the hydrogenation step until after the planned Suzuki cross-coupling. In preparation for this step, alkene **145** now had to be transformed into boronic acid **148** (Scheme 3.23). The previously detailed reliable aqueous precipitation conditions were attempted. After quenching the Et_2O with water, the phases were separated as normal and the aqueous (pH 12) phase acidified to pH 7. However, to our surprise, no product precipitated from solution upon acidification. Instead, concentration of the organic phase yielded the desired boronic acid **148** in excellent yield. It appears that the long octyl chain was aiding transfer of the product into the organic phase even at pH 12.

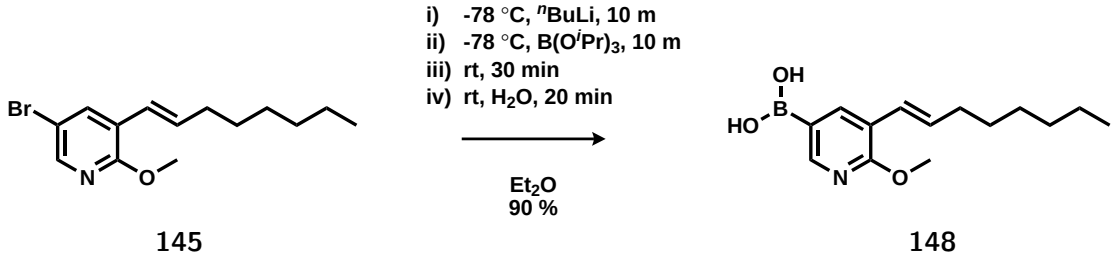

Scheme 3.23 Formation of boronic acid **148** from bromide **145**.

3.3.5 Suzuki Coupling

We were now ready to perform the Suzuki coupling between aryl bromide **116** and boronic acid **148**. Once again, our favoured coupling conditions proved reliable, providing the bipyridine **149** in excellent yield (Scheme 3.24).

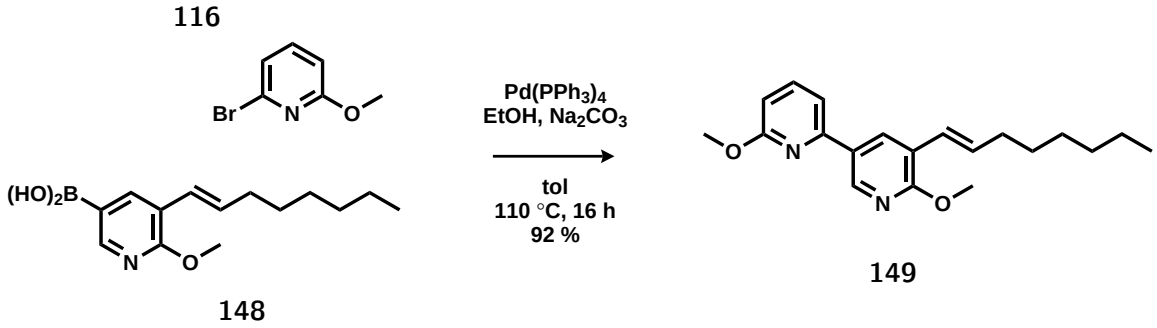

Scheme 3.24 Suzuki cross-coupling to afford bismethoxypyridine **149**.

At this point we could have employed the NaI/TMSCl conditions to deprotect bipyridine **149** in the presence of the neighbouring alkene side chain. However, it was thought that there would likely be little difference between the solubility properties of the fully saturated octyl compound and the unsaturated alkene derivative **149**. We therefore chose to only synthesise the fully saturated compound, and thus hydrogenated alkene **149** under the conditions used previously. To our delight, bispyridine **150** was isolated in excellent yield. The subsequent deprotection step in the presence of HBr and AcOH was straightforward, and proceeded in acceptable yield to afford our target compound, bispyridone **151** (Scheme 3.25).

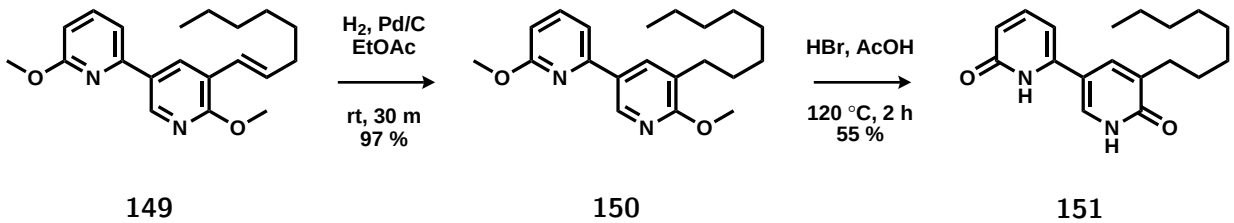

Scheme 3.25 Hydrogenation and deprotection of alkene **149**.

3.3.6 Solubility

Frustratingly, despite the presence of a long, lipophilic octyl side-chain, octylbispyridone **151** was completely insoluble in $CDCl_3$. Given this result, we were beginning to wonder if any side-chain would enable a bipyridone to dissolve in this solvent. To investigate these fears further, we coupled bromide **145** with the boronic acid **148** of itself (Scheme 3.26). This would provide a compound with two octyl chains whose solubility in $CDCl_3$ could be investigated following the requisite hydrogenation and deprotection of this bipyridone precursor.

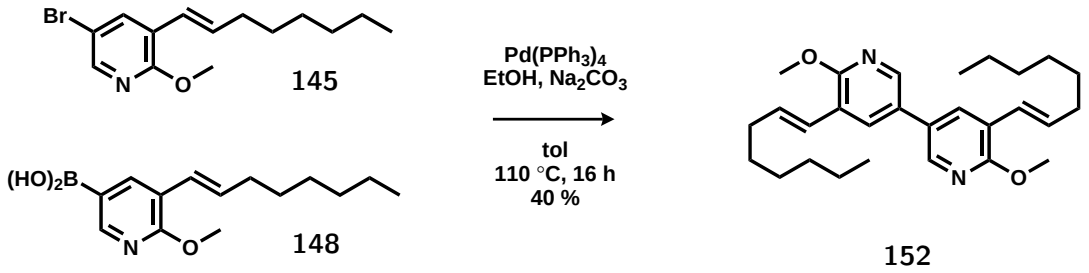

Scheme 3.26 Suzuki cross-coupling of bromide **145** with the boronic acid of itself, **148**.

The hydrogenation and deprotection (Scheme 3.27) both proceeded smoothly to provide bipyridone **153**. Gratifyingly, it was perfectly soluble in $CDCl_3$. Finally, we had demonstrated that with sufficiently large side-chains, a compound containing our desired bipyridone architecture could be dissolved in $CDCl_3$. We therefore set about synthesizing versions of Unit A that contained larger and more greasy groups.

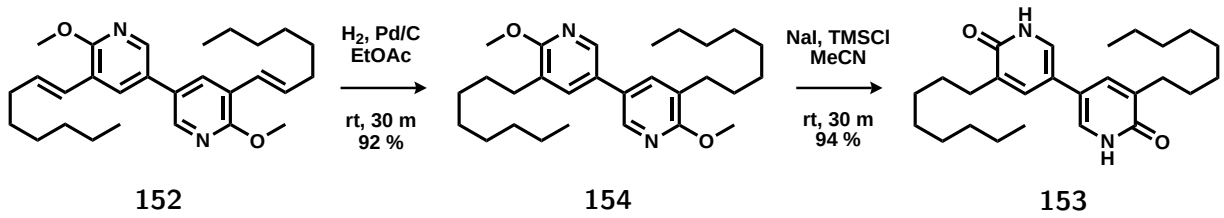

Scheme 3.27 Hydrogenation and deprotection of bisalkene **152**.

3.4 Alternative Side Chains

3.4.1 Hydroboration

Installation of a number of alternative side chains were concomitantly investigated, utilising the allyl group of previously synthesised precursor **130** as a synthetic handle. It was hoped that building a small library of substituted compounds would greatly assist our search for a variant of Unit A

with desirable solubility properties. Hydroboration[131–134] of the allyl group was an immediately attractive strategy, as it would provide a terminal alcohol functionality at which a solubilising group could be added (Scheme 3.28). Using borane dimethyl sulfide complex and hydrogen peroxide work-up, a yield of 42 % was achieved for this transformation. While reactions involving the use of 9-BBN as a hydroborating agent were also successful, the yields were inferior.

With the desired alcohol functionality now in place, benzyl bromide was successfully reacted with compound **155**, this step being mediated by NaH (Scheme 3.28).

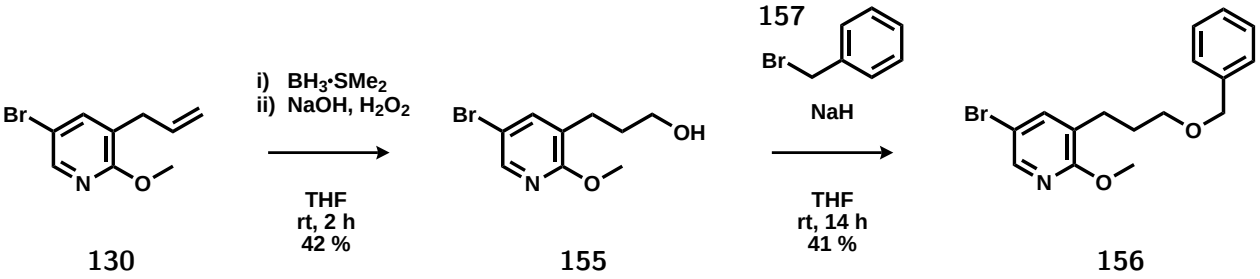

Scheme 3.28 Hydroboration and benzyl protection of allyl pyridone **130**.

In order to investigate whether deprotection of the pyridone could be successfully achieved in the presence of a benzyl group, pyridine **156** was subjected to a small range of appropriate conditions. Attempts using the acidic HBr/AcOH conditions were successful in removing the methyl, but also removed the benzyl group. The deprotection of methoxypyridine **156** with NaI/TMSCl was more successful. The masking methoxy group was removed as desired, while the benzyl group remained intact (Scheme 3.29). Gratifyingly, the resulting pyridone **158** was soluble in $CDCl_3$.

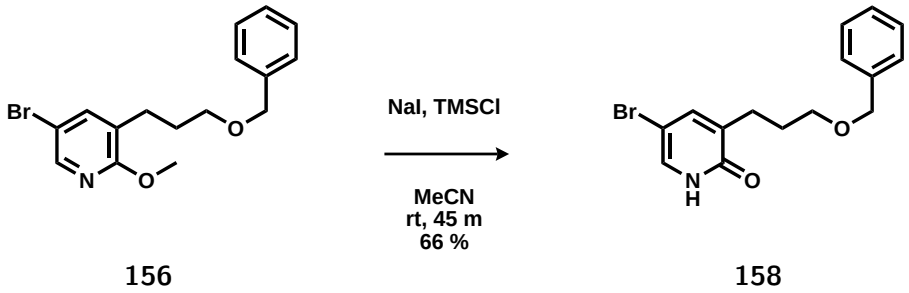

Scheme 3.29 Deprotection of methoxypyridine **156**.

3.4.2 Grubbs Cross-Metathesis

Once again utilising the allyl functionality of subunit **130**, it was proposed that Grubbs cross-metathesis methodology[135,136] could be used to further extend the side chain of Unit A.

TBS alkene **159** was chosen as coupling partner with allyl pyridone **130** due to its ready availability and TBS group, which is well-known to aid with organic solvent solubility (Scheme 3.30). Based on

literature precedent,[137,138] the Grubbs II catalyst was employed for this transformation, affording compound **160** in a modest 32 % yield, with 28 % starting material returned. The *E*:*Z* ratio was 3:1. We also attempted a cross-metathesis between allyl pyridone **130** and unprotected 3-buten-1-ol **161** (Scheme 3.30). Again, the obtained yield of 26 % for **162** was disappointingly low, with the starting material returned in a 39 % yield. A 3:1 *E*:*Z* ratio was observed for this transformation. A possible reason for the low yields is the presence of the methoxy group, which can coordinate to the Ru catalyst. Methyl acrylate **163** was proposed to be an alternative and attractive cross-metathesis partner, as the ester moiety could subsequently be utilised in a transesterification reaction. Thus, a cross-metathesis was performed between allyl pyridone **130** and methyl acrylate **163** (Scheme 3.30). The reaction was successful, affording ester **164** in a 42 % yield and thus further extending our library of potential side chains.

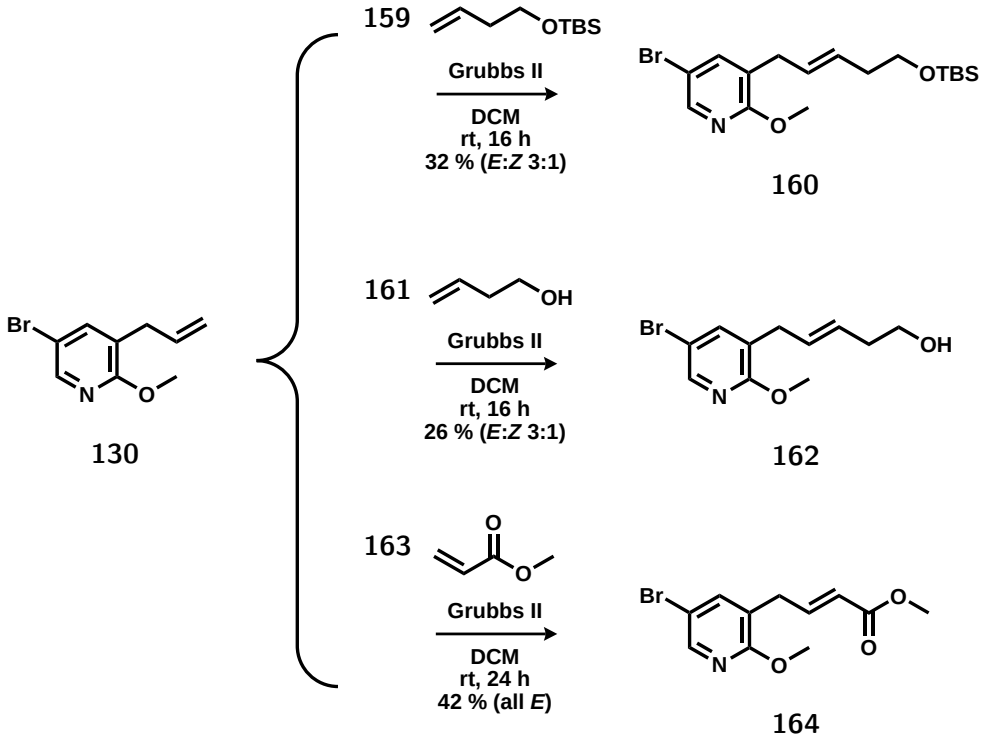

Scheme 3.30 Grubbs cross-metathesis between allyl pyridone **130** and TBS alkene **159**, butenol **161**, and methyl acrylate **163**.

3.4.3 Side Chain Extension of Allyl Bipyridines

The aforementioned cross-metathesis strategy was also investigated for allyl bipyridine **125**. This previously synthesised precursor was reacted with readily-available 3-buten-1-ol **161** (Scheme 3.31), providing a terminal alcohol on which further modifications could be performed. The resulting product **165** was obtained in a 29 % yield, however 33 % of the starting material was recovered. A

3:1 *E*:*Z* ratio was observed for this reaction.

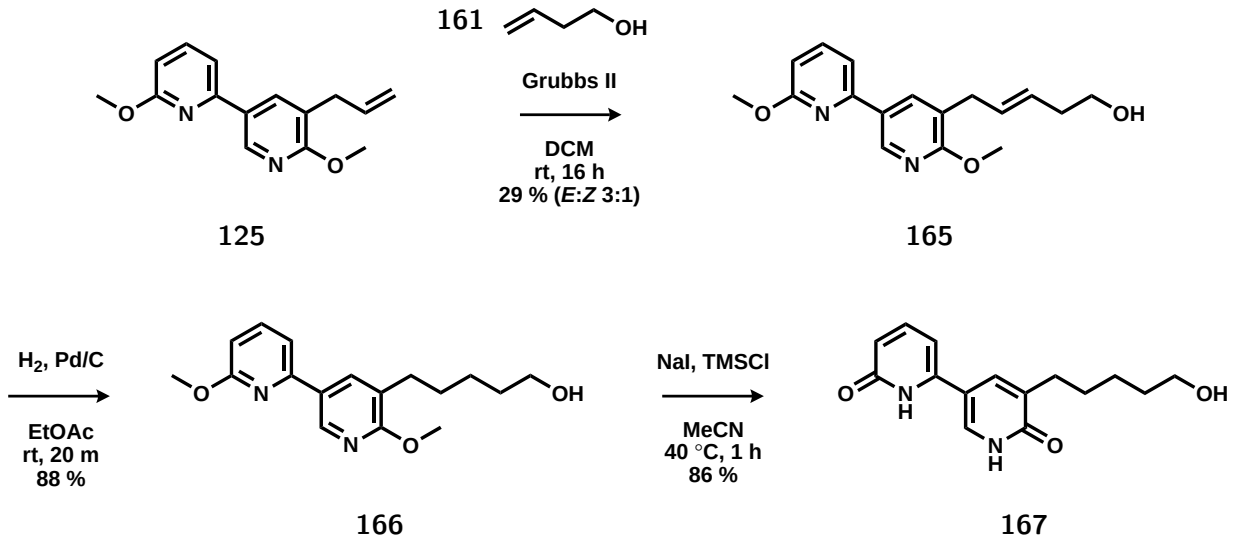

Scheme 3.31 Grubbs cross-metathesis between allyl bipyridone **125** and 3-buten-1-ol **161**, followed by hydrogenation and deprotection.

The alkene functionality of alcohol **165** was subsequently hydrogenated in 88 % yield under the same hydrogenation conditions as previously utilised (Scheme 3.31).

Bismethoxypyridine **166** was then smoothly deprotected in the presence of NaI and TMSCl (Scheme 3.31). Only the desired product was isolated, suggesting that the free primary alcohol moiety present was not acting to hinder the deprotection. As expected, bipyridone **167** was only soluble in DMSO.

Investigation of an alternative side chain derivative saw the initial protection of the primary alcohol functionality prior to deprotection. We selected the TBS group as it is well-known to help compounds dissolve in less polar solvents.

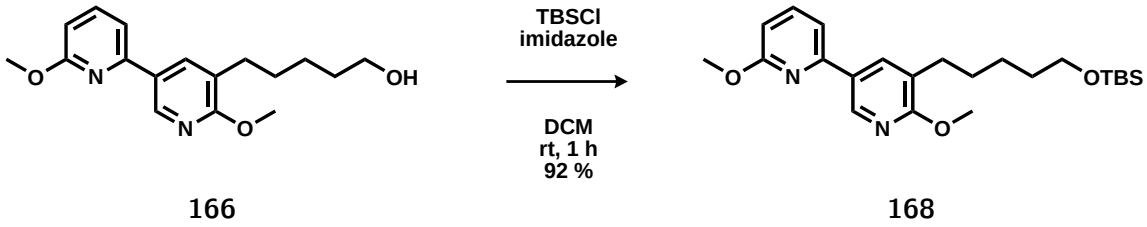

Scheme 3.32 TBS protection of alcohol **166**.

However, the primary silyl ether moiety of compound **168** was thought to be a potentially delicate functionality, and thus the milder (NaI/TMSCl) deprotection conditions were employed on TBS-protected bismethoxypyridine **168** (Scheme 3.33). Disappointingly, none of the desired compound **169** was isolated. Instead, both TBS-deprotected bismethoxy **166** and TBS-deprotected and methoxy-deprotected bipyridone **167** were isolated. This shows that the TBS alcohol as a

solubilising group along with the methoxy deprotection route was not a viable combination.

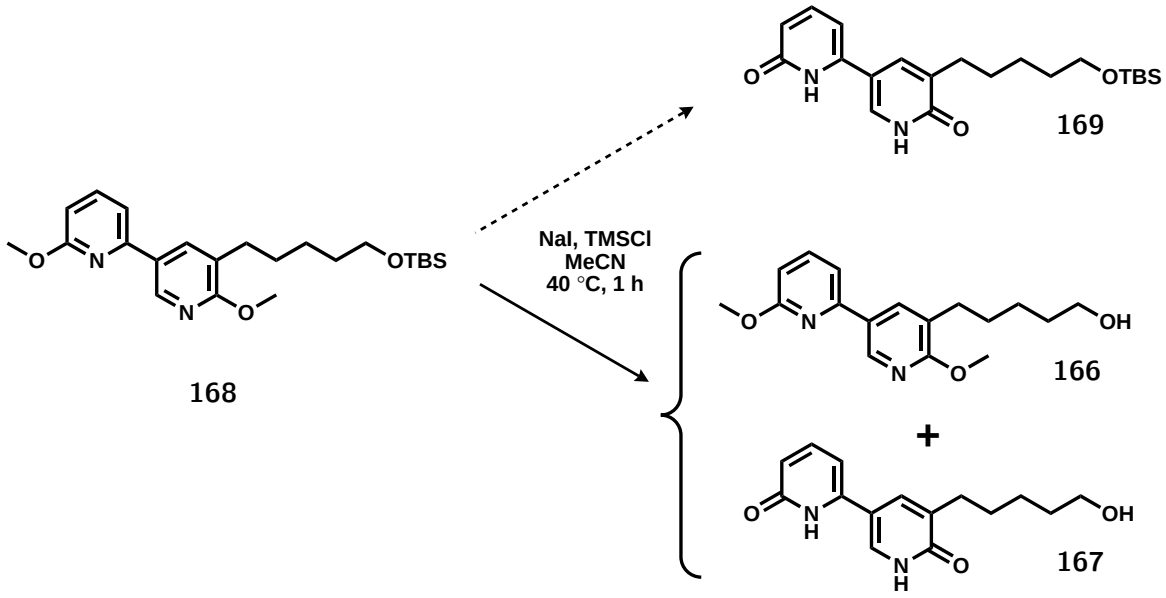

Scheme 3.33 Attempted deprotection of TBS-protected bismethoxypyridine **168**.

Although a small library of side-chain functionalised compounds had now been successfully synthesised, the decision was ultimately made to neglect pursuing their solubilising potential further. We were becoming increasingly convinced that considerable modification of Unit A would be necessary to achieve the desired solubility profile, and thus our attentions turned towards the investigation of more significant alterations that could be applied to the bipyridone framework.

3.5 Addition of Multiple Side Chains

At this stage we had successfully added a side-chain to one of the pyridone building blocks of Unit A. Our studies had suggested that the presence of multiple side chains may confer the desired solubility upon this bipyridone architecture, and so we elected to explore such modifications further. In order to synthesise a variant of Unit A with two side-chains, we had to address the more synthetically challenging 2,6-pyridone subunit (Fig. 3.2). From inspection of the structure, positions 3 and 4 would both be suitable, whereas position 5 should be avoided as it was proposed that a substituent in this position would cause steric interference with the other ring.

The installation of a side chain on the 3- or 4-position of a 6-bromo-2-pyridone building block is synthetically non-trivial, with little literature precedent. Our solution was to instead employ 3-aminopyridine **170** (Scheme 3.34). There was good precedent[97,139] for the bromination of 3-aminopyridine in the 2- and 6-positions. This presented the possibility of a selective S_NAr reaction

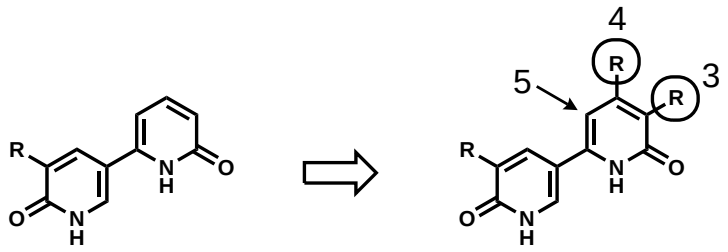

Fig. 3.2 Installation of a second side-chain on Unit A.

on the 2-bromine while leaving the 6-bromine available for the Suzuki coupling.

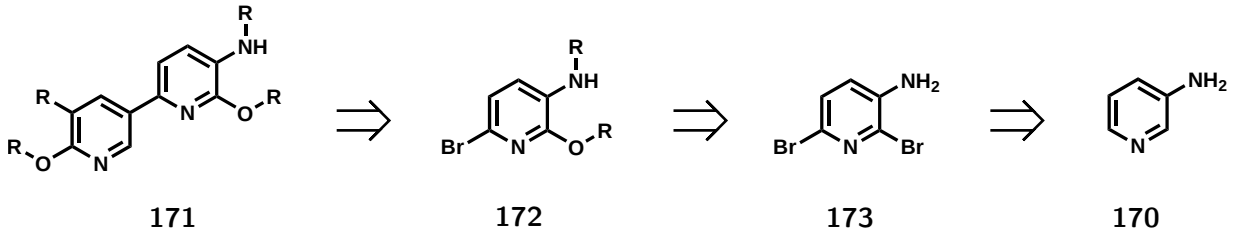

171 **172** **173** **170**

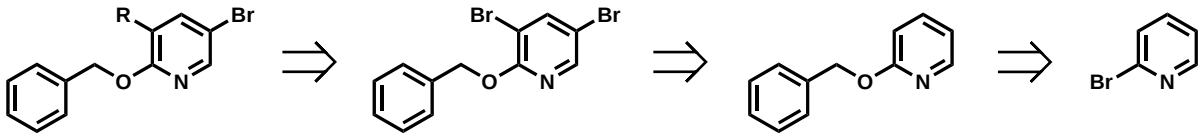

174 **175** **176** **177**

Scheme 3.34 Synthetic strategy to install a second side-chain on Unit A, and to use a benzyl protecting group on the 2,3,5-pyridine ring of Unit A.

This strategy is also appealing as it allows for a choice of nucleophile in the S_NAr reaction (on **173**) which was proposed to provide the protecting group for the pyridone. The final deprotection conditions of both NaI/TMSCl and HBr/AcOH are rather harsh, and milder, orthogonal deprotection conditions would be highly desirable. The benzyl protecting group was selected for its relative ease of synthesis, but crucially its orthogonal and relatively straightforward deprotection conditions of hydrogenation.

This new strategy of benzyl deprotection rather than methoxy deprotection required a rethink on the 2,3,5-side of the molecule where the side-chain had been previously installed (Scheme 3.34). It was proposed that the same double bromination strategy followed by selective lithiation and trapping would be perfectly suitable, in just the same way as for the methoxy compound. It was therefore first necessary to synthesise benzyloxypyridine **176**.

A test reaction was performed to confirm that the benzyl group would indeed be removed from 2-benzyloxypyridine **176** by hydrogenation (Scheme 3.35). Benzyl alcohol was deprotonated with

sodium hydride and reacted with 2-bromopyridine in an S_NAr reaction to afford 2-benzyloxypyridine **176** in high yield. When this compound was subjected to the standard hydrogenation conditions, the benzyl group was indeed efficiently removed, to yield 2-pyridone **178**.

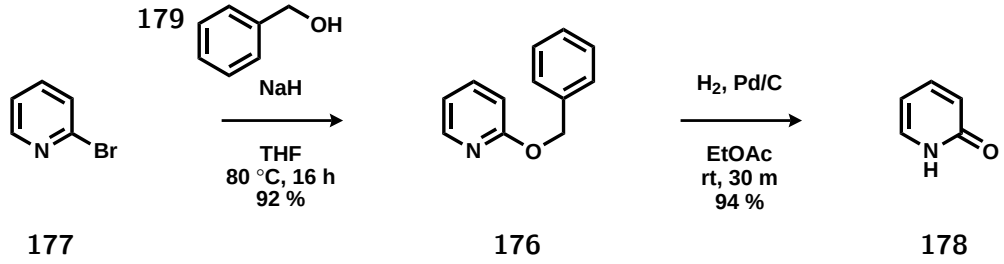

Scheme 3.35 Confirmation that hydrogenation successfully deprotects 2-benzyloxypyridine **176**.

3.5.1 2,3,5-Substituted Pyridine Subunit

We had benzyloxypyridine **176** already in hand from the test deprotection. Double-bromination of this compound would deliver our intended target **175**, although there was no precedent for this precise transformation in the literature. Unfortunately, despite many attempts, the bromination was unsuccessful (Scheme 3.36). ^{1}H NMR analysis of the crude reaction mixture did not indicate the presence of the desired compound **175**.

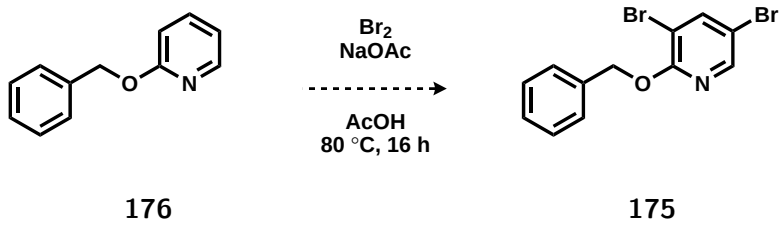

Scheme 3.36 Attempted bromination of **176**.

The failure of the bromination of benzyl pyridine **176** meant that we had to revise our strategy. It was instead proposed that the same target **175** could be reached *via* the benzylation of 2-pyridone **178** following bromination (Scheme 3.37). Happily, there was good precedent for the bromination of 2-pyridone **178** in the 3- and 5-positions,[97,140] and one example of the benzylation of 3,5-substituted pyridone **180**.[141]

The bromination of 2-pyridone **178** was first attempted with our familiar NBS/MeCN conditions,[97] using 2 equivalents of NBS. This was successful and 2-pyridone was doubly-brominated as desired in 47 % yield (Scheme 3.38). The succinimide bi-product was washed out of the crude reaction mixture with water to afford the desired compound **180** in good purity. Despite the presence of a small spot on the TLC plate that was thought to correspond to the singly-brominated product, this

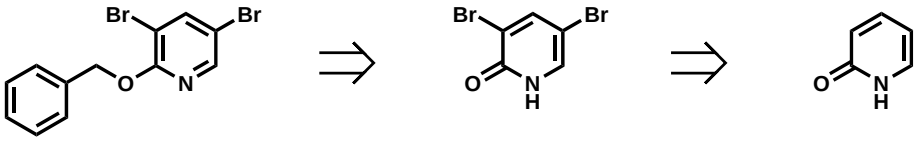

175 **180** **178**

Scheme 3.37 Synthetic strategy to use a benzyl protecting group starting with pyridone **178**.

compound was not evident during the ^{1}H NMR analysis of the crude reaction mixture, suggesting it may have been sufficiently soluble in water to be washed out. However, the low yield does suggest that some of the desired doubly-brominated product **180** was also washed into the aqueous phase during workup.

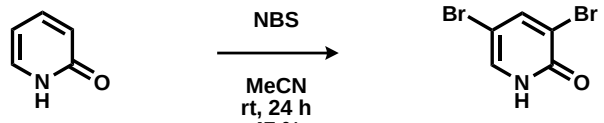

178 **180**

Scheme 3.38 Bromination of **178** to yield bisbromopyridine **180**.

The next step was to benzylate bisbromopyridine **180** (Scheme 3.39). The literature procedure[141] involved a straightforward reaction with benzyl bromide, mediated by silver carbonate in benzene. The reaction was attempted using these conditions, except the benzene was replaced with the more polar ethyl acetate. Pleasingly, the desired benzyloxypyridine **175** was isolated in good yield at the first attempt.

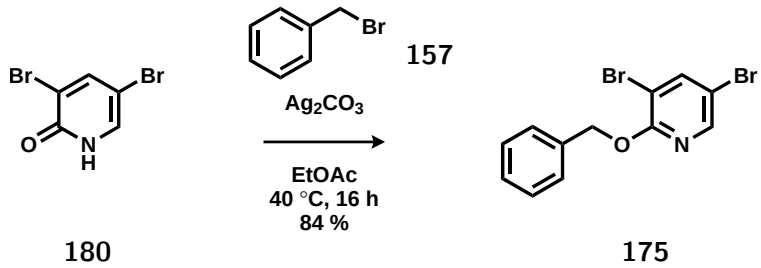

180 **175**

Scheme 3.39 Successful benzylation of bisbromopyridine **180** using silver carbonate.

We now had to perform the same selective ortho-lithiation and trapping procedure upon bromopyridine **175** that had worked so well for the methoxy equivalent **124**. The only difference between the compounds is the presence of a benzyl group on the oxygen instead of a methyl, but it was feared that this additional steric bulk might hinder the selective lithiation and trapping. Gratifyingly, benzyl-pyridine **175** also proved to be amenable towards selective ortho-lithiation (Scheme 3.40), with the desired benzyl-pyridine **181** successfully isolated on the first attempt using the same CuI conditions as previously employed.

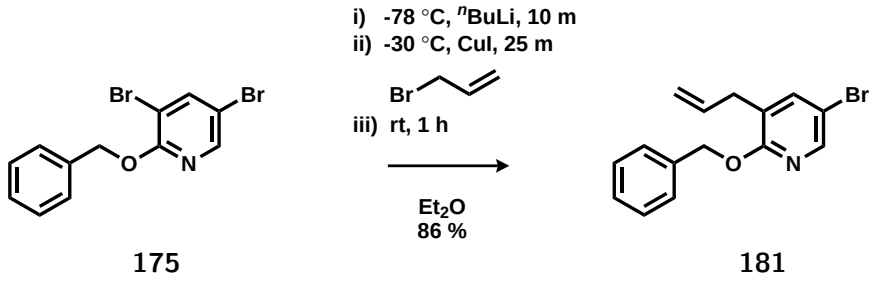

175 181

Scheme 3.40 Lithiation and trapping of bisbromopyridine **175** with allyl bromide.

Bromopyridine **181** was then smoothly converted into boronic acid **182** using the same procedure that had previously proven successful (Scheme 3.41). As with the octyl-substituted pyridine subunit **148**, boronic acid **182** was isolated by extracting into Et_2O, rather than precipitating it from the aqueous phase. Once again, it is proposed that the apolar nature of the allyl and benzyl substituents are crucial in governing the organic solubility of this boronic acid.

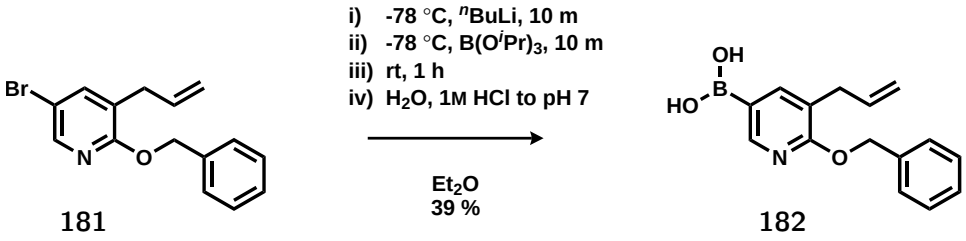

181 182

Scheme 3.41 Conversion of bromopyridine **181** into boronic acid **182**.

3.5.2 2,3,6-Substituted Pyridine Subunit

As previously discussed, our proposed approach to an appropriately-substituted subunit of Unit A required the synthesis of dibrominated compound **173**. Our preferred bromination conditions of NBS in MeCN at room temperature were found to be suitable for the bromination of 3-aminopyridine **170** to bisbromopyridine **173**, despite the low yield (Scheme 3.42).

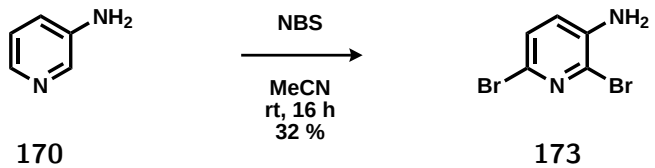

170 173

Scheme 3.42 Bromination of 3-aminopyridine to yield bisbromopyridine **173**.

There was precedent for the displacement of a single bromine on 2,6-dibromopyridine with benzyl alcohol to form 2-benzyloxy-6-bromopyridine,[142] and also for the selective substitution of the 2-bromine by methoxide on 2,6-bromo-3-aminopyridine.[143] This precedent suggested that the same substitution with benzyl alcohol would be successful, and thus similar conditions were employed in

our investigations (Scheme 3.43).

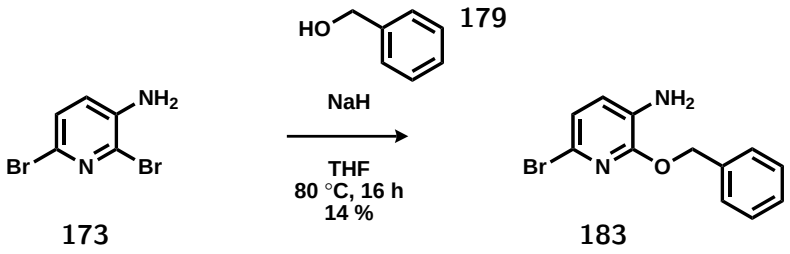

Scheme 3.43 Selective S_NAr reaction on bromopyridine **173** with benzyl alcohol **179**.

The experiment produced mixed results. ^{1}H NMR analysis of the crude reaction mixture suggested very good conversion to the desired product **183**. This was extremely encouraging, as it showed that the reaction was indeed selective for the 2-position, affording only the desired product **183**. However, the compound did not behave favourably during flash column chromatography, demonstrating instability on silica. This instability resulted in a low purified yield of 14 %. Further attempts at optimisation of the purification protocol did not yield better results.

For these reasons, the subsequent amide coupling reaction was attempted with the crude reaction mixture of **183** (Scheme 3.44). The experiment was not a success. ^{1}H NMR analysis suggested that all starting material was consumed, yet only a 3 % yield could be achieved following purification by flash column chromatography. The remaining components of the reaction mixture could not be identified following spectroscopic analysis.

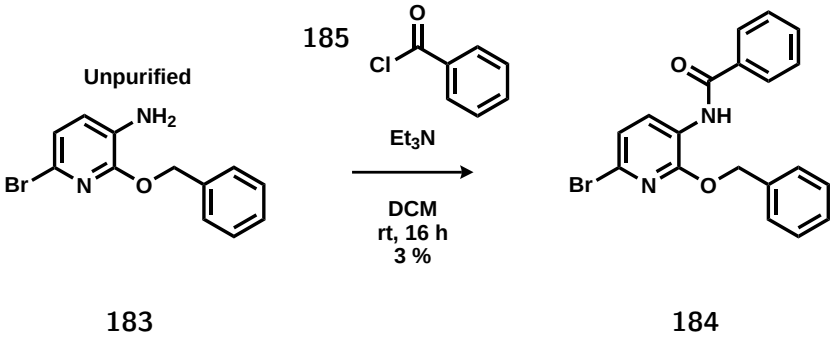

Scheme 3.44 Installation of side-chain on amine **183** *via* formation of an amide bond.

The small amount of pure benzylaminopyridine **183** that was isolated was subsequently subjected to treatment with benzoyl chloride (Scheme 3.45). ^{1}H NMR analysis of the crude reaction mixture suggested that the starting material was consumed, but the yield of the desired amide **184** was only 17 %. Again, the remaining components of the reaction mixture could not be identified.

The difficulty in purifying **183**, and the low yields of reactions on both crude and pure **183** to produce **184**, suggested that an alternative synthetic strategy should be sought. It was thus

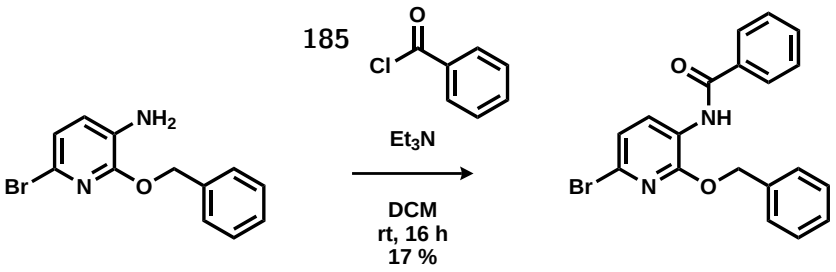

Scheme 3.45 Installation of side-chain on amine **183** *via* formation of an amide bond.

proposed that the amide-bond-forming reaction be performed first, followed by the selective S_NAr to install the benzyl moiety.

As expected, the amide reaction worked well. Using standard conditions of Et_3N in DCM at room temperature,[144] the desired product **186** was isolated in 72 % yield (Scheme 3.46).

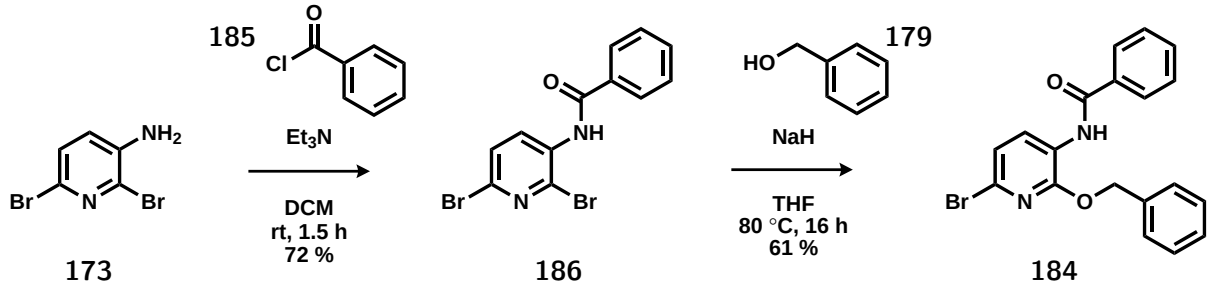

Scheme 3.46 Installation of side-chain on **173** followed by selective S_NAr reaction with benzyl alcohol **179**.

It was now time for the crucial selective substitution reaction. Despite the low yield problems experienced previously with the free amine precursor **173**, spectroscopic analysis of that reaction did indicate that it was indeed selective for the intended 2-bromine. Our optimism proved to be well founded. Treatment of bromopyridine **186** with one equivalent of deprotonated benzyl alcohol **179** afforded the target compound in an acceptable 61 % yield (Scheme 3.46). This was an excellent result. The inductive effect of the electron-withdrawing amide group allowed the bromine in the 2-position to react selectively with the alkoxide nucleophile.

3.5.3 Suzuki Coupling and Final Steps

We now had both the bromide **184** and boronic acid **182** in hand, and thus proceeded to the Suzuki coupling of these subunits. The coupling proceeded smoothly under the favoured conditions to provide bis-benzylpyridine **187** in good yield (Scheme 3.47).

With bipyridine **187** successfully synthesised, it was proposed that the allyl side-chain be further

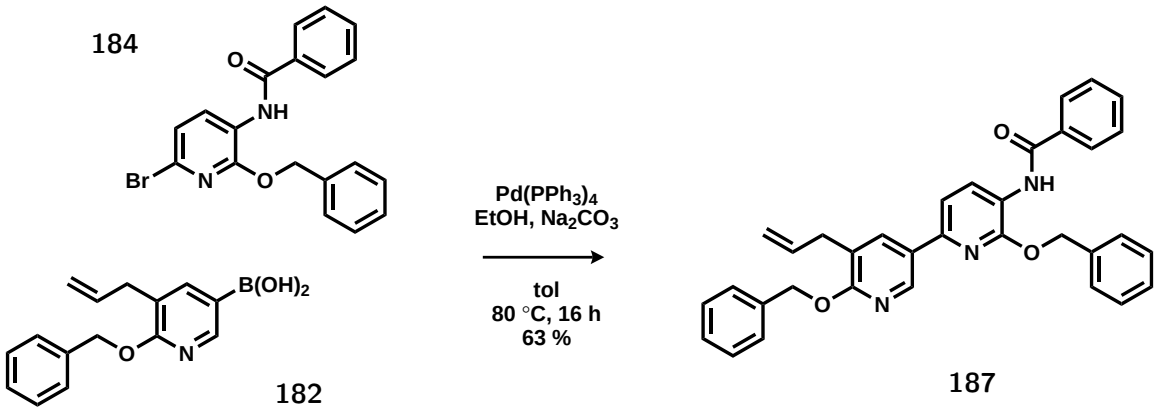

Scheme 3.47 Suzuki cross-coupling to afford bisbenzylpyridine **187**.

extended, utilising the hydroboration methodology that had been previously explored. The resultant alcohol from this transformation can be readily converted to an apolar silyl ether. The hydroboration was indeed a success, with alkene **187** smoothly converted to the alcohol **188** in excellent yield (Scheme 3.48).

The bulky, apolar *tert*-butyldiphenylsilyl group was selected as an appropriate masking group for the free primary alcohol present in compound **188**. The alcohol **188** was therefore treated with TBDPS chloride[145,146] to give TBDPS-protected **189** in an acceptable 64 % yield (Scheme 3.48).

Bisbenzylpyridine **189** could now be deprotected by hydrogenation. Gratifyingly, as we had planned, the relatively mild hydrogenation conditions did not interfere with the rest of the molecule, efficiently removing both benzyl protecting groups to afford highly substituted bispyridone **190** in 77 % yield (Scheme 3.48). This was a pleasing result as, despite benzyl deprotection by hydrogenation being a well-known technique, there are a limited number of literature examples where it is used to reveal a pyridone.

3.5.4 Solubility

With this less polar variant of Unit A now successfully synthesised, we began to explore the solubility properties of this molecule further. To our dismay, bipyridone **190** was only partially soluble in $CDCl_3$. It formed an opaque suspension in this solvent, even after vigorous shaking. The ^{1}H NMR spectrum did register peaks in the aromatic region, but they were very broad and indistinct, and certainly completely inappropriate for NMR binding measurements.

It is true that there are groups other than an amide side-chain that would perhaps be better for increasing lipophilicity. However, our faith in the 2-pyridone architecture of Unit A was waning, and it was thought a better use of the limited time remaining to explore solutions to the solubility

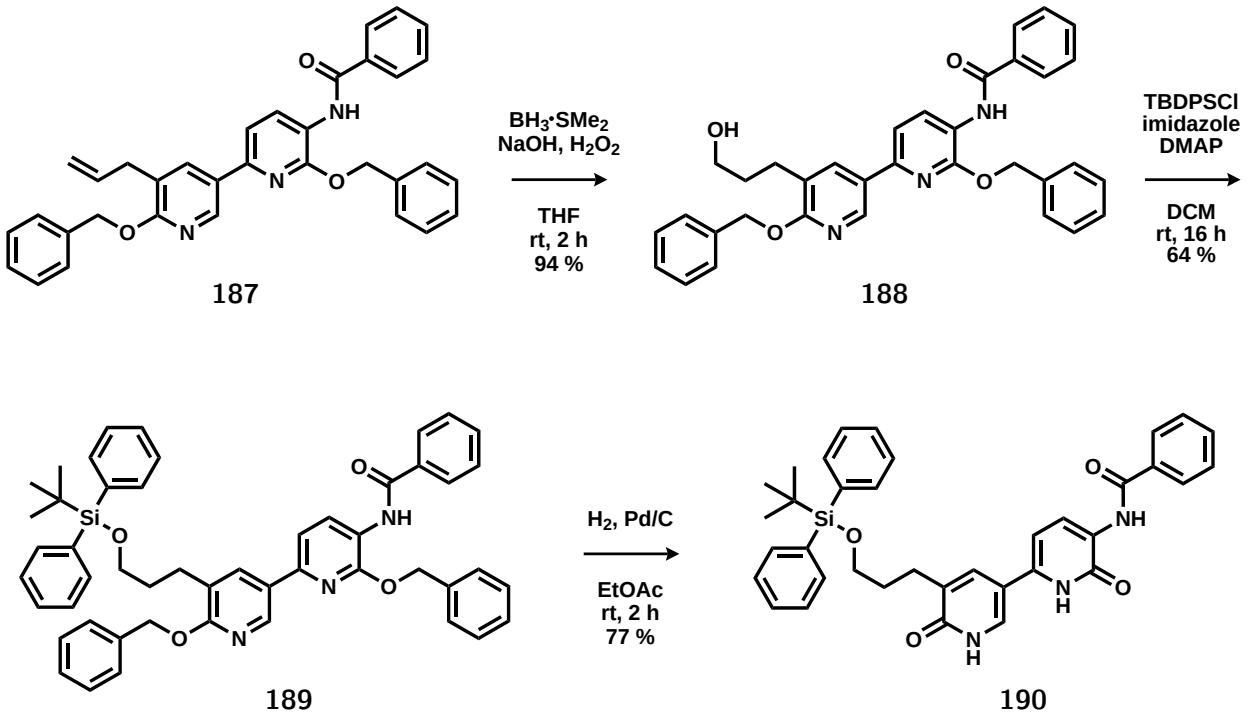

Scheme 3.48 Hydroboration, TBDPS-protection, and benzyl deprotection of bispyridylalkene **187** to give bispyridone **190**.

problems that were not based on the bipyridone architecture.

4 Amide Design

4.1 Introduction

Following considerable investigation, and the consistent solubility problems of the bipyridone units, a new strategy was considered. It was proposed that an amide bond could be used as part of the binding array (Fig. 4.1), which would not only allow for the removal of one of the two pyridone subunits of Unit A, but also help to shorten the synthesis.

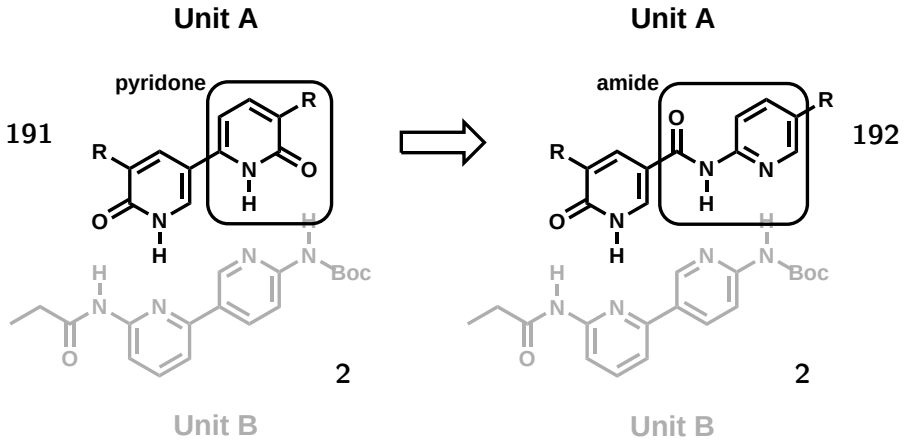

Fig. 4.1 Redesign of Unit A, using an amide bond as part of the binding array.

4.2 Synthesis

An appropriate retrosynthetic strategy was devised, initiating with the commercially available building blocks **83** and **193** (Scheme 4.1). In theory, the desired compound **194** could be synthesised in a single step; an amide bond-forming reaction between 2-aminopyridine **83** and 6-hydroxynicotinic acid **193**.

To begin the synthesis, 6-hydroxynicotinic acid **195** was converted into the acyl chloride **193** using thionyl chloride **196**[147,148] (Scheme 4.2). A coupling between acyl chloride **193** and amine **83** was then attempted (Scheme 4.2). Unfortunately, despite numerous attempts, this amide bond-forming

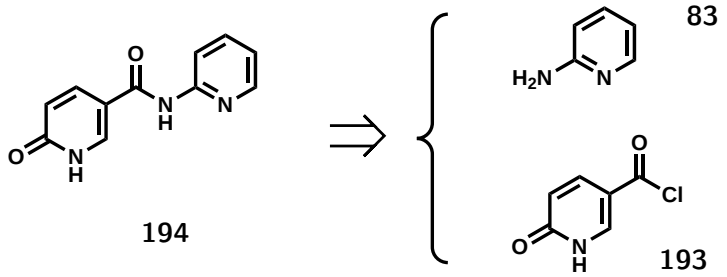

Scheme 4.1 Retrosynthetic approach to amide Unit A **194**.

reaction could not be achieved.

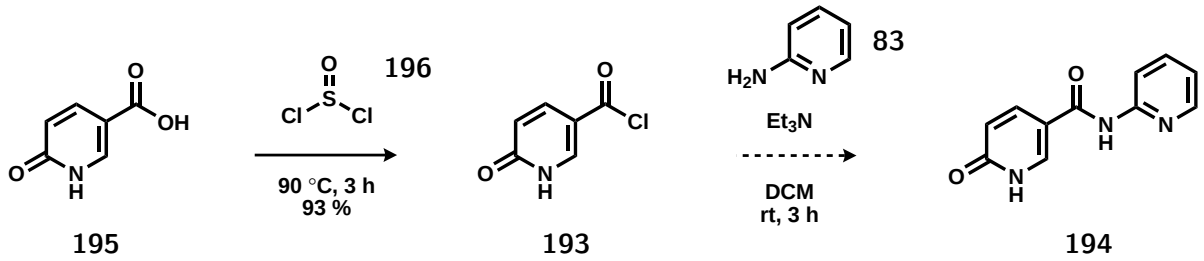

Scheme 4.2 Formation of acyl chloride **193** from 6-hydroxynicotinic acid **195**, and attempted coupling of **193** with 2-aminopyridine **83**.

4.2.1 Chloropyridine Strategy

The failure of the direct coupling led us to revise our strategy. It was suggested that the pyridone functionality of acyl chloride **193** was somehow preventing successfully coupling. Therefore, this compound was replaced with 6-chloro coupling partner **197** (Scheme 4.3).

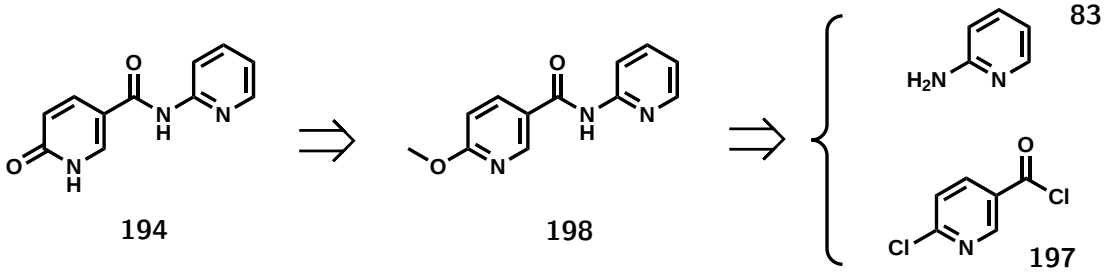

Scheme 4.3 Revised retrosynthetic approach to amide Unit A **194**.

Initial efforts at achieving the desired amide coupling involved the attempted formation of the acyl chloride **197** *in situ* from the nicotinyl chloride **199** using thionyl chloride **196**, followed by immediate reaction with 2-aminopyridine **83** to form the amide **200** (Scheme 4.4). The chloride substituent would then be displaced with methoxide in an S_NAr reaction to afford intermediate **198**. Unfortunately, this one-pot reaction did not work. Despite the absence of starting materials from the crude reaction mixture, no desired product could be isolated.

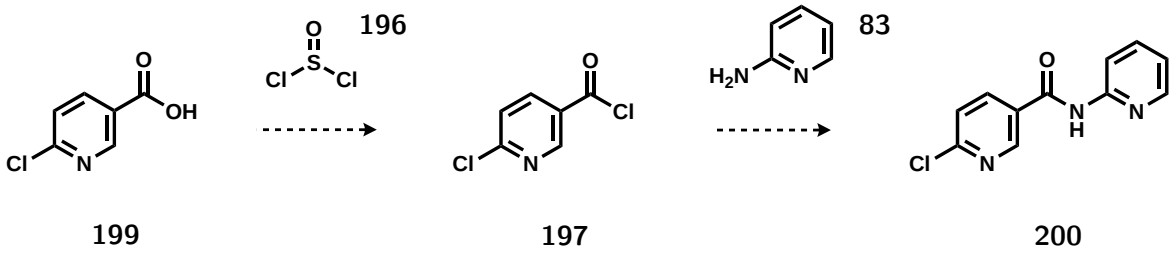

Scheme 4.4 Attempted formation of amide **200** in a one-pot reaction sequence.

Instead, we coupled the commercially-available acyl chloride **197** with 2-aminopyridine **83** using standard conditions.[149,150] The reaction was a success, delivering amide **200** in an acceptable yield of 57 % (Scheme 4.5).

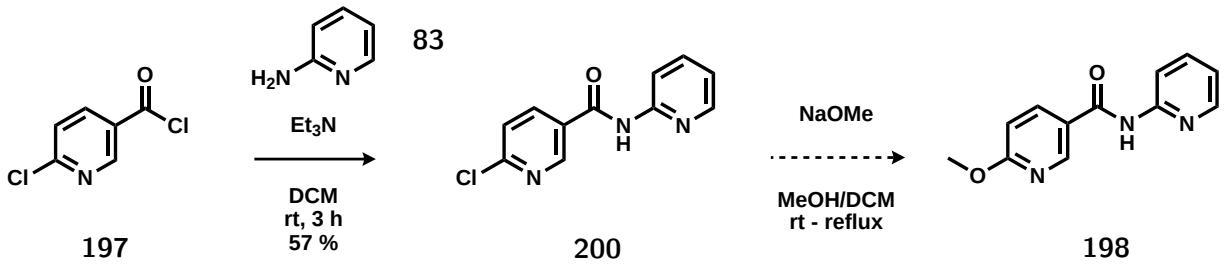

Scheme 4.5 Formation of amide **200** from acyl chloride **197**, and failure to displace the chlorine of **200** to reach methoxypyridine **198**.

We then attempted to react chloropyridine **200** with sodium methoxide in order to synthesise the methoxypyridine **198** (Scheme 4.5). We found that in both MeOH and DCM solvent systems at room temperature, no reaction occurred. However, in MeOH at 75 °C, methanolysis of the amide bond took place, returning 2-aminopyridine **83**. In DCM at reflux over a 16 h reaction period, mainly starting material was returned. Spectroscopic analysis of the reaction mixture was not able to elucidate the compounds formed under these conditions. For these reasons, this acyl chloride/amine coupling approach was abandoned.

4.2.2 Carbodiimide Classical Coupling

Given the failure of these acyl chloride coupling reactions, we instead investigated alternative methods of amide bond formation. If the carboxylic acid **195** could be directly coupled with 2-aminopyridine **83** we could access Unit A in one step, and thus diimide-type couplings[151–153] were thought to be synthetically attractive (Scheme 4.6). DCC was employed as a coupling partner in DMF, but unfortunately only starting material was returned, with no reaction taking place.

It was proposed that the pyridone/hydroxypyridine moiety was somehow preventing coupling from taking place. We therefore designed a synthesis based on DCC coupling but in which the

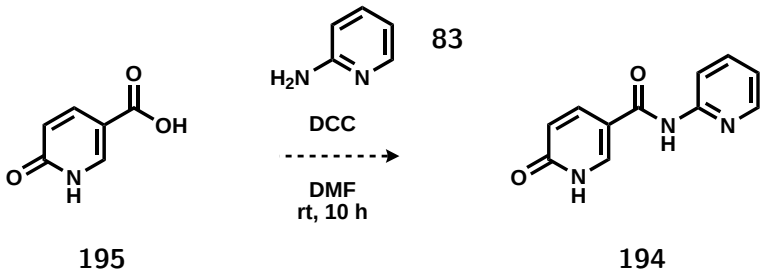

Scheme 4.6 Attempted direct coupling of carboxylic acid **195**.

pyridone oxygen was protected. Methoxy deprotection was desirable as we were familiar with the methodology. The pyridone would be protected with a methyl group prior to the DCC coupling, which is followed by deprotection using our reliable HBr/AcOH or TMSCl/NaI conditions.

In order to employ well-known methodology,[154–158] but at the slight expense of inelegance, our planned synthetic route initiated with esterification of 6-chloronicotinic acid **199** followed ester hydrolysis to yield the carboxylic acid **201** (Scheme 4.7). The carboxylic acid **199** was smoothly converted to the 6-methoxy methyl ester **202** using a known procedure.[154] These strongly forcing conditions simultaneously form an ester moiety while the desired S_NAr reaction is taking place on the chlorine. The methyl ester **202** was then converted back to the acid **201** in high yield using standard hydrolysis conditions,[158] leaving the 2-methoxy pyridine intact.

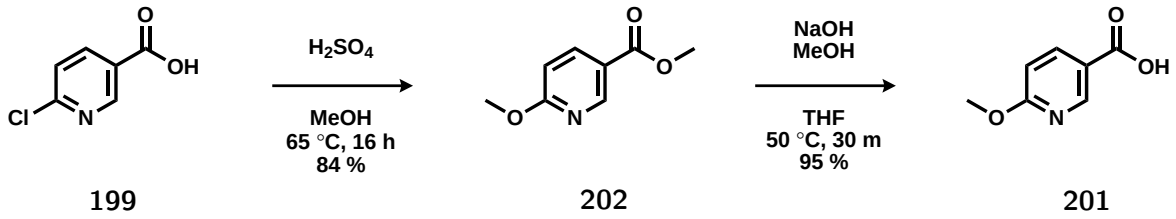

Scheme 4.7 Conversion of carboxylic acid **199** into methyl ester **202** and then the acid **201**.

Gratifyingly, the coupling between methoxypyridine **201** and aminopyridine **83** was successful, albeit in low yield (Scheme 4.8). The yields improved when a catalytic amount of DMAP was added. Couplings using EDC instead of DCC were also attempted. These again provided the target compound, but at slightly lower yields.

We were now in a position to conduct the final step towards our redesigned Unit A **194**, the familiar transformation of methoxy deprotection. Many different deprotection conditions were attempted (Table 11.2, Appendix C). The HBr/AcOH conditions proved to be unsuitable, returning only starting material at both room temperature and 70 °C. However at 120 °C, the amide bond was cleaved, with 2-aminopyridine isolated following the work-up. At 95 °C, the amide bond was cleaved again, returning 2-aminopyridine. Given the difficulties in selecting an appropriate temperature for

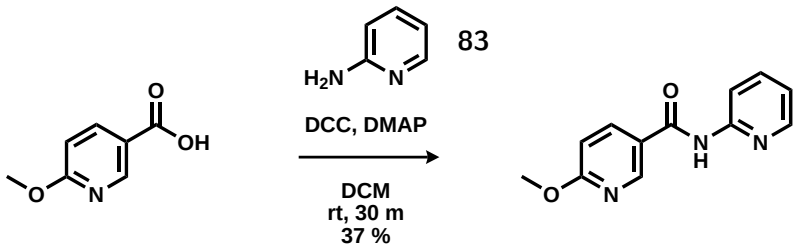

201 198

Scheme 4.8 Coupling of carboxylic acid **201** with 2-aminopyridine **83** to form the precursor to Unit A.

this transformation, we instead decided to investigate alternative deprotection conditions.

The TMSCl/NaI conditions were proposed to be more suitable for this transformation. At room temperature, all of the starting material was consumed. However, no product could be isolated, with spectroscopic analysis suggesting that the amide oxygen had instead been silylated. To our delight, further investigations showed that the reaction produced the desired pyridone **194** at both 40 °C and 70 °C.

We also investigated deprotection with BBr_3 in DCM.[112,159] When this reaction was performed at room temperature, only an unidentifiable product was isolated. However, these conditions worked well at both 70 °C and 40 °C, providing slightly cleaner product and slightly better yields than the TMSCl/NaI conditions (Scheme 4.9).

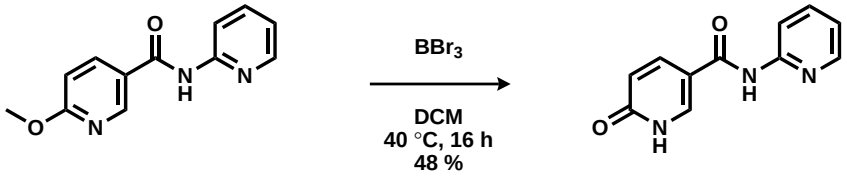

198 194

Scheme 4.9 Deprotection of methoxypyridine **198** to form the amide version of Unit A **194**.

With our redesigned Unit A now successfully synthesised, our attentions were once again drawn to the solubility properties of this compound.

4.2.3 Solubility

Sadly, amide pyridone **194** was completely insoluble in $CDCl_3$. Despite only one 2-pyridone motif now being present, the polarity of amide **194** was such that it could only be solubilised in DMSO, and was thus unsuitable for our planned binding experiments. However, with the amide coupling methodology now proceeding well, we decided to investigate the coupling between the methoxy carboxylic acid **201** and 2-amino-4,6-methylpyridine **203** as the latter compound would be more

soluble in organic solvents than 2-aminopyridine **83**. Pleasingly, this amine coupled smoothly under the same conditions as previously to afford amide **204**, albeit in low yield (Scheme 4.10).

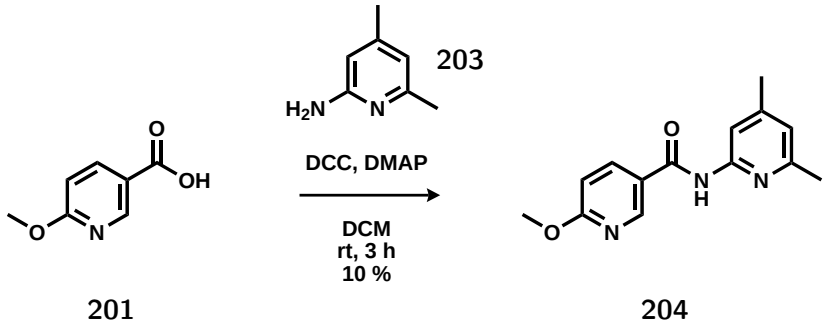

Scheme 4.10 Coupling of carboxylic acid **201** with 2-amino-4,6-methylpyridine **203** to form precursor **204** to Unit A.

BBr_3 was once again employed to deprotect the methoxy derivative **204** (Scheme 4.11). This worked well again, providing pyridone amide **205** in a yield of 88 %.

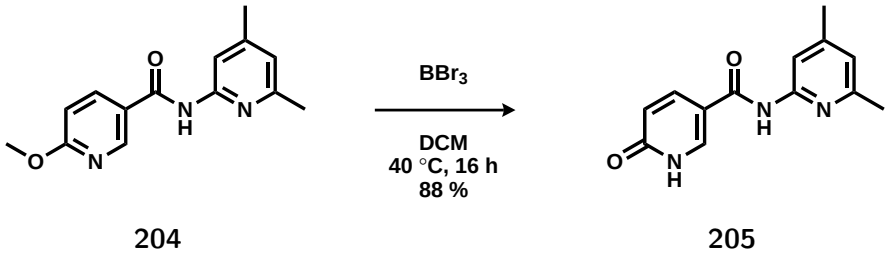

Scheme 4.11 Deprotection of methoxypyridine **204** to form the amide version of Unit A **205**.

Once again, pyridone **205** was not soluble in $CDCl_3$. However, it should be noted that this compound could be dissolved in water, whereas amide **194** was insoluble.

These disappointing results indicated strongly that other molecular architecture for Units A and C beyond the 2-pyridone motif should instead be considered. Thus, our original designs for these molecules were abandoned and a completely new approach was instead sought.

5 Complete Redesign

5.1 Introduction

Our previous studies now strongly suggested that the 2-pyridone motif should be completely avoided. Therefore, after considerable thought, Units A and C were completely redesigned, retaining an identical staggered ADDA H-bond array, but without any reliance on the 2-pyridone motif. By 'inverting' the 2-amino pyridine motif (Fig. 5.1), the appropriate H-bond binding pattern could be achieved, resulting in the design of new Units A **206** and C **207**.

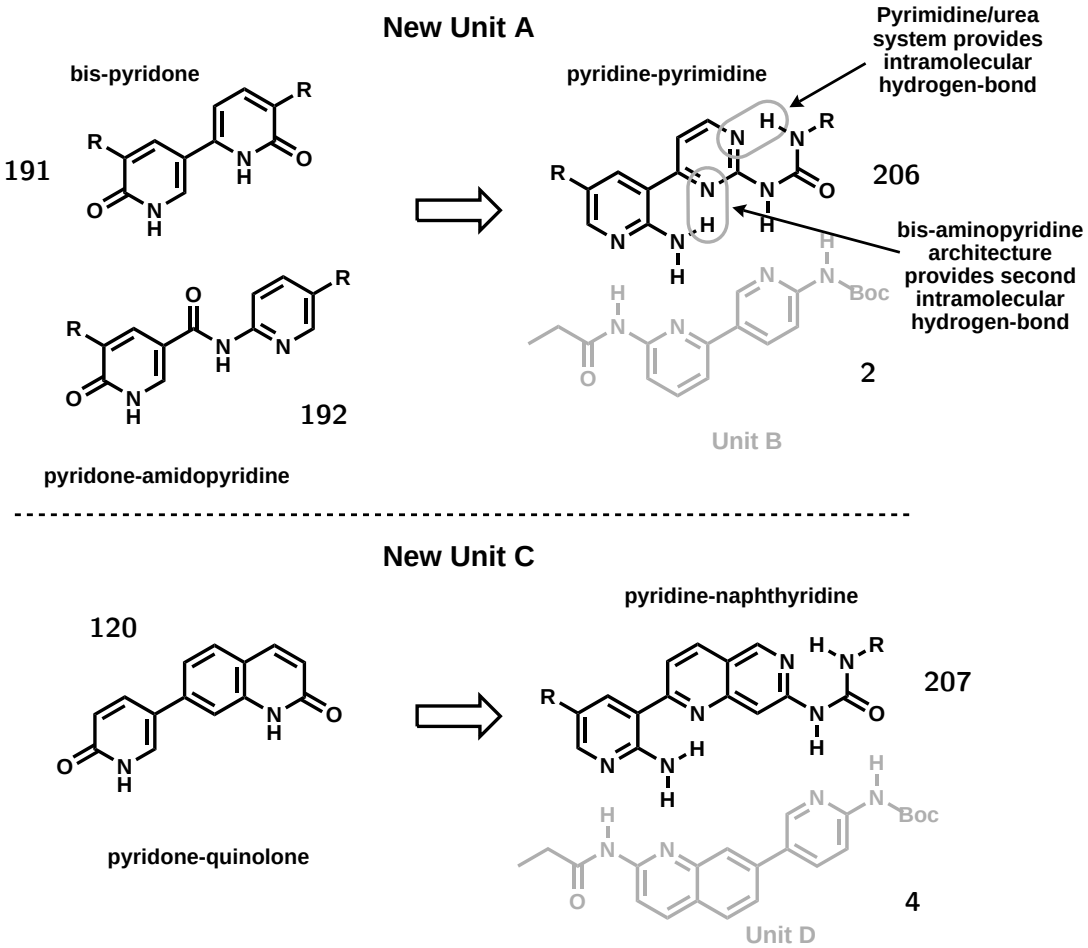

Fig. 5.1 Redesign of Units A and C, involving no pyridones.

An intramolecular hydrogen-bond was thought to be an additional desirable property, as it would lock the side-chain in place, and thus potentially increase the binding strength of interaction. This was achieved by the use of a pyrimidine, in conjunction with a urea in the side chain to provide the N-H donor.

The designs in Fig. 5.1 represent the ideal targets. We were however aware that for Unit A, the synthesis of a pyrimidine building block would be more challenging than the synthesis of a pyridine. Likewise, for Unit C, the synthesis of a naphthyridine building block would be more difficult than the synthesis of a quinoline. As such, we also started work on simplified versions of the new units (Fig. 5.2).

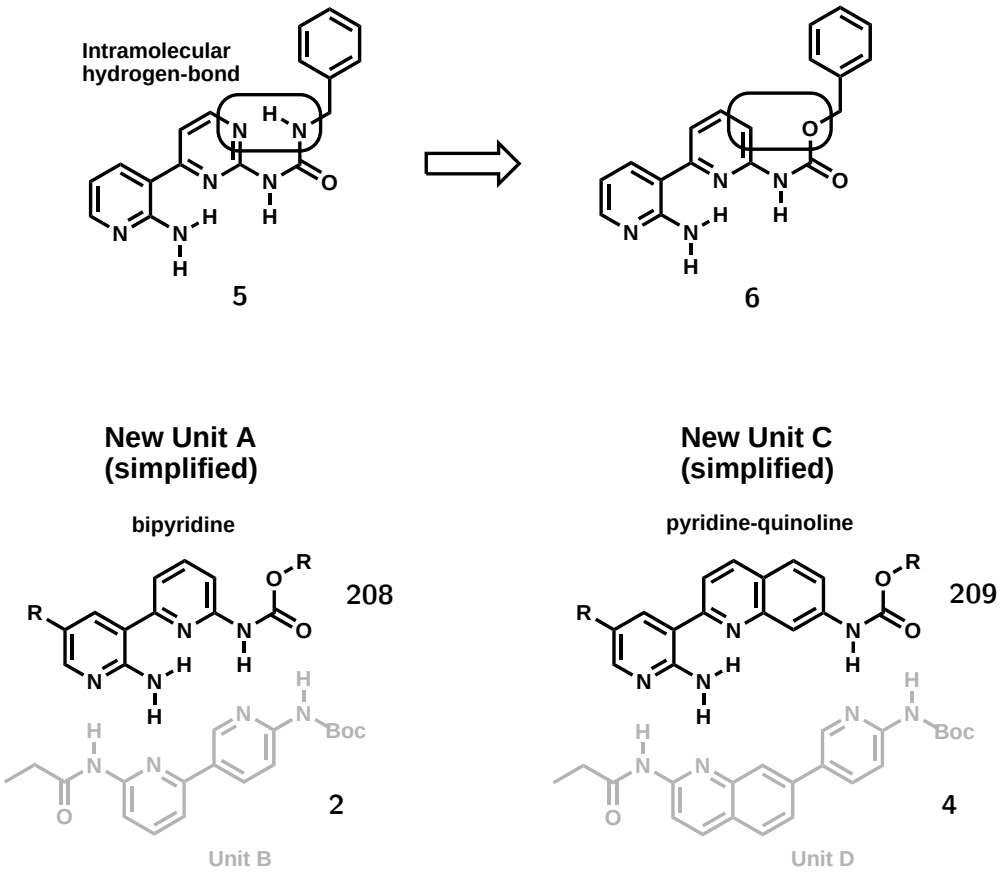

Fig. 5.2 Simplified redesign of Units A and C.

Due to time constraints, more progress was made with the synthesis of the new versions of Unit A than the new versions of Unit C. As such, the progress made with Unit C will be described first, followed by the more extensive investigations on Unit A.

5.2 Unit C

5.2.1 Initial Steps – Simplified Quinolone Unit C

An initial retrosynthetic analysis suggested that aminoquinolone **210** would be a key component in the route towards Unit C **211** (Scheme 5.1).

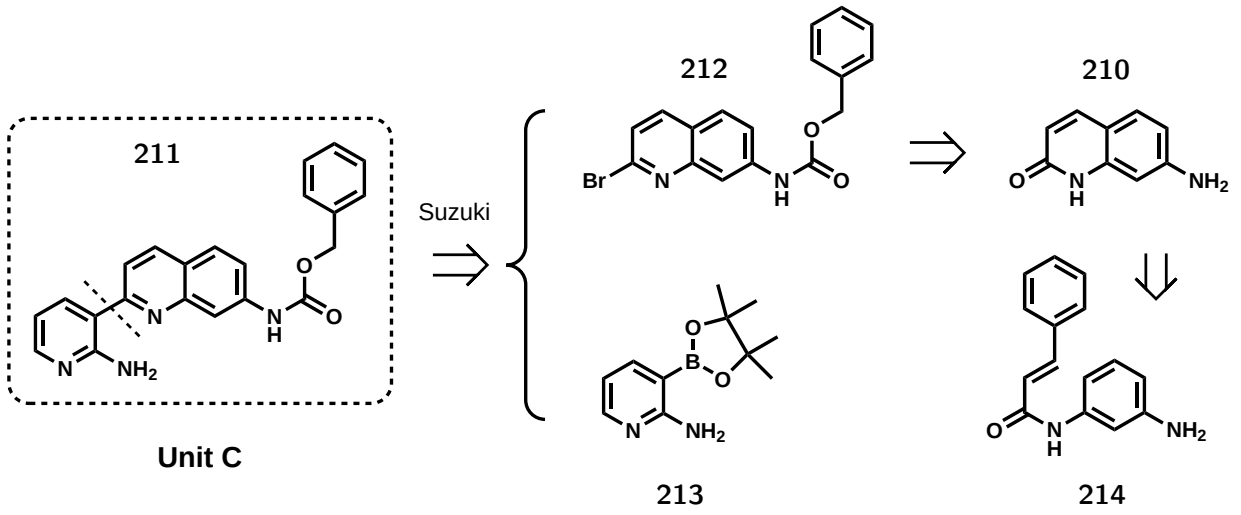

Scheme 5.1 Planned route towards 7-aminoquinoline Unit C **211**.

This compound could in theory again be accessed by performing the same $AlCl_3$-directed Doebner-Miller cyclisation/elimination on compound **214** with the concomitant loss of benzene. Amine **214** was readily synthesised *via* a mono-cinnamoylation[160] of diamine **215** (Scheme 5.2). Purification by flash column chromatography provided the product in good purity in 73 % yield.

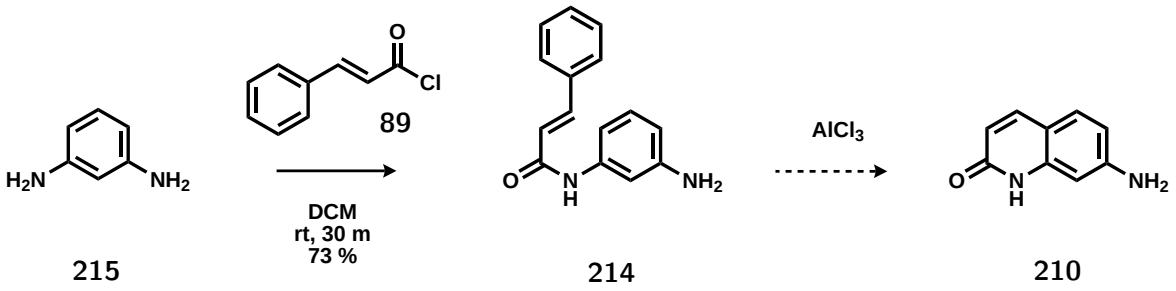

Scheme 5.2 Synthesis of amine **214**, and the failed cyclisation.

The next step was the previously-described $AlCl_3$-mediated cyclisation (Scheme 5.2), for which a large variety of conditions were attempted (Table 11.3, Appendix C). Refluxing in THF, dioxane and toluene, with or without base, all returned purely starting material. In 1,2-dichlorobenzene, at 130 °C for 30 minutes, there was no starting material remaining as evidenced by ^{1}H NMR analysis of the crude reaction mixture. However, a number of unidentifiable by-products were found to be

present. The same result was achieved with longer reaction times and higher temperatures. The failure of this reaction is likely due to the presence of the primary amine, which would coordinate to the $AlCl_3$ and draw electron density away from the position para to the amine, thus preventing the cyclisation.

The failure of this cyclisation dictated that a slightly new approach be investigated. We first protected **215** with benzyl chloroformate **216** to afford amine-carbamate **217** (Scheme 5.3). The chloroformate was added slowly to the amine to minimize formation of the bis-protected by-product. With amine-carbamate **217** in hand, the free amine could now be reacted to afford bis-amide **218** in excellent yield. We could now attempt the $AlCl_3$-mediated cyclisation again, but with a protected amine now in the other position.

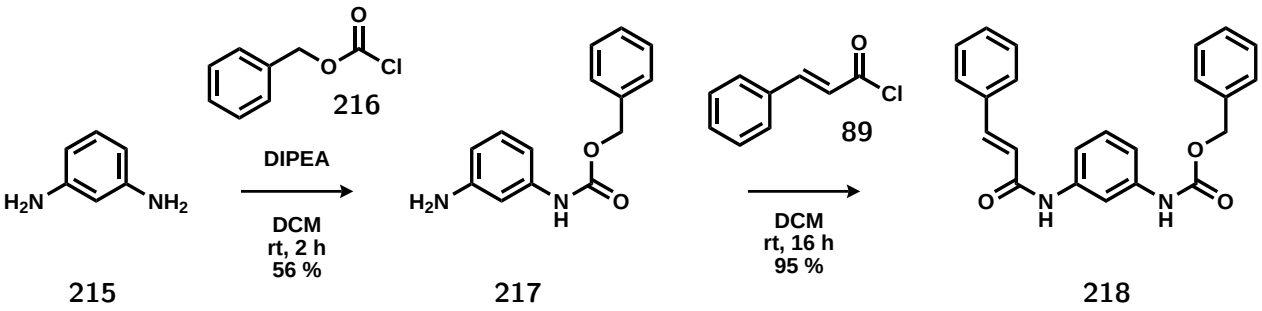

Scheme 5.3 Synthesis of amine **217** and subsequent transformation into carbamate-amide **218**.

Unfortunately, once again attempts to synthesise quinolone **219** *via* a Doebner-Miller cyclisation of **218** did not produce good results (Scheme 5.4). ^{1}H NMR analysis of the crude reaction mixture indicated the presence of a wide range of unidentifiable compounds. Purification by flash column chromatography did not provide any clean samples to aid characterisation.

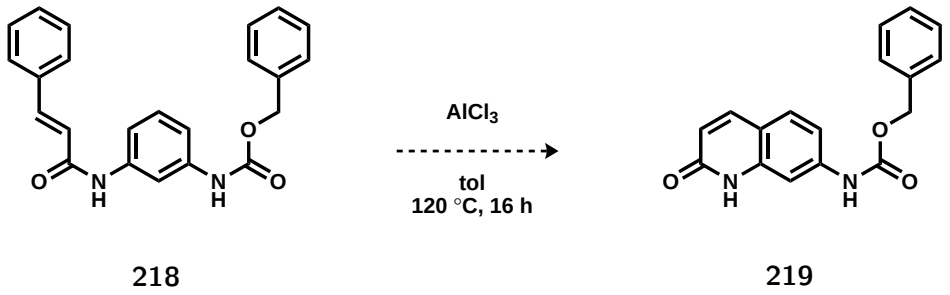

Scheme 5.4 Attempted cyclisation of **218** to afford quinolone **219**.

We performed a test reaction on **217** with $AlCl_3$ in toluene at reflux (Scheme 5.5), in order to investigate the ability of the carbamate group to withstand such forcing reaction conditions. As feared, benzene-1,3-diamine **215** was isolated. The carbamate was being cleaved under these conditions, and thus a more robust protecting group was sought.

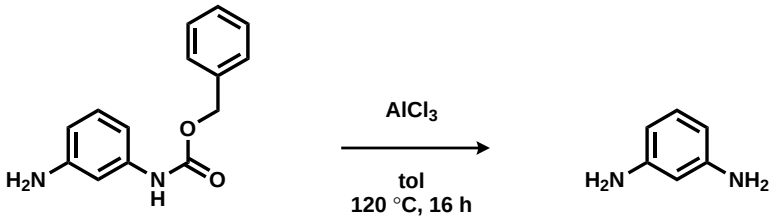

217 **215**

Scheme 5.5 Test reaction on **217** with $AlCl_3$ in toluene at reflux.

We decided to investigate the use of an acyl protecting group on the amine (Scheme 5.6). Acetic anhydride **220** was slowly added to a concentrated excess of bisamine **215** to minimise formation of the undesired bis-acylated by-product. The resultant amide **221** was subsequently reacted with cinnamoyl chloride under the same reaction conditions as previously employed, affording **222** in low yield (Scheme 5.6).

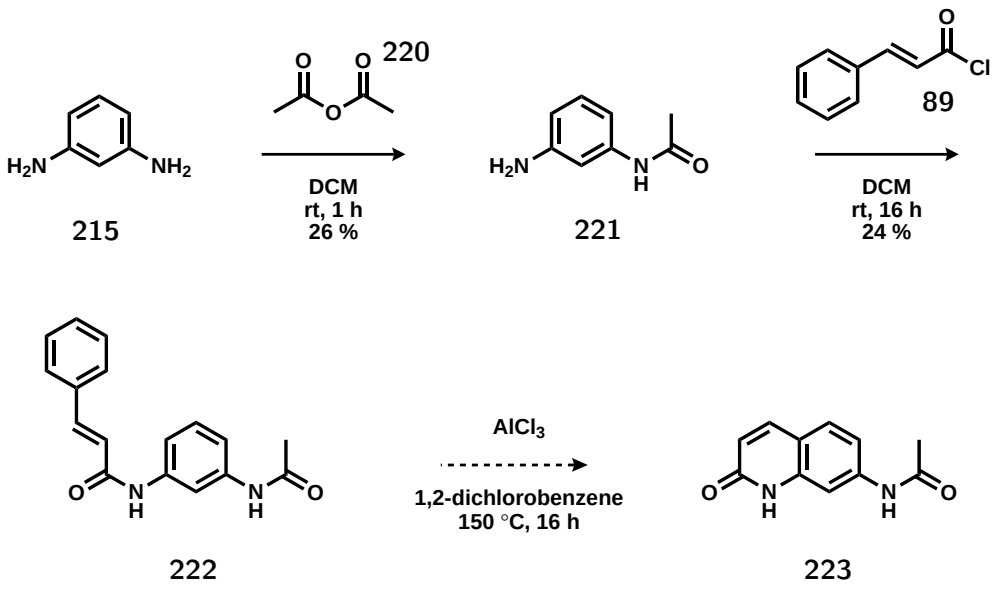

215 **221** **222** **223**

Scheme 5.6 Attempted cyclisation of doubly-protected amine **215**.

The $AlCl_3$-mediated cyclisation of **222** could now be attempted with the acyl protecting group (Scheme 5.6). However, once again the results were similar to the previous cyclisation attempts. Under a wide range of reaction conditions, a complex mixture of products was repeatedly obtained. Further attempts to achieve the cyclisation of this substrate were thus abandoned.

The traditional Doebner-Miller cyclisation utilises benzene as a leaving group, and so we decided to investigate alternative functionalities that might fulfill this role. We therefore prepared acyl chloride **224** (Scheme 5.7),[161] which would ultimately lead to a cyclisation substrate containing an ethoxy leaving group.

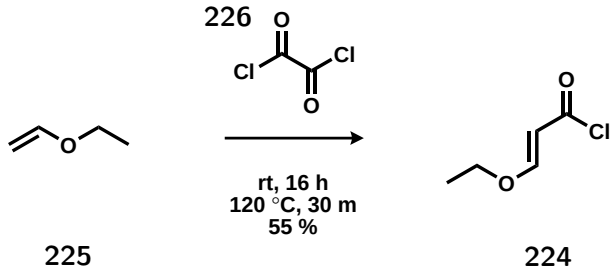

Scheme 5.7 Synthesis of ether **224**.

However, attempts to form **227** by reacting acyl chloride **224** with amine **215** did not meet with success (Scheme 5.8). The experiments returned starting material alone, suggesting that no reaction was taking place.

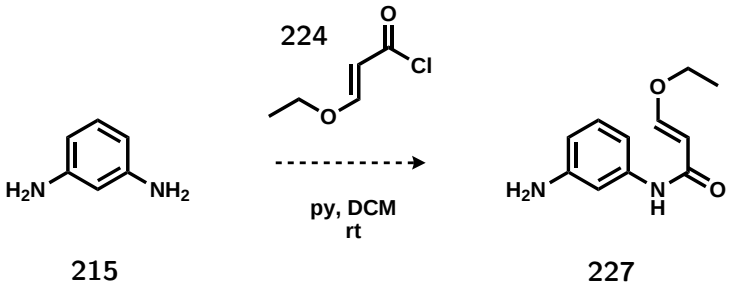

Scheme 5.8 Attempted synthesis of amide **227**.

The synthesis of substrate **227** was not pursued further, and a compound containing a chloride leaving group was instead targeted. Propanoyl chloride **228**, when reacted with amine **221**, would enable the synthesis of such a substrate **229**. However, initial attempts at this reaction with the mono-protected starting material **221** were unsuccessful (Scheme 5.9).

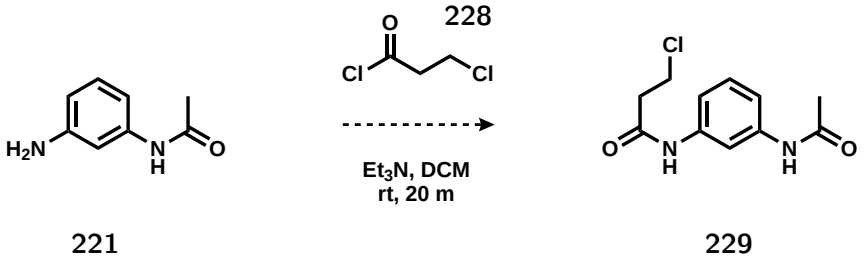

Scheme 5.9 Attempted synthesis of **229**.

The reaction of 3-Chloropropanoyl chloride **228** with aminobenzene **215** was a success (Scheme 5.10). Under standard conditions[162] the target compound **230** was isolated in 40 % yield. However, while it was pleasing to have arrived at amine **230**, conditions could not be found which resulted in a successful Friedel-Crafts cyclisation to quinolone **231** (Scheme 5.10). $AlCl_3$ in DCM at reflux for 4 hours returned pure starting material, as did the same reaction in toluene at reflux. In

THF at reflux, ^{1}H NMR analysis suggested that a complex mixture of compounds had been formed. Thus, given the repeated difficulties in achieving the desired cyclisation, alternative methodology was sought to provide access to the desired quinolone motif.

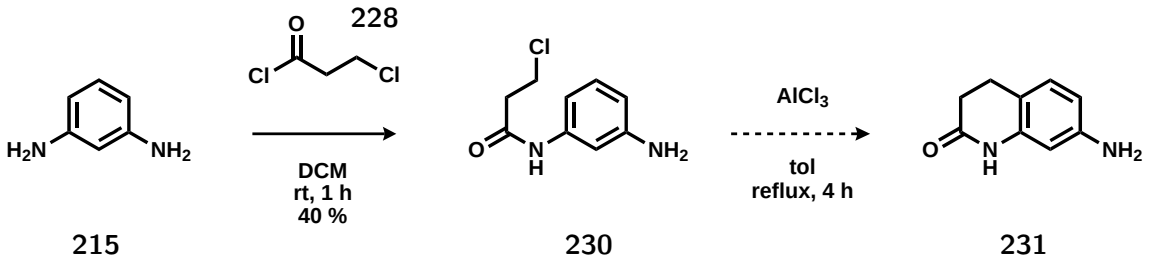

Scheme 5.10 Synthesis and attempted cyclisation of amine **230**.

5.2.2 Acetamide Reaction

We postulated that our target compound **223** could be reached by reacting bromoquinolone **70** with acetamide[163,164] (Scheme 5.11). The reaction was performed on the isomer mix of 7-bromoquinolone **70** and 5-bromoquinolone **90** previously obtained during the synthesis of Units C and D. In dioxane at reflux no reaction took place. However, in an NMP solvent system at 150 °C the desired quinolone **223** was isolated in a respectable 62 % yield. Interestingly, a significant amount of the 5-bromo starting material remained, but none of the 7-bromo starting material. This could possibly be because the 7-position is less sterically hindered, but may also be due to electronic effects resulting from the relative positioning of the quinolone moiety.

While this synthetic strategy did show promise, time constraints dictated that our attentions instead be focussed upon the synthesis of the naphthyridine variant of Unit C.

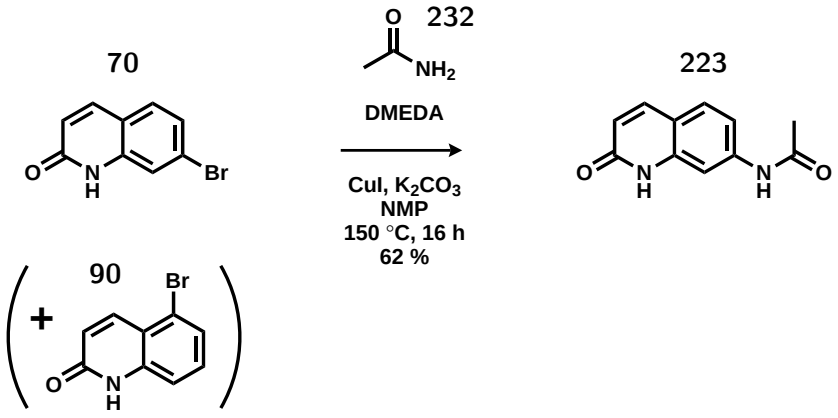

Scheme 5.11 Reaction of bromoquinolone **70** with acetamide **232**.

5.2.3 Initial Steps – Naphthyridine Unit C

This more desirable version of Unit C **233** is based around a 1,6-naphthyridine architecture with groups at the 2 and 7 positions – a highly synthetically challenging motif. Our retrosynthetic strategy was based upon the initial synthesis of naphthyridine **234** (Scheme 5.12). At the time of investigation there was only one example of **234** in the literature[165] (although recently a much simpler synthesis has been published[166]).

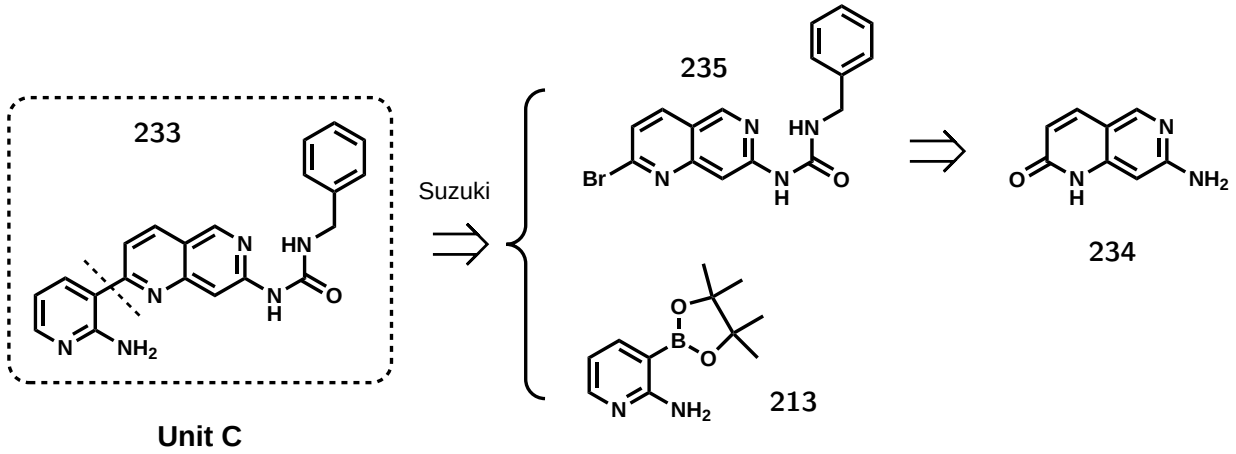

Scheme 5.12 Planned route towards 2,6-naphthyridine Unit C **233**.

The synthesis described by Barvian and co-workers[165] was non-trivial (Scheme 5.13). It involved five steps, the first three of which were particularly challenging.

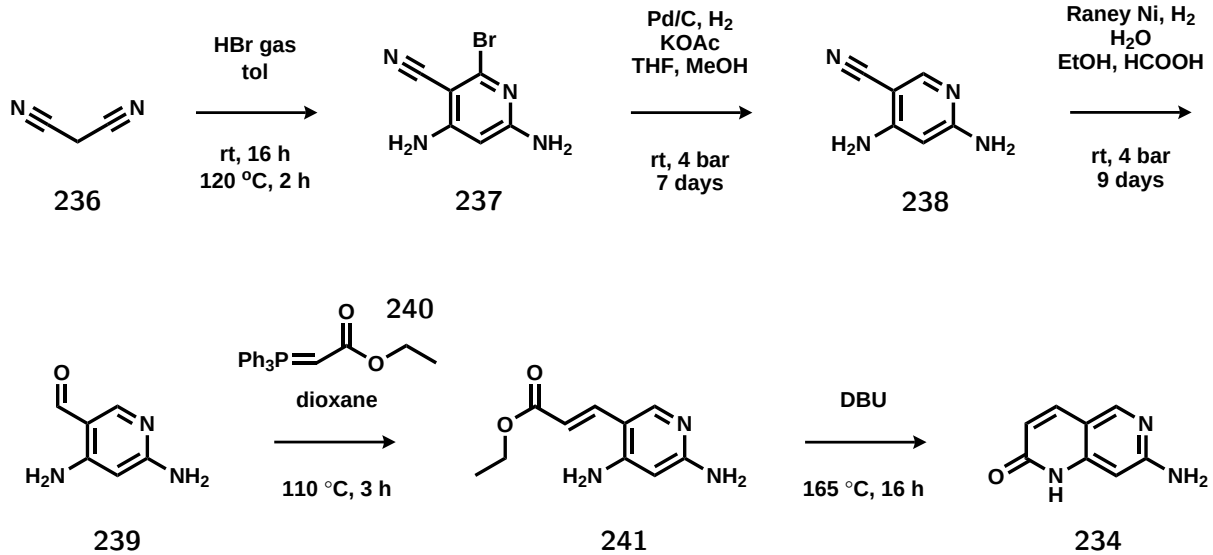

Scheme 5.13 Literature synthesis of 2,6-naphthyridone **234**.[165]

Initially, dry HBr gas was reacted with malononitrile **236** to form pyridine **237**. This highly corrosive acidic reagent was produced *in situ* by following a very convenient procedure reported in

1994 by Schlosser and co-workers.[167] The experimental setup is shown in Fig. 5.3.

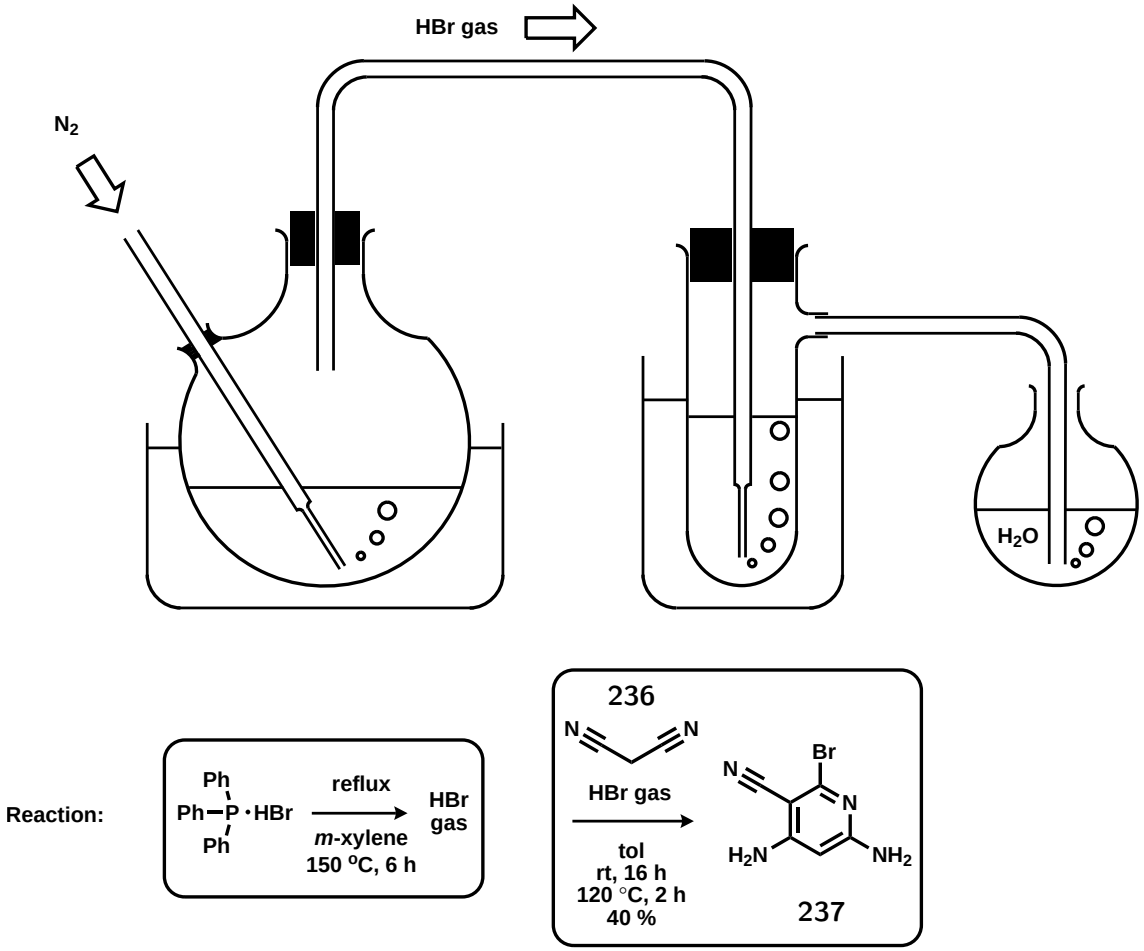

Fig. 5.3 Experimental setup for simultaneous generation of HBr gas and formation of pyridine **237**.

A 1:1 mixture of *tert*-butyl bromide and triphenylphosphine was refluxed with a catalytic amount of tetrabutylammonium bromide, this reagent serving to accelerate the decomposition of *tert*-butyl bromide (Scheme 5.14). Isobutene was released, and the HBr combined with the PPh_3 in a quarternization reaction. After 90 minutes only the solid PPh_3·HBr salt remained in the flask. At this point, xylene was added to the reaction vessel and the mixture was heated to reflux. The PPh_3·HBr salt rapidly decomposed, evolving dry HBr gas. A gentle stream of nitrogen was sent through the solution, thus evacuating the HBr through a custom-made glass tube fitted to the top of the condenser, guiding the HBr gas into a second flask containing malononitrile in toluene at room temperature. The main challenge was ensuring that the *tert*-butyl bromide did not evaporate during the first phase of HBr generation – the main reason for unsuccessful initial experiments.

The HBr was produced continuously for around 6 hours, at which point the glass tube was removed and the malononitrile reaction mixture was stirred for 16 hours, then refluxed for 2 hours. The

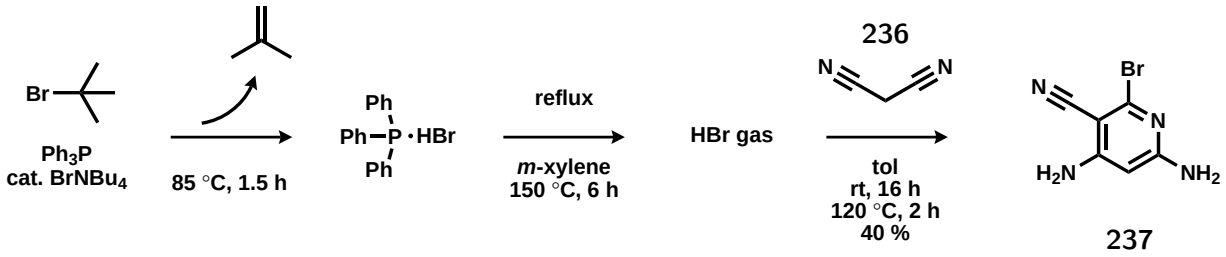

Scheme 5.14 Formation of dry HBr gas for reaction with malononitrile **236** to form pyridine **237**.

product was isolated in 40 % yield by filtration, with subsequent spectroscopic analysis confirming that pyridine **237** had indeed been synthesised.

The next step in the synthesis of naphthyridine **234** was to replace the bromine with a hydrogen substituent. Initial experiments focussed on ways to improve upon the Barvian synthesis[165] and avoid, if at all possible, a 7-day hydrogenation under pressure en route to pyridine **238** (Table 11.4, Appendix C).

We attempted to improve upon this methodology by treating pyridine **237** with DIBAL, the hope being this would not only reduce the nitrile to an aldehyde,[168,169] but result in debromination.[170,171] Following literature procedure for the reduction of a nitrile on a related compound,[172] pyridine **237** was stirred at −78 ℃ with DIBAL in toluene. Spectroscopic analysis suggested that a potential reaction may be taking place, but time constraints did not allow for any further investigation.

We also tried to remove the bromine simply by treating pyridine **242** with *n*-BuLi then quenching with water, an attempt for which the results were once again inconclusive.

Based upon a report by Zhang and co-workers,[173] a catalytic debromination with Cs_2CO_3, $Pd(PPh_3)_4$, and EtOH was attempted, to no avail. Finally, several experiments utilising Bu_3SnH as a hydride donor were attempted, in the presence of AIBN and $Pd(PPh_3)_4$ respectively. To our disappointment, these reactions again yielded a complex mixture of compounds in which the desired pyridine **238** was not evident.

Eventually, we accepted that the long hydrogenation from the literature was our best hope (Scheme 5.15). Bromopyridine **237** was stirred under a hydrogen atmosphere of 4.5 bar, with Pd/C and KOAc in a solvent system of THF and MeOH, for 10 days. Gratifyingly, spectroscopic analysis confirmed that the desired pyridine **238** had been synthesised in excellent yield. However, time constraints halted our investigations at this juncture, and our efforts were focussed upon furthering the synthesis of an improved variant of Unit A.

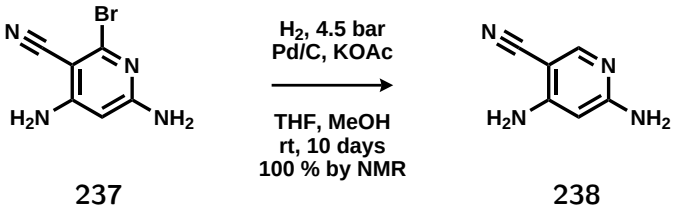

Scheme 5.15 Successful debromination of pyridine **237**.

5.3 Unit A – Pyridine

5.3.1 Retrosynthesis

It was proposed that the key disconnection of Unit A could again be achieved by a Suzuki coupling, a particularly attractive strategy given the expertise we had developed in that area. Such an approach would require the preparation of bromopyridine **243** and boron derivative **244** ready for Suzuki coupling (Scheme 5.16).

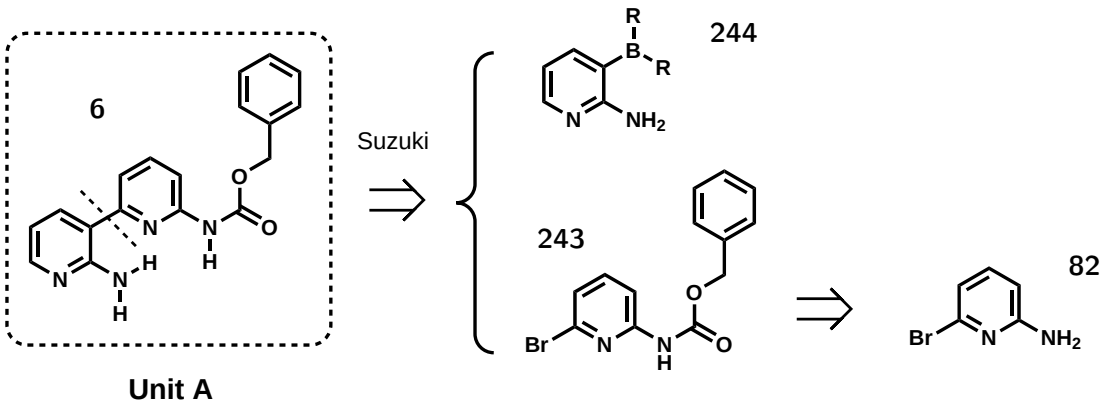

Scheme 5.16 Retrosynthetic approach to bisaminopyridine Unit A **6**.

5.3.2 Boronic Acid Synthesis

It was thought that the presence of a primary amine may be detrimental to the outcome of a bromine-lithiation protocol, when installing the necessary boronic acid functionality. Therefore, we instead investigated an ortho-lithiation strategy, utilising Boc-protected aminopyridine **245** (Scheme 5.17).

Under well-documented Et_3N/DMAP/DCM conditions,[174] the initial Boc-protection step did not proceed well. A small amount of product was produced, along with at least two other unidentifiable impurities, which were the major components of the reaction mixture. However, the protection did work well using *tert*-butanol as solvent and only Boc_2O as reagent,[175] providing **245** in good yield.

The Boc group is well-known as a good directing group for ortho-lithiation.[121] However, despite

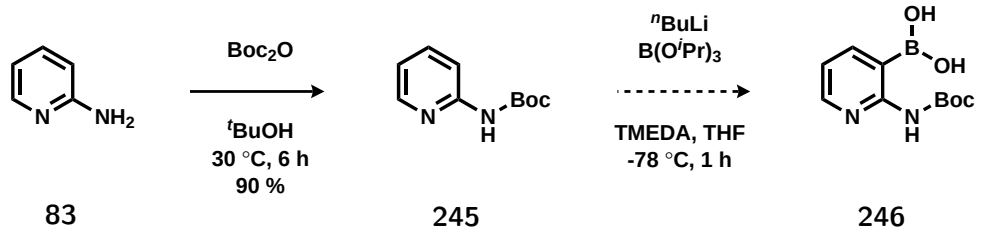

Scheme 5.17 Boc-protection and attempted ortho-lithiation of 2-aminopyridine **83**.

our best efforts, compound **246** could not be synthesised, with starting material recovered on every occasion.

We decided a better approach would be to employ commonly-available 2-amino-3-bromopyridine **247** as a substrate, with the aim of pursuing a bromine-lithium exchange approach towards boronic acid **246**.

Firstly, amine **247** was Boc-protected. The desired compound **248** was synthesised in acceptable yield using the same conditions as previously for 2-aminopyridine (Scheme 5.18).

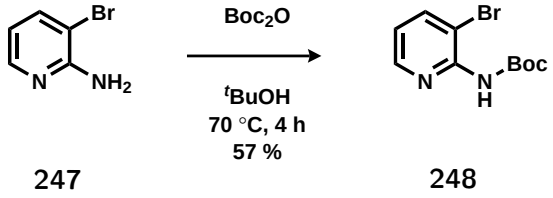

Scheme 5.18 Boc-protection of 2-amino-3-bromopyridine **247**.

The next step was to transform bromopyridine **248** into boronic acid **246** (Scheme 5.19). However, repeated attempts to synthesise the acid were unsuccessful. Despite using three equivalents of *n*-BuLi, mainly starting material **248** was recovered, with a small fraction of quenched material **245** present in the reaction mixture. These results suggest that bromide **248** was reluctant to undergo bromine-lithium exchange; and even when this could be achieved, the lithiation species thus formed did not undergo trapping with $B(O^iPr)_3$.

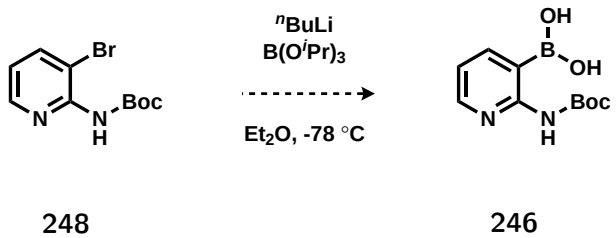

Scheme 5.19 Attempted transformation of **248** into boronic acid **246**.

Our experience with boronic acids led us to believe that there was a chance that the boronic acid **246** was being formed, but not isolated. We therefore attempted to instead synthesise the pinacol

ester **249**, which was thought to be easier to isolate (Scheme 5.20).

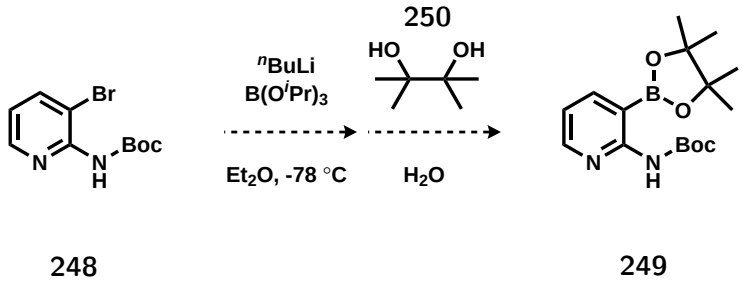

Scheme 5.20 Attempted formation of pinacol ester **249**.

Following lithiation, B(O^{i}Pr)$_3$ was again added to the reaction mixture before quenching and acidification to neutral pH. 2,3-Dimethylbutane-2,3-diol **250** was then added, and the reaction stirred. Disappointingly, this attempt returned mostly debrominated starting material, with none of the desired pinacol ester present. Experiments with trimethyl borate and tri-*tert*-butyl borate produced the same result. When the solution was deliberately quenched with water following the addition of *n*-BuLi, purely debrominated pyridine **245** was isolated. In contrast to our earlier experiments when forming the boronic acid, this result shows that bromine-lithium exchange was now readily taking place, but the anion was not trapping the borate. It is possible that the Boc group was preventing the trapping from taking place due to steric considerations, or the carbonyl was coordinating to the lithium anion.

Given these difficulties, we instead attempted to synthesise the boronic acid **251** from the primary amine **247**. Boronic acid **251** had been previously reported in the literature but only on a single occasion.[176] However, there was found to be good precedent[177–179] for the formation of pinacol boron esters from brominated heteroaryl systems containing a primary amine moiety, utilising a Suzuki-type coupling to achieve the desired transformation.

In exploring this methodology, we found that catalytic systems using both Pd(dppf)Cl$_2$ and Pd$_2$dba$_3$ produced the desired boron pinacol ester **213**. However, this compound did prove to be very sensitive to exposure to silica gel. Despite repeated attempts at purification by flash column chromatography, only small amounts of the boronic acid **251** could be recovered, with none of the pinacol compound **213** isolated (Scheme 5.21).

For this reason, the crude reaction mixture containing **213** was merely filtered through celite and then concentrated *in vacuo* (Scheme 5.22). ^{1}H NMR analysis indicated pleasingly good conversion for this transformation, with the Pd(dppf)Cl$_2$ conditions performing better than the Pd$_2$dba$_3$ conditions (80 % yield versus 62 %). We proposed to submit the unpurified boronic ester **213**

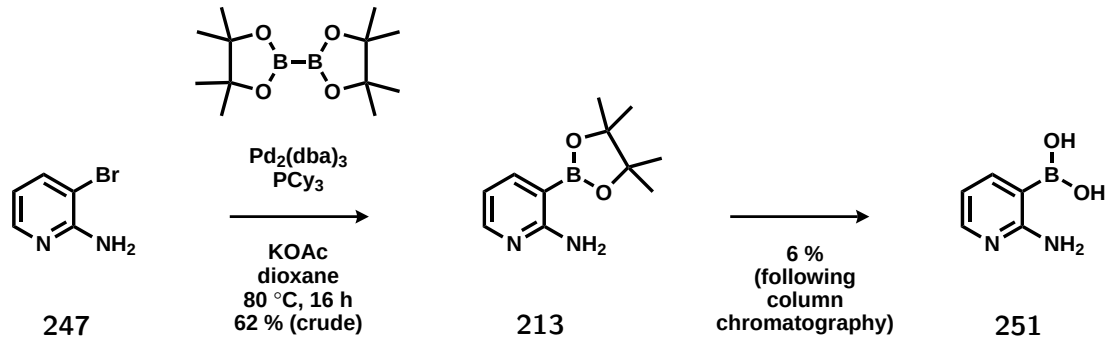

Scheme 5.21 Synthesis of pyridine boronic acid **251**.

directly to the subsequent Suzuki coupling with the hope that any impurities present would not adversely affect this key transformation.

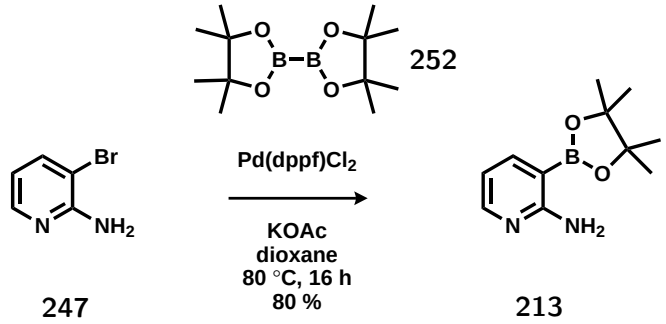

Scheme 5.22 Synthesis of pyridine pinacol ester **213**.

5.3.3 Coupling Partner Synthesis

With boronic ester **213** now successfully synthesised, our attention turned towards the synthesis of the brominated coupling partner **243**. The synthesis was achieved by reacting 2-amino-6-bromopyridine **82** with benzyl chloroformate **216** (Scheme 5.23), the product being isolated in good yield by recrystallization.

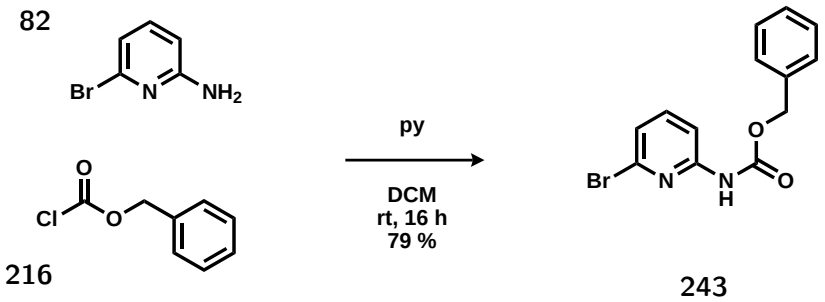

Scheme 5.23 Synthesis of pyridine carbamate **243**.

5.3.4 Alternative Coupling Partner

A similar coupling partner to bromopyridine **243** was also synthesised. Bromopyridine **253** was formed by reacting 2-amino-6-bromopyridine **82** with benzoyl chloride **185** (Scheme 5.24).

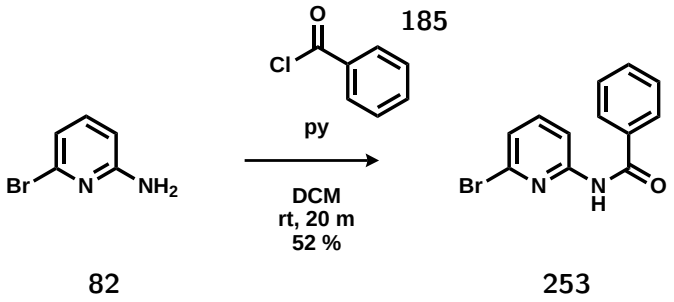

Scheme 5.24 Synthesis of bromopyridine **253**.

In order to investigate alternative routes towards Unit A, we proposed that bromopyridine **253** be converted to the boronic acid **254** and the pinacol ester **255**. Unfortunately, this approach failed despite multiple attempts (Scheme 5.25). Again, bromine-lithium exchange was thought to be taking place, but the lithiated species did not trap the borate as only quenched material could be isolated. Using freshly distilled $B(OMe)_3$ made no difference. Subsequent attempts to repeat the successful Suzuki coupling of pinacolato diboron **252** with 2-amino-3-bromopyridine **247** (Scheme 5.22) by trying to couple pinacolato diboron **252** with bromopyridine **253** were all unsuccessful, returning only starting material.

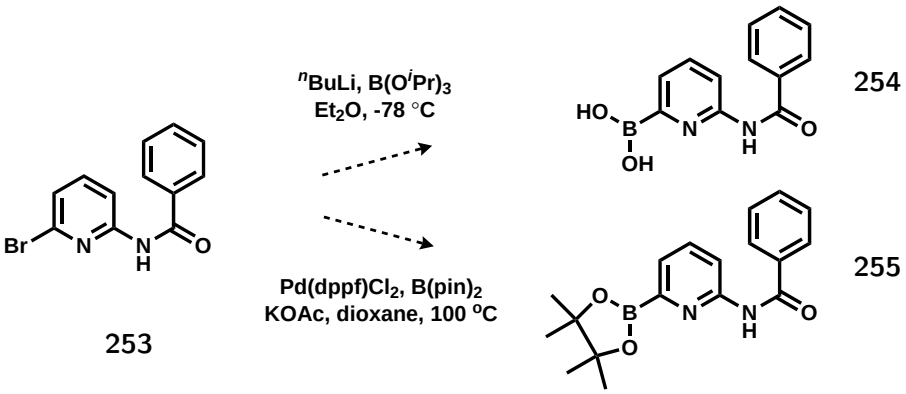

Scheme 5.25 Failed attempts to convert bromopyridine **253** to the boronic acid **254** and pinaol ester **255**.

5.3.5 Suzuki Coupling

With the two subunits now synthesised, the stage was set for the key bond-forming transformation. To our delight, the Suzuki coupling between the pyridine carbamate **243** and the pinacol ester

213 yielded bipyridine Unit A **6** in 72 % yield (Scheme 5.26). This reaction performed best when the pinacol ester **213** was concentrated *in vacuo* in the flask, and the same flask used for the Suzuki coupling. Small crystals of **6** just large enough for X-ray crystallography could be formed by slow evaporation from Et_2O. The crystal structure is shown in Fig. 5.4. It is pleasing that the two pyridine rings lie in a mostly planar conformation, with a torsion angle of 29 °C (Appendix B, Chapter 10).

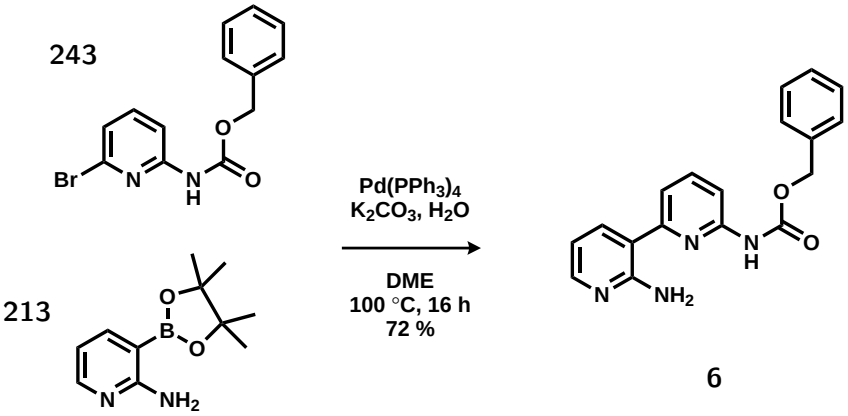

Scheme 5.26 Suzuki coupling of pyridine carbamate **243** with boron pinacol ester **213** to give Unit A **6**.

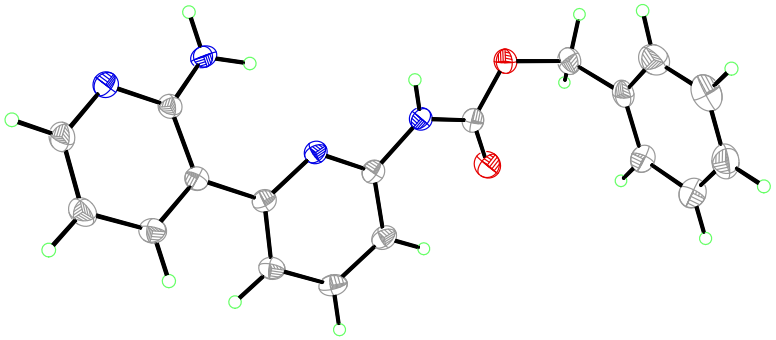

Fig. 5.4 Crystal structure of Unit A **6**.

The alternative bromopyridine coupling partner **253** was also successfully coupled under Suzuki conditions to boron pinacol ester **213** (Scheme 5.27). The desired compound **256** was isolated in a disappointing 27 % yield.

Again with the aim to investigate divergent synthetic routes towards Unit A, we also coupled the boron pinacol ester **213** with 2-amino-6-bromopyridine **82** (Scheme 5.28). The coupling was successful, although the product **257** was difficult to separate from a number of other unidentifiable aromatic impurities by flash column chromatography.

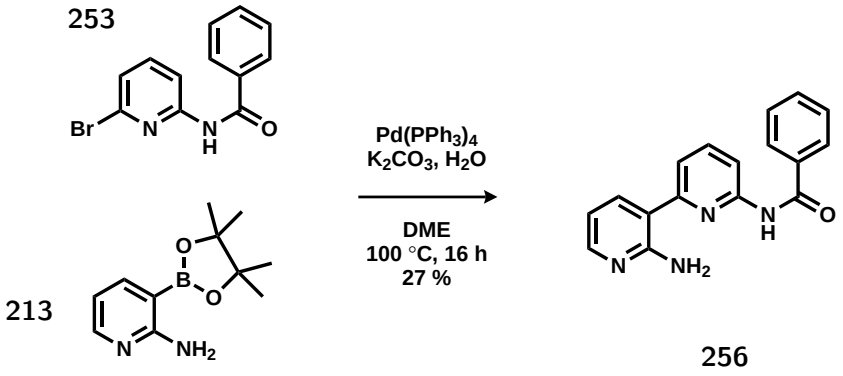

Scheme 5.27 Suzuki coupling of bromopyridine **253** with boron pinacol ester **213**.

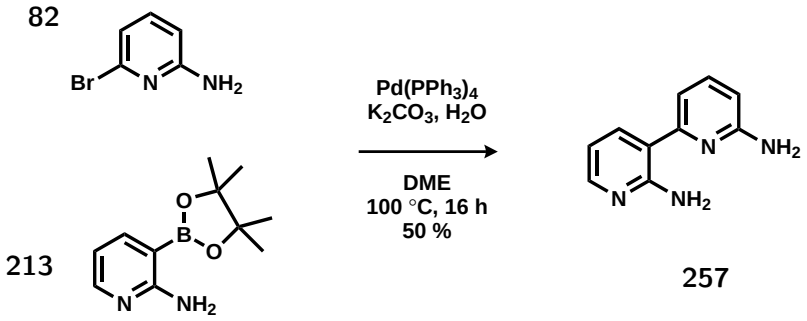

Scheme 5.28 Suzuki coupling of 2-amino-6-bromopyridine **82** with boron pinacol ester **213**.

5.3.6 Solubility

It was to our great delight that non-pyridone Unit A **6** was soluble in $CDCl_3$. Needless to say, we were extremely gratified to find that the solubility problems, which had for so long been a major obstacle in these investigations, could be overcome. This pleasing result further confirmed our growing conviction that the 2-pyridone motif is unsuitable for use in such molecular architectures.

5.4 Unit A – Pyrimidine

5.4.1 Retrosynthesis

Following the successful synthesis of the simplified variant of Unit A, our attentions turned to the pyrimidine-based version, in which an intramolecular H-bond is believed to be present. This new variant of Unit A **5** can be synthesised using the same Suzuki coupling methodology as for the pyridine-based Unit A **5** (Scheme 5.29). With boron pinacol **213** already in hand, the synthesis of pyrimidine precursor **258** alone remained. This subunit could be accessed in one step by reacting benzyl isocyanate **259** with pyrimidine amine **260**.

To our concern, there was only one example,[180] reported in 1947 by Golding and Senear, of

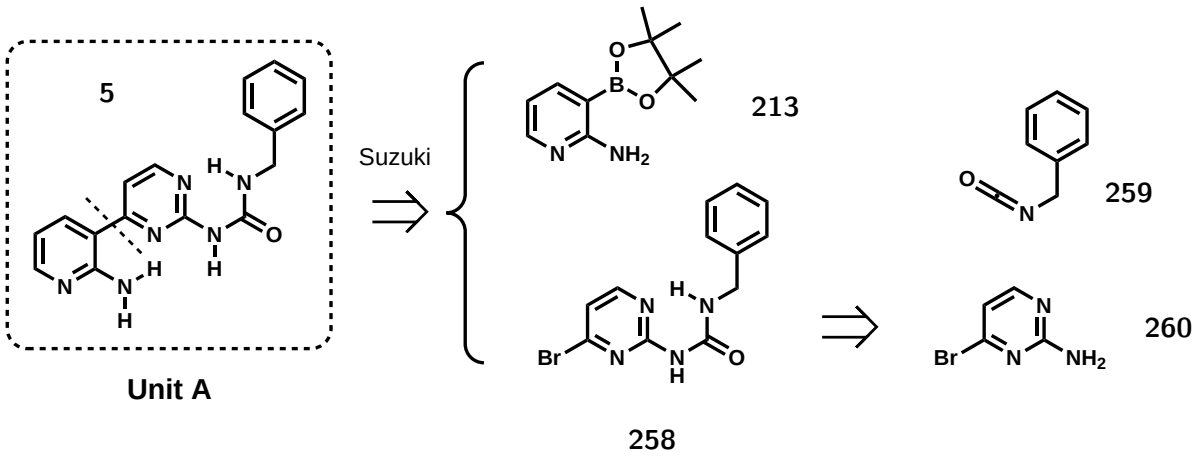

Scheme 5.29 Retrosynthetic approach to pyrimidine urea Unit A **5**.

2-amino-4-bromopyrimidine **260** present in the literature, and only two examples of the similar 2-amino-4-bromo-6-methylpyrimidine **261**.[180,181] Golding and Senear synthesised bromopyridine **260** by treating isocytosine **262** with phosphorus oxybromide at 135 °C. The reported yield was only 16 %, with limited spectroscopic analysis available.

Despite this unencouraging precedent, we attempted the aforementioned synthesis of pyrimidine **260**, with isocytosine **262** thus being the first synthetic target. We were pleased to note that there was considerable literature precedent for the synthesis of isocytosine **262**.[182–186] We thus elected to react dimethyluracil **263** with guanidine **264**.[185,186] The dimethyluracil **263** was in turn easily accessible *via* the methylation of uracil **265**, again following a straightforward literature procedure[187] (Scheme 5.30).

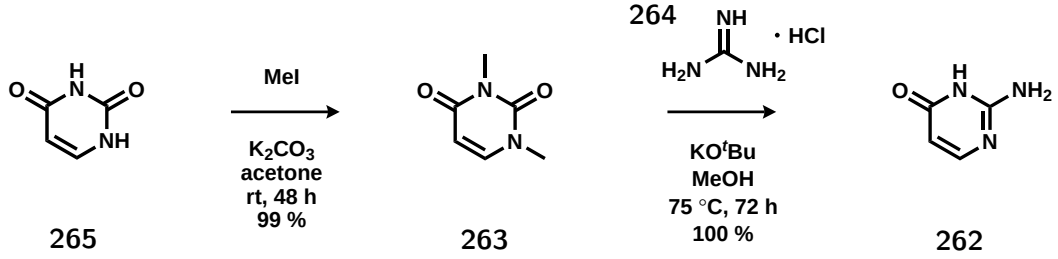

Scheme 5.30 Methylation of uracil **265** followed by reaction of diemethyluracil **263** with guanidine **264** to make isocytosine **262**.

5.4.2 Synthesis

The initial methylation step in our synthesis of the pyrimidine-based version of Unit A proceeded in excellent yield. However, the reaction of diemethyluracil **263** with guanidine **264** to yield isocytosine **262** proved to be rather more challenging (Scheme 5.30).

The solubility of uracil **263** in organic solvents was found to be limited, and thus it was necessary for the reaction to be conducted in MeOH rather than EtOH. Based upon literature precedent,[185,186] our initial investigations employed NaOMe as a deprotonating agent. ^{1}H NMR analysis of the crude reaction mixture suggested that isocytosine **262** was successfully synthesised when freshly-prepared NaOMe was added. The use of commercially-prepared NaOMe was found to extend the reaction time. Following further investigation, we were pleased to note that KO^{t}Bu could instead be employed as a base, again affording isocytosine **262** as desired.

Further challenges arose during attempts at isolating isocytosine **262**. This product is soluble in water, but not in typical organic solvents such as DCM or Et_2O, making separation from the excess guanidine reagent **264** difficult. Thus, we aimed to reduce the quantities of guanidine present in the reaction mixture in the hope that it would aid isocytosine **262** isolation. The literature example utilised 8 equivalents of guanidine and base, providing a mixture following reaction that was approximately 80 % guanidine.

We thus reduced the loading of this reagent incrementally, but noted a concomitant increase in reaction time to 96 hours when 3 equivalents were employed. Reducing the guanidine loading below 3 equivalents resulted in incomplete conversion to the desired product **262**.

Following these investigations, many attempts were made at separating isocytosine **262**, guanidine **264**, and the dimethyl urea (DMU) side-product. Washing the reaction mixture with DCM made no difference to the relative amounts of all three. Some progress was made when MeOH was added, as all three reaction components dissolved. DCM was slowly added on top of the MeOH, resulting in the formation of a precipitate in the DCM phase. The MeOH/DCM mixture was decanted off, concentrated *in vacuo*, and subjected to ^{1}H NMR analysis. The resulting spectra indicated the presence of isocytosine **262** and DMU, a promising outcome given that the guanidine **264** had been successfully removed. Unfortunately the DMU proved to be difficult to separate from the isocytosine: water was added and the solution extracted with DCM or EtOAc. To our dismay, the organic phase was devoid of the desired product **262**.

A little more progress was made by dissolving the reaction mixture in MeOH, then slowly adding Et_2O on top of the MeOH. An oily substance appeared at the bottom of the flask. The MeOH/Et_2O was decanted off and concentrated, and the oily substance isolated. ^{1}H NMR analysis of the decant showed a product:DMU ratio of 1:17. In contrast, the oily substance was found to be a product:DMU mixture in the ratio 1:3. The DMU was therefore dissolving preferentially in the MeOH/Et_2O solvent, and thus repeating this decanting procedure improved the purity of the isocytosine product.

Following these extensive purification attempts, isocytosine **262**, in as good a state of purity as could be achieved, was carried forward to the next reaction; the transformation into bromopyrimidine **260** (Scheme 5.31).

Scheme 5.31 Transformation of isocytosine **262** into bromopyrimidine **260**.

Treating **262** with both neat PBr_3 and neat $POBr_3$ produced the desired bromopyrimidine **260**, with $POBr_3$ affording much better yields. Purification by continuous extraction for 16 hours into EtOAc enabled bromopyridine **260** to be isolated in 67 % yield, with only minor contamination from the isocytosine starting material **262**.

5.4.3 Methyl Isocytosine

The methyl isocytosine **266** was also proposed as a desirable alternative subunit. The methyl group would not interfere with the synthesis or function of Unit A, and there were many examples of the construction of **266** in the literature.[185,188–191]

Drawing inspiration from Braker and co-workers,[190] ethyl acetoacetate **267** was stirred with guanidine hydrochloride **264** and sodium methoxide at reflux in EtOH (Scheme 5.32).

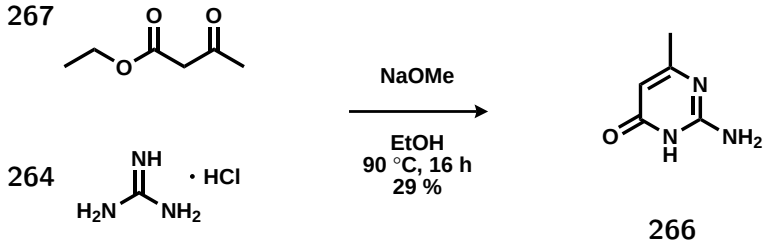

Scheme 5.32 Synthesis of methyl isocytosine **266**.

Once again however, the purification of the resulting reaction mixture was very difficult. Methyl isocytosine **266** is water-soluble, and separation from NaOH was a problem. The crude reaction mixture contained an insoluble precipitate, which was isolated by sinter filtration and dissolved in MeOH, then sinter-filtered again. The filtrate was found to contain the product **266**, but in even lower purity than before. Similarly, filtering through an inch of silica reduced the purity further. Attempts at further purification did not prove successful. We found that the purity was slightly improved by concentrating the crude reaction mixture *in vacuo*, then dissolving in a small amount

of water and filtering. However, ^{1}H NMR analysis in $CDCl_3$ showed the product to still be a minor compound. The highest purity product achieved was isolated by removing the EtOH solvent under reduced pressure, washing the remaining mixture with EtOAc, and allowing the H_2O phase to stand overnight. The product precipitated out of solution and was filtered off. However, ^{1}H NMR analysis still showed the presence of some guanidine.

Given these considerable difficulties with purification, we attempted to react the impure methyl isocytosine **266** with phenyl isocyanate **268** to form urea **269** (Scheme 5.33). The experiments were not successful, returning only starting material and phenyl isocyanate.

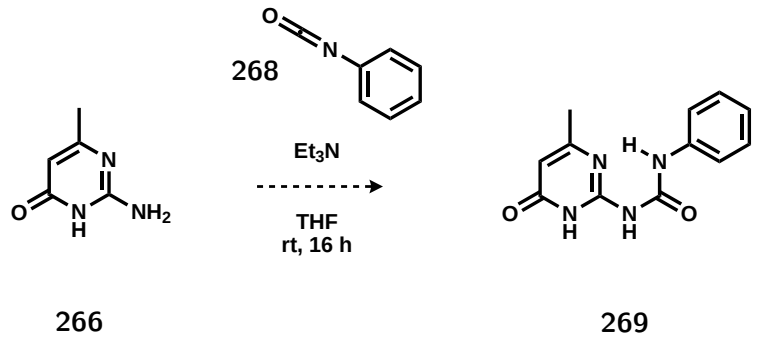

Scheme 5.33 Attempted synthesis of urea **269**.

Attempts were then made to transform methyl isocytosine **266** into pyrimidine bromide **261** with $POBr_3$, and into the pyrimidine chloride **270** with $POCl_3$ (Scheme 5.34). After refluxing for 3 hours in $POBr_3$, quenching with water, and basifying to pH 14, the extraction into DCM yielded only a very small amount of the desired product **261**, with ^{1}H NMR analysis indicating the presence of a range of unidentifiable impurities. Following the same procedure for $POCl_3$, a similar result was obtained.

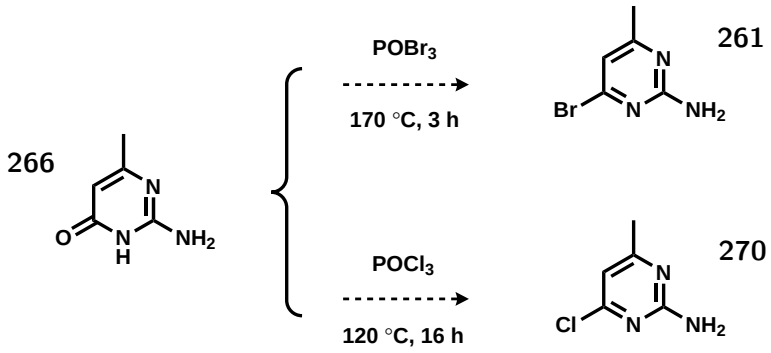

Scheme 5.34 Attempted synthesis of pyrimidine bromide **261**.

Given the considerable difficulties experienced in synthesising and isolating bromopyridine **260** and methyl isocytosine **266**, the decision was made to abandon this route towards the pyrimidine-

based variant of Unit A.

5.4.4 Cyclisation

An alternative strategy towards the pyrimidine architecture of Unit A was developed, again utilising a guanidine cyclisation as the key step (Scheme 5.35). There was considerable literature precedent for the synthesis of pyrimidines *via* the reaction of an ynone with a guanidine functionality.[192–195] It was therefore proposed that treating ynone **271** with a guanidine-urea **272** would directly deliver the pyrimidine **273** that we required.

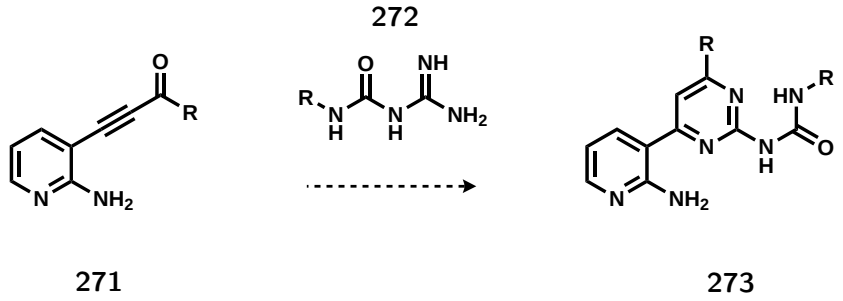

Scheme 5.35 Cyclisation strategy to form pyrimidine-based Unit A **273**.

Therefore, this approach required the synthesis of an alkyne-substituted pyridine, which could then be treated with DMF·DMA to install an ynone functionality. We employed a Sonogashira coupling of 2-amino-3-bromopyridine **247** and trimethylsilylacetylene **274** to give alkyne pyridine **275** (Scheme 5.36). Following initially unsuccessful literature conditions[196] using CuI, DIPEA, NMP, and $Pd(PPh_3)_4$, we found that palladium acetate in DMF at 50 °C delivered the desired product **275** in 69 % yield.

We next needed to remove the trimethylsilyl group on **275** to give the alkyne **276** (Scheme 5.36). Pleasingly, the desilylation reaction with K_2CO_3 in MeOH proceeded to completion in two hours at room temperature, and produced clean product. TBAF in THF delivered the product, but these conditions required heating to 50 °C for 16 hours in order to achieve the desired transformation.

Next, alkyne **276** was Boc-protected to afford Boc-pyridine **277** in good yield (Scheme 5.37). However, the planned transformation from Boc-pyridine **277** to the ynone **278** using DMF·DMA could not be achieved (Scheme 5.37). Even following purification by flash column chromatography, there were at least three unidentifiable aromatic compounds present. For this reason, and the development of an alternative alkynol Sonogashira strategy (see below), investigation of this synthetic route was put on hold.

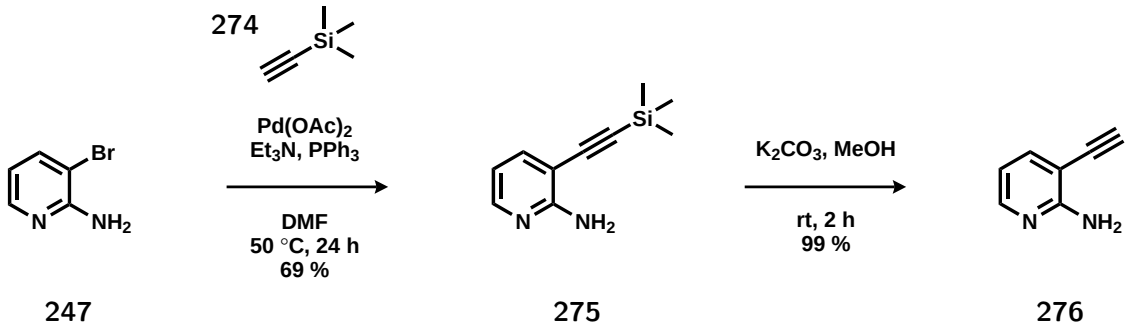

Scheme 5.36 Sonagashira coupling of 2-amino-3-bromopyridine **247** and trimethylsilylacetylene **274**, followed by removal of the trimethylsilyl group to give alkyne **276**.

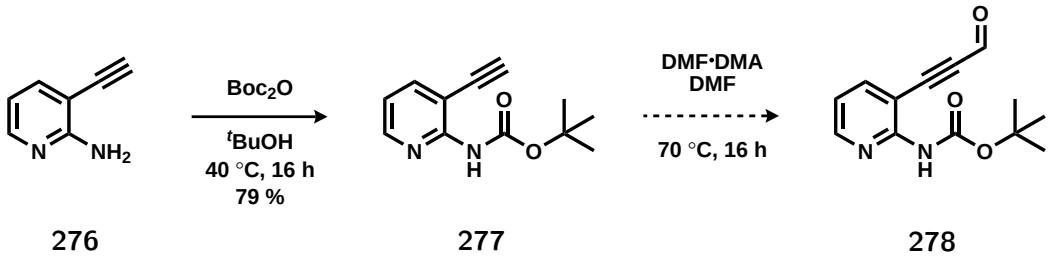

Scheme 5.37 Boc-protection of alkyne **276** to give boc-pyridine **277**, and attempted synthesis of ynal **278**.

5.4.5 Alkynol Sonogashira

It was proposed that the desired ynone motif could instead be accessed by performing a Sonogashira coupling with an appropriate alkynol species, and subjecting the resulting alcohol to oxidation conditions.

After some experimentation, the Sonogashira coupling between 2-amino-3-bromopyridine **247** and 1-octyn-3-ol **279** was achieved, providing alkyne pyridine **280** in a respectable 81 % yield (Scheme 5.38).

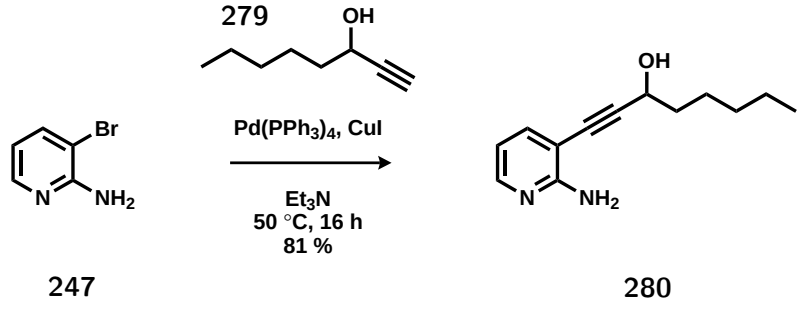

Scheme 5.38 Sonagashira coupling of 2-amino-3-bromopyridine **247** and 1-octyn-3-ol **279** to give alkyne pyridine **280**.

The oxidation of alcohol **280** to provide ynone **281** was surprisingly challenging (Table 5.1). Manganese dioxide[197,198] produced the desired product, but it could only be isolated in low yield.

Table 5.1 Oxidation of ynol **280**.

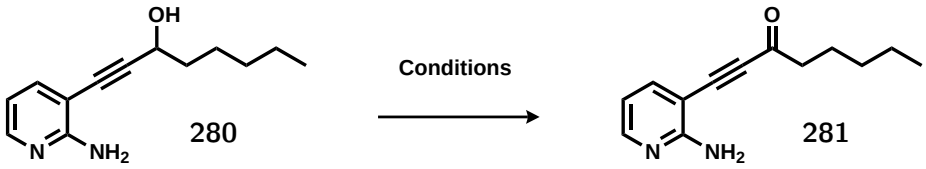

	Conditions	Yield	Comments
1	MnO_2	12 %	Very difficult to repeat
2	PCC	20 %	Good crude yields, but poor yields following column chromatography
3	IBX	78 % (crude)	Poor yields following column chromatography. Difficult to repeat
4	Parikh-Doering	62 %	Scaling up the reaction made no difference to yields
5	DMP	64 %	Best conditions found

Moreover, the reaction proved very difficult to repeat. PCC[199,200] with celite produced promising results, but the mass recovery following flash column chromatography was very poor, giving a yield of 20 %. It was not clear exactly how the compound was being lost. Like PCC, oxidations with IBX[201,202] produced good crude yields, as high as 78 %, although some aromatic impurities were evident following ^{1}H NMR analysis. However, these results proved very difficult to repeat.

The Parikh-Doering oxidation[203,204] was attempted under standard conditions. The reaction appeared to proceed to completion by TLC analysis. Despite this positive observation, yields above 62 % could not be obtained following purification by flash column chromatography. Scaling-up the reaction did not improve the yield. No starting material was ever recovered from the reaction mixture, and we thus proposed that the ynol product was unstable on silica.

Oxidation under Dess-Martin conditions[205,206] again appeared to proceed to completion by TLC analysis, but yields above 64 % could not be obtained following purification by flash column chromatography, adding weight to the suggestion that the product is unstable on silica. However, of all the conditions tried (Table 5.1), DMP provided the highest yield (Scheme 5.39).

With ynone **281** now in hand, the next step in the synthetic pathway was the protection of the amine in preparation for the subsequent cyclisation step. Ynone **281** was smoothly Boc-protected

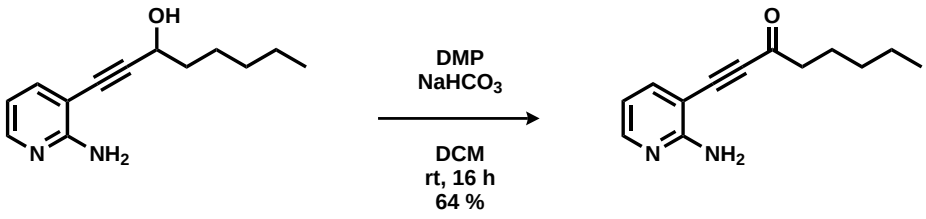

280 281

Scheme 5.39 Final oxidation of ynol **280** to provide pyridine ynone **281**.

in a 42 % yield under standard conditions[207,208] (Scheme 5.40).

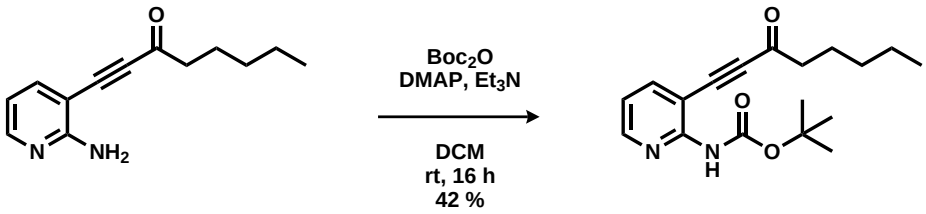

281 282

Scheme 5.40 Boc-protection of ynone **281**.

We were now in a position to attempt the cyclisation of Boc-protected ynone **282** to make Boc-protected precursor **283** to Unit A (Scheme 5.41). Multiple attempts at this reaction provided complex reaction mixtures, with very low mass recovery. We therefore put the Boc-protected cyclisation on hold, and instead attempted this process in the absence of the Boc protecting group.

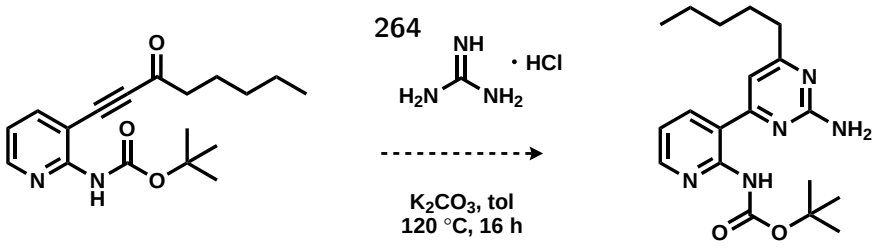

282 283

Scheme 5.41 Attempted formation of Boc-protected Unit A **283**.

The initial cyclisation attempts of pyridine ynone **281** with guanidine hydrochloride **264** to give biaryl **284** produced an interesting result (Scheme 5.42). The experiments were performed at reflux in ethanol, and none of the desired cyclised product could be isolated. However, naphthyridine **285** was isolated in excellent purity, albeit in only 13 % yield. It was proposed that the ethanol attacked the alkyne moiety, allowing the amine functionality access to the ketone, and thus enabling a cyclisation to take place, forming the naphthyridine. It was clear that nucleophilic solvents must be avoided if we were to achieve our desired cyclisation product.

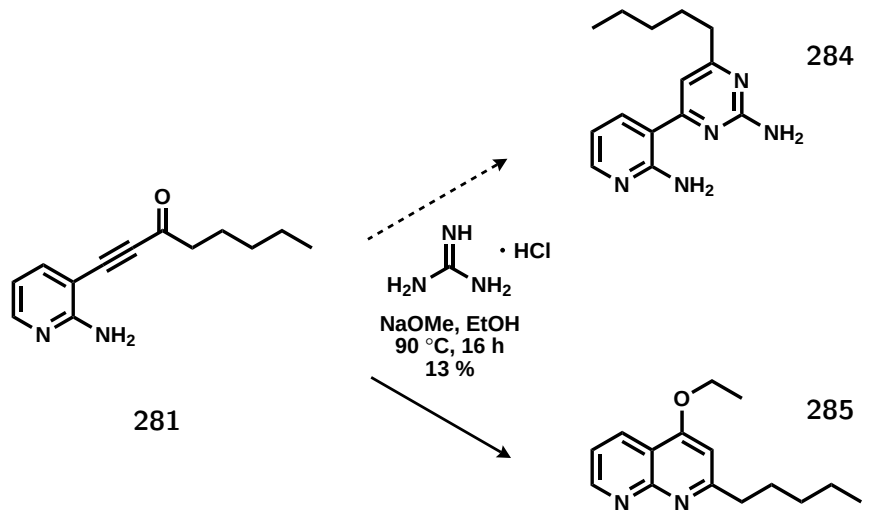

Scheme 5.42 Unexpected synthesis of naphthyridine **285**.

The proposed reaction mechanism is shown in Scheme 5.43. To our knowledge this is the first time a pyridine ring (in this case part of a naphthyridine) has been synthesised *via* this reaction.

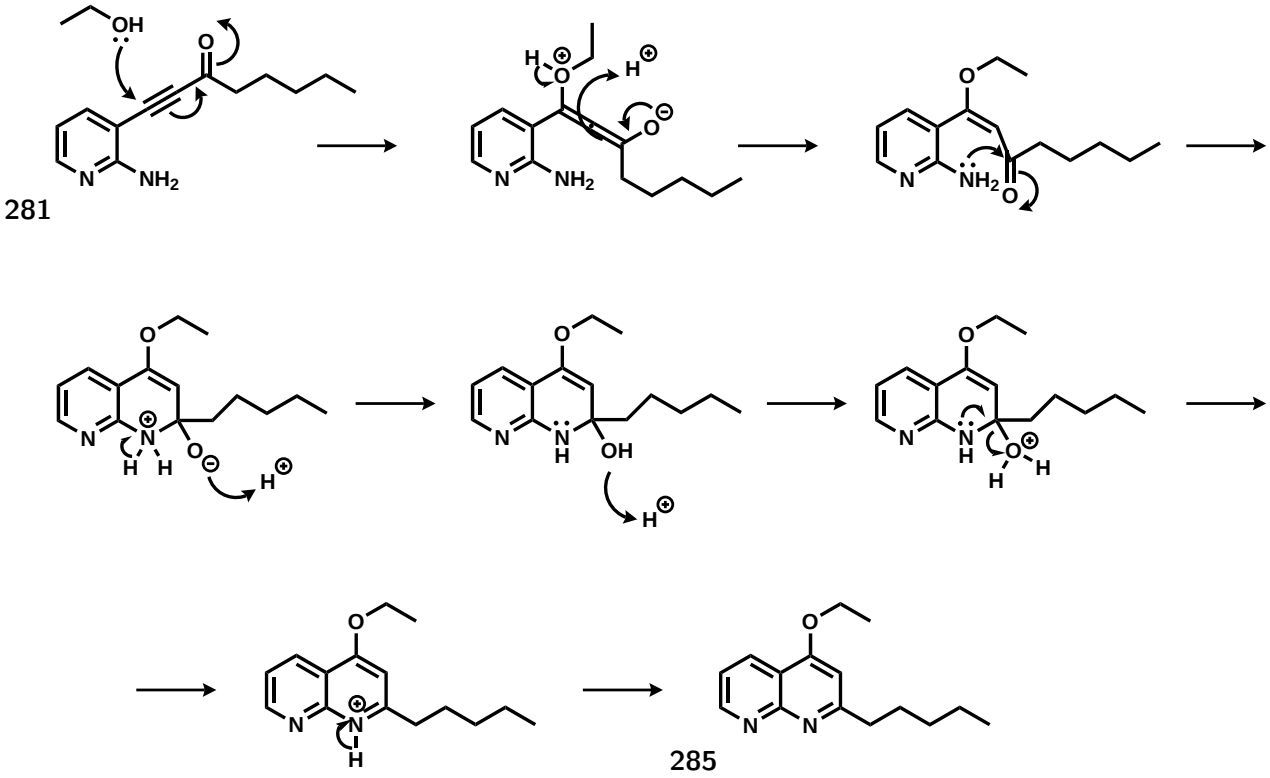

Scheme 5.43 Proposed mechanism during formation of naphthyridine **285**.

As a result, the reaction was instead attempted in toluene, with use of K_2CO_3 as a base affording the best results. An overnight reflux provided biaryl **284** in an acceptable 58 % yield (Scheme 5.44). This was an excellent result. It demonstrated that the challenging pyridine-pyrimidine structure could be synthesised using a Sonogashira coupling and ynone cyclisation strategy. It now only

remained to install the urea on the pyrimidine amine to arrive at Unit A **286**.

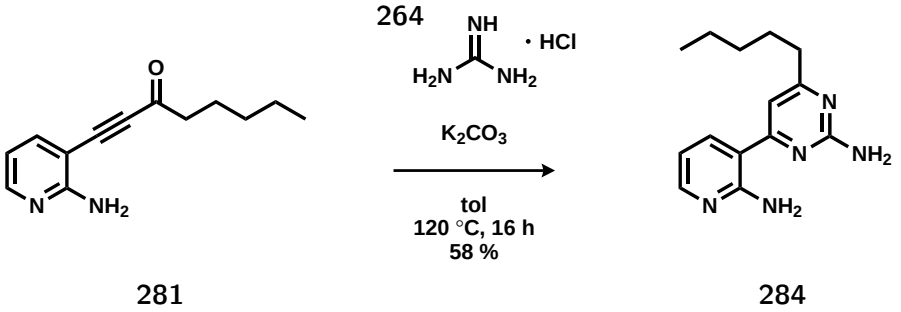

Scheme 5.44 Cyclisation of pyridine ynone **281** with guanidine **264** to give biaryl **284**.

Disappointingly, initial experiments utilising benzyl chloroformate were unsuccessful, with only starting material **284** isolated from the reaction mixture. We therefore focussed our next experiments on the reaction of phenyl isocyanate **268** with biaryl **284** to afford phenyl urea Unit A **286**. To our disappointment, but not total surprise, the pyridine amine proved to be the more reactive, and the reaction instead produced only biaryl **287** (Scheme 5.45).

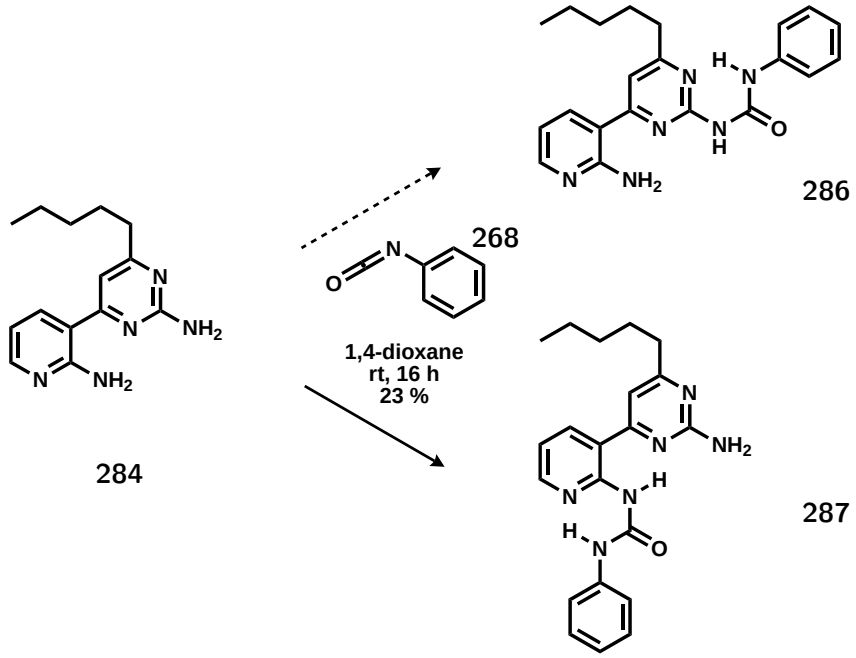

Scheme 5.45 Functionalisation of **284** with phenyl isocyanate **268** to give **287**, rather than the intended **286**.

A protection strategy was therefore attempted to arrive at Boc-protected Unit A **288**. As expected, the Boc anhydride reacted preferentially with the pyridine amine over the pyrimidine amine of biaryl **284** (Scheme 5.46). Despite using 3 equivalents of the Boc anhydride reagent, the pyrimidine amine did not react.

The Boc-protected biaryl **283** could now be reacted with benzyl isocyanate **259** in an attempt

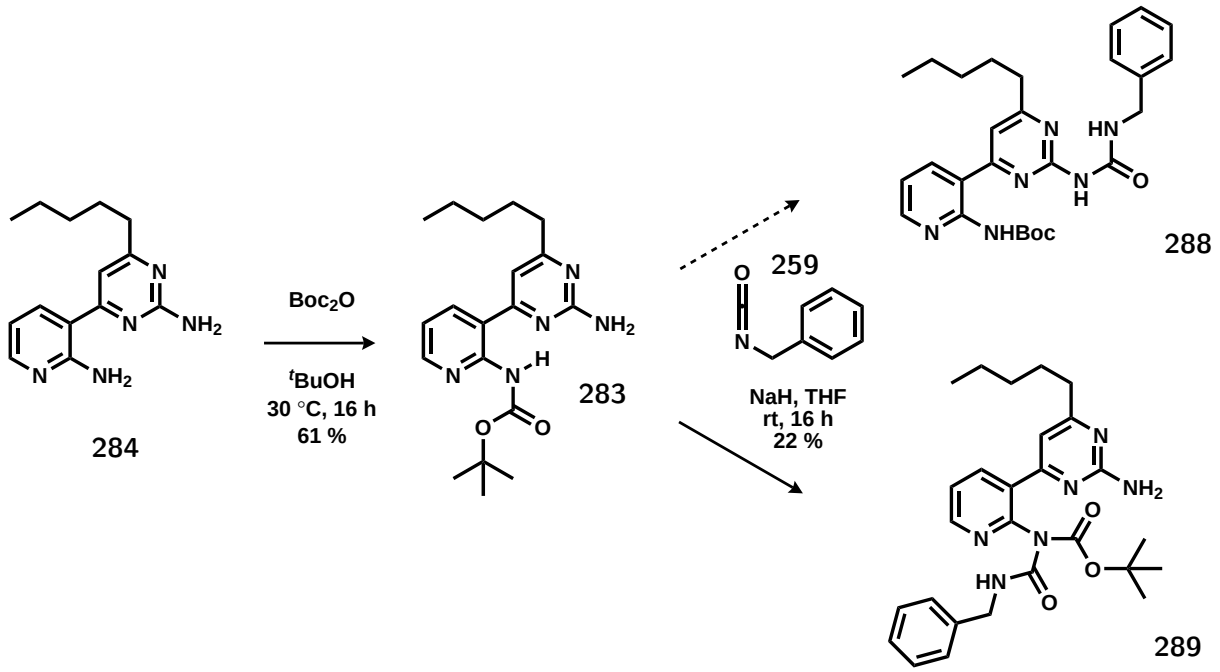

Scheme 5.46 Boc-protection of biaryl **284**, followed by attempted synthesis of boc-protected Unit A **288**.

to synthesise Boc-protected Unit A **288** (Scheme 5.46). In DCM with Et_3N, no reaction occurred, and only starting material was isolated. However, with NaH in THF the isocyanate did react, but the Boc-protected nitrogen was again the more reactive moiety, affording biaryl **289** in poor yield. The pyrimidine amine again remained unreactive.

5.4.6 Pre-Formed Urea

The failure of the protection strategy forced us to attempt cyclisation with the urea moiety already installed. This approach required the synthesis of guanidine-urea **290** (Scheme 5.47), for which there was found to be some literature precedent.[209] Unfortunately, in our hands this synthesis could not be repeated. Benzyl amine **291** was reacted with CDI **292** to form intermediate **293**, followed by the addition of guanidine hydrochloride to form **290** in a one-pot procedure. Only the double-adduct **294** was isolated, suggesting that the amine **291** had not fully reacted with the CDI in the first step.

Gratifyingly, further experimentation led to success. We deprotonated the guanidine salt **264** with sodium hydride in a solvent of MeCN, then added benzyl isocyanate (Scheme 5.48). Two different products were isolated; the desired compound **290**, and the bis-adduct **295**. The bis-adduct **295** could be isolated by quenching with water, removing the MeCN solvent under reduced pressure, and filtering off the solids from the aqueous phase. The single adduct **290** was isolated following

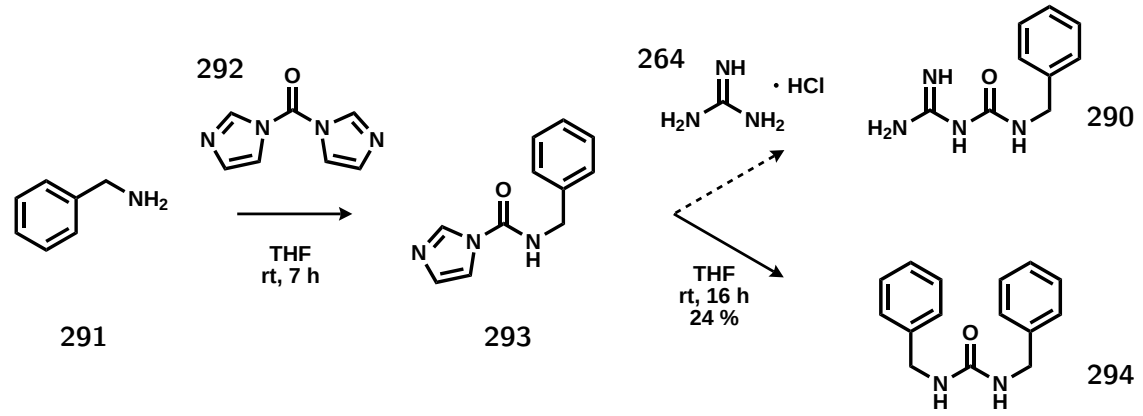

Scheme 5.47 Attempted synthesis of guanidine urea **290**, instead getting double-adduct **294**.

extraction of the filtrate with DCM. Attempts at further purification were unsuccessful, resulting in little improvement to the purity of the adducts, with a large reduction in yield. As such, both compounds **290** and **295** were carried forward into the cyclisation without further purification.

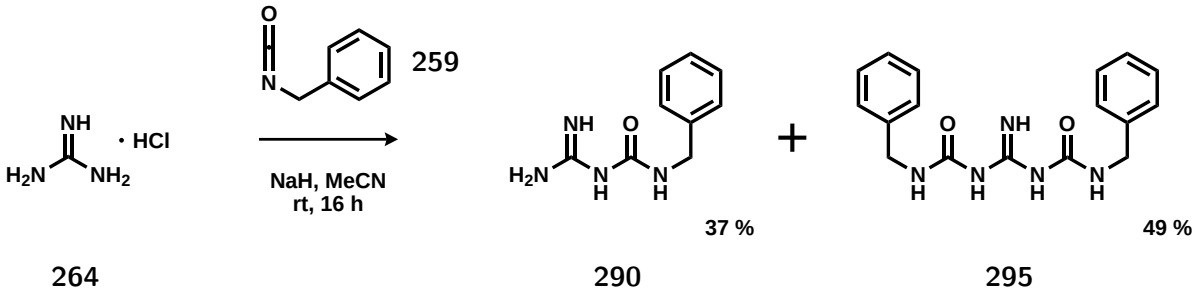

Scheme 5.48 Synthesis of guanidine benzylurea **290** and guanidine bis-benzylurea **295**.

5.4.7 Cyclisation

The cyclisation was attempted with both the single adduct **290** and the bis adduct **295**, with K_2CO_3 employed as base. Toluene was employed as solvent due to the high boiling point of this compound. To our great delight, both experiments were successful, with little difference in the reaction outcome between the single adduct **290** and the bis adduct **295**. However, the solid nature of the bis adduct **295** made this variant easier to handle, and thus it was preferred as a cyclisation precursor over mono adduct **290** (Scheme 5.49). A pure sample of Unit A **5** was isolated by flash column chromatography, and was found to be soluble in $CDCl_3$, enabling our proposed binding experiments with Unit B **2** to be performed.

We were intrigued to note that the bis adduct **295** performed well in the cyclisation, given the absence of an unprotected reactive centre. We proposed that the reaction proceeds *via* an identical mechanistic pathway as proposed for the single adduct **290**, with loss of the benzyl urea occurring

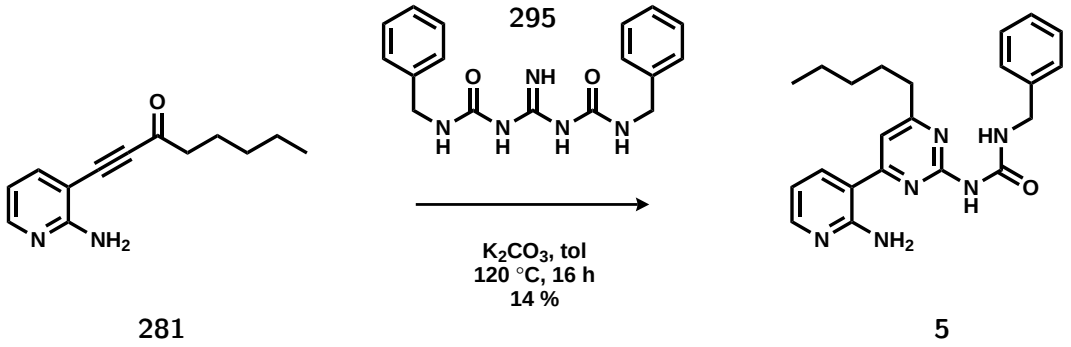

Scheme 5.49 Final synthesis of Unit A **5**.

following cyclisation (Scheme 5.50).

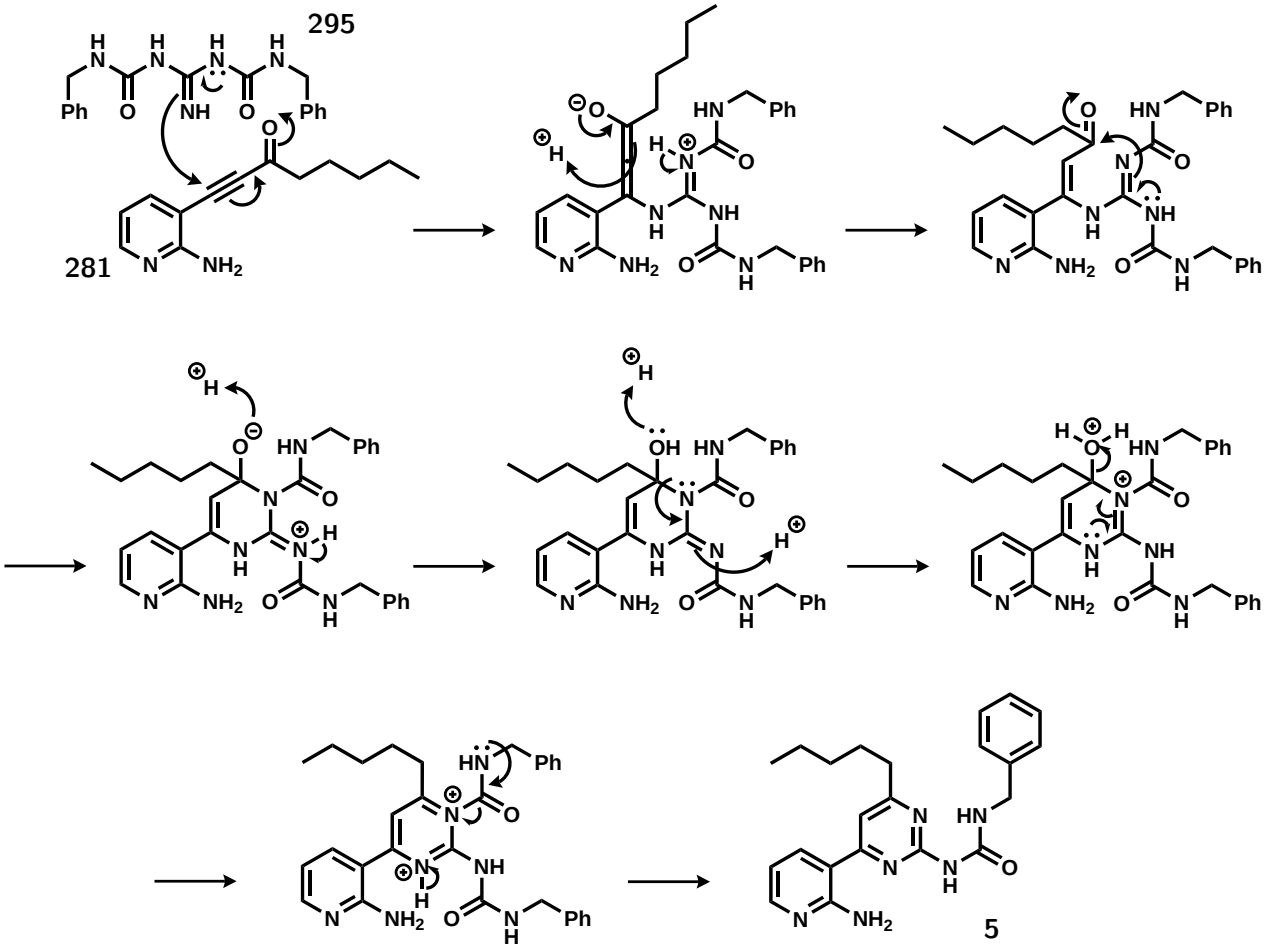

Scheme 5.50 Proposed mechanism during formation of Unit A **5**.

We could now not only perform binding experiments with Unit B **2**, but we could compare the results with the binding results between Unit B **2** and the pyridine variant of Unit A **6**, in an attempt to quantify the effect that the extra intramolecular H-bond might have on the binding strength of this interaction. Regrettably, the synthesis of Unit C, for binding experiments with Unit D, could not be pursued further due to time constraints.

6 Binding Experiments

6.1 Introduction

With the successful synthesis of Units A and B, measurement of the binding constants could finally be attempted. Experiments were performed according to the procedure described by Fielding,[210,211] using ^{1}H NMR spectroscopy. One of the two binding species is present in an NMR tube at constant concentration, and the second species is titrated in, sweeping through a large range of concentrations. Following the analysis of Fielding, we will describe the species already present in the NMR tube at constant concentration as the guest, and the species that is titrated in as the host. Here, we have two versions of Unit A. Henceforth, we shall designate the optimum (pyridine–pyrimidine) version **5** as 'A', and the bis-pyridine version **6** as 'A′'.

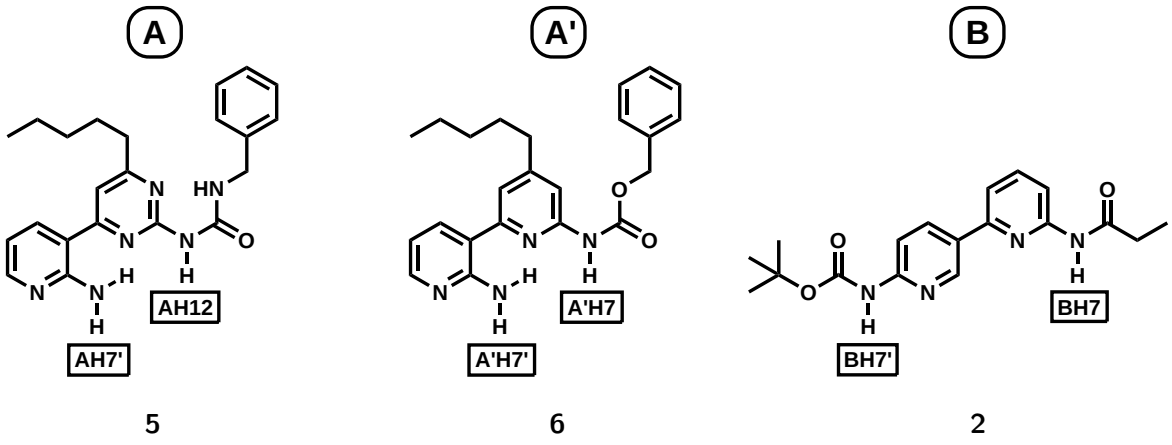

Fig. 6.1 Protons involved in H-bonding in Units A **5**, A′ **6**, and B **2**.

The first procedure necessary is to test the stoichiometry of binding by the method of continuous variations, known as 'Job's method'.[212–214] Job Plots are plotted in order to check that binding is occurring in a 1:1 fashion. A series of solutions are prepared, each containing a certain amount of Unit A and Unit B, in which the total concentration ($[A]_0 + [B]_0$) is constant, so that a complete range of mole ratios is sampled ($0 > [B]_0/([B]_0 + [A]_0) < 1$). In other words, the relative amounts of Unit A and Unit B are varied from low A and high B, through 1:1 A:B, to high A and low B. The

Table 6.1 List of terms used for measurement of binding constant K_a.

Term	Explanation
K_a	Association Constant/Binding Constant
$\Delta\delta_{AH7'}$	Measured change in chemical shift (upon addition of host species) of proton H7′ of species A (the guest), referenced to that of the uncomplexed A
X_A	Mole fraction of species A in equilibrium mixture
[A]	Concentration of (unbound) species A at equilibrium
[AB]	Concentration of bound pair A·B at equilibrium
$[A]_0$	Known total concentration of guest (constant). Thus: $[A]_0 = [A] + [AB]$

observed parameter is the change in chemical shift $\Delta\delta$ of the binding protons of the guest. There are four observable protons, and a single Job Plot corresponds to the change in chemical shift of each: $\Delta\delta_{AH12}$ and $\Delta\delta_{AH7'}$ when A is the guest, and $\Delta\delta_{BH7}$ and $\Delta\delta_{BH7'}$ when B is the guest. There are therefore four Job Plots plotted for binding between A and B. In the case of proton AH7′ for example, the Job plot is created by plotting $[A] \times \Delta\delta_{AH7'}$ versus X_A. The position of the maximum indicates the stoichiometry, and should be at 0.5 for 1:1 binding. The whole process was repeated for binding between A′ and B, yielding a total of eight Job Plots. The results are shown in Table 6.2, with the recorded data in Appendix A (Chapter 9).

The next step necessary is to check the variation of chemical shift of the observable H-bonding protons when the binding species is alone in solution at different concentrations. We have three binding species: A, A′, and B. Each species was measured at concentrations covering two orders of magnitude. The results are shown in Table 6.3, Table 6.4, and Table 6.5. At some of the lower concentrations, the concentration is too low or the peak too broad to be observed in the ^{1}H NMR spectrum (indicated by 'Doesn't show' in the tables).

The third and final step is to perform the binding experiments themselves. Experiments were performed for binding between A and B, both for A acting as the guest and B as the host, and for B as the guest and A as the host; and for binding between A′ and B, again both for A′ acting as

the guest and B as the host, and for B as the guest and A′ as the host. In this way, for binding between Units A and B for example, two measurements of the binding constant can be calculated: one for A as host and B as guest, and a second one for B as host and A as guest. In theory, the two values should be the same. By comparison with the binding constants of literature complexes (Section 1), the binding constant between Units A and B was expected to be somewhere in the range 10^4–$10^6\,\mathrm{M}^{-1}$. This made the K_a suitable for measurement by NMR, which according to Fielding should be in the range 10–10^6. The binding experiments were performed twice. The first set of experiments were done by taking each data point in a separate NMR tube. The second set were done using the same NMR tube for each chart, with a constant guest concentration, and adding the host bit by bit.[94,215,216]

The procedure for the first set of experiments (multiple NMR tubes) for binding, for example, between A and B, with A as guest and B as host, was as follows. Fielding suggested choosing an $[A]_0$ of around 2 mM. Based on the limited amount of completely pure material available, we used a concentration of 1.22 mM. A stock solution of A at known concentration was prepared, and a stock solution of B at known concentration was also prepared. Some of the stock solution of A was added to the NMR tube (less than 0.6 mL). Some of the stock solution of Unit B was removed, and diluted by the appropriate degree, then added to the NMR tube such that the total combined volume was 0.6 mL. The combined volume was always 0.6 mL and calculations took into account the fact that when mixed together in the NMR tube, the final volume of each solution would be 0.6 mL. This procedure was repeated for different concentrations of Unit B, sweeping through a range from 0.1 equivalents of Unit B, to more than 10 equivalents. An NMR tube was also prepared that contained purely A at 1.22 mM. At the end of the procedure, we had 10 or so NMR tubes ready for measurement. Each NMR tube was shaken vigorously before the NMR spectrum was recorded. The $CDCl_3$ used was dried with molecular sieves and the acidity neutralized with K_2CO_3.

In this example the guest species, Unit A, is the 'observed' species, the one for which the chemical shifts are measured. So, the chemical shift of the two relevant protons of the guest (in the case of Unit A, protons H7′ and H12) was noted from the spectrum of pure Unit A at 1.22 mM. The value $\Delta\delta_{\mathrm{AH7'}}$ (in the case of proton H7′ on Unit A) is the difference between this chemical shift and the chemical shift for the same protons in the presence of Unit B at the different concentrations ([B]). Plots were made of both $\Delta\delta_{\mathrm{AH7'}}$ versus [B] and $\Delta\delta_{\mathrm{AH12}}$ versus [B] so that the binding constant calculated for each could be compared. In theory, the two values should be the same. The binding plots are shown in Table 6.6, Table 6.7, and Table 6.8, with the recorded data in Appendix A

(Chapter 9).

The procedure for the second set of experiments (single NMR tube) for binding, for example, between A and B, with A as guest and B as host, was as follows. A known amount of A was dissolved in 0.6 mL of $CDCl_3$, and added to the NMR tube. The same amount of A was dissolved in another 0.6 mL of $CDCl_3$ in a vial, along with the entirety of B (around 20 equivalents). This provided the stock solution of B from which, for each NMR measurement, a fraction was removed with a micropipette and added to the NMR tube. The 1 equivalent of A mixed with B in the stock solution meant that the concentration of A was constant throughout the entire range of measurements. The NMR tube was shaken vigorously every time more B was added, prior to the NMR spectrum being measured.

As for the multiple NMR tube experiments, plots were made of both $\Delta\delta_{\mathrm{AH7'}}$ versus [B] and $\Delta\delta_{\mathrm{AH12}}$ versus [B] so that the binding constant calculated for each could be compared. The binding plots are shown in Table 6.9, Table 6.10, Table 6.11 and Table 6.12, with the recorded data in Appendix A (Chapter 9).

Table 6.2 All Job Plots.

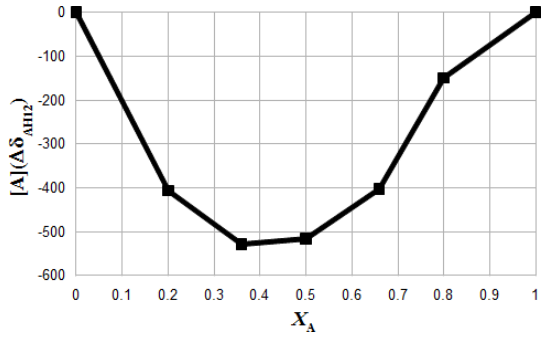

$[\mathrm{A}]_0(\Delta\delta_{\mathrm{AH12}})$ vs. X_{A}

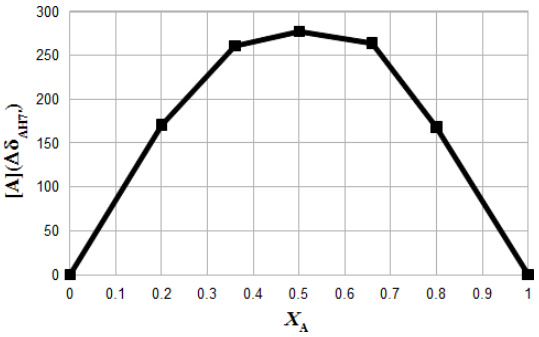

$[\mathrm{A}]_0(\Delta\delta_{\mathrm{AH7'}})$ vs. X_{A}

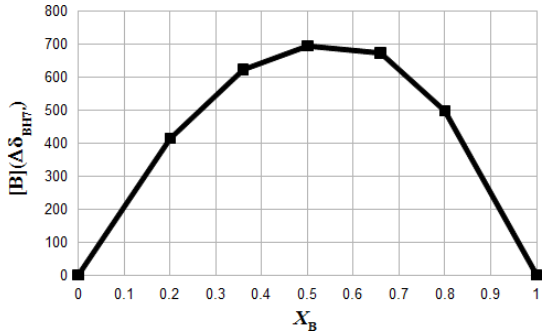

$[\mathrm{B}]_0(\Delta\delta_{\mathrm{BH7'}})$ vs. X_{B}

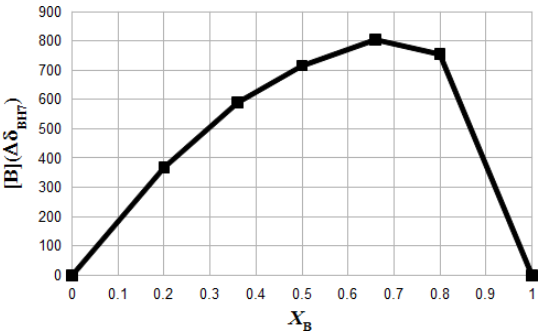

$[\mathrm{B}]_0(\Delta\delta_{\mathrm{BH7}})$ vs. X_{B}

Job Plots for binding between Unit A and Unit B.

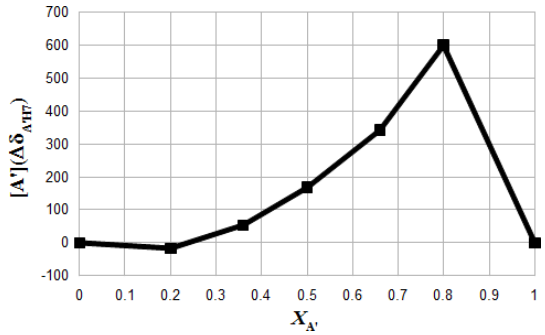

$[\mathrm{A}']_0(\Delta\delta_{\mathrm{A'H7}})$ vs. $X_{\mathrm{A'}}$

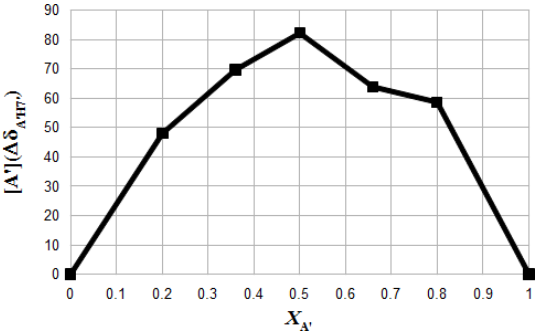

$[\mathrm{A}']_0(\Delta\delta_{\mathrm{A'H7'}})$ vs. $X_{\mathrm{A'}}$

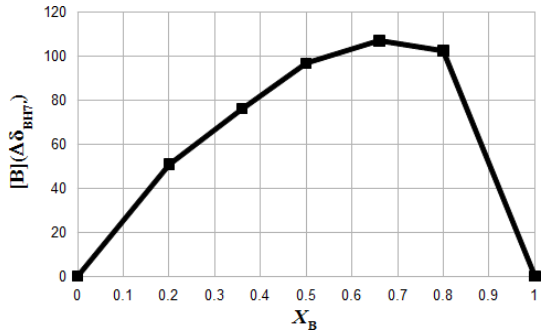

$[\mathrm{B}]_0(\Delta\delta_{\mathrm{BH7'}})$ vs. X_{B}

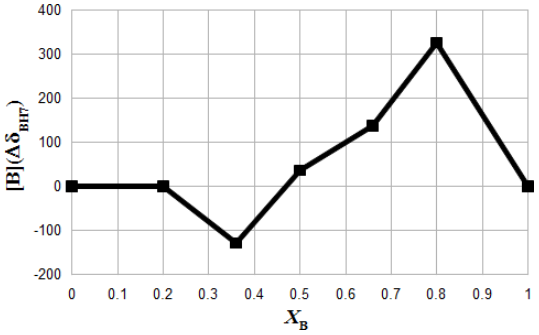

$[\mathrm{B}]_0(\Delta\delta_{\mathrm{BH7}})$ vs. X_{B}

Job Plots for binding between Unit A′ and Unit B.

Table 6.3 Chemical shift data for A alone in solution over a range of concentrations.

Conc. of A in mM ([A] / mM)	H12 shift (δH12)	H7′ shift (δH7′)
0.07	Doesn't show	Doesn't show
0.2	Doesn't show	Doesn't show
0.5	Doesn't show	Doesn't show
2	7.759	6.643
7.3	8.257	6.598

Table 6.4 Chemical shift data for A′ alone in solution over a range of concentrations.

Conc. of A′ in mM ([A′] / mM)	H7 shift (δH7)	H7′ shift (δH7′)
0.07	Doesn't show	6.253
0.2	Doesn't show	6.253
0.5	Doesn't show	6.252
2	Doesn't show	6.254
7.3	7.662	6.256

Table 6.5 Chemical shift data for B alone in solution over a range of concentrations.

Conc. of B in mM ([B] / mM)	H7 shift (δH7)	H7′ shift (δH7′)
0.07	Doesn't show	Doesn't show
0.2	Doesn't show	Doesn't show
0.5	7.883	Doesn't show
2	7.88	7.4
7.3	7.861	7.545

Table 6.6 Multiple NMR tubes experiment:
Binding Plots for binding between Unit A and Unit B.
A is guest (observed species) and B is host (titrated in) in both plots.
Top: A guest (1.22 mM, AH12 observed species); B host.
Bottom: A guest (1.22 mM, AH7′ observed species); B host.

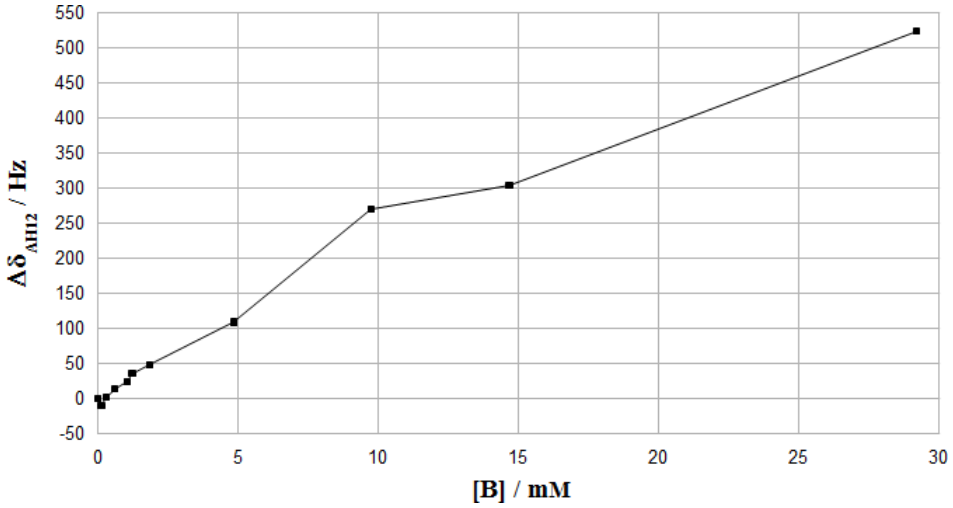

$\Delta\delta_{\mathrm{AH12}}$ / Hz vs. [B] / mM

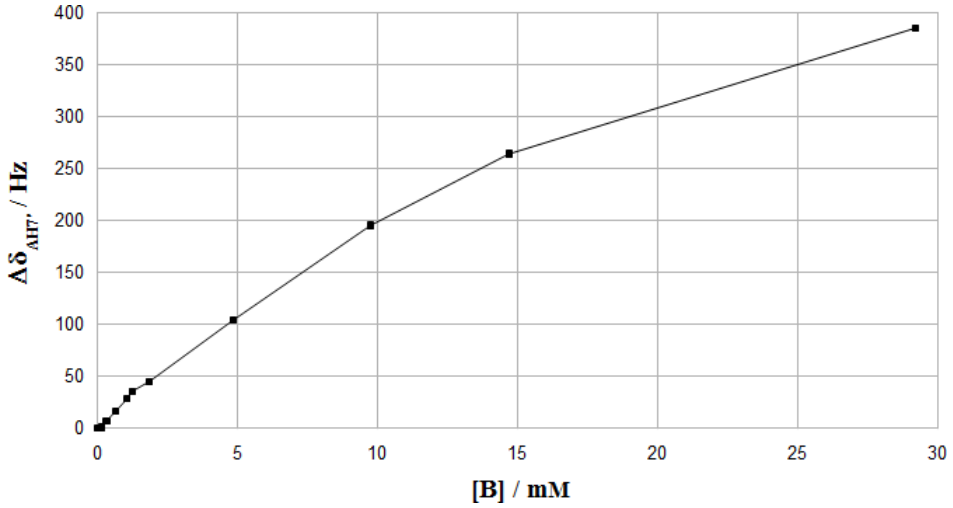

$\Delta\delta_{\mathrm{AH7'}}$ / Hz vs. [B] / mM

Table 6.7 Multiple NMR tubes experiment:
Binding Plots for binding between Unit A and Unit B.
B is guest (observed species) and A is host (titrated in) in both plots.
Top: B guest (1.22 mM, BH7 observed species); A host.
Bottom: B guest (1.22 mM, BH7′ observed species); A host.

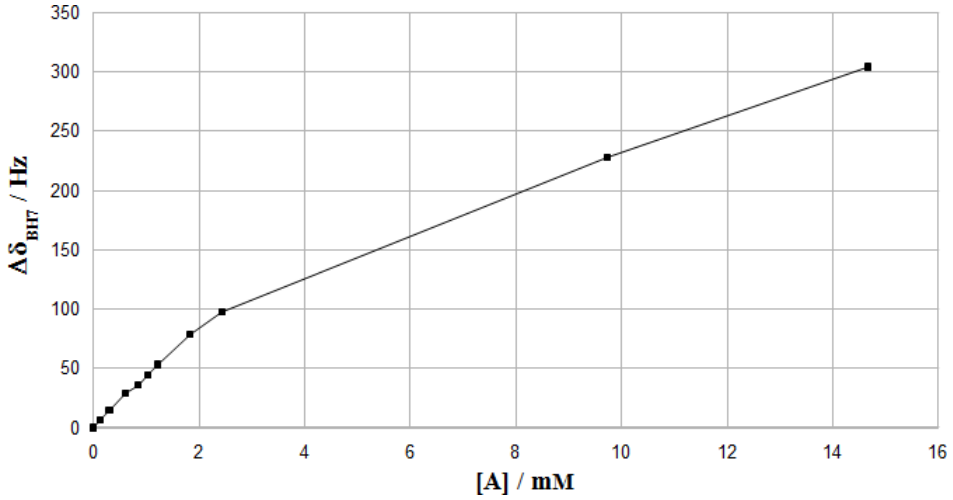

$\Delta\delta_{\mathrm{BH7}}$ / Hz vs. [A] / mM

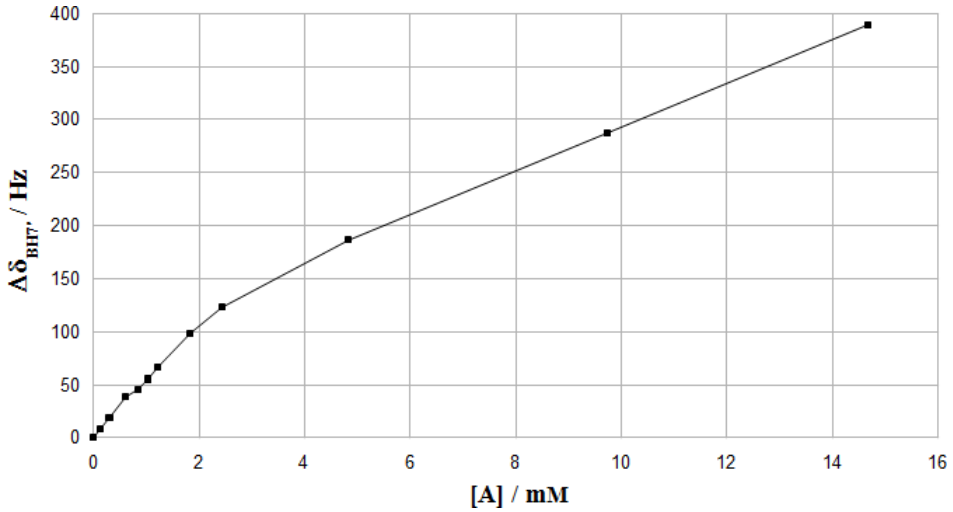

$\Delta\delta_{\mathrm{BH7'}}$ / Hz vs. [A] / mM

Table 6.8 Multiple NMR tubes experiment:
Binding Plots for binding between Unit A′ and Unit B.
Top: A′ guest (1.22 mM, A′H7′ observed species); B host.
Bottom: B guest (1.22 mM, BH7 observed species); A′ host.

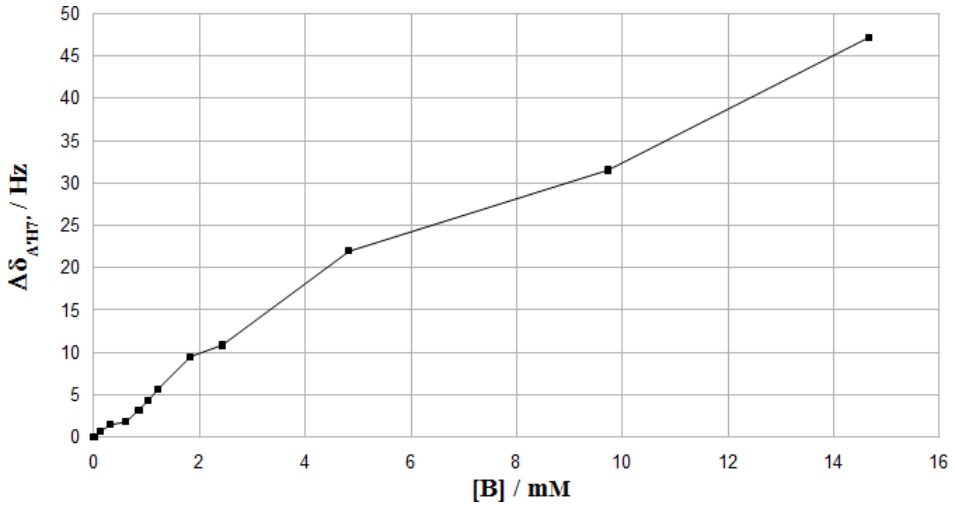

$\Delta\delta_{\mathrm{A'H7'}}$ / Hz vs. [B] / mM

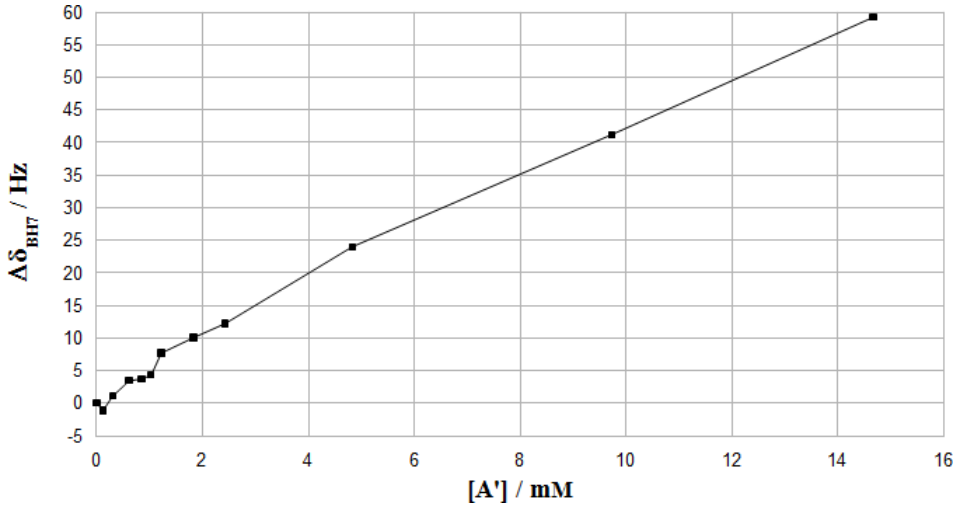

$\Delta\delta_{\mathrm{BH7}}$ / Hz vs. [A′] / mM

Table 6.9 Single NMR tube experiment:
Binding Plots for binding between Unit A and Unit B.
A is guest (observed species) and B is host (titrated in) in both plots.
Top: A guest (3.68 mM, AH12 observed species); B host.
Bottom: A guest (3.68 mM, AH7′ observed species); B host.

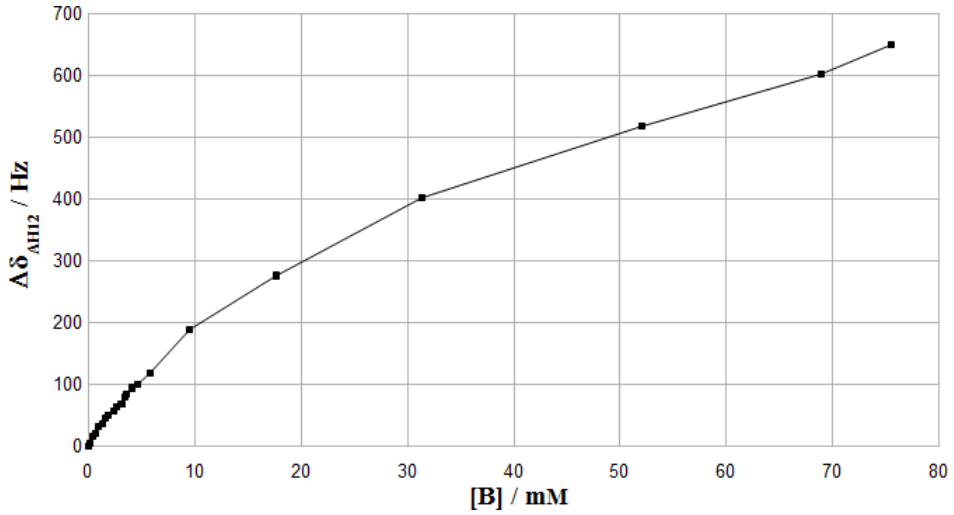

$\Delta\delta_{\mathrm{AH12}}$ / Hz vs. [B] / mM

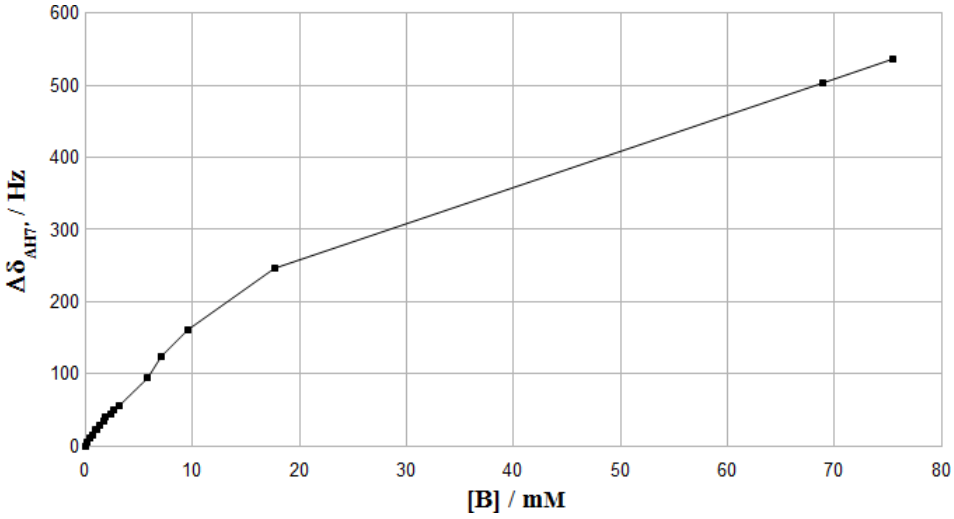

$\Delta\delta_{\mathrm{AH7'}}$ / Hz vs. [B] / mM

Table 6.10 Single NMR tubes experiment:
Binding Plots for binding between Unit A and Unit B.
B is guest (observed species) and A is host (titrated in) in both plots.
Top: B guest (3.83 mM, BH7 observed species); A host.
Bottom: B guest (3.83 mM, BH7′ observed species); A host.

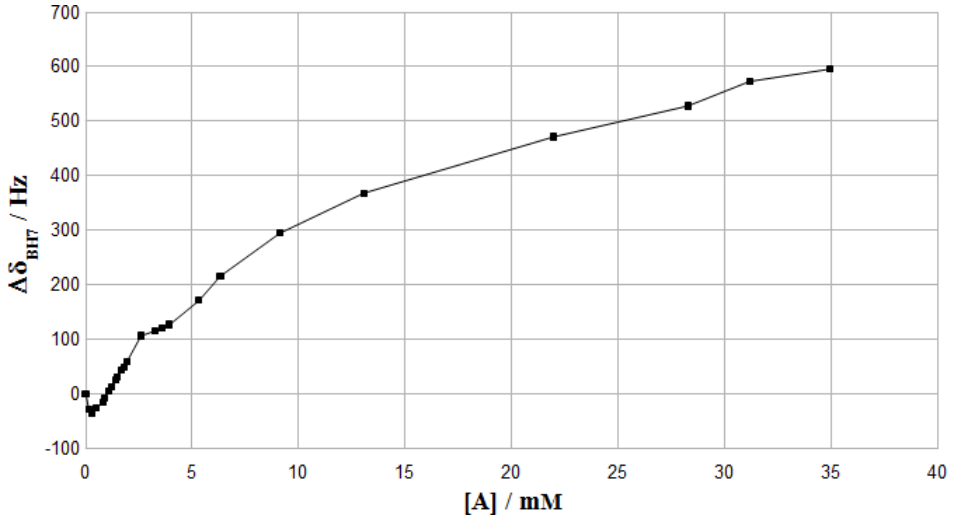

$\Delta\delta_{\mathrm{BH7}}$ / Hz vs. [A] / mM

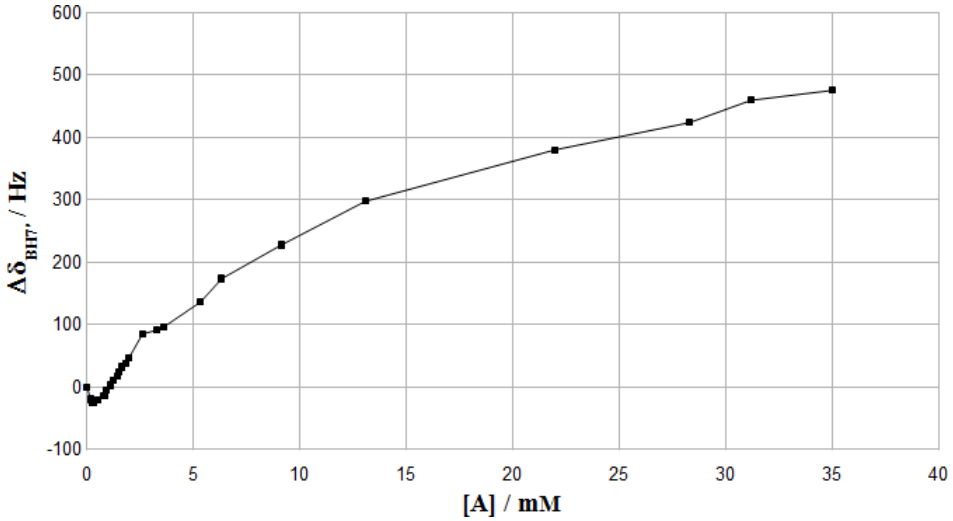

$\Delta\delta_{\mathrm{BH7'}}$ / Hz vs. [A] / mM

Table 6.11 Single NMR tube experiment:
Binding Plots for binding between Unit A′ and Unit B.
A′ is guest (observed species) and B is host (titrated in) in both plots.
Top: A′ guest (2.80 mM, A′H7 observed species); B host.
Bottom: A′ guest (2.80 mM, A′H7′ observed species); B host.

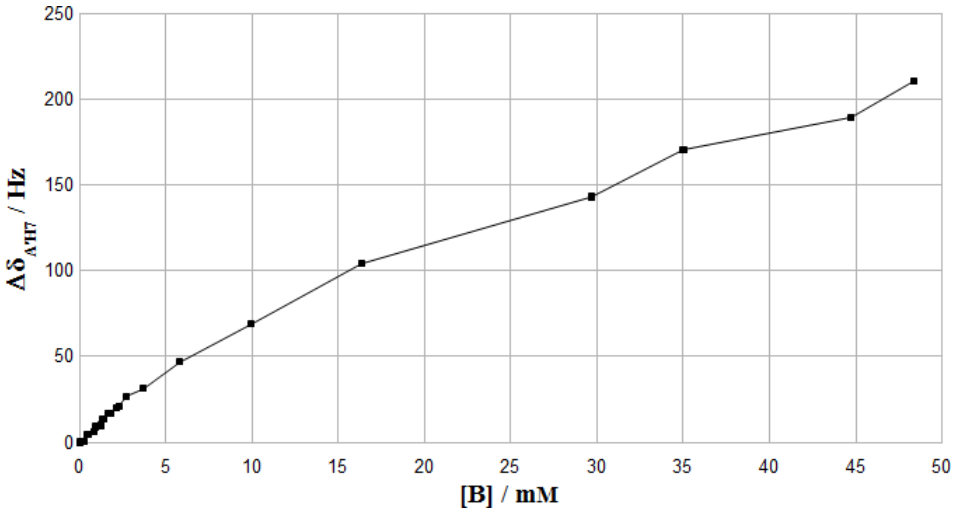

$\Delta\delta_{\mathrm{A'H7}}$ / Hz vs. [B] / mM

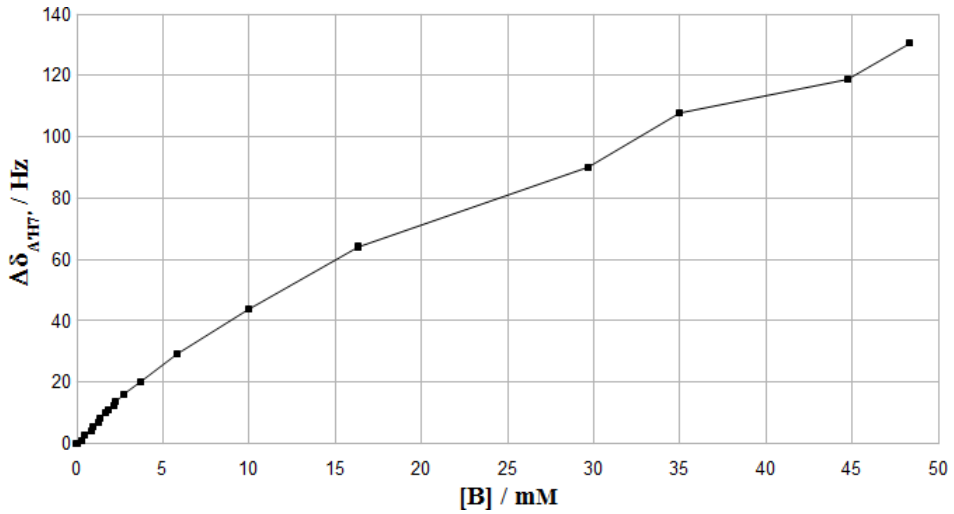

$\Delta\delta_{\mathrm{A'H7'}}$ / Hz vs. [B] / mM

Table 6.12 Single NMR tubes experiment:
Binding Plots for binding between Unit A′ and Unit B.
B is guest (observed species) and A′ is host (titrated in) in both plots.
Top: B guest (4.25 mM, BH7 observed species); A′ host.
Bottom: B guest (4.25 mM, BH7′ observed species); A′ host.

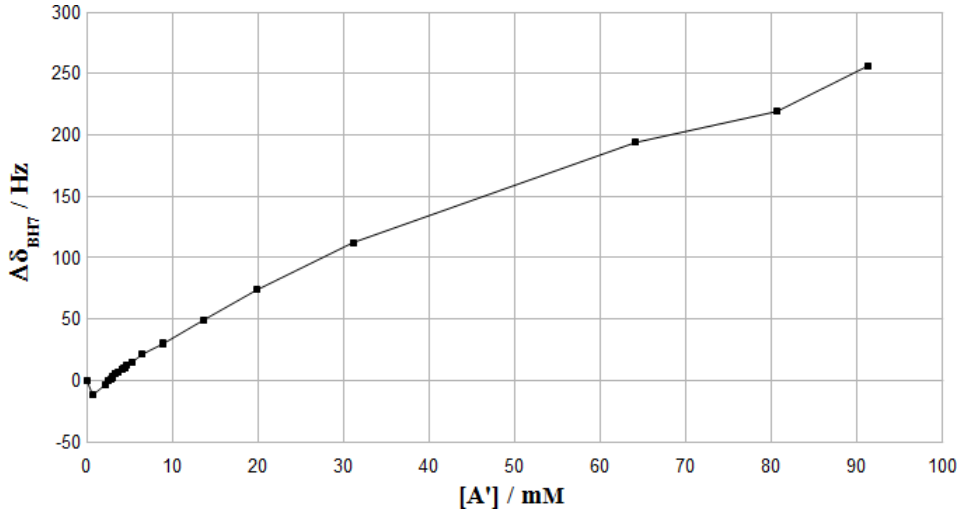

$\Delta\delta_{\mathrm{BH7}}$ / Hz vs. [A′] / mM

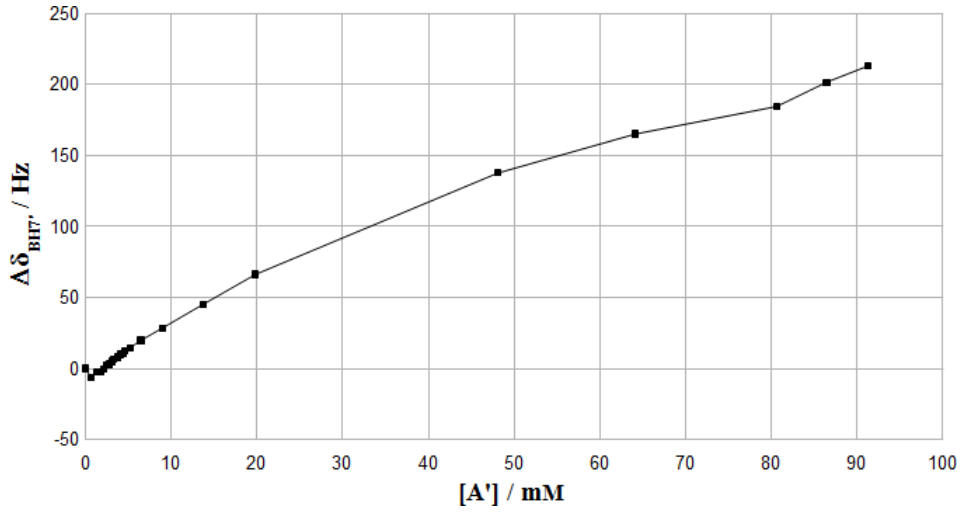

$\Delta\delta_{\mathrm{BH7'}}$ / Hz vs. [A′] / mM

6.2 Results

Two of the eight Job Plots have negative values, but this is not unusual,[217] as it merely indicates that the change in proton shift is to the right (more shielded) rather than to the left. For 1:1 binding, each Job Plot should peak at 0.5. However, only three of the eight Job Plots demonstrate this behaviour. Moreover, neither A–B binding nor A′–B binding demonstrated a complete set of four plots that all peak in the same position. This shows that 1:1 binding is not taking place between A and B, nor between A′ and B. Unsymmetrical Job Plot patterns such as these are often seen in systems in which a non-1:1 binding stoichiometry is occurring, perhaps involving chains or aggregates.[218,219] There are a number of possible causes for this irregular stoichiometry. Self-overlapping may be taking place between the units (Fig. 6.2). In this case, the guest would form long, potentially branched chains in solution, which would be gradually disrupted by the host species as it is titrated in. Also, steric interference may be taking place between protons in the cramped inter-unit space between A and B. In this case, self-binding in the manner shown may be energetically favourable over the alternative A–B binding. Thus, complicated aggregate structures may be forming from intermolecular binding in multiple directions, and rotation around the C–C bond joining the two rings would aid this mode of binding.

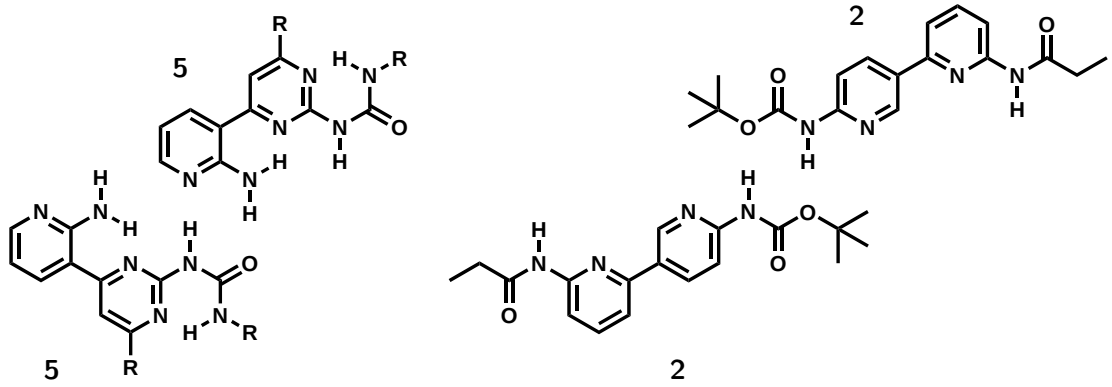

Fig. 6.2 Self-overlapping shown for Unit A **5** and Unit B **2**.

The concentration data (chemical shift data for each Unit alone in solution over a range of concentrations) is inconclusive. Unfortunately, in most cases at low concentrations, the peak is too broad or too small to be observed in the ^{1}H NMR spectrum. The H7′ proton on Unit A′ is the only H-bonding proton visible over the entire range of concentrations (Table 6.4). Pleasingly in this case, the shift remains constant over the entire concentration range, suggesting that the A′H7′ proton is not binding to anything else over all concentrations. Unfortunately, the A′H7 proton is only visible at the highest concentration. If Unit A′ is indeed self-overlapping or interfering with itself in

some manner, it would seem likely that were the A′H7 proton visible at the lower concentrations, the chemical shift values would all be different. There is the suggestion that this is indeed what is happening in the other two tables (Table 6.3 and Table 6.5), although definitive conclusions cannot be drawn. There is a large change in chemical shift for Unit A between 2 mM and 7.3 mM. We observe similar differences for AH7′ and BH7′, again suggesting that self-interaction is taking place, although the BH7 shift remains constant. For reliable determination of binding constants, a consistent chemical shift is required at higher (> 1:1) concentrations (the guest and host were at 1:1 equivalents at 1.22 mM). This is not observed, again pointing to higher aggregation processes taking place.

Mindful that the Job Plots had demonstrated that 1:1 binding was not occurring, the NMR binding titration results were nevertheless analysed to attempt to interpret the mode of binding taking place (Table 6.6 to Table 6.12). In all cases, the data points did not produce a smooth curve shape. In fact, in every plot, the points are staggered, forming a series of small plateaus followed by sharp rises. This is slightly more pronounced in the plots when B is the guest, for both multiple-tube and single-tube experiments. The lower concentration region is the most interesting, where small plateaus can be seen most clearly in the plots for binding between A′ and B (multiple-tube, Table 6.8), and between A and B (single-tube, Table 6.10). There is even the suggestion in Table 6.8 that the binding curve has flattened out as the concentration approaches 1:1 equivalents (1.22 mM). A similar pattern can be seen in Table 6.10 – there is a clear disconnect at around [A] = 3 mM. Patterns such as these can be observed in systems involving aggregation and unusual binding stoichiometries.[217,220] Moreover, in Table 6.6, Table 6.8, Table 6.10 and Table 6.12, the change in shift alters direction, thus producing negative values of $\Delta\delta$ and a 'U'-shaped curve at low concentrations. Again, this is possible in non-1:1 binding systems as you move from low to high concentrations.[221,222]

We sought expert advice on our binding titration results from Dr. Dan Pantoş of the University of Bath. We are advised that patterns such as ours are indeed observed in systems in which 1:1 binding is not taking place, and more complicated oligomeric structures are forming. Thus, the behaviour suggested by both the Job Plots and the binding plots is consistent, and we conclude that the NMR binding titration plots provide further evidence to the Job Plots that we do not have a 1:1 binding stoichiometry, and aggregation or chain formation among the binding species is likely. This result leaves open the possibility that strong binding is after all taking place between A and B, but when the host concentration begins to exceed that of the guest, further interactions between

the excess host and the already-bound host-guest complexes create further chemical shift changes, and the binding plots continue on an upward trajectory. Furthermore, it is also possible that steric interference between the protons in the intermolecular space between Units A and B (and A′ and B) may after all not be a problem, and the design architecture which we worked so hard to develop may be perfectly viable.

Despite the staggered and step-like shape of the NMR binding titration plots, the data points were still regularly spaced enough to be curve-fitted, and a value for a binding constant to be calculated. Calculations were performed with the assistance of the NMR Service at the University of Oxford, using the software program OriginPro to curve-fit the data.*

The first set of experiments to be performed were the multiple NMR tube experiments. In each case, the guest concentration was 1.22 mM. As mentioned above, the range of sampling concentrations was chosen because we expected a binding constant of order 10^4–$10^6\,\mathrm{M}^{-1}$. Over this concentration range, a binding constant of this order of magnitude would produce a steeply rising graph in the lower concentration ranges, which flattens out to a virtual constant over the higher ranges. However, in all our plots, the curve rises gently, and has not flattened out by the time it reaches the higher concentrations. This behaviour would suggest weak binding. It is for this reason that the binding experiments were repeated at a higher concentration, using a single NMR tube for all NMR measurements.[94,215,216] For each of the four single-tube experiments, the concentration of the guest was chosen as high as the availability of material would allow (in the event, it was found that higher concentrations were not practical due to the material precipitating out of solution in the NMR tube). The binding experiment results are shown in Table 6.13.

The binding constant values suggest weak binding. For the multiple-tube experiments, binding between A and B, with A as the observed species, values of $22\,\mathrm{M}^{-1}$ and $37\,\mathrm{M}^{-1}$ were measured for the two H-bonding protons. In theory, these values should be the same, but at least they are of the same order of magnitude. For binding between A and B with B as the observed species, values of $106\,\mathrm{M}^{-1}$ and $92\,\mathrm{M}^{-1}$ were measured. Unfortunately, for binding between A′ and B, proton H7 of A could not be seen in the NMR spectra. Similarly, proton H7′ of B could not be observed. We therefore only have a single value of the K_a with each unit as the observed species. With A′ as the observed species, a value of $40\,\mathrm{M}^{-1}$ was measured. With B as the observed species, a value of $24\,\mathrm{M}^{-1}$ was measured.

For the single-tube experiments, binding between A and B, with A as the observed species, values

*With thanks to Ivanhoe Leung of the University of Oxford for calculating the binding constants.

Table 6.13 Binding constants as measured by ^{1}H NMR.

Guest (observed species)	Host	Binding Constant K_a (multiple NMR tubes)	Binding Constant K_a (single NMR tube)
AH12	B	22 M^{-1}	26 M^{-1}
AH7′	B	37 M^{-1}	28 M^{-1}
BH7	A	106 M^{-1}	42 M^{-1}
BH7′	A	92 M^{-1}	42 M^{-1}
A′H7	B	–	23 M^{-1}
A′H7′	B	40 M^{-1}	24 M^{-1}
BH7	A′	24 M^{-1}	3.7 M^{-1}
BH7′	A′	–	5.3 M^{-1}

of 26 M^{-1} and 28 M^{-1} were measured for the two H-bonding protons. These values show a closer agreement to each other than for the multiple-tube values, which is perhaps to be expected - the change in each proton shift is measured in the same NMR tube at exactly the same concentration, unlike for the multiple-tube experiments. For binding between A and B with B as the observed species, values of 42 M^{-1} were measured in both cases. For binding between A′ and B, with A′ as the observed species, values of 23 M^{-1} and 24 M^{-1} were measured for the two H-bonding protons. For binding between A′ and B with B as the observed species, values of 3.7 M^{-1} and 5.3 M^{-1} were measured. Thus, for both multiple-tube and single-tube experiments, we measure stronger binding between Unit A and Unit B than between Unit A′ and Unit B. This is in line with our expectations: the intramolecular H-bond in Unit A providing greater rigidity and a higher binding constant. However, we are aware that we do not have 1:1 binding occurring, and these results must not be over-interpreted.

There is good agreement between the multiple-tube and single-tube binding values for A–B binding with A as guest. However, in all three of the other cases, the values for the single-tube experiments are significantly lower. Plus, the values for A′–B binding with B constant for the single-tube experiments are noticeably lower than the corresponding values for both the multiple-tube experiment, and the values for A′–B binding with A constant. We would expect differences between

the two sets of experiments. For example, the binding values are very sensitive to the amount of water present in the $CDCl_3$. While every effort was made to reduce this to a minimum, there will naturally be a small amount present, and a different amount for the multiple-tube experiments compared to the single-tube experiments. It is possible that more moisture entered the NMR tube for the experiments for single-tube A′–B binding with B constant.

This sensitivity to precise experimental conditions is demonstrated in both the multiple-tube and single-tube results in the difference between the measured K_a values for each of the four sets of measurements (A–B, A guest; A–B, B guest; A′–B, A′ guest; A′–B, B guest). In theory, the values for binding between the two species should be the same no matter which of the two is operating as the guest and which as the host. It is however gratifying that the multiple-tube and single-tube experiments both demonstrate the same general binding pattern: A–B binding is stronger than A′–B binding; and the values are higher in all cases for when A or A′ is guest over when B is guest. This general pattern shows a degree of consistency between all the experiments, boosting confidence in the experiments being performed correctly and the validity of the results.

Increasing the concentration of the binding species and repeating the binding experiments (in a single NMR tube) did indeed have the desired effect of producing plots with a more pronounced curve. The curve is most pronounced in the plot for binding between A and B with B as guest (Table 6.10). However, it is still quite far off the ideal shape, in which the plot rises more steeply for the lower concentrations and then tails off to a virtual constant for the higher concentrations – after all, the binding is much lower than we expected, so even in the higher concentration single-tube experiments, the curve would not approach a constant at the higher concentrations.

Over all experiments, the binding constant values are in the range $3.7\,\mathrm{M}^{-1}$ to $106\,\mathrm{M}^{-1}$. These are four orders of magnitude lower than expected, and are actually in the range expected for binding between 2-H-bond arrays (Section 1.3.2). Such a vast difference between the expected and the measured values could be explained by steric interference between protons in the inter-unit space between A and B (see Fig. 7.1, Section 7.2). If this were so, it would mean that the design of Units A and B is fundamentally flawed. As discussed in Section 1.7.3, it was reasonable to hope that this interaction would not be too detrimental to binding if the two halves of the unit can twist slightly around the joining C–C bond. However, the low measured binding values do suggest that our optimism was perhaps ill-founded. The most likely reason for a low binding constant is a steric clash between the protons on each binding species. Again, we must bear in mind that we do not have 1:1 binding, and this interpretation is predicated on curve-fitting for 1:1 binding.

7 Conclusions and Future Work

7.1 Chemistry

As discussed in Section 1.7, we do believe that non-covalent synthesis would benefit greatly from the development of binding motifs that are both non-symmetrical and non-self-complementary. We proposed the staggered array design, and synthesised (to our knowledge) the first ever non-self-complementary and non-symmetrical binding arrays, and in doing so demonstrated that the staggered architecture is synthetically possible. It was very frustrating that there was insufficient time to complete the full set of two pairs of orthogonally-binding motifs. However, we did complete much of the necessary chemistry for the synthesis of all four motifs, and we do not believe there is any reason, from a synthetic standpoint, why they could not be completed.

The staggered ADDA architecture proved to be a difficult synthetic challenge. The 2-pyridone motif would at first glance appear to be the ideal solution, but we saw that these chemical moieties were too unreliable. Their poor solubility properties severely hindered the rate of progress of the entire project. These solubility problems were not anticipated, but with perseverance and continual redesign and strategy updating, they were overcome. The inverted 2-pyridine structure, which achieved the same ADDA binding pattern but without the use of a 2-pyridone, proved to be an excellent solution. That the final pyridine-pyrimidine version of Unit A **5** was soluble in $CDCl_3$ was extremely gratifying following all the failures that we had encountered. It was very satisfying to first invent the novel inverted 2-aminopyridine design, plan the synthesis, then revise the synthesis a number of times following synthetic dead-ends, to eventually triumph with a working version of Unit A.

We optimised a work-up procedure for the isolation of boronic acids which involved the isolation of the negatively-charged borate in the aqueous phase, followed by acidification to neutral pH with the concomitant precipitation of the boronic acid from solution. This proved to be a highly reliable procedure, providing our desired boronic acid time after time during this project.

The Suzuki reaction proved to be very reliable for the heterocyclic systems studied throughout the project. The vast majority of our Suzuki couplings were between two pyridyl systems with the bromine in the 2-position and the boronic acid or boron pinacol in the 3-position, for which there is no precedent. Moreover, for couplings between pyridines with the boron in any position and substituted bromobenzene rings, and also for between pyridines with the bromine in any position and substituted benzene boron species, there is also no precedent. We have therefore expanded the scope of the Suzuki reaction for the coupling of heteroaryl systems.

We also demonstrated the robustness of the Suzuki reaction and the boronic acids themselves by coupling with boronic acids in a wide variety of forms (Section 2.4.3). The Suzuki couplings completed (albeit at fairly low yields) when the boronic acid was acidic, neutral, or basic. Boronic acids are often difficult to synthesise and/or isolate. These results suggest that if the next step in a synthesis is a Suzuki coupling, the explicit isolation and purification of the boronic acid is not necessarily required. This may unlock potential synthetic pathways in the synthesis of compounds for which a Suzuki coupling could be utilised in one or more of the steps.

7.2 Binding Experiments

The binding experiments were inconclusive. The Job Plots showed that the binding stoichiometry between Unit A and Unit B (and Units A′ and B) was not 1:1, so the binding constant K_a could not be reliably measured. The actual strength of binding may be very high or very low. Despite this, binding measurements were performed by ^{1}H NMR spectroscopy. Binding experiments were performed in two sets of experiments, the first (in multiple NMR tubes) at a lower concentration, the second set (in a single NMR tube) at a higher concentration. Increasing the binding species' concentration and repeating the binding experiments did successfully produce binding plots with a more pronounced curve, although the measured binding constant values for the repeat experiments were even lower than those for the original lower-concentration experiments.

For these reasons, the binding experiments did not shed much light on the potential steric clash between the central proton of Units A and B, and this remains an area of concern. The steric problems are highlighted in Fig. 7.1. Definitively strong 1:1 binding would suggest that steric interference is not taking place; definitively weak 1:1 binding would strongly suggest that it is. If the units are binding weakly, we have a serious design flaw in the A–B pairing, and the bis-pyridine or pyridine/pyrimidine architecture may not be a viable design option (Fig. 7.1, Unit A/Unit B).

Rather, motifs may require more inter-unit space, such as that of Units C and D (Fig. 7.1, Unit C/Unit D). It can clearly be seen that the presence of the extra 'spacer' ring in the architecture of Units C and D results in a much less congested intermolecular space.

Much further binding experimentation is clearly necessary, but unfortunately time constraints did not allow for this. It would be very constructive to compare the Job Plots for binding between Units C and D. If their Job Plots all showed 1:1 binding, it would be a very good result, boosting our confidence in the staggered ADDA/DAAD design. It would suggest that the non-1:1 binding between A and B is an artefact of steric clashes. On the other hand, if the C and D Job Plots also demonstrated non-1:1 binding, this would perhaps hint at a design flaw within the chemical structures. For example, overlapping could be taking place, so a design that prevented overlapping may be necessary.

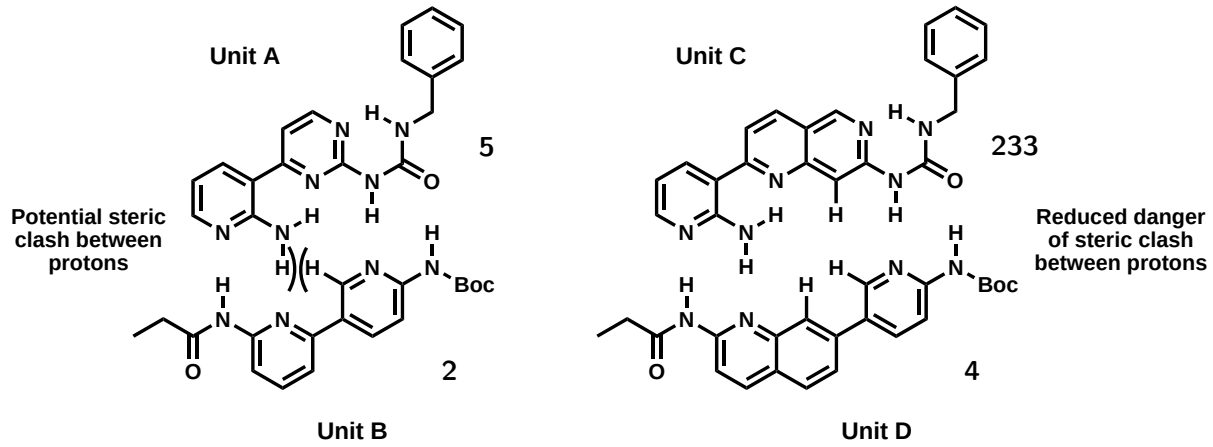

Fig. 7.1 Potential steric clash between protons of Units A **5** and B **2** during binding.

7.3 Future Work

Following discussions with Dr. Dan Pantoş, the binding experiments should be repeated with many more data points, especially in the lower concentration regions where the guest/host molar ratio is greater than 1 and the $\Delta\delta$ values are negative. The precise shape of the plot in this region would be elucidated, shedding much light on the nature of the binding. Unfortunately, this was not possible due to time constraints.

Synthetically, the first thing to do is complete the synthesis of Unit C (Scheme 7.1). As mentioned in Section 5.2.3, our synthesis of the key compound, naphthyridine **234**, was based on the only known synthesis of **234** at the time,[165] which was highly non-trivial. The recent paper by Johnson and co-workers[166] describes a much-improved synthesis of **234**, and this would be a good place to start.

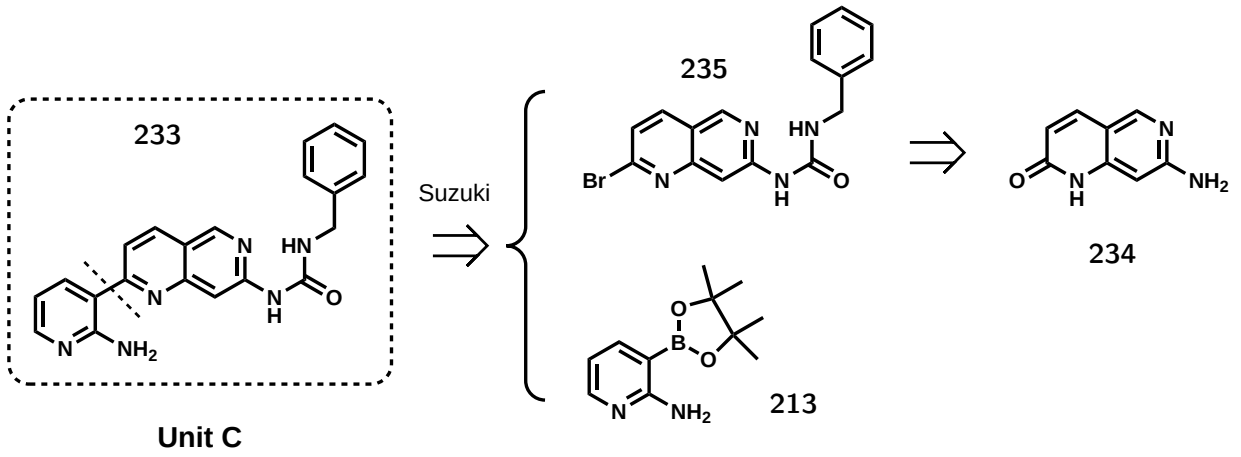

Scheme 7.1 Planned route towards 2,6-naphthyridine Unit C **233**.

The completion of Unit C would shed some light on the issue of steric interference between Units A and B. As shown in Fig. 7.1, steric clashing between Units C and D is much less likely than between Units A and B. Once binding experiments between Units C and D have been performed, the value of the binding constant will give a good indication if steric interference is happening between Units A and B. If the binding constant between Units C and D is significantly higher, it would indicate that sterics are indeed reducing the binding strength between Units A and B.

When we have all four Units A, B, C and D in hand, the crucial experiment to demonstrate binding orthogonality (self-sorting) can be performed. This is to demonstrate that the units all bind in the intended pairwise orthogonal manner. That is to say, when all four units are in solution together, A binds solely to B, and C binds solely to D. This behaviour can be demonstrated by taking a 1:1 mixture of A and B in an NMR tube, and then titrating in Unit C. When there is 1 equivalent of Unit C present, a single equivalent of Unit D will be titrated in. If orthogonal binding is indeed taking place, the chemical shifts of the H-bonding protons on Units A and B will not change during the entire process. The change in the chemical shifts of Units C and D should change in the same fashion that they did when the same binding experiment was performed with only Units C and D present.

7.3.1 Alkyne linker

We can not be sure that there is no steric interference taking place between the protons of Units A and B during binding. The synthesis of alkyne versions of Units A and B, **296** and **297**, would completely eliminate the possibility of steric interference (Fig. 7.2). If the binding constant between **296** and **297** was much higher than between the current units **5** and **2**, it would suggest that steric

interference was indeed taking place.

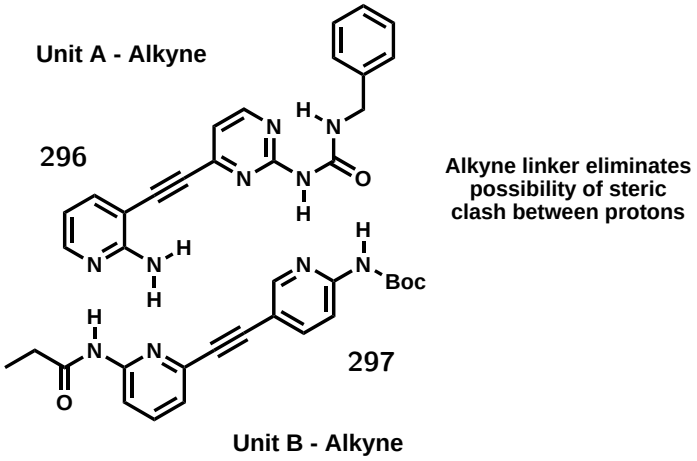

Fig. 7.2 Alkyne versions **296** and **297** of Unit A and Unit B.

7.3.2 Pyridazine Unit B

Another way to eliminate steric clashing between Units A and B is to use a pyridazine ring in Unit B instead of a pyridine, giving pyridazine Unit B **298** (Fig. 7.3). This design also has the benefit of increasing the number of H-bonds. The new nitrogen in the ring would form a H-bond with one or both of the protons of the amine of Unit A, thus potentially increasing the binding strength.

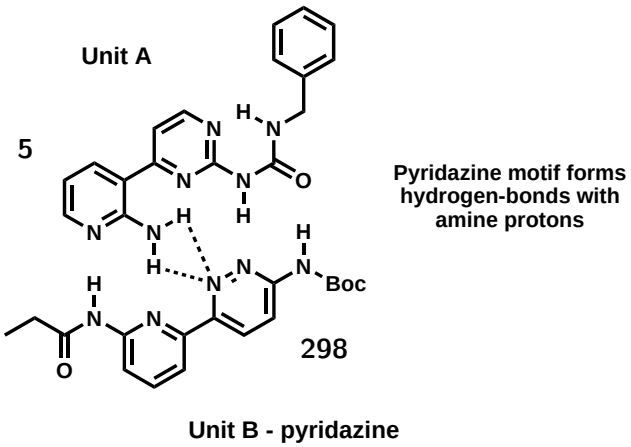

Fig. 7.3 Pyridazine version of Unit B **298** binding to Unit A **5**.

7.3.3 Naphthyridine Architecture

As mentioned above, Units C and D during binding have a reduced potential for steric clashing between protons compared to Units A and B (Fig. 7.1). However, the proton on the pyridine half of Unit D that points into the inter-unit space is involved in two potential steric clashes that

may affect binding strength (Fig. 7.4). To address this, both Units C and D could be updated to the designs shown. The pyridopyrimidine design **299** of Unit C is synthetically challenging. The simplified naphthyridine design **300** would sacrifice the intramolecular H-bond, but would considerably improve the ease of synthesis, as it is based on the same naphthyridine as Unit D functionalised in the 2- and 7-positions, for which there is much literature precedent.

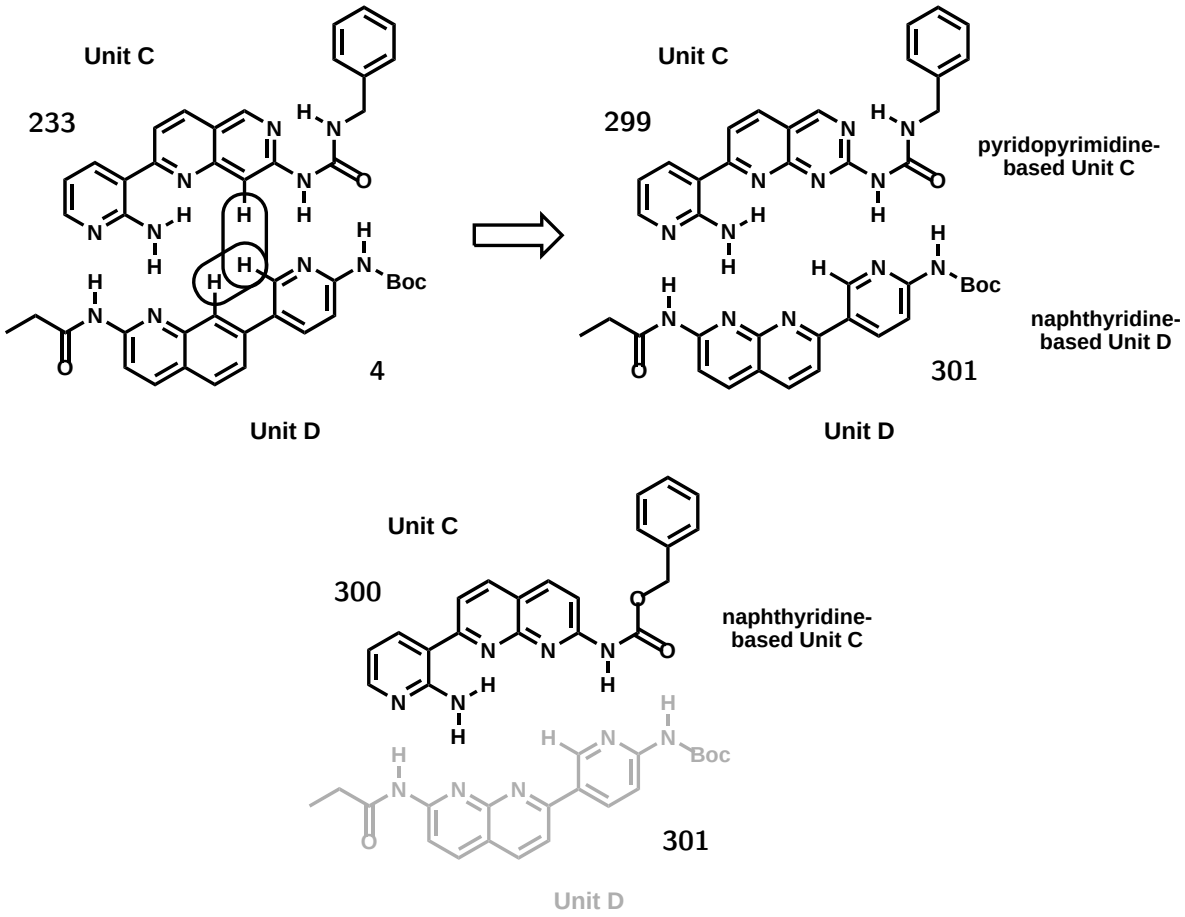

Fig. 7.4 Potential future versions of Units C and D.

7.3.4 Expanding the Pairwise Set

Units A and B and Units C and D form a staggered ADDA/DAAD pattern, and together form two pairs in an orthogonally-binding set. However, by expanding the staggered array pattern to include AAAD/DDDA, AADA/DDAD and AAAA/DDDD, the set can be vastly expanded to include five orthogonal pairs (Fig. 7.5). The beauty of the staggered design allows for twice the number of possible units for the AAAD/DDDA and AADA/DDAD pattern compared to if the pattern were in a straight row. The pattern AADD/DDAA, even if staggered, is self-complementary, and therefore is not included as it fails our design criteria. The designs are purely speculative, although the

attempt has been made to make them as synthetically feasible as possible. All include at least one nitrogen on one of the rings to reduce the intra-unit strain discussed above. Of all the five new suggested units, we propose Units G and H (**302** and **303**) as the outstanding pair in terms of likely ease of synthesis of both units.

In principle, many of the new arrays are very attractive, maintaining our key design requirements of non-self-complementarity and non-symmetry. However, a difficulty with such designs is the DD motif. Such a motif requires an N–H on the 'inside' position, which is chemically challenging to achieve. This problem was solved using a urea in Unit A **5**, but there are few other architectures that achieve the same thing. The problem arises when a proton is placed on the pyridine nitrogen, as there is a driving force for the ring to aromatise. The possible solutions shown include a urea (for example in Unit H **303**), and a 4-pyridone (for example in Unit K **304**). However, the urea would possibly suffer from rotation around the C=O/NH bond, for example producing an ADAD array in Unit H **303**, which would be self-complementary.

The AA motif is much more appealing from a synthetic point of view. This pattern can be achieved with naphthyridine (for example Unit E **305**), methoxypyridine (for example Unit G **302**), or methoxynaphthyridine (for example Unit J **306**). The oxygen (acceptor) of the methoxy would form a weaker H-bond than say the nitrogen of a pyridine. However, as discussed in Section 1.2.1, the sum of an array of H-bonds acting together is much greater than the sum of its parts. Plus, the AA/DD pair has positive secondary interactions (Section 1.3.1). Therefore, the synthetic simplicity of this motif makes it very appealing.

The designs have been created following the 'Units C and D architecture' as opposed to the 'Units A and B architecture'. This is to avoid steric clashes between protons in the inter-unit space, which we suspect may reduce binding strength. Unit L **307** contains a ring that juts into the space in the same way Unit A **5** does. However, the use of a pyrazine reduces the danger of steric clashing, and actually provides a second acceptor site for the N–H donor on Unit K **304**. On the other hand, there may still be steric clashing with Unit K **304** from the one remaining proton on the pyrazine ring of Unit L **307** that sticks into the inter-unit space.

7.3.5 Other Possibilities

There are many other possible complementary binding arrays and the design possibilities are limited only by imagination. Fig. 7.6 shows a variety of designs, some of which may prove to be successful were they ever to be synthesised. Again, the designs are purely speculative, intended more to

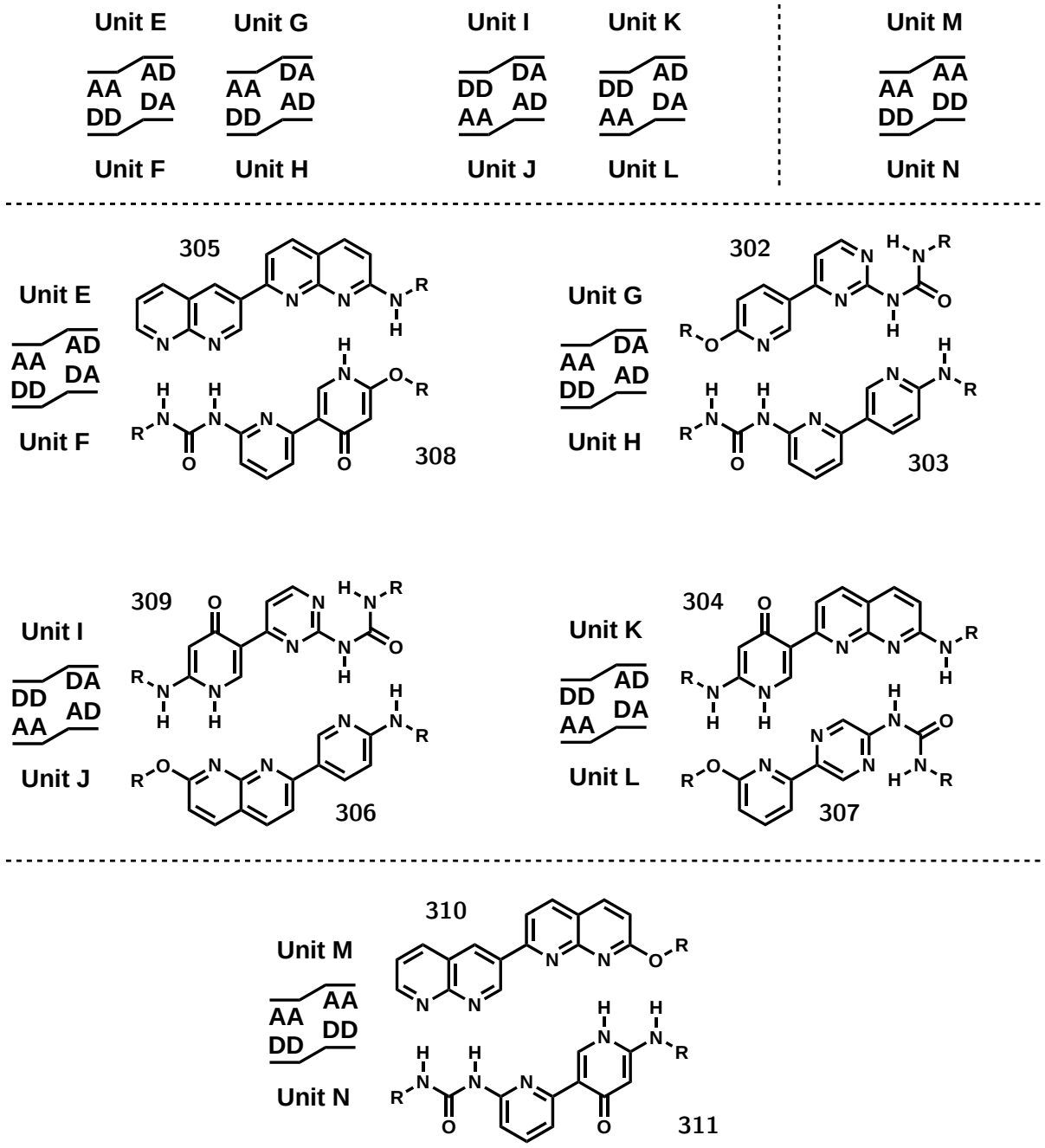

Fig. 7.5 Expansion of the set of orthogonally-binding pairs.

stimulate ideas than as rigorously-planned synthetic proposals.

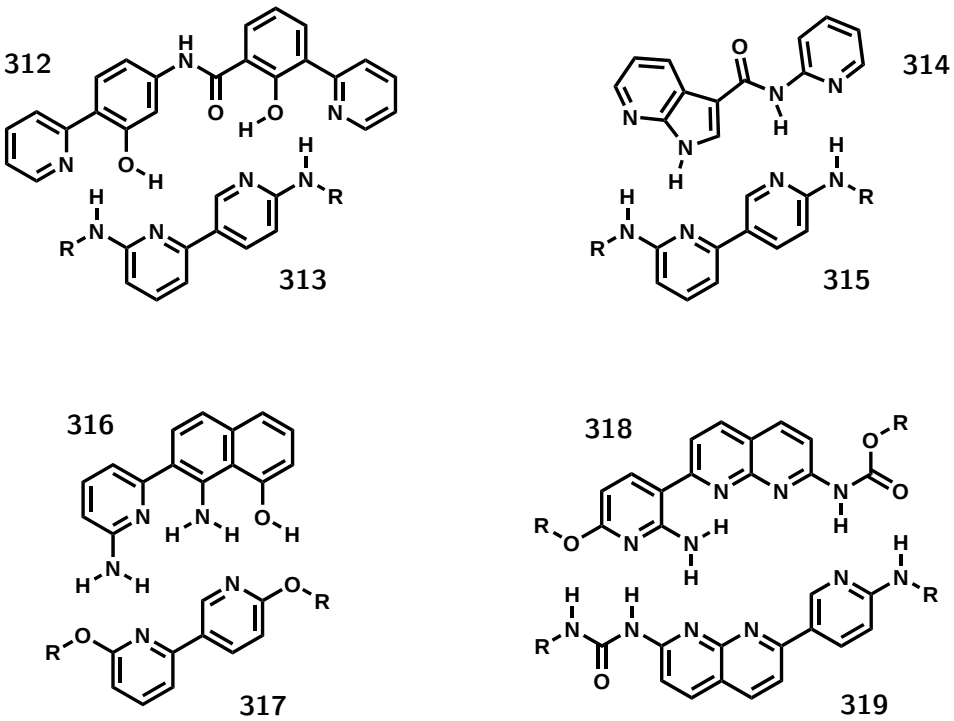

Fig. 7.6 Potential future designs.

8 Experimental

8.1 General Comments

^{1}H NMR spectra were recorded in $CDCl_3$ (δ_H 7.26 ppm), DMSO (δ_H 2.50 ppm), D_2O (δ_H 4.79 ppm), acetone-d_6 (δ_H 2.05 ppm), CD_3CN (δ_H 1.94 ppm), or CD_3OD (δ_H 3.31 ppm) at ambient probe temperatures on the following instruments: Bruker AVII 500 (500 MHz), Bruker DPX400 (400 MHz), Bruker DPX250 (250 MHz) and Bruker DPX200 (200 MHz) spectrometers. ^{13}C NMR spectra were recorded in $CDCl_3$ (δ_C 77.16 ppm), DMSO (δ_C 39.52 ppm), D_2O, acetone-d_6 (δ_C 29.84 and 206.26 ppm), CD_3CN (δ_C 1.32 and 118.26 ppm), or CD_3OD (δ_C 49.00 ppm) at ambient probe temperatures on the following instruments: Bruker AVII 500 (125 MHz), Bruker AV400 (100 MHz), Bruker DPX250 (62.9 MHz) and Bruker DPX200 (50 MHz) spectrometers. Chemical shifts are given in ppm on a δ scale relative to $\delta_{\mathrm{TMS}} = 0$. Data are presented as follows: integration, multiplicity (s = singlet, d = doublet, t = triplet, q = quartet, m = multiplet), coupling constant (J / Hz) and assignment. Assignments were determined on the basis of ^{1}H and ^{13}C NMR chemical shift, coupling pattern, and COSY, HSQC and HMBC experiments, or by analogy to fully interpreted spectra for related compounds.

Infra-red spectra were recorded on a Bruker Tensor 27 FT-IR spectrometer. The sample was prepared as a thin film or as a KBr disc. Wavelengths of maximum absorbance (ν_{max}) are quoted in cm^{-1}.

Low resolution mass spectra were recorded on a Waters LCT Premier EX mass spectrometer, using electron spray (ES^+, ES^-) techniques. High resolution mass spectra were recorded by the Departmental Mass Spectrometry Service, University of Oxford, using electron spray ionisation (ESI^+/ESI^-) and field ionisation (FI) techniques. The parent ion $[M+H]^+$, $[M-H]^-$ or $[M+Na]^+$ is quoted.

Melting points were obtained using a Reichert-Koffler block and are uncorrected.

Analytical thin layer chromatography (TLC) was carried out on Merck Kieselgel 60 F_{254} plates

with visualisation by ultraviolet light (254 nm) and $KMnO_4$ dip. Flash column chromatography was carried out on Merck Kieselgel 60 (230 - 400 mesh) under positive pressure using distilled solvents; the procedure includes the subsequent evaporation of solvents *in vacuo*.

Reagents and solvents were purified by standard means.[223] Diethyl ether (Et_2O), methanol (MeOH), ethanol (EtOH), toluene (PhMe) and benzene (PhH) were distilled from calcium hydride and stored under an argon atmosphere. Triethylamine (Et_3N), pyridine (pyr) and *N,N′*-dimethylethylenediamine (DMEDA) were distilled from and stored over calcium hydride. All other chemicals were used as received, except where otherwise noted in the experimental text. All solutions of sodium bicarbonate ($NaHCO_3$), ammonium chloride (NH_4Cl), and sodium thiosulfate ($Na_2S_2O_3$) were aqueous and saturated.

All experiments were performed under anhydrous conditions under an atmosphere of argon, except where stated, using oven-dried apparatus and employing standard techniques for handling air-sensitive materials. Unless stated otherwise, reactions were performed at room temperature (r.t.).

8.2 Compounds

5-bromopyridin-2-amine 84

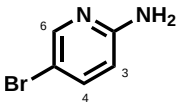

84

To a stirred solution of 2-aminopyridine **83** (2.0 g, 21.3 mmol, 1.0 eq.) in MeCN (50 mL) at 0 °C was added NBS (3.78 g, 21.3 mmol, 1.0 eq.). The solution was stirred at r.t. for 16 h and the solvent removed under reduced pressure. The residue was dissolved in $CHCl_3$, washed with water, and concentrated under reduced pressure to afford 5-bromopyridin-2-amine **84** (3.35 g, 19.4 mmol, 91 %) as brown flakes; **^{1}H NMR** (400 MHz, $CDCl_3$) δ_H 8.10 (1H, d, J = 2.40 Hz, H6), 7.49 (1H, dd, J = 8.70 and 2.41 Hz, H4), 6.42 (1H, d, J = 8.70 Hz, H3), 4.46 (2H, s, NH_2). Data agrees with literature.[97]

tert-butyl (5-bromopyridin-2-yl)carbamate 76

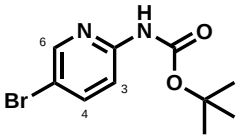

76

To a stirred solution of 5-bromopyridin-2-amine **84** (3.25 g, 18.77 mmol, 1.0 eq.) in THF (60 mL) at r.t. was added NaHMDS (50.68 mL, 1.0 M in THF, 50.68 mmol, 2.7 eq.). After 20 m a solution of Boc_2O (5.10 g, 23.36 mmol, 1.25 eq.) in THF (10 mL) was added. After 3 h the reaction mixture was concentrated under reduced pressure, aqueous NH_4Cl was added, and the solution extracted with DCM (3 × 60 mL). The combined organic phases were concentrated under reduced pressure to afford tert-butyl (5-bromopyridin-2-yl)carbamate **76** (4.71 g, 17.31 mmol, 92 %) as a white crystalline solid; **^{1}H NMR** (400 MHz, $CDCl_3$) δ_H 9.38 (1H, s, NH), 8.41 (1H, d, J = 2.37 Hz, H6), 7.96 (1H, d, J = 9.00 Hz, H3), 7.76 (1H, dd, J = 8.92 Hz and 2.45 Hz, H4), 1.56 (9H, s, $C(CH_3)_3$). Data agrees with literature.[98]

N-(6-bromopyridin-2-yl)propionamide 77

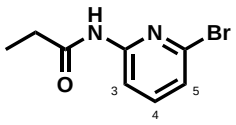

77

A solution of 6-bromopyridin-2-amine **82** (500 mg, 2.89 mmol, 1.0 eq.), propionyl chloride (0.28 mL, 3.18 mmol, 1.1 eq.), and pyridine (0.31 mL, 3.82 mmol, 1.2 eq.) in DCM (10 mL) was stirred at r.t. for 20 m. Aqueous sodium bicarbonate was added and the solution extracted with DCM (3 × 20 mL). The combined organic phases were concentrated under reduced pressure to afford **77** (451 mg, 1.98 mmol, 68 %) as light yellow flakes; $\mathbf{R_f}$ 0.42 (1:1 P.E.:Et_2O); **mp** 68.4–71.4 °C; $\boldsymbol{\nu_{max}}$ (thin film) / cm^{-1} 3228, 3077, 2975, 2361, 2341, 1663, 1561, 1524, 1456, 1429, 1387, 1324, 1302, 1242, 1210, 1154, 1132, 1081, 1064, 1009, 981, 869, 784, 728, 691 and 635; ^{1}**H NMR** (400 MHz, $CDCl_3$) δ_H 8.78 (1H, s, NH), 8.09 (1H, d, J = 8.18 Hz, ArH), 7.43 (1H, t, J = 7.95 Hz, H4), 7.06 (1H, d, J = 7.71 Hz, ArH), 2.39 (2H, q, J = 7.54 Hz, CH_2), 1.11 (3H, t, J = 7.56 Hz, CH_3), ^{13}**C NMR** (100 MHz, $CDCl_3$) δ_C 172.9, 151.6, 140.5, 138.9, 123.1, 112.5, 30.4 and 9.2; $\boldsymbol{m/z}$ (ESI^+) 252.96 (100 %, $[M+Na]^+$); **HRMS** (ESI^+) found 252.9771 ($[M+Na]^+$, $C_8H_9BrN_2ONa$ requires 252.9770).

(6-((tert-butoxycarbonyl)amino)pyridin-3-yl)boronic acid 75

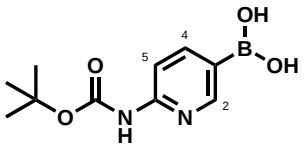

75

To a solution of tert-butyl (5-bromopyridin-2-yl)carbamate **76** (500 mg, 1.84 mmol, 1.0 eq.) in dry Et_2O (7 mL) at −78 °C was added *n*-BuLi (2.9 mL, 2.5 M, 7.36 mmol, 4.0 eq.) dropwise over 10 m. The solution was stirred at −78 °C for 15 m, then triisopropylborate (1.70 mL, 7.36 mmol, 4.0 eq.) was added, and the solution stirred at −78 °C for 15 m. Water (10 mL) was added, and the solution stirred at r.t. for 15 m. The Et_2O was removed under reduced pressure, and the aqueous phase washed once with Et_2O. Any remaining Et_2O in the aqueous phase was removed under reduced pressure, and then it was acidified to pH 7, during which time the product crashed out of solution. It was isolated by sinter filtration and dried under vacuum over P_2O_5 to afford (6-((tert-butoxycarbonyl)amino)pyridin-3-yl)boronic acid **75** (141 mg, 0.59 mmol, 32 %); $\mathbf{R_f}$ 0.41 (100% EtOAc); **mp** > 250 °C; $\boldsymbol{\nu_{max}}$ (thin film) / cm^{-1} 2979, 1727, 1584, 1530, 1393, 1369, 1304, 1251, 1155, 1128, 1060, 840 and 772; ^{1}**H NMR** (500 MHz, $(CD_3)_2CO$) δ_H 9.57 (1H, s, NH), 8.76

(1H, s, H2), 8.16 (1H, dd, J = 8.40 and 1.89 Hz, H4), 7.97 (1H, d, J = 8.43 Hz, H5), 7.34 (2H, s, $B(OH)_2$), 1.54 (9H, s, $C(CH_3)_3$); **^{13}C NMR** (125 MHz, $(CD_3)_2CO$) δ_C 154.9, 149.3, 144.7, 141.4, 114.6, 111.8, 80.9 and 28.5 ($C(CH_3)_3$); ***m/z*** (ESI^+) 237.13 (100 %), 261.11 (53 %, $[M+Na]^+$); **HRMS** (ESI^+) found 261.1026 ($[M+Na]^+$, $C_{10}H_{15}BN_2O_4Na$ requires 261.1019).

phenylboronic acid 85

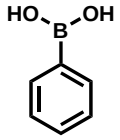

85

To a stirred solution of bromobenzene **111** (1.0 mL, 9.50 mmol, 1.0 eq.) in THF (20 mL) at −78 °C was added *n*-BuLi dropwise (4.2 mL, 2.5 M solution, 10.45 mmol, 1.1 eq.). The solution was stirred for 30 m at −78 °C then $B(OMe)_3$ (3.16 mL, 28.5 mmol, 3.0 eq.) was subsequently added over 1 m. The solution was stirred for 30 m at −78 °C, then allowed to warm to room temperature. Stirring was continued for a futher hour at r.t. before quenching with 1 M HCl solution (15 mL). The phases were separated, the aqueous phase extracted with DCM (3 × 20 mL) and the combined organic phases dried ($MgSO_4$) and concentrated under reduced pressure to afford phenylboronic acid **85** (900 mg, 7.38 mmol, 78 %) as a white crystalline solid; **^{1}H NMR** (400 MHz, $CDCl_3$) δ_H 8.26 (2H, dd, J = 8.02 and 1.35 Hz, ArH), 7.62 (1H, tt, J = 7.36 and 1.50 Hz, ArH), 7.52 (2H, t, J = 7.71 Hz, ArH). Data agrees with literature.[224]

N-(6-phenylpyridin-2-yl)propionamide 86

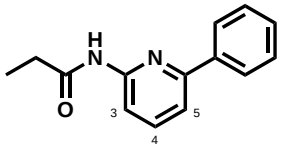

86

A solution of N-(6-bromopyridin-2-yl)propionamide **77** (200 mg, 0.88 mmol, 1.0 eq.), phenyl boronic acid (118 mg, 0.97 mmol, 1.1 eq.), aqueous Na_2CO_3 solution (0.73 mL, 2 M, 1.7 eq.) and EtOH (0.4 mL) in toluene (8 mL) was degassed with argon for 30 m. $Pd(PPh_3)_4$ (20 mg, 0.017 mmol, 0.02 eq.) was subsequently added and the solution stirred at 110 °C for 24 h. Brine (10 mL) was then added, the phases separated and the aqueous phase extracted with EtOAc (3 × 15 mL). The combined organic phases were dried ($MgSO_4$) and concentrated *in vacuo*. The combined

organic phases were purified by flash chromatography (100 % DCM mobile phase) to afford N-(6-phenylpyridin-2-yl)propionamide **86** (129 mg, 0.57 mmol, 65 %) as a white crystalline solid; $\mathbf{R_f}$ 0.35 (100 % DCM); $\boldsymbol{\nu_{max}}$ (KBr disc) / cm^{-1} 3268, 2923, 1668, 1572, 1445, 1386, 1280, 1193, 1155, 1072, 1028, 929, 816, 764, 696; ^{1}**H NMR** (400 MHz, $CDCl_3$) δ_H 8.24 (1H, s, NH), 8.18 (1H, d, J = 10.15 Hz, ArH), 7.95–7.92 (2H, m, ArH), 7.77 (1H, t, J = 9.95 Hz, H4), 7.49–7.45 (3H, m, ArH), 7.43–7.39 (1H, m, ArH), 2.36 (2H, m, CH_2), 1.21 (3H, m, CH_3); ^{13}**C NMR** (125 MHz, $CDCl_3$) δ_C 172.6, 156.0, 151.3, 139.3 (C4), 138.9, 129.2, 128.9, 126.9, 116.5, 112.3, 29.8 (CH_2) and 9.5 (CH_3); $\boldsymbol{m/z}$ (ESI^+) 475.18 (100 %), 249.09 ($[M+Na]^+$, 76 %), 227.11 ($[M+H]^+$, 66 %); **HRMS** (ESI^+) found 249.0997 ($[M+Na]^+$), $C_{14}H_{14}N_2NaO$ $[M+Na]^+$ requires 249.0998).

N-(6′-amino-[2,3′-bipyridin]-6-yl)propionamide 87

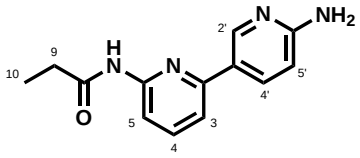

87

A solution of N-(6-bromopyridin-2-yl)propionamide **77** (50 mg, 0.22 mmol, 1.0 eq.), (6-((tert-butoxycarbonyl)amino)pyridin-3-yl)boronic acid **75** (58 mg, 0.24 mmol, 1.1 eq.), aqueous Na_2CO_3 solution (0.19 mL, 2 M, 0.38 mmol, 1.7 eq.), EtOH (0.10 mL), and toluene (1.8 mL) was degassed for 20 m. Tetrakis(triphenylphosphine)palladium (5 mg, 0.0043 mmol, 0.02 eq.) was added and the solution stirred at 110 ℃ for 48 h. After cooling to room temperature, brine was added, and the mixture extracted with EtOAc (3 × 15 mL). The combined organic phases were concentrated under reduced pressure and purified by flash chromatography (2:1 EtOAc:DCM mobile phase) to afford N-(6′-amino-[2,3′-bipyridin]-6-yl)propionamide **87** (11 mg, 0.045 mmol, 21 %); $\mathbf{R_f}$ 0.30 (100 % EtOAc); **mp** 173.3–175.1 ℃; $\boldsymbol{\nu_{max}}$ (thin film) / cm^{-1} 3357, 2937, 1592 and 1448; ^{1}**H NMR** (500 MHz, $CDCl_3$) δ_H 8.66 (1H, d, J = 2.09 Hz, H2′), 8.10 (1H, d, J = 7.96 Hz, H5), 8.03 (1H, dd, J = 8.53 and 2.35 Hz, H4′), 8.02 (1H, s, NH), 7.72 (1H, t, J = 8.02 Hz, H4), 7.35 (1H, d, J = 7.66 Hz, H3), 6.57 (1H, d, J = 8.63 Hz, H5′), 4.65 (2H, s, NH_2), 2.45 (2H, q, J = 7.53 Hz, CH_2), 1.26 (3H, t, J = 7.53 Hz, CH_3); ^{13}**C NMR** (125 MHz, $CDCl_3$) δ_C 172.5, 158.9, 153.8, 151.3, 147.1, 139.3 (C4), 136.4, 125.2, 115.1 (C3), 111.7 (C5), 108.4, 29.8 (C9) and 9.6 (C10); $\boldsymbol{m/z}$ (ESI^+) 243.11 ($[M+H^+]$, 100 %); **HRMS** (ESI^+) found 243.1241 ($[M+H]^+$, $C_{13}H_{15}N_4O$ requires 243.1240).

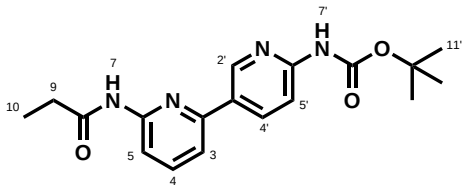

2

tert-butyl (6-propionamido-[2,3′-bipyridin]-6′-yl)carbamate 2

A solution of N-(6-bromopyridin-2-yl)propionamide **77** (40 mg, 0.18 mmol, 1.0 eq.), (6-((tert-butoxycarbonyl)amino)pyridin-3-yl)boronic acid **75** (46 mg, 0.19 mmol, 1.1 eq.), tetrakis(triphenylphosphine)palladium (5 mg, 0.0045 mmol, 0.025 eq.), aqueous Na_2CO_3 (0.16 mL, 2 M solution, 0.31 mmol, 1.7 eq.), EtOH (0.08 mL) and toluene (1.5 mL) was degassed for 10 m and then stirred at 80 °C for 16 h. After cooling to room temperature the mixture was concentrated under reduced pressure and purified by flash chromatography (100 % DCM mobile phase) to afford tert-butyl (6-propionamido-[2,3′-bipyridin]-6′-yl)carbamate **2** (43 mg, 0.13 mmol, 72 %) as a white crystalline solid; $\mathbf{R_f}$ 0.30 (1:1 P.E.:Et_2O); $\boldsymbol{\nu_{max}}$ (thin film) / cm^{-1} 2978, 1728, 1575, 1536, 1447, 1410, 1367, 1271, 1157, 1072 and 803; ^{1}**H NMR** (500 MHz, $CDCl_3$) δ_H 8.85 (1H, dd, J = 0.72 and 2.38 Hz, H2′), 8.24 (1H, dd, J = 2.38 and 8.79 Hz, H4′), 8.16 (1H, d, J = 8.29 Hz, H5), 8.10 (1H, s, H7′), 8.05 (1H, d, J = 8.29 Hz, H5′), 7.94 (1H, s, H7), 7.76 (1H, t, J = 7.96 Hz, H4), 7.42 (1H, dd, J = 0.68 and 7.66 Hz, H3), 2.47 (2H, q, J = 7.54 Hz, H9), 1.55 (9H, s, H11′), 1.28 (3H, t, J = 7.54 Hz, H10); ^{13}**C NMR** (125 MHz, $CDCl_3$) δ_C 172.5, 153.1, 152.6, 152.5, 151.4, 146.5 (C2′), 139.4 (C4), 136.6 (C4′), 129.3, 115.7 (C3), 112.4 (C5), 112.0 (C5′), 81.4, 31.0 (C9), 28.5 (C11′) and 9.6 (C10); $\boldsymbol{m/z}$ (ESI^-) 341.15 (100 %, [M-H^-]); **HRMS** (ESI^+) found 365.1582 ([M+Na]$^+$, $C_{18}H_{22}N_4O_3Na$ requires 365.1584).

N-(3-bromophenyl)cinnamamide 88

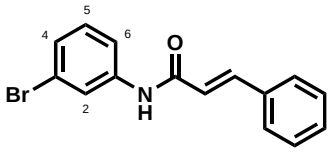

88

To a stirred solution of 3-bromoaniline **80** (2.00 mL, 18.3 mmol, 1.0 eq.) and pyridine (1.78 mL, 22.0 mmol, 1.2 eq.) in DCM (25 mL) at r.t. was slowly added cinnamoyl chloride (3.35 g, 20.1 mmol, 1.1 eq.). After 30 m the reaction mixture was washed first with $NaHCO_3$ solution then 1 M HCl solution. The organic phase was concentrated under reduced pressure to afford N-(3-bromophenyl)-

cinnamamide **88** (4.75 g, 15.73 mmol, 86 %) as a white solid; **^{1}H NMR** (400 MHz, $CDCl_3$) δ_H 7.88 (1H, s, NH), 7.76 (1H, d, J = 15.51 Hz, HC=CH), 7.58–7.49 (4H, m, ArH), 7.40–7.35 (3H, m, ArH), 7.25 (1H, d, J = 7.37 Hz, ArH), 7.20 (1H, t, J = 8.04 Hz, ArH), 6.55 (1H, d, J = 15.53 Hz, HC=CH). Data agrees with literature.[225]

Isomeric mix: 7-bromoquinolin-2(1H)-one 70 and 5-bromoquinolin-2(1H)-one 90

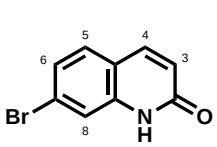

70

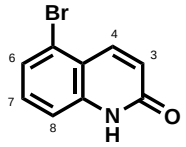

90

A mixture of N-(3-bromophenyl)cinnamamide **88** (2.0 g, 6.62 mmol, 1.0 eq.) and $AlCl_3$ (2.6 g, 19.9 mmol, 3.0 eq.) was stirred without solvent at 100 °C for 90 m, after a heat gun was employed to initate the reaction. After cooling to room temperature the flask was cooled to 0 °C and the mixture was slowly quenched with ice and water. The precipitate was collected by vacuum filtration, washed with 1 M HCl, and dried over P_2O_5 under reduced pressure to afford a 3:2 isomeric mix of 7-bromoquinolin-2(1H)-one **70** : 5-bromoquinolin-2(1H)-one **90** (combined yield 1.47 g, 6.62 mmol, 100 %) as a light red/brown powder; NMR data reported from the same spectrum: 7-bromoquinolin-2(1H)-one **70** (985 mg, 4.44 mmol, 67 %) **^{1}H NMR** (400 MHz, $CDCl_3$) δ_H 7.78 (1H, d, J = 9.51 Hz, H4), 7.59 (1H, s, H8), 7.44 (1H, d, J = 8.39 Hz, H5), 7.36 (1H, m, H6), 6.73 (1H, d, J = 9.45 Hz, H3). Data agrees with literature.[226] 5-bromoquinolin-2(1H)-one **90** (485 mg, 2.18 mmol, 33 %) **^{1}H NMR** (400 MHz, $CDCl_3$) δ_H 8.23 (1H, d, J = 9.78 Hz, H4), 7.48 (1H, dd, J = 6.83 and 1.89 Hz, ArH), 7.36 (2H, m, ArH), 6.80 (1H, d, J = 9.81 Hz, H3). Data agrees with literature.[227]

7-bromo-2-chloroquinoline 96

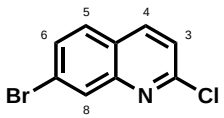

96

A solution of 5/7-bromoquinolin-2(1H)-one (3:2 7-br **70**:5-br **90**) (5.0 g, 22.52 mmol, 1.0 eq.) and $POCl_3$ (10.29 mL, 113 mmol, 5.0 eq.) was stirred at reflux (115 °C) for 4 h. After cooling to room temperature the flask was placed in an ice bath (0 °C), a condenser placed on top of the flask, and ice-cold water added from the bath very slowly down the condenser. After all $POCl_3$ had been

quenched, the pH was raised to neutral with aqueous NaOH. The mixture was extracted with DCM (3 × 50 mL), the combined organic phases concentrated under reduced pressure, and purified by flash chromatography (3:1 P.E.:Et_2O) to afford 7-bromo-2-chloroquinoline **96** (1.445 g, 5.97 mmol, 44 % from the 3.0 g of 7-br starting material); **^{1}H NMR** (400 MHz, $CDCl_3$) δ_H 8.21 (1H, d, J = 1.72 Hz, H8), 8.08 (1H, d, J = 8.55 Hz, ArH), 7.69 (1H, d, J = 8.66 Hz, H5), 7.66 (1H, dd, J = 8.69 and 1.84 Hz, H6), 8.41 (1H, d, J = 8.54 Hz, ArH). Data agrees with literature.[228]

5-bromo-2-chloroquinoline 97

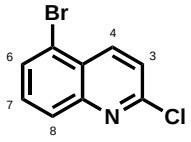

97

A solution of 5/7-bromoquinolin-2(1H)-one (3:2 7-br **70**:5-br **90**) (5.0 g, 22.52 mmol, 1.0 eq.) and $POCl_3$ (10.29 mL, 113 mmol, 5.0 eq.) was stirred at reflux (115 °C) for 4 h. After cooling to room temperature the flask was placed in an ice bath (0 °C), a condenser placed on top of the flask, and ice-cold water added from the bath very slowly down the condenser. After all $POCl_3$ had been quenched, the pH was raised to neutral with aqueous NaOH. The mixture was extracted with DCM (3 × 50 mL), the combined organic phases concentrated under reduced pressure, and purified by flash chromatography (3:1 P.E.:Et_2O) to afford 5-bromo-2-chloroquinoline **97** (740 mg, 3.06 mmol, 34 % from the 2.0 g of 5-br starting material); **^{1}H NMR** (400 MHz, $CDCl_3$) δ_H 8.50 (1H, d, J = 8.86 Hz, ArH), 8.00 (1H, d, J = 8.47 Hz, ArH), 7.84 (1H, dd, J = 7.57 and 0.93 Hz, ArH), 7.60 (1H, t, J = 8.03 Hz, H7), 7.49 (1H, d, J = 8.87 Hz, ArH). Data agrees with literature.[229]

7-bromoquinolin-2-amine 98

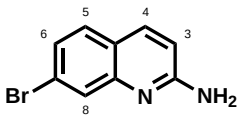

98

A solution of 7-bromo-2-chloroquinoline **96** (625 mg, 2.58 mmol, 1.0 eq.), acetamide (3.05 g, 51.65 mmol, 20 eq.) and potassium carbonate (1.78 g, 12.9 mmol, 5.0 eq.) was stirred at 200 °C for 1 h. After reducing to room temperature, water (20 mL) was added, and the aqueous phase extracted with DCM (3 x 20 mL). The combined organic phases were dried with Mg_2SO_4, concentrated under

reduced pressure, and purified by flash chromatography (100 % Et_2O mobile phase) to afford 7-bromoquinolin-2-amine **98** (502 mg, 2.25 mmol, 87 %) as a dark yellow solid; $\mathbf{R_f}$ 0.14 (100 % Et_2O); **mp** 126.1–129.4 °C; $\boldsymbol{\nu_{max}}$ (thin film) / cm^{-1} 3329, 3188, 1619, 1561, 1498, 1463, 1391, 1349, 1146, 1129, 924, 834 and 769; ^{1}**H NMR** (500 MHz, $CDCl_3$) δ_H 7.83 (1H, d, J = 7.52 Hz, H4), 7.82 (1H, s, H8), 7.47 (1H, d, J = 8.59 Hz, H5), 7.34 (1H, dd, J = 8.52 and 1.99 Hz, H6), 6.71 (1H, d, J = 8.79 Hz, H3), 4.84 (2H, s, NH_2), ^{13}**C NMR** (125 MHz, $(CD_3)_2CO$) δ_C 157.6, 148.8, 137.9 (C4), 128.8 (C5), 128.7 (C8), 126.2 (C6), 124.0, 122.4 and 112.0 (C3); $\boldsymbol{m/z}$ (ESI^+) 224.98 (100 %, $[M+H]^+$); **HRMS** (ESI^+) found 224.9843 ($[M+H]^+$, $C_9H_8BrN_2$ requires 224.9845).

N-(7-bromoquinolin-2-yl)propionamide 81

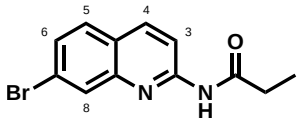

81

A solution of 7-bromoquinolin-2-amine **98** (588 mg, 2.64 mmol, 1.0 eq.), propionyl chloride (0.34 mL, 3.96 mmol, 1.5 eq.), pyridine (0.42 mL, 5.27 mmol, 2.0 eq.) and DCM (10 mL) was stirred at r.t. for 6 h. Sodium bicarbonate was added and the mixture extracted into DCM (3 x 15 mL). The organic phase was concentrated under reduced pressure and purified by flash chromatography (3:1 EtOAc:P.E. mobile phase) to afford N-(7-bromoquinolin-2-yl)propionamide **81** (405 mg, 1.45 mmol, 55 %) as a white solid; $\mathbf{R_f}$ 0.38 (1:1 P.E.:Et_2O); **mp** 135.5–137.9 °C; $\boldsymbol{\nu_{max}}$ (thin film) / cm^{-1} 3058, 2981, 2940, 2361, 1699, 1611, 1595, 1491, 1463, 1438, 1399, 1313, 1265, 1203, 1184, 1144, 1126, 1060, 1026, 965, 938, 893, 845, 806, 769 and 627; ^{1}**H NMR** (500 MHz, $CDCl_3$) δ_H 8.65 (1H, s, NH), 8.47 (1H, d, J = 8.99 Hz, H3), 8.14 (1H, d, J = 8.99 Hz, H4), 7.98 (1H, d, J = 1.86 Hz, H8), 7.63 (1H, d, J = 8.63 Hz, H5), 7.53 (1H, dd, J = 8.62 and 1.90 Hz, H6), 2.51 (2H, q, J = 7.53 Hz, H11), 1.28 (3H, t, J = 7.54 Hz, H12); ^{13}**C NMR** (125 MHz, $(CD_3)_2CO$) δ_C 173.2, 152.0, 147.2, 138.8 (C4), 129.4 (C8), 128.9 (C5), 128.8 (C6), 124.9, 124.4, 114.7 (C3), 31.1 (C11) and 9.4 (C12); $\boldsymbol{m/z}$ (ESI^-) 278.98 (100 %, $[M-H]^-$); **HRMS** (ESI^+) found 302.9923 ($[M+Na]^+$, $C_{12}H_{11}BrN_2ONa$ requires 302.9927).

ethyl (5-(2-propionamidoquinolin-7-yl)pyridin-2-yl)carbamate 99

A solution of (6-((tert-butoxycarbonyl)amino)pyridin-3-yl)boronic acid **75** (50 mg, 0.21 mmol, 1.3 eq.), N-(7-bromoquinolin-2-yl)propionamide **81** (45 mg, 0.16 mmol, 1.0 eq.), tetrakis(triphenyl-

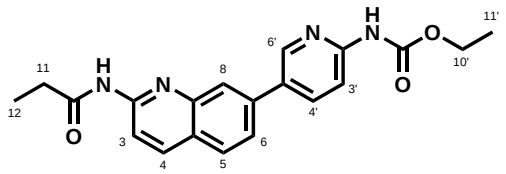

99

phosphine)palladium (9 mg, 0.008 mmol, 0.05 eq.), aqueous Na_2CO_3 (0.14 mL, 2 M solution, 0.27 mmol, 1.7 eq.), EtOH (0.07 mL) and toluene (1.5 mL) was degassed for 10 m and then stirred at 110 °C for 16 h. After cooling to room temperature the mixture was concentrated under reduced pressure and purified by flash chromatography (1:1 P.E.:Et_2O mobile phase) to afford ethyl (5-(2-propionamido-quinolin-7-yl)pyridin-2-yl)carbamate **99** (20 mg, 0.055 mmol, 34 %); $\mathbf{R_f}$ 0.39 (100 % Et_2O); $\boldsymbol{\nu_{max}}$ (thin film) / cm^{-1} 2973, 1724, 1665, 1598, 1545, 1511, 1486, 1418, 1360, 1311, 1286, 1253, 1223, 1074, 840, 805 and 765; ^{1}**H NMR** (500 MHz, $CDCl_3$) δ_H 8.76 (1H, s, NH), 8.69 (1H, d, J = 2.20 Hz, H6′), 8.45 (1H, d, J = 8.80 Hz, H3), 8.34 (1H, s, NH), 8.19 (1H, d, J = 8.97 Hz, H4), 8.14 (1H, d, J = 8.74 Hz, H3′), 8.04 (1H, dd, J = 8.71 and 2.45 Hz, H4′), 8.00 (1H, s, H8), 7.86 (1H, d, J = 8.37 Hz, H5), 7.66 (1H, dd, J = 8.41 and 1.69 Hz, H6), 4.29 (2H, q, J = 7.05 Hz, H10′), 2.51 (2H, q, J = 7.57 Hz, H11), 1.34 (3H, t, J = 7.12 Hz, H11′), 1.29 (3H, t, J = 7.52 Hz, H12); ^{13}**C NMR** (125 MHz, $CDCl_3$) δ_C 172.9 (C10), 153.6, 151.7, 147.1, 146.5 (C6′), 145.7, 139.2, 138.5 (C4), 137.3 (C4′), 131.2, 128.5 (C5), 125.7, 124.8 (C8), 124.1 (C6), 114.5 (C3), 112.5 (C3′), 61.7 (C10′), 31.2 (C11), 14.7 (C11′), and 9.5 (C12); $\boldsymbol{m/z}$ (ESI^+) 413.26 (100 %), 365.15 (94 %, $[M+H^+]$); **HRMS** (ESI^+) found 365.1600 ($[M+H]^+$, $C_{20}H_{21}N_4O_3$ requires 365.1608).

ethyl (5-(2-propionamidoquinolin-7-yl)pyridin-2-yl)carbamate 4

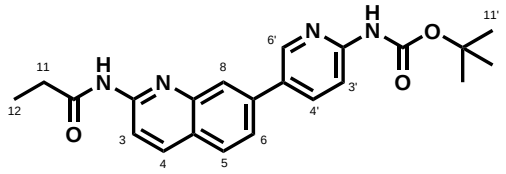

4

A solution of (6-((tert-butoxycarbonyl)amino)pyridin-3-yl)boronic acid **75** (67 mg, 0.28 mmol, 1.1 eq.), N-(7-bromoquinolin-2-yl)propionamide **81** (71 mg, 0.25 mmol, 1.0 eq.), tetrakis(triphenyl-phosphine)palladium (7 mg, 0.006 mmol, 0.025 eq.), aqueous Na_2CO_3 (0.22 mL, 2 M solution, 0.43 mmol, 1.7 eq.), EtOH (0.11 mL) and toluene (3.0 mL) was degassed for 10 m and then stirred at 80 °C for 16 h. After cooling to room temperature the mixture was concentrated under reduced

pressure and purified by flash chromatography (1:1 P.E.:Et_2O mobile phase) to afford ethyl (5-(2-propionamidoquinolin-7-yl)pyridin-2-yl)carbamate **4** (55 mg, 0.14 mmol, 57 %); $\mathbf{R_f}$ 0.38 (1:1 P.E.: EtOAc); **mp** 168.2–170.7 °C; $\boldsymbol{\nu_{max}}$ (thin film) / cm^{-1} 2978, 1703, 1602, 1507, 1413, 1367, 1316, 1251, 1156, 1062 and 842; ^{1}**H NMR** (500 MHz, $CDCl_3$) δ_H 8.65 (1H, d, J = 2.20 Hz, H6′), 8.53 (1H, s, NH), 8.46 (1H, d, J = 8.95 Hz, H3), 8.28 (1H, s, NH), 8.20 (1H, d, J = 8.97 Hz, H4), 8.09 (1H, d, J = 8.32 Hz, H3′), 8.02 (1H, dd, J = 8.74 and 2.40 Hz, H4′), 8.00 (1H, s, H8), 7.86 (1H, d, J = 8.42 Hz, H5), 7.66 (1H, dd, J = 8.41 and 1.69 Hz, H6), 2.52 (2H, q, J = 7.59 Hz, H11), 1.52 (9H, s, H11′), 1.29 (3H, t, J = 7.43 Hz, H12); ^{13}**C NMR** (125 MHz, $CDCl_3$) δ_C 173.1 (C10), 152.7, 152.0, 151.7, 146.4 (C6′), 139.5, 138.7 (C4), 137.1 (C4′), 130.9, 128.5 (C5), 126.3, 125.6, 124.8 (C8), 124.2 (C6), 114.5 (C3), 112.6 (C3′), 81.4 (C10′), 31.1 (C11), 28.4 (C11′) and 9.5 (C12); $\boldsymbol{m/z}$ (ESI^+) 413.26 (100 %), 393.19 (75 %, $[M+H^+]$); **HRMS** (ESI^+) found 393.1938 ($[M+H]^+$, $C_{22}H_{25}N_4O_3$ requires 393.1921).

2,4,6-tribromopyrimidine 105

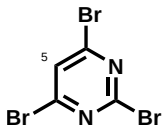

105

A solution of barbituric acid **104** (602 mg, 4.70 mmol, 1.0 eq.), phosphorus oxytribromide (5.0 g, 18.65 mmol, 4.0 eq.), N,N-diethylaniline (1.30 g, 8.72 mmol, 1.85 eq.), and toluene (10 mL) was stirred at 120 °C for 3 h. After cooling to r.t. the flask was cooled to 0 °C and water was slowly added. The solution was extracted with toluene (3 × 20 mL) and concentrated under reduced pressure to afford 2,4,6-tribromopyrimidine **105** (1.34 g, 4.25 mmol, 90 %) as a yellow crystalline solid; ^{1}**H NMR** (400 MHz, $CDCl_3$) δ_H 7.74 (1H, s, H5). Data agrees with literature.[111]

4-bromo-2,6-dimethoxypyrimidine 100

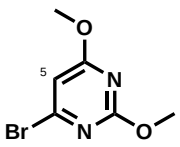

100

To a stirred solution of 2,4,6-tribromopyrimidine **105** (828 mg, 2.63 mmol, 1.0 eq.), in dry MeOH (6 mL) and dry Et_2O (3 mL) at r.t. was added dropwise NaOMe solution (10.5 mL, 0.5 M, 2.0 eq.) over 10 m. The solution was stirred at r.t. for 72 h, concentrated under reduced pressure and purified by flash chromatography (3:1 P.E.:DCM) to afford 4-bromo-2,6-dimethoxypyrimidine **100** (294 mg, 1.42 mmol, 54 %); **^{1}H NMR** (400 MHz, $CDCl_3$) δ_H 6.60 (1H, s, H5), 4.00 (3H, s, OMe), 3.96 (3H, s, OMe). Data agrees with literature.[111]

5-bromo-2-methoxypyridine 106

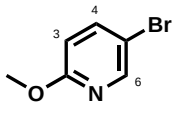

106

A solution of 2-methoxypyridine **103** (4.0 mL, 38.17 mmol, 1.0 eq.), N-bromosuccinimide (6.80 g, 38.17 mmol, 1.0 eq.) and MeCN (100 mL) was stirred at 90 °C for 16 h in darkness. The solution was concentrated under reduced pressure and purified by flash chromatography (10:1 P.E.:EtOAc) to afford 5-bromo-2-methoxypyridine **106** (4.11 g, 21.87 mmol, 57 %) as a yellow flaky solid; **^{1}H NMR** (400 MHz, $CDCl_3$) δ_H 8.20 (1H, d, J = 2.50 Hz, H6), 7.63 (1H, dd, J = 8.76 and 2.56 Hz, H4), 6.66 (1H, d, J = 8.79 Hz, H3), 3.90 (3H, s, OMe). Data agrees with literature.[230]

(6-methoxypyridin-3-yl)boronic acid 101

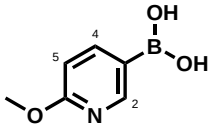

101

To a solution of 5-bromo-2-methoxypyridine **106** (1.0 g, 5.32 mmol, 1.0 eq.) in Et_2O at −78 °C was added *n*-BuLi (2.8 mL, 6.91 mmol, 1.3 eq.). The solution was stirred for 10 m, then triisopropylborate (1.60 mL, 6.91 mmol, 1.3 eq.) was added. The solution was stirred for 10 m at −78 °C then r.t. for 30 m. Water was added and the mixture stirred at r.t. for 10 m. The Et_2O was removed under reduced pressure, and the remaining aqueous solution acidified to pH 6 with 1 M HCl. The product crashed out of solution at around pH 8 and was filtered off and dried under reduced pressure over P_2O_5 to afford (6-methoxypyridin-3-yl)boronic acid **101** (714 mg, 4.67 mmol, 88 %) as white flakes; **^{1}H NMR** (400 MHz, $(CD_3)_2CO$) δ_H 8.61 (1H, d, J = 1.59 Hz, H2), 8.05 (1H, dd, J = 8.36

and 2.05 Hz, H4), 7.30 (2H, s, $B(OH)_2$), 6.72 (1H, dd, J = 8.28 and 0.70 Hz, H5), 3.89 (3H, s, OMe). Data agrees with literature.[231]

2,4-dimethoxy-6-(6-methoxypyridin-3-yl)pyrimidine 102

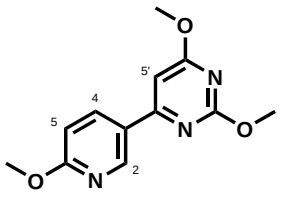

102

A solution of 4-bromo-2,6-dimethoxypyrimidine **100** (200 mg, 0.97 mmol, 1.0 eq.), 6-methoxy-pyridin-3-ylboronic acid **101** (163 mg, 1.06 mmol, 1.1 eq.), Na_2CO_3 (0.83 mL, 2 M aqueous solution, 1.7 eq.) and EtOH (0.45 mL) in toluene (9 mL) was degassed with argon for 30 m. $Pd(PPh_3)_4$ (22 mg, 0.019 mmol, 0.02 eq.) was added and the solution stirred at reflux (110 °C) for 24 h. Brine (10 mL) was then added, the phases separated and the aqueous phase extracted with EtOAc (3 × 10 mL). The combined organic phases were dried ($MgSO_4$) and concentrated *in vacuo*. Purification by flash chromatography (100 % DCM mobile phase) afforded 2,4-dimethoxy-6-(6-methoxypyridin-3-yl)pyrimidine **102** (132 mg, 0.53 mmol, 55 %) as a white flaky solid; $\mathbf{R_f}$ 0.23 (100 % DCM); **mp** 129.5–132.8 °C; $\boldsymbol{\nu_{max}}$ (KBr disc) / cm^{-1} 1585, 1559, 1505, 1456, 1375, 1351, 1292, 1222, 1204, 1105, 1014, 943, 817; ^{1}**H NMR** (500 MHz, $CDCl_3$) δ_H 8.85 (1H, d, J = 2.44 Hz, H2), 8.23 (1H, dd, J = 8.71 and 2.47 Hz, H4), 6.82 (1H, d, J = 8.72 Hz, H5), 6.70 (1H, s, H5′), 4.06 (3H, s, OMe), 4.00 (3H, s, OMe), 3.99 (3H, s, OMe); ^{13}**C NMR** (125 MHz, $CDCl_3$) δ_C 172.6, 165.8, 165.7, 163.8, 146.5 (C2), 137.3 (C4), 126.1, 111.0 (C5), 96.3 (C5′), 54.9 (OMe), 54.1 (OMe) and 53.9 (OMe); $\boldsymbol{m/z}$ (ESI^+) 517.14 ($[2M+Na]^+$, 100%), 248.09 ($[M+H]^+$, 77 %), 270.09 ($[M+Na]^+$, 49%); **HRMS** (ESI^+) found 270.0849 ($[M+Na]^+$, $C_{12}H_{13}N_3O_3Na$ requires 270.0849).

(6-chloropyridin-3-yl)boronic acid 107

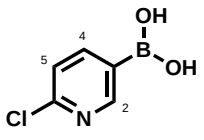

107

To a solution of 5-bromo-2-chloropyridine **108** (1.0 g, 5.2 mmol, 1.0 eq.) in dry Et_2O at −78 °C was added *n*-BuLi (2.6 mL, 2.5 M, 1.25 eq.) dropwise over 15 m. After 1 h at −78 °C, was added to the reaction triisopropylborate (2.4 mL, 10.4 mmol, 2.0 eq.). The solution was stirred for 1 h at r.t. before water was added. The solution was stirred at r.t. for 16 h. The mixture was concentrated under reduced pressure and the remaining aqueous solution washed once with Et_2O. The remaining aqueous solution was acidified to neutral pH with 48 % HBr, whereupon the product crashed out of solution. It was filtered off and dried under vacuum over P_2O_5 to afford (6-chloropyridin-3-yl)boronic acid **107** (550 mg, 3.50 mmol, 67 %) as a light orange powder; ^{1}**H NMR** (500 MHz, $CDCl_3$) δ_H 8.76 (1H, d, J = 1.83 Hz, H2), 8.17 (1H, dd, J = 7.95 and 1.95 Hz, H4), 7.64 (2H, s, $B(OH)_2$), 7.43 (1H, d, J = 7.90 Hz, H5). Data agrees with literature.[231]

4-(6-chloropyridin-3-yl)-2,6-dimethoxypyrimidine 114

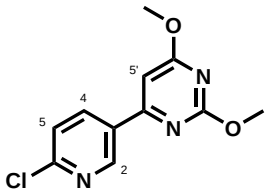

114

A solution of 4-bromo-2,6-dimethoxypyrimidine **100** (50 mg, 0.24 mmol, 1.0 eq.), 6-chloropyridin-3-ylboronic acid **107** (42 mg, 0.27 mmol, 1.1 eq.), Na_2CO_3 (0.21 mL, 2 M solution, 0.41 mmol, 1.7 eq.) and EtOH (0.12 mL) in toluene (2 mL) was degassed with argon for 30 m. $Pd(PPh_3)_4$ (7 mg, 0.006 mmol, 0.025 eq.) was added and the solution stirred at 80 °C for 24 h. Brine (2 mL) was then added, the phases separated and the aqueous phases extracted with EtOAc (3 × 5 mL). The combined organic phases were dried ($MgSO_4$), concentrated *in vacuo*, and purified by flash chromatography (100 % DCM mobile phase) to afford 4-(6-chloropyridin-3-yl)-2,6-dimethoxypyrimidine **114** (33 mg, 0.13 mmol, 54 %) as a white solid; $\mathbf{R_f}$ 0.25 (100 % DCM); **mp** 132.5–133.6 °C; $\boldsymbol{\nu_{max}}$ (thin film) / cm^{-1} 1600, 1576, 1557, 1482, 1461, 1417, 1375, 1338, 1300, 1223, 1202, 1104, 1026, 1006, 982, 941, 865, 817, 781, 740, 704, 634; ^{1}**H NMR** (500 MHz, $CDCl_3$) δ_H 9.00 (1H, d, J = 2.39 Hz, H2), 8.30 (1H, dd, J = 8.35 and 2.50 Hz, H4), 7.42 (1H, d, J = 8.37 Hz, H5), 6.77 (1H, s, H5′), 4.07 (3H, s, OMe), 4.02 (3H, s, OMe); ^{13}**C NMR** (125 MHz, $CDCl_3$) δ_C 172.8, 165.9, 162.4, 153.4, 148.5 (C2), 137.3 (C4), 131.5, 124.4 (C5), 97.7 (C5′), 55.1 (OMe) and 54.3 (OMe); $\boldsymbol{m/z}$ (ESI^+) 579.18 (100%), 301.08 ($[M+MeOH+NH_4]^+$, 96%), 279.10 (88%), 274.04 ($[M+Na]^+$, 44%), 252.06 ($[M+H]^+$, 39%); **HRMS** (ESI^+) found 252.0535 ($[M+H]^+$, $C_{11}H_{11}ClN_3O_2$ requires

252.0534).

6-(6-oxo-1,6-dihydropyridin-3-yl)pyrimidine-2,4(1H,3H)-dione 1

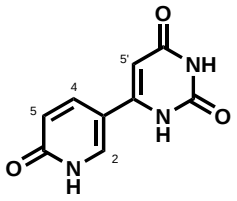

1

A solution of 2,4-dimethoxy-6-(6-methoxypyridin-3-yl)pyrimidine **102** (18 mg, 0.073 mmol, 1.0 eq), 48 % HBr (0.6 mL) and AcOH (0.3 mL) was stirred at 120 °C for 30 m. After cooling to r.t., the reaction mixture was concentrated and the solid residue was washed with $CHCl_3$ (2 × 1 mL) and water (1 × 2 mL). The residue was then dried under vacuum to afford 6-(6-oxo-1,6-dihydropyridin-3-yl)pyrimidine-2,4(1H,3H)-dione **1** (7 mg, 0.034 mmol, 47 %) as an off-white solid; $\mathbf{R_f}$ 0.50 (10:1 EtOAc:MeOH); **mp** > 300 °C; $\boldsymbol{\nu_{max}}$ (thin film) / cm^{-1} 3049, 1688, 1657, 1619, 1545, 1494, 1463, 1424, 1371, 1329, 1240, 1147, 1039, 1002, 835, 760, 643; ^{1}**H NMR** (500 MHz, DMSO) δ_H 12.15 (1H, s, NH), 11.04 (1H, s, NH), 10.91 (1H, s, NH), 7.98 (1H, d, J = 2.65 Hz, H2), 7.78 (1H, dd, J = 9.72 and 2.81 Hz, H4), 6.39 (1H, d, J = 9.71 Hz, H5), 5.77 (1H, s, H5′); ^{13}**C NMR** (125 MHz, DMSO) δ_C 164.1 (C4′), 162.0 (C6), 151.8 (C2′), 149.0 (C3), 138.6 (C4), 136.2 (C2), 120.0 (C5), 109.2 (C6′) and 95.7 (C5′); $\boldsymbol{m/z}$ (ESI$^-$) 204.05 ([M-H]$^-$, 100 %), 250.16 (51 %), 255.25 (43 %); **HRMS** (ESI$^-$) found 204.0412 ([M-H]$^-$, $C_9H_6N_3O_3$ requires 204.0415).

(6-methoxypyridin-3-yl)boronic acid 79

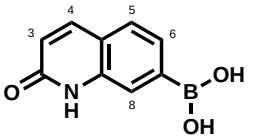

79

To a solution of 7-bromo-2-chloroquinoline **96** and 5-bromoquinolin-2(1H)-one **90** (3:2 7-br:5-br isomer mix, combined 200 mg, 0.90 mmol, 1.0 eq.) in dry THF at −78 °C was added n-BuLi (1.08 mL, 2.5 M, 2.70 mmol, 3.0 eq.). The solution was stirred for 1 h, then triisopropylborate (0.62 mL, 2.70 mmol, 3.0 eq.) was added. The solution was stirred for 1 h at −78 °C. Water was added and the mixture stirred at r.t. for 16 h. The THF was removed under reduced pressure, the remaining aqueous phase washed once with Et_2O, then acidified to pH 6 with aqueous HBr. The product was

filtered off, dried under reduced pressure over P_2O_5, and purified by column chromatography (9:1 EtOAc:MeOH mobile phase) to afford (6-methoxypyridin-3-yl)boronic acid **79** (36 mg, 0.19 mmol, 21 %); **^{1}H NMR** (400 MHz, $(CD_3)_2CO$) δ_H 7.96 (1H, s, ArH), 7.93 (1H, d, J = 9.55 Hz, ArH), 7.75 (1H, s, ArH), 7.67 (1H, dd, J = 7.75 and 0.80 Hz, ArH), 7.61 (1H, d, J = 7.77 Hz, ArH).

2-bromo-6-methoxypyridine 116

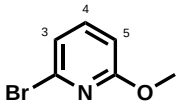

116

To a solution of 2,6-dibromopyridine **118** (5.0 g, 21.1 mmol, 1.0 eq.) in MeOH (20 mL) was added a solution of NaOMe in MeOH (15 mL, 42.2 mmol, 2.0 eq,). The mixture was stirred for 16 h at reflux temperature. The solvent was removed under reduced pressure, water added, and the aqueous mixture extracted with Et_2O. The combined organic phases were concentrated under reduced pressure to afford 2-bromo-6-methoxypyridine **116** (3.13 g, 16.64 mmol, 79 %); **^{1}H NMR** (400 MHz, $CDCl_3$) δ_H 7.41 (1H, t, J = 7.84 Hz, H4), 7.05 (1H, d, J = 7.46 Hz, ArH), 6.69 (1H, d, J = 8.22 Hz, ArH), 3.93 (3H, s, OMe). Data agrees with literature.[232]

6,6′-dimethoxy-2,3′-bipyridine 117

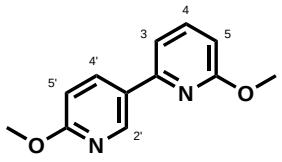

117

A solution of 2-methoxy-6-bromopyridine **116** (56 mg, 0.30 mmol, 1.0 eq.), 6-methoxypyridin-3-ylboronic acid **101** (50 mg, 0.33 mmol, 1.1 eq.), aqueous Na_2CO_3 solution (2.0 M, 0.26 mL, 1.7 eq.) and EtOH (0.13 mL) in toluene (2 mL) was degassed with argon for 15 min. $Pd(PPh_3)_4$ (9 mg, 0.0075 mmol, 0.025 eq.) was added and the solution was stirred at reflux (110 °C) for 18 h. After cooling to room temperature the solvent was removed under reduced pressure and the residue purified by flash chromatography (5:1 P.E.:EtOAc mobile phase) to afford 6,6′-dimethoxy-2,3′-bipyridine **117** (53 mg, 0.25 mmol, 82 %) as a white solid; $\mathbf{R_f}$ 0.29 (5:1 P.E.:Et_2O); **mp** 75.5–76.5 °C; $\boldsymbol{\nu_{max}}$ (thin film) / cm^{-1} 2952, 2361, 2341, 1602, 1581, 1500, 1465, 1410, 1365, 1332, 1308, 1288, 1254, 1158, 1120, 1031, 1011, 884, 831 and 795; **^{1}H NMR** (500 MHz, $CDCl_3$) δ_H 8.84 (1H, d, J =

2.42 Hz, H2′), 8.23 (1H, dd, J = 8.66 and 2.48 Hz, H4′), 7.61 (1H, t, J = 7.82 Hz, H4), 7.25 (1H, d, J = 7.41 Hz, H3), 6.82 (1H, d, J = 8.66 Hz, H5′), 6.67 (1H, d, J = 8.21 Hz, H5), 4.01 (3H, s, MeO), 3.99 (3H, s, MeO); **^{13}C NMR** (125 MHz, $CDCl_3$) δ_C 164.6, 163.9, 152.4, 145.7 (C2′), 139.4 (C4), 137.1 (C4′), 128.4, 112.0 (C3), 110.8 (C5′), 109.3 (C5), 53.8 (OMe) and 53.3 (OMe); ***m/z*** (ESI^+) 579.20 (100 %), 217.11 (48 %, $[M+H]^+$); **HRMS** (ESI^+) found 239.0791 ($[M+Na]^+$, $C_{12}H_{12}N_2O_2Na$ requires 239.0791).

6-bromopyridin-2(1H)-one 119

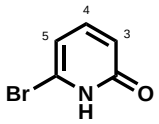

119

A solution of 2-bromo-6-methoxypyridine **116** (300 mg, 1.60 mmol, 1.0 eq.), sodium iodide (500 mg, 3.33 mmol, 2.0 eq.), and trimethylsilyl chloride (0.42 mL, 3.33 mmol, 2.0 eq.) in acetonitrile (5.0 mL) was stirred at 40 °C for 1 h. After cooling to r.t., water was added, the phases separated and the aqueous phase extracted with DCM (3 × 10 mL). The combined organic phases were concentrated under reduced pressure to afford 6-bromopyridin-2(1H)-one **119** (231 mg, 1.33 mmol, 83 %) as a brown crystalline solid; **R_f** 0.41 (2:1 P.E.:EtOAc); **mp** 118.4–122.9 °C; ***ν_{max}*** (thin film) / cm^{-1} 2927, 1655, 1606, 1577, 1478, 1433, 1334, 1245, 1158, 1131, 996, 893, 835, 782, 724 and 675; **^{1}H NMR** (400 MHz, $CDCl_3$) δ_H 11.52 (1H, s, NH), 7.44 (1H, dd, J = 8.59 and 7.59 Hz, H4), 6.83 (1H, d, J = 7.33 Hz, ArH), 6.71 (1H, d, J = 8.62 Hz, ArH); **^{13}C NMR** (100 MHz, $CDCl_3$) δ_C 165.2, 142.2, 132.0, 116.5 and 113.2; ***m/z*** (ESI^+) 175.95 ($[M+H]^+$, 100 %); **HRMS** (ESI^+) found 175.9542 ($[M+H]^+$, C_5H_5BrNO requires 175.9529).

[2,3′-bipyridine]-6,6′(1H,1′H)-dione 115

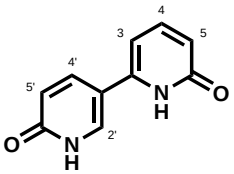

115

A solution of 6,6′-dimethoxy-2,3′-bipyridine **125** (206 mg, 0.95 mmol, 1.0 eq.), 48 % HBr (6 mL) and AcOH (3 mL) was stirred under an argon atmosphere at 120 °C for 30 m. After cooling to

room temperature the solution was quenched with aqueous $NaHCO_3$ solution (10 mL). The product precipitated as a white suspension and was collected by vacuum filtration and dried under vacuum to afford [2,3′-bipyridine]-6,6′(1H,1′H)-dione **115** (115 mg, 0.62 mmol, 65 %) as an off-white solid; $\mathbf{R_f}$ 0.25 (3:1 EtOAc:MeOH); **mp** > 300 °C; $\boldsymbol{\nu_{max}}$ (thin film) / cm^{-1} 2961, 1648, 1590, 1544, 1472, 1420, 1294, 1231, 1167, 995, 916, 835, 796, 724, 703; ^{1}**H NMR** (500 MHz, DMSO) δ_H 7.90 (1H, d, J = 2.45 Hz, H2′), 7.81 (1H, dd, J = 9.63 and 2.82 Hz, H4′), 7.43 (1H, dd, J = 8.81 and 7.17 Hz, H4), 6.57 (1H, d, J = 7.09 Hz, H3), 6.34 (1H, dd, J = 9.61 and 0.54 Hz, H5′), 6.25 (1H, dd, J = 8.81 and 0.77 Hz, H5); ^{13}**C NMR** (125 MHz, DMSO) δ_C 163.4 (C6), 162.0 (C6′), 145.7 (C2), 140.9 (C4), 139.1 (C4′), 134.8 (C2′), 119.8 (C5′), 114.4 (C5), 113.0 (C3′) and 104.4 (C3); $\boldsymbol{m/z}$ (ESI^-) 100.95 (100 %), 220.90 (34 %), 222.90 (25 %), 187.06 (22 %, $[M-H]^-$); **HRMS** (ESI^-) found 187.0512 ($[M-H]^-$, $C_{10}H_7N_2O_2$ requires 187.0513).

2-methoxy-5-phenylpyridine 112

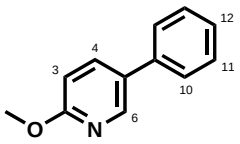

112

A solution of (6-methoxypyridin-3-yl)boronic acid **101** (87 mg, 0.57 mmol, 1.0 eq.), bromobenzene (0.09 mL, 0.86 mmol, 1.5 eq.), aqueous Na_2CO_3 solution (2.0 M, 0.48 mL, 1.7 eq.) and EtOH (0.24 mL) in toluene (5.0 mL) was degassed with argon for 20 m. $Pd(PPh_3)_4$ (16 mg, 0.0143 mmol, 0.025 eq.) was added and the solution was stirred at reflux (110 °C) for 16 h. After cooling to room temperature the solution was concentrated under reduced pressure and purified by flash chromatography (5:1 P.E.:EtOAc mobile phase) to afford 2-methoxy-5-phenylpyridine **112** (62 mg, 0.34 mmol, 59 %) as a yellow oil; ^{1}**H NMR** (400 MHz, $CDCl_3$) δ_H 8.40 (1H, dd, J = 2.56 and 0.54 Hz, H6), 7.79 (1H, dd, J = 8.53 and 2.55 Hz, H4), 7.55–7.51 (2H, m, PhH), 7.47–7.42 (2H, m, PhH), 7.36 (1H, m, H12), 6.83 (1H, dd, J = 8.54 and 0.68 Hz, H3), 3.99 (3H, s, OMe). Data agrees with literature.[233]

6,6′-dimethoxy-3,3′-bipyridine 113

A solution of (6-methoxypyridin-3-yl)boronic acid **101** (20 mg, 0.13 mmol, 1.1 eq.), bromobenzene (12 μL, 0.11 mmol, 1.0 eq.), aqueous Na_2CO_3 solution (2.0 M, 0.1 mL, 1.7 eq.) and EtOH (0.05 mL) in toluene (1.0 mL) was degassed with argon for 20 m. $Pd(PPh_3)_4$ (3 mg, 0.00275 mmol, 0.025 eq.) was added and the solution was stirred at reflux (110 °C) for 16 h. After cooling to room temperature

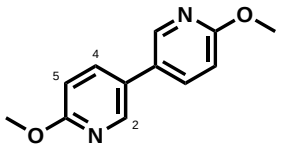

113

the solution was concentrated under reduced pressure and purified by flash chromatography (5:1 P.E.:EtOAc mobile phase) to afford 6,6′-dimethoxy-3,3′-bipyridine **113** (6 mg, 0.028 mmol, 26 %) as a white solid; ^{1}**H NMR** (400 MHz, $CDCl_3$) δ_H 8.32 (2H, d, J = 2.47 Hz, H2), 7.72 (2H, dd, J = 8.59 and 2.53 Hz, H4), 6.83 (2H, d, J = 8.61 Hz, H5), 3.97 (6H, s, OMe). Data agrees with literature.[231] (2-methoxy-5-phenylpyridine **112** was also isolated: 5 mg, 0.027 mmol, 25 %).

7-(6-methoxypyridin-3-yl)quinolin-2(1H)-one 121 and 5-(6-methoxypyridin-3-yl)quinolin-2(1H)-one 122

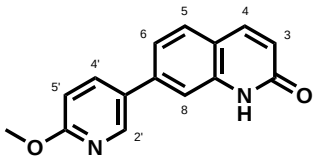

121

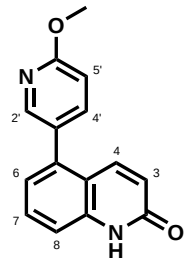

122

A solution of (6-methoxypyridin-3-yl)boronic acid **101** (63 mg, 0.41 mmol, 1.0 eq.), 7-bromoquinolin-2(1H)-one **70** and 5-bromoquinolin-2(1H)-one **90** isomer mixture (7-br:5-br 1.5:1. Total: 100 mg, 0.45 mmol, 1.1 eq.; 7-br: 60 mg, 0.27 mmol, 0.66 eq.; 5-br: 40 mg, 0.18 mmol, 0.33 eq.), $Pd(PPh_3)_4$ (12 mg, 0.010 mmol, 0.025 eq.), Na_2CO_3 (0.35 mL, 2.0 M, 1.7 eq.), EtOH (0.18 mL), and toluene (3.0 mL) was degassed for 10 m, then stirred at 110 °C for 16 h. After cooling to room temperature the solution was concentrated under reduced pressure and purified by flash chromatography (10:1 EtOAc:MeOH mobile phase) to afford 7-(6-methoxypyridin-3-yl)quinolin-2(1H)-one **121** (44 mg of pure 7-br isomer, 0.18 mmol, 65 % from the 60 mg of 7-isomer starting material); $\mathbf{R_f}$ 0.33 (100 % EtOAc); $\boldsymbol{\nu_{max}}$ (thin film) / cm^{-1} 2920, 1668, 1605, 1568, 1489, 1412, 1357, 1291, 1237, 1127, 1017, 876, 840, 824, 673 and 623; ^{1}**H NMR** (500 MHz, $CDCl_3$) δ_H 11.94 (1H, s, NH), 8.48 (1H, d, J = 2.48 Hz, ArH), 7.88 (1H, dd, J = 8.61 and 2.52 Hz, ArH), 7.83 (1H, d, J = 9.47 Hz, ArH), 7.63 (1H, d, J = 8.09 Hz, ArH), 7.52 (1H, s, ArH), 7.40 (1H, dd, J = 8.08 and 1.58 Hz, ArH), 6.86 (1H, d, J = 8.61 Hz, ArH), 6.72 (1H, d, J = 9.45 Hz, ArH), 4.01 (3H, s, OMe); ^{13}**C NMR** (125 MHz, $CDCl_3$) δ_C 164.5, 164.3, 145.5, 140.8, 140.6, 139.1, 137.8, 129.0, 128.6, 121.6, 121.5,

119.2, 113.6, 111.2 and 53.9; ***m/z*** (ESI^+) 253.08 ($[M+H]^+$, 100 %); **HRMS** (ESI^+) found 253.0973 ($[M+H]^+$, $C_{15}H_{13}N_2O_2$ requires 253.0972); and 5-(6-methoxypyridin-3-yl)quinolin-2(1H)-one **122** (34 mg of pure 5-br isomer, 0.14 mmol, 75 % from the 40 mg of 5-isomer starting material); ^{1}**H NMR** (400 MHz, $CDCl_3$) δ_H 11.15 (1H, s, NH), 8.21 (1H, d, J = 2.34 Hz, ArH), 7.87 (1H, d, J = 9.80 Hz, ArH), 7.64 (1H, d, J = 7.63 Hz, ArH), 7.57 (1H, t, J = 7.85 Hz, ArH), 7.46 (1H, d, J = 8.15 Hz, ArH), 7.15 (1H, dd, J = 7.17 and 1.20 Hz, ArH), 6.88 (1H, d, J = 8.48 Hz, ArH), 6.70 (1H, d, J = 9.81 Hz, ArH), 4.01 (3H, s, OMe).

7-(6-oxo-1,6-dihydropyridin-3-yl)quinolin-2(1H)-one 120

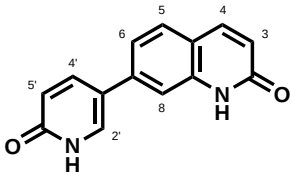

120

A solution of 7-(6-methoxypyridin-3-yl)quinolin-2(1H)-one **121** (50 mg, 0.20 mmol, 1.0 eq.), 48 % HBr (1.5 mL), and AcOH (0.75 mL) was stirred at 120 °C in a sealed vial for 30 m. After cooling to room temperature the product was filtered off, washed with water, and dried under reduced pressure over P_2O_5 to afford 7-(6-oxo-1,6-dihydropyridin-3-yl)quinolin-2(1H)-one **120** (40 mg, 0.17 mmol, 85 %); $\mathbf{R_f}$ 0.37 (20:1 EtOAc:MeOH); **mp** denatured > 170 °C, no melting > 250 °C; $\boldsymbol{\nu_{max}}$ (thin film) / cm^{-1} 2922, 2852, 2358, 2341, 1698, 1649, 1606, 1459, 1411, 1275, 1205, 1127, 847, 730, 667, 656, 641, 633, 625 and 612; ^{1}**H NMR** (500 MHz, DMSO) δ_H 7.89 (1H, d, J = 9.54 Hz, ArH), 7.81 (1H, dd, J = 9.49 and 2.79 Hz, ArH), 7.75 (1H, d, J = 2.64 Hz, ArH), 7.68 (1H, d, J = 8.11 Hz, ArH), 7.39 (1H, dd, J = 8.19 and 1.75 Hz, ArH), 7.37 (1H, s, ArH), 6.50 (1H, d, J = 9.53 Hz, ArH), 6.46 (1H, d, J = 9.47 Hz, ArH); ^{13}**C NMR** (125 MHz, DMSO) δ_C 162.0, 161.7, 139.9, 139.7, 139.4, 138.1, 133.5, 128.5, 121.4, 120.3, 119.3, 117.9, 117.2 and 111.0.

7-bromoquinolin-2(1H)-one 70

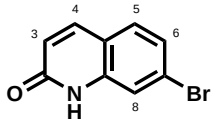

70

A solution of 7-bromo-2-chloroquinoline **96** (30 mg, 0.12 mmol, 1.0 eq.), H_2SO_4 (0.35 mL), and H_2O (1.0 mL) was stirred at 120 °C for 16 h. After cooling to room temperature aqueous $NaHCO_3$ was added until the pH was 7. The mixture was extracted with DCM (3 × 15 mL) and the combined organic phases were concentrated under reduced pressure to afford 7-bromoquinolin-2(1H)-one **70** (24 mg, 0.11 mmol, 87 %); **^{1}H NMR** (400 MHz, $CDCl_3$) δ_H 10.34 (1H, s, NH), 7.74 (1H, d, J = 9.56 Hz, H4), 7.44 (1H, d, J = 2.07 Hz, H8), 7.43 (1H, d, J = 9.48 Hz, H5), 7.34 (1H, dd, J = 8.35 and 1.72 Hz, H6), 6.69 (1H, d, J = 9.50 Hz, H3). Data agrees with literature.[226]

5-bromoquinolin-2(1H)-one 90

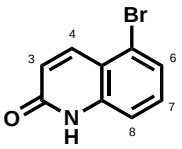

90

A solution of 5-bromo-2-chloroquinoline **97** (120 mg, 0.50 mmol, 1.0 eq.), H_2SO_4 (0.35 mL), and H_2O (1.0 mL) was stirred at 120 °C for 16 h. After cooling to room temperature aqueous $NaHCO_3$ was added until the pH was 7. The mixture was extracted with DCM (3 × 15 mL) and the combined organic phases were concentrated under reduced pressure to afford 5-bromoquinolin-2(1H)-one **90** (102 mg, 0.45 mmol, 91 %); **^{1}H NMR** (400 MHz, $CDCl_3$) δ_H 8.20 (1H, d, J = 9.82 Hz, H4), 7.47 (1H, dd, J = 7.17 and 1.61 Hz, ArH), 7.34 (1H, d, J = 7.18 Hz, ArH), 7.33 (1H, d, J = 1.62 Hz, ArH), 6.77 (1H, d, J = 9.84 Hz, H3). Data agrees with literature.[227]

3,5-dibromo-2-methoxypyridine 124

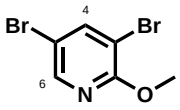

124

To a solution of 2-methoxypyridine **103** (3.83 g, 35.0 mmol, 1.0 eq.) and sodium acetate (5.80 g, 70.0 mmol, 2.0 eq.) in AcOH (30 mL) was added Br_2 (3.15 mL, 123 mmol, 3.5 eq.). The mixture was stirred at 80 °C for 40 h, then poured into water, extracted (3 × 20 mL) into DCM, washed once with aqueous sodium hydroxide and once with aqueous sodium thiosulfate, and purified by column chromatography (10:1 P.E.:EtOAc mobile phase) to afford 3,5-dibromo-2-methoxypyridine

124 (6.40 g, 24.0 mmol, 68 %); ^{1}**H NMR** (400 MHz, $CDCl_3$) δ_H 8.14 (1H, d, J = 2.15 Hz, H6), 7.92 (1H, d, J = 2.17 Hz, H4), 3.99 (3H, s, OMe). Data agrees with literature.[120]

2-methoxy-3,5-diphenylpyridine 127, 3-bromo-2-methoxy-5-phenylpyridine 128, and 5-bromo-2-methoxy-3-phenylpyridine 129.

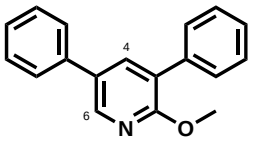

127

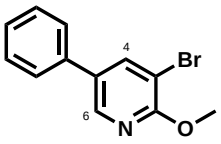

128

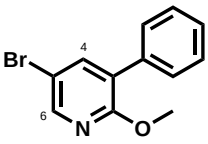

129

A solution of 3,5-dibromo-2-methoxypyridine **124** (130 mg, 0.49 mmol, 1.2 eq.), phenylboronic acid **85** (50 mg, 0.41 mmol, 1.0 eq.), $Pd(PPh_3)_4$ (12 mg, 0.01 mmol, 0.025 eq.), Na_2CO_3 (0.35 mL, 2 M aq. sol., 1.7 eq.), EtOH (0.2 mL), and toluene (1.0 mL) was degassed for 10 m. The solution was stirred at reflux (115 °C) for 24 h. Brine (10 mL) was added and the mixture extracted with EtOAc (3 × 10 mL). The combined organic phases were concentrated under reduced pressure to afford compounds **127** (0.0363 mmol by nmr, 7 %), **128** (0.0653 mmol by nmr, 13 %), and **129** (0.2396 mmol by nmr, 49 %); (31 % start material **124** returned);

2-methoxy-3,5-diphenylpyridine **127**: ^{1}**H NMR** (500 MHz, $CDCl_3$) δ_H 8.39 (1H, d, J = 2.53 Hz, H6), 7.85 (1H, d, J = 2.45 Hz, H4), 7.56–7.36 (10H, m, ArH), 4.03 (3H, s, CH_3);

3-bromo-2-methoxy-5-phenylpyridine **128**: ^{1}**H NMR** (500 MHz, $CDCl_3$) δ_H 8.33 (1H, d, J = 2.21 Hz, H6), 8.05 (1H, d, J = 2.21 Hz, H4), 7.56–7.36 (5H, m, ArH), 4.07 (3H, s, CH_3);

5-bromo-2-methoxy-3-phenylpyridine **129**: ^{1}**H NMR** (500 MHz, $CDCl_3$) δ_H 8.19 (1H, d, J = 2.53 Hz, H6), 7.72 (1H, d, J = 2.51 Hz, H4), 7.56–7.36 (5H, m, ArH), 3.95 (3H, s, CH_3).

3-allyl-5-bromo-2-methoxypyridine 130

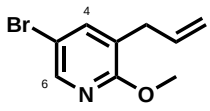

130

To a solution of 3,5-dibromo-2-methoxypyridine **124** (1.0 g, 3.75 mmol, 1.0 eq.) in Et_2O (30 mL) at −78 °C under an argon atmosphere was added n-BuLi (1.85 mL, 2.5 M, 1.23 eq.). Ten minutes later the bath temperature was raised to -30 °C. To the reaction was then added copper iodide (72 mg, 0.38 mmol, 0.1 eq.) and allyl bromide (0.66 mL, 7.50 mmol, 2.0 eq.). The reaction was

then stirred at -30 ℃ for 25 minutes and then at room temperature for two hours. Water was added and the solution stirred for 25 minutes. The mixture was then extracted into Et_2O and the organic phase concentrated under reduced pressure to afford 3-allyl-5-bromo-2-methoxypyridine **130** (832 mg, 3.65 mmol, 97 %) as an oil; $\mathbf{R_f}$ 0.50 (10:1 P.E.:Et_2O); $\boldsymbol{\nu_{max}}$ (thin film) / cm^{-1} 2950, 1640, 1569, 1465, 1415, 1390, 1303, 1248, 1139, 1021, 918, 753, 669; ^{1}**H NMR** (500 MHz, $CDCl_3$) δ_H 8.06 (1H, d, J = 2.41 Hz, H6), 7.48 (1H, d, J = 2.41 Hz, H4), 5.92 (1H, ddt, J = 16.96, 10.19 and 6.74 Hz, CH_2CH=CH_2), 5.14–5.08 (2H, m, CH_2CH=CH_2), 3.93 (3H, s, MeO), 3.30 (2H, d, J = 6.7 Hz, CH_2CH=CH_2); ^{13}**C NMR** (125 MHz, $CDCl_3$) δ_C 160.9, 145.0, 140.0, 134.8, 125.1, 117.3, 111.8, 53.9 and 33.7; **HRMS** (FI^+) found 226.9947 ($[M]^+$), $C_9H_{10}NOBr$ requires 226.9946).

5-allyl-6-methoxypyridin-3-ylboronic acid 131

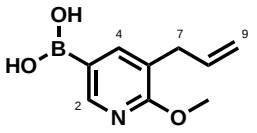

131

To a stirred solution of 3-allyl-5-bromo-2-methoxypyridine **130** (507 mg, 2.22 mmol, 1.0 eq.) in anhydrous Et_2O (10 mL) at −78 ℃ under an argon atmosphere was added *n*-BuLi (1.16 mL, 2.5 M, 1.3 eq.) dropwise. The solution was stirred for 10 minutes and then triisopropylborate (0.77 mL, 3.33 mmol, 1.5 eq.) was added over 1 minute and the reaction stirred at room temperature for 15 minutes. Water was added and the solution stirred for 20 minutes. The Et_2O was removed under reduced pressure and the aqueous phase washed once with Et_2O and then subjected to reduced pressure to remove any remaining Et_2O. The aqueous phase was then acidified to pH 6 with 1 M HCl. The precipitate was filtered off and dried under reduced pressure to afford 5-allyl-6-methoxypyridin-3-ylboronic acid **131** (385 mg, 2.0 mmol, 90 %) as a white solid; $\mathbf{R_f}$ 0.38 (100 % EtOAc); **mp** 139.5–141.2 ℃; $\boldsymbol{\nu_{max}}$ (thin film) / cm^{-1} 3341, 1608, 1576, 1477, 1456, 1409, 1355, 1323, 1295, 1272, 1256, 1181, 1134, 1068, 1019, 920, 789, 764, 667; ^{1}**H NMR** (500 MHz, $(CD_3)_2CO$) δ_H 8.49 (1H, s, H2), 7.88 (1H, s, H4), 7.25 (2H, s, $B(OH)_2$), 5.98 (1H, ddt, J = 16.97, 10.17 and 6.75 Hz, H8), 5.09–5.02 (2H, m, H9), 3.94 (3H, s, OMe), 3.32 (2H, d, J = 6.69 Hz, H7); ^{13}**C NMR** (125 MHz, $(CD_3)_2CO$) δ_C 164.2, 152.1, 144.1, 136.9, 122.2, 116.3, 53.6, and 34.4; $\boldsymbol{m/z}$ (ESI^+) 413.30 (100 %), 208.12 (76 %), 194.11 ($[M+H]^+$, 35 %); **HRMS** (ESI^+) found 194.0991 ($[M+H]^+$, $C_9H_{13}BNO_3$ requires 194.0985).

5′-allyl-6,6′-dimethoxy-2,3′-bipyridine 125

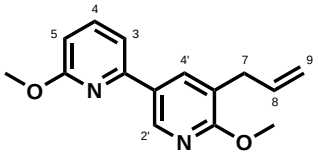

125

A solution of 2-methoxy-6-bromopyridine **116** (107 mg, 0.57 mmol, 1.1 eq.), 5-allyl-6-methoxypyridin-3-ylboronic acid **131** (100 mg, 0.52 mmol, 1.0 eq.), aqueous Na_2CO_3 solution (2 M solution, 0.44 mL, 1.7 eq.) and EtOH (0.22 mL) in toluene (5 mL) was degassed with argon for 15 m. $Pd(PPh_3)_4$ (15 mg, 0.013 mmol, 0.025 eq.) was added and the solution stirred at 110 °C for 16 h. After cooling to r.t. the solvent was removed under reduced pressure and the residue purified by flash chromatography (5:1 P.E.:EtOAc mobile phase) to afford 5′-allyl-6,6′-dimethoxy-2,3′-bipyridine **125** (100 mg, 0.39 mmol, 75 %) as an oil; $\mathbf{R_f}$ 0.45 (5:1 P.E.:EtOAc); $\boldsymbol{\nu_{max}}$ (thin film) / cm^{-1} 2948, 1727, 1640, 1578, 1465, 1412, 1384, 1256, 1199, 1157, 1089, 1025, 916, 844, 800, 761, 734, 694, 627, 608; ^{1}**H NMR** (500 MHz, $CDCl_3$) δ_H 8.72 (1H, d, J = 2.34 Hz, H2′), 8.04 (1H, d, J = 2.34 Hz, H4′), 7.60 (1H, t, J = 7.81 Hz, H4), 7.25 (1H, d, J = 7.41 Hz, H3), 6.66 (1H, d, J = 8.20 Hz, H5), 6.06–5.98 (1H, m, H8), 5.15–5.10 (2H, m, H9), 4.02 (3H, s, OMe), 4.01 (3H, s, OMe), 3.40 (2H, d, J = 6.66 Hz, H7); ^{13}**C NMR** (125 MHz, $CDCl_3$) δ_C 163.9, 162.5, 152.7, 143.3, 139.3 (C4), 136.2, 135.7, 128.4, 122.6, 116.6, 112.1 (C3), 109.1 (C5), 53.8 (OMe), 53.4 (OMe) and 34.1; $\boldsymbol{m/z}$ (ESI^+) 380 (100 %), 279.10 ($[M+Na]^+$, 48 %), 257.14 ($[M+H]^+$, 29 %); **HRMS** (ESI^+) found 279.0931 ($[M+Na]^+$, $C_{15}H_{16}N_2O_2Na$ requires 279.1104).

6-(2-methyl-2,3-dihydrofuro[2,3-b]pyridin-5-yl)pyridin-2(1H)-one 135

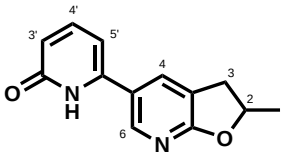

135

A solution of 5′-allyl-6,6′-dimethoxy-2,3′-bipyridine (23 mg, 0.090 mmol, 1.0 eq.), HBr (0.5 mL) and AcOH (1.0 mL) was stirred at 120 °C for 1 hour. The mixture was quenched with saturate aqueous sodium bicarbonate until bubbling ceased, and extracted with DCM (4 × 10 mL). The organic phase was concentrated under reduced pressure to afford 6-(2-methyl-2,3-dihydrofuro[2,3-b]pyridin-5-yl)pyridin-2(1H)-one **135** (9 mg, 0.039 mmol, 44 %) as an off-white solid; $\mathbf{R_f}$ 0.20 (9:1 MeOH:

EtOAc); **mp** 229.2–232.1 °C; $\boldsymbol{\nu_{max}}$ (thin film) / cm^{-1} 2920, 1647, 1612, 1482, 1417, 1226, 1160, 1081, 1035, 993, 914, 875, 828, 800, 759, 728, 696, 622, 556, 528; ^{1}**H NMR** (500 MHz, $CDCl_3$) δ_H 8.33 (1H, s, H6), 7.85 (1H, s, H4), 7.48 (1H, dd, J = 9.09 and 7.01 Hz, H4′), 6.51 (1H, dd, J = 9.08 and 0.89 Hz, H3′), 6.41 (1H, dd, J = 6.99 and 0.91 Hz, H5′), 5.10–5.03 (1H, m, H2), 3.45 (1H, dd, J = 16.26 and 8.94 Hz, H3), 2.92 (1H, dd, J = 16.27 and 7.20 Hz, H3), 1.55 (3H, d, J = 6.30 Hz, CH_3); ^{13}**C NMR** (125 MHz, $CDCl_3$) δ_C 169.4, 165.6, 146.2 (C6), 145.1, 141.8 (C4′), 132.2 (C4), 123.2, 121.0, 118.3 (C3′), 104.8 (C5′), 78.9 (C2), 35.4 (C3) and 22.2 (CH_3); $\boldsymbol{m/z}$ (ESI^+) 479.15 ([2M+Na]+, 100%), 251.08 ([M+Na]+, 73%), 229.10 ([M+H]+, 51%); **HRMS** (ESI^+) found 229.0976 ([M+H]+ $C_{13}H_{13}N_2O_2$ requires 229.0972).

3-allyl-5-bromopyridin-2(1H)-one 133

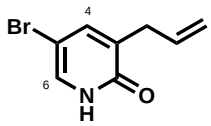

133

A solution of 3-allyl-5-bromo-2-methoxypyridine **130** (394 mg, 1.73 mmol, 1.0 eq.), sodium iodide (779 mg, 5.19 mmol, 3.0 eq.), and trimethylsilyl chloride (0.66 mL, 5.19 mmol, 3.0 eq.) in acetonitrile (8.0 mL) was stirred at 50 °C for 1 h. After cooling to r.t., water was added, the phases separated and the aqueous phase extracted with DCM (3 × 15 mL). The combined organic phases were concentrated under reduced pressure and purified by column chromatography (100 % EtOAc mobile phase) to afford 3-allyl-5-bromopyridin-2(1H)-one **133** (240 mg, 1.12 mmol, 65 %); $\mathbf{R_f}$ 0.50 (100 % EtOAc); $\boldsymbol{\nu_{max}}$ (thin film) / cm^{-1} 1644, 1614, 1555, 1473, 1429, 1339, 1252, 1000, 934, 870, 755, 666, 628; ^{1}**H NMR** (400 MHz, $CDCl_3$) δ_H 7.41 (1H, d, J = 2.54 Hz, ArH), 7.35 (1H, d, J = 2.53 Hz, ArH), 5.94 (1H, ddt, J = 16.85, 10.26 and 6.67 Hz, CH_2CH=CH_2), 5.19–5.14 (2H, m, CH_2CH=CH_2), 3.28 (2H, d, J = 6.55 Hz, CH_2CH=CH_2), ^{13}**C NMR** (100 MHz, $CDCl_3$) δ_C 163.6, 154.7, 141.5, 134.3, 133.3, 132.6, 117.9 and 99.7; $\boldsymbol{m/z}$ (ESI^+) 237.97 ($[M+Na]^+$, 100 %), 216.00, $[M+H]^+$, 30 %); **HRMS** (ESI^+) found 237.9669 ($[M+Na]^+$, $C_8H_8BrNONa$ requires 237.9661).

5′-allyl-[2,3′-bipyridine]-6,6′(1H,1′H)-dione 126

A solution of 5′-allyl-6,6′-dimethoxy-2,3′-bipyridine **125** (50 mg, 0.20 mmol, 1.0 eq.), NaI (120 mg, 0.80 mmol, 4.0 eq.), TMSCl (87 mg, 0.80 mmol, 4.0 eq.) and MeCN (1 mL) was stirred at 50 °C for 1 h. After cooling to room temperature the mixture was poured into water and washed (3 × 5 mL)

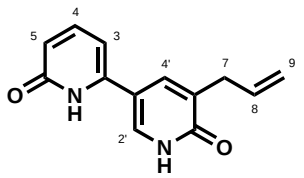

126

with DCM. The aqueous solution was concentrated under reduced pressure to afford 5′-allyl-[2,3′-bipyridine]-6,6′(1H,1′H)-dione **126** (33 mg, 0.145 mmol, 74 %); ^{1}**H NMR** (400 MHz, DMSO) δ_H 7.86 (1H, d, J = 3.05 Hz, H4′), 7.70 (1H, d, J = 2.27 Hz, H2′), 7.54 (1H, m, H4), 6.66 (1H, d, J = 7.52 Hz, H3), 6.34 (1H, d, J = 10.91 Hz, H5), 6.03–5.93 (1H, m, H8), 5.16–5.01 (2H, m, H9), 3.18 (2H, d, J = 8.43 Hz, H7).

5′-allyl-6-methoxy-[2,3′-bipyridin]-6′(1′H)-one 138

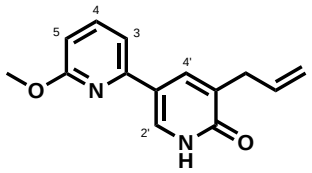

138

A solution of 5′-allyl-6,6′-dimethoxy-2,3′-bipyridine **125** (52 mg, 0.20 mmol, 1.0 eq.), NaI (60 mg, 0.40 mmol, 2.0 eq.), TMSCl (50 μL, 0.40 mmol, 2.0 eq.) and MeCN (2 mL) was stirred at r.t. for 1 h. The MeCN was removed under reduced pressure, water added, and the solution extracted (3 × 5 mL) with DCM. The organic solution was concentrated under reduced pressure and purified by flash chromatography (100 % EtOAc mobile phase) to yield 5′-allyl-6-methoxy-[2,3′-bipyridin]-6′(1′H)-one **138** (10 mg, 0.041 mmol, 20 %); ^{1}**H NMR** (400 MHz, $CDCl_3$) δ_H 8.19 (1H, d, J = 2.41 Hz, H4′), 7.98 (1H, d, J = 2.19 Hz, H2′), 7.59 (1H, t, J = 7.81 Hz, H4), 7.12 (1H, d, J = 7.51 Hz, H3), 6.64 (1H, d, J = 8.19 Hz, H5), 6.07 (1H, m, $CH_2CH{=}CH_2$), 5.21 (2H, m, $CH{=}CH_2$), 3.99 (3H, s, OMe), 3.42 (2H, d, J = 6.51 Hz, CH_2).

6,6′-dimethoxy-5′-propyl-2,3′-bipyridine 139

A solution of 5′-allyl-6,6′-dimethoxy-2,3′-bipyridine **125** (117 mg, 0.46 mmol) in EtOAc (5 mL) and a spatula tip of palladium on carbon was stirred vigourously under a hydrogen atmosphere for 80 m. The crude reaction solution was filtered through silica and the eluent evaporated under reduced pressure to afford 6,6′-dimethoxy-5′-propyl-2,3′-bipyridine **139** (112 mg, 0.43 mmol, 95 %) as a clear oil; $\mathbf{R_f}$ 0.45 (5:1 P.E.:EtOAc); $\boldsymbol{\nu_{max}}$ (thin film) / cm^{-1} 2958, 2870, 1579, 1465, 1412, 1385, 1330,

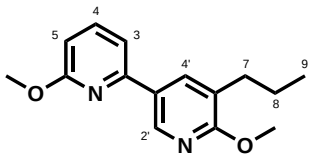

139

1254, 1164, 1094, 1025, 986, 918, 843, 800, 734, 687; **^{1}H NMR** (500 MHz, $CDCl_3$) δ_H 8.67 (1H, d, J = 2.33 Hz, H2′), 8.01 (1H, d, J = 2.31 Hz, H4′), 7.59 (1H, t, J = 7.82 Hz, H4), 7.24 (1H, d, J = 7.51 Hz, H3), 6.65 (1H, d, J = 8.19 Hz, H5), 4.00 (3H, s, OMe), 3.99 (3H, s, OMe), 2.60 (2H, t, J = 7.67 Hz, H7), 1.66 (2H, dq, J = 15.03 and 7.48 Hz, H8), 0.97 (3H, t, J = 7.35 Hz, H9); **^{13}C NMR** (125 MHz, $CDCl_3$) δ_C 163.9, 162.8, 152.9, 142.8, 139.3 (C4), 136.2, 128.3, 124.9, 112.1 (C3), 109.0 (C5), 53.7 (OMe), 53.4 (OMe), 32.2, 22.4 and 14.1 (C9′); ***m/z*** (ESI^+) 259.14 ($[M+H]^+$, 100 %), 281.13 ($[M+Na]^+$, 83 %); **HRMS** (ESI^+) found 259.1440 ($[M+H]^+$, $C_{15}H_{19}N_2O_2$ requires 259.1441).

5′-propyl-[2,3′-bipyridine]-6,6′(1H,1′H)-dione 140

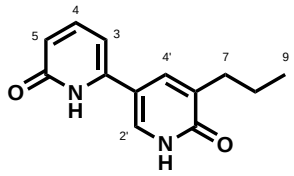

140

A solution of 6,6′-dimethoxy-5′-propyl-2,3′-bipyridine **139** (33 mg, 0.13 mmol, 1.0 eq.), HBr (48 %, 1.0 mL) and AcOH (0.5 mL) was stirred in a vial at 120 °C for two hours. After cooling to r.t. the solution was quenched with aqueous NaOH. The solids were isolated by sinter filtration and dried over P_2O_5 under reduced pressure to afford 5′-propyl-[2,3′-bipyridine]-6,6′(1H,1′H)-dione **140** (25 mg, 0.11 mmol, 85 %) as an off-white powder; **R_f** 0.16 (10:1 EtOAc:MeOH); **mp** > 270 °C; ***ν_{max}*** (thin film) / cm^{-1} 2961, 1682, 1645, 1616, 1563, 1470, 1379, 1278, 1004, 875, 788, 722 and 695; **^{1}H NMR** (500 MHz, DMSO) δ_H 7.81 (1H, d, J = 2.73 Hz, H4′), 7.70 (1H, d, J = 2.68 Hz, H2′), 7.47 (1H, dd, J = 8.83 and 7.17 Hz, H4), 6.61 (1H, d, J = 7.09 Hz, H3), 6.28 (1H, dd, J = 8.82 and 0.71 Hz, H5), 2.39 (2H, t, J = 7.54 Hz, H7), 1.55 (2H, dq, J = 14.99 and 7.47 Hz, H8), 0.90 (3H, t, J = 7.37 Hz, H9); **^{13}C NMR** (125 MHz, DMSO) δ_C 163.4 (C6), 162.1 (C6′), 145.8, 140.8 (C4), 135.2 (C2′), 132.3, 131.8 (C4′), 114.5, 112.6, 104.0 (C3), 32.0 (C7), 21.1 (C8) and 13.9 (C9); ***m/z*** (ESI^-) 229.09 (100 %, $[M-H]^-$), 277.08 (44 %); **HRMS** (ESI^+) found 253.0944 ($[M+Na]^+$, $C_{13}H_{14}N_2O_2Na$ requires 253.0947).

5′-allyl-6′-methoxy-[2,3′-bipyridin]-6(1H)-one 132

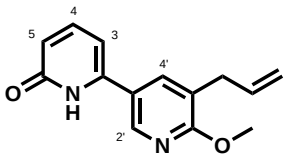

132

A solution of (5-allyl-6-methoxypyridin-3-yl)boronic acid **131** (84 mg, 0.44 mmol, 1.0 eq.), 6-bromopyridinone **119** (84 mg, 0.48 mmol, 1.1 eq.), aqueous sodium carbonate (0.38 mL, 0.75 mmol, 1.7 eq.), ethanol (0.19 mL) and tetrakis(triphenylphosphine)palladium (13 mg, 0.011 mmol, 0.025 eq.) in a solvent of toluene (3 mL) was degassed for 10 m and then stirred at 110 °C for 16 h. The toluene was then removed under reduced pressure and the residue purified by flash chromatography (100 % EtOAc) to afford 5′-allyl-6′-methoxy-[2,3′-bipyridin]-6(1H)-one **132** (63 mg, 0.26 mmol, 59 %); $\mathbf{R_f}$ 0.17 (100 % EtOAc); $\boldsymbol{\nu_{max}}$ (thin film) / cm^{-1} 2931, 1671, 1619, 1575, 1473, 1417, 1371, 1312, 1251, 1158, 1146, 1095, 1028, 963, 921, 797, 761, 730, 560, 523; ^{1}**H NMR** (400 MHz, $CDCl_3$) δ_H 12.76 (1H, s, NH), 8.38 (1H, d, J = 2.52 Hz, H2′), 7.80 (1H, d, J = 2.51 Hz, H4′), 7.48 (1H, dd, J = 9.11 and 6.99 Hz, H4), 6.51 (1H, dd, J = 9.09 and 0.88 Hz, H3), 6.43 (1H, dd, J = 6.99 and 0.92 Hz, H5), 6.04 (1H, m, $CH_2CH{=}CH_2$), 5.15 (2H, m, $CH{=}CH_2$), 4.02 (3H, s, OCH_3), 3.40 (2H, d, J = 6.73 Hz, CH_2); ^{13}**C NMR** (100 MHz, $CDCl_3$) δ_C 165.6, 163.1, 145.0, 143.3, 141.6, 136.1, 135.1, 123.5, 123.3, 118.2, 117.2, 104.6, 54.1 and 33.9; $\boldsymbol{m/z}$ (ESI^+) 991.43 (100 %), 265.12 ($[M{+}Na]^+$, 33 %), 243.14 ($[M{+}H]^+$, 14 %); **HRMS** (ESI^+) found 265.0946 ($C_{14}H_{14}N_2NaO_2$ $[M{+}Na]^+$ requires 265.0947).

(5-allyl-6-oxo-1,6-dihydropyridin-3-yl)boronic acid 134

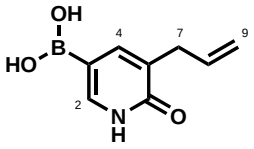

134

To a stirred solution of 3-allyl-5-bromopyridin-2(1H)-one **133** (100 mg, 0.47 mmol, 1.0 eq.) in anhydrous Et_2O (5 mL) at −78 °C was added *n*-BuLi (0.63 mL, 2.5 M, 1.55 mmol, 3.3 eq.) dropwise. The solution was stirred for 10 m and then triisopropylborate (0.36 mL, 1.55 mmol, 3.3 eq.) was added and the reaction stirred at room temperature for 10 m. Water was added and the solution stirred for 10 m. The Et_2O was removed under reduced pressure and the aqueous phase washed

once with Et_2O and then subjected to reduced pressure to remove any remaining Et_2O. The aqueous phase was then acidified to pH 6 with 1 M HCl. The precipitate was filtered off and dried under reduced pressure to afford (5-allyl-6-oxo-1,6-dihydropyridin-3-yl)boronic acid **134** (53 mg, 0.30 mmol, 63 %); ^{1}**H NMR** (400 MHz, $(CD_3)_2CO$) δ_H 10.69 (1H, s, NH), 7.52 (1H, s, ArH), 7.31 (1H, s, ArH), 6.02–5.91 (1H, m, H8), 5.17–5.06 (2H, m, H9), 3.20 (2H, d, J = 6.89 Hz, H7).

octyl trifluoromethanesulfonate 142

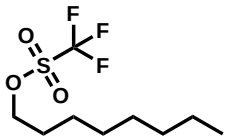

142

To a solution of octanol **141** (0.6 mL, 3.85 mmol, 1.0 eq.) in dry DCM (10 mL) at 0 °C was added triflic anhydride (1.2 g, 4.24 mmol, 1.1 eq.), and the solution stirred for 3 h at room temperature. Water was added and the solution extracted with DCM (3 × 30 mL). The combined organic phases were concentrated under reduced pressure to afford octyl trifluoromethanesulfonate **142** (969 mg, 3.70 mmol, 96 %); ^{1}**H NMR** (400 MHz, $CDCl_3$) δ_H 4.54 (2H, t, J = 6.54 Hz, CH_2), 1.89–1.79 (2H, m, CH_2), 1.47–1.22 (10H, m, $(CH_2)_5$), 0.88 (3H, t, J = 6.93 Hz, CH_3). Data agrees with literature.[124]

1-(5-bromo-2-methoxypyridin-3-yl)octan-1-ol 144

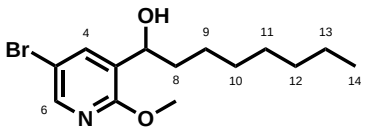

144

To a solution of 3,5-dibromo-2-methoxypyridine **124** (2.0 g, 7.4 mmol, 1.0 eq.) in dry Et_2O (20 mL) at −78 °C was added *n*-BuLi (3.6 mL, 2.5 M, 1.2 eq.), and the solution stirred for 10 m. Then, octanal (7.4 mL, 2 M solution in dry Et_2O, 2.0 eq.) was added and the solution raised to room temperature and stirred for 30 m before quenching with water (50 mL). The organic phase was isolated and the aqueous phase extracted with Et_2O (3 × 50 mL). The combined organic phases were concentrated under reduced pressure and the product purified by flash chromatorgaphy (5:1 P.E.:Et_2O mobile phase) to afford 1-(5-bromo-2-methoxypyridin-3-yl)octan-1-ol **144** (1.473 g, 4.66 mmol, 62 %) as a clear oil; $\mathbf{R_f}$ 0.43 (5:1 P.E.:EtOAc); $\boldsymbol{\nu_{max}}$ (thin film) / cm^{-1} 3384, 2926, 1570, 1462, 1415, 1244,

1116, 1022, 903, 771; **^{1}H NMR** (400 MHz, $CDCl_3$) δ_H 8.07 (1H, s, H6), 7.72 (1H, s, H4), 4.76 (1H, q, J = 6.04 Hz, H7), 3.93 (3H, s, OMe), 2.48 (1H, s, OH), 1.75–1.62 (2H, m, CH_2), 1.41–1.27 (10H, m, $(CH_2)_5$), 0.91–0.85 (3H, m, H14); **^{13}C NMR** (100 MHz, $CDCl_3$) δ_C 159.6, 145.7, 137.8, 129.3, 112.3, 53.8 (OMe), 36.9, 31.9, 29.5, 29.43, 29.3, 25.8, 22.8 and 14.2 (C14); ***m/z*** (ESI^-) 631.19 (100%), 314.10 ([M-H]$^-$, 33 %); **HRMS** (ESI^+) found 338.0718 ($C_{14}H_{22}BrNNaO_2$ requires 338.0726).

1-(5-bromo-2-methoxypyridin-3-yl)octyl methanesulfonate 146

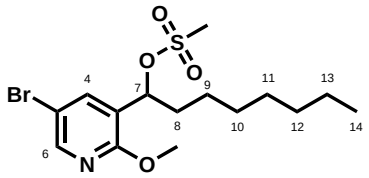

146

To a solution of 1-(5-bromo-2-methoxypyridin-3-yl)octan-1-ol **144** (927 mg, 2.93 mmol, 1.0 eq.) and triethylamine (0.82 mL, 5.86 mmol, 2.0 eq.) in DCM (15 mL) at 0 °C was added methanesulfonate-chloride (0.27 mL, 3.52 mmol, 1.2 eq.). The ice bath was removed and the solution stirred at r.t. for 15 m and then quenched with aqueous ammonium chloride. The organic phase was isolated and the aqueous phase extracted with DCM (2 × 15 mL). The combined organic phases were dried ($MgSO_4$), concentrated *in vacuo*, and purified by flash chromatography (4:1 P.E.:EtOAc mobile phase) to afford 1-(5-bromo-2-methoxypyridin-3-yl)octyl methanesulfonate **146** (490 mg, 1.24 mmol, 42 %) as an oil (the compound is unstable on silica, the crude yield by NMR is quantitative); $\mathbf{R_f}$ 0.33 (5:1 P.E.:EtOAc); $\boldsymbol{\nu_{max}}$ (thin film) / cm^{-1} 2926, 2855, 2361, 1570, 1464, 1416, 1393, 1344, 1295, 1245, 1174, 1016, 912, 772, 657; **^{1}H NMR** (400 MHz, $CDCl_3$) δ_H 8.16 (1H, m, H6), 7.76 (1H, m, H4), 5.78 (1H, t, J = 6.41 Hz, H7), 3.95 (3H, s, OMe), 2.91 (3H, s, SO_2Me), 1.94–1.78 (2H, m, CH_2), 1.43–1.25 (10H, m, $(CH_2)_5$), 0.86 (3H, t, J = 6.05 Hz, H14); **^{13}C NMR** (100 MHz, $CDCl_3$) δ_C 158.9, 147.5, 138.2, 124.0, 112.1, 77.7, 54.2 (OMe), 38.7, 35.9, 31.8, 29.10, 29.07, 25.1, 22.7 and 14.2 (C14); ***m/z*** (ESI^+) 691.45 (100%), 394.08 ([M+H]$^+$, 81 %); **HRMS** (ESI^+) found 394.0676 ([M+H]$^+$, $C_{15}H_{25}BrNO_4S$ requires 394.0682).

(E)-5-bromo-2-methoxy-3-(oct-1-en-1-yl)pyridine 145

A mixture of 1-(5-bromo-2-methoxypyridin-3-yl)octyl methanesulfonate **146** (2.592 g, 6.58 mmol, 1.0 eq.) and Et_3N (15 mL) was stirred at 100 °C for 16 h. After cooling to room temperature aqueous

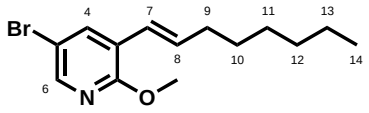

145

sodium bicarbonate was added, and the mixture extracted with DCM (3 × 30 mL). Purification by flash chromatography (5:1 P.E.:EtOAc mobile phase) afforded (E)-5-bromo-2-methoxy-3-(oct-1-en-1-yl)pyridine **145** (897 mg, 3.01 mmol, 46 %) as a clear oil; $\mathbf{R_f}$ 0.39 (30:1 P.E.:Et_2O); $\boldsymbol{\nu_{max}}$ (thin film) / cm^{-1} 2927, 2855, 1690, 1646, 1560, 1464, 1394, 1293, 1246, 1153, 1021, 968, 894, 760, 655; ^{1}**H NMR** (400 MHz, $CDCl_3$) δ_H 8.02 (1H, d, J = 2.13 Hz, H6), 7.70 (1H, d, J = 2.16 Hz, H4), 6.45 (1H, d, J = 15.98 Hz, H7), 6.28 (1H, dt, J = 15.38 and 7.41 Hz, H8), 3.94 (3H, s, OMe), 2.22 (2H, q, J = 7.17 Hz, CH_2), 1.49–1.42 (2H, m, CH_2), 1.30 (6H, m, $(CH_2)_3$), 0.89 (3H, m, H14); ^{13}**C NMR** (100 MHz, $CDCl_3$) δ_C 159.5, 145.0, 136.5, 135.6, 123.3, 122.4, 112.1, 53.9 (OMe), 33.6, 31.9, 29.3, 29.1, 22.8 and 14.2 (C14); **HRMS** (FI^+) found 297.0724 ($C_{14}H_{20}NOBr$ requires 297.0728).

2-methoxy-3-octylpyridine 147

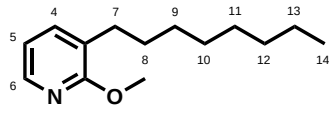

147

A solution of (E)-5-bromo-2-methoxy-3-(oct-1-en-1-yl)pyridine **145** (32 mg, 0.107 mmol, 1.0 eq.) and palladium on carbon (about 10 mg) in MeOH (5 mL) was stirred under a hydrogen atmosphere for 30 m. The mixture was filtered through celite and concentrated under reduced pressure to afford 2-methoxy-3-octylpyridine **147** (22 mg, 0.097 mmol, 91 %); ^{1}**H NMR** (400 MHz, $CDCl_3$) δ_H 8.03 (1H, dd, J = 4.93 and 1.47 Hz, H6), 7.43 (1H, d, J = 6.85 Hz, H4), 6.85 (1H, dd, J = 5.20 and 7.42 Hz, H5), 4.01 (3H, s, OMe), 2.56 (2H, t, J = 7.69 Hz, H7), 1.66–1.49 (2H, m, CH_2), 1.37–1.19 (10H, m, $(CH_2)_5$), 0.88 (3H, m, H14).

(E)-(6-methoxy-5-(oct-1-en-1-yl)pyridin-3-yl)boronic acid 148

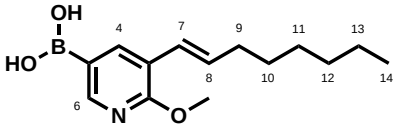

148

To a solution of (E)-5-bromo-2-methoxy-3-(oct-1-en-1-yl)pyridine **145** (601 mg, 1.99 mmol, 1.0 eq.) in dry Et_2O (15 mL) at −78 °C was added *n*-BuLi (0.96 mL, 2.39 mmol, 2.5 M solution, 1.2 eq.). The solution was stirred for 10 m, then triisopropylborate (0.92 mL, 3.98 mmol, 2.0 eq.) was added. The solution was stirred for 10 m at −78 °C then r.t. for 30 m. Water was added and the mixture stirred at r.t. for 20 m. The solution was extracted with Et_2O (4 × 20 mL) and the combined organic phases concentrated under reduced pressure to afford (E)-(6-methoxy-5-(oct-1-en-1-yl)pyridin-3-yl)boronic acid **148** (470 mg, 1.79 mmol, 90 %); **^{1}H NMR** (400 MHz, $(CD_3)_2CO$) δ_H 8.47 (1H, d, J = 2.00 Hz, H6), 8.18 (1H, d, J = 1.87 Hz, H4), 6.56 (1H, d, J = 16.01 Hz, H7), 6.36 (1H, dt, J = 15.93 and 6.84 Hz, H8), 3.95 (3H, s, OMe), 2.24 (2H, qd, J = 7.17 and 1.41 Hz, CH_2), 1.52–1.44 (2H, m, CH_2), 1.41–1.26 (6H, m, $(CH_2)_3$), 0.89 (3H, t, J = 6.90 Hz, H14); **HRMS** (ESI^-) found 262.1625 ($C_{14}H_{21}BNO_3$ requires 262.1623).

(E)-2-methoxy-3-(oct-1-en-1-yl)pyridine 320

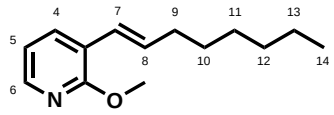

320

To a solution of (E)-5-bromo-2-methoxy-3-(oct-1-en-1-yl)pyridine **145** (165 mg, 0.55 mmol, 1.0 eq.) in dry Et_2O (5 mL) at −78 °C was added *n*-BuLi (0.29 mL, 0.72 mmol, 2.5 M solution, 1.3 eq.). The solution was stirred for 10 m, then triisopropylborate (0.38 mL, 1.65 mmol, 3.0 eq.) was added. The solution was stirred for 10 m at −78 °C then r.t. for 30 m. Water was added and the mixture stirred at r.t. for 20 m. The solution was extracted with Et_2O (3 × 20 mL) and the combined organic phases concentrated under reduced pressure and purified by flash chromatography (30:1 P.E.:Et_2O mobile phase) to afford (E)-2-methoxy-3-(oct-1-en-1-yl)pyridine **320** (72 mg, 0.33 mmol, 60 %) as an oil; $\mathbf{R_f}$ 0.27 (30:1 P.E.:Et_2O); $\boldsymbol{\nu_{max}}$ (thin film) / cm^{-1} 2926, 2855, 2360, 2342, 1578, 1462, 1406, 1258, 1099, 1022, 970, 781 and 669; **^{1}H NMR** (500 MHz, $CDCl_3$) δ_H 8.01 (1H, dd, J = 4.95 and 1.85 Hz, H6), 7.62 (1H, dd, J = 7.39 and 1.48 Hz, H4), 6.83 (1H, dd, J = 7.36 and 4.96 Hz, H5), 6.54 (1H, d, J = 15.96 Hz, H7), 6.28 (1H, dt, J = 15.94 and 6.95 Hz, H8), 3.98 (3H, s, OMe), 2.23 (2H, qd, J = 7.34 and 1.20 Hz, CH_2), 1.50–1.44 (2H, m, CH_2), 1.37–1.24 (6H, m, $(CH_2)_3$), 0.91–0.87 (3H, m, H14); **^{13}C NMR** (100 MHz, $CDCl_3$) δ_C 160.8, 144.8 (C6), 134.4 (C4), 134.0 (C8), 123.5 (C7), 121.5, 117.0 (C5), 53.5 (OMe), 33.7, 31.9, 29.5, 29.1, 22.8 and 14.3 (C14); $\boldsymbol{m/z}$ (ESI^+) 220.18 (100 %, $[M+H]^+$); **HRMS** (ESI^+) found 220.1695 ($C_{14}H_{22}NO$ requires 220.1696).

(E)-6,6′-dimethoxy-5′-(oct-1-en-1-yl)-2,3′-bipyridine 149

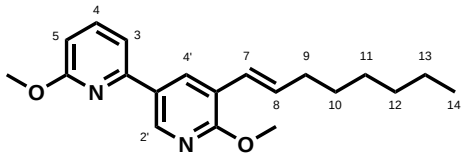

149

A solution of (E)-(6-methoxy-5-(oct-1-en-1-yl)pyridin-3-yl)boronic acid **148** (459 mg, 1.75 mmol, 1.0 eq.), 2-bromo-6-methoxypyridine **321** (658 mg, 3.50 mmol, 2.0 eq.), Na_2CO_3 (2.98 mmol, 1.5 mL of 2 M solution, 1.7 eq.), EtOH (0.8 mL) and toluene (15 mL) was degassed for 10 min before adding tetrakis(triphenylphosphine)palladium (51 mg, 0.044 mmol, 0.025 eq.). The mixture was stirred under an argon atmosphere at 110 °C for 16 hours, reduced to room temperature, concentrated under reduced pressure and purified by flash chromatography (10:1 P.E.:Et_2O mobile phase) to afford (E)-6,6′-dimethoxy-5′-(oct-1-en-1-yl)-2,3′-bipyridine **149** (524 mg, 1.61 mmol, 92 %) as a clear oil; $\mathbf{R_f}$ 0.18 (10:1 P.E.:Et_2O); $\boldsymbol{\nu_{max}}$ (thin film) / cm^{-1} 2360, 2342, 1578, 1467, 1414, 1257, 669; **^{1}H NMR** (400 MHz, $CDCl_3$) δ_H 8.69 (1H, d, J = 2.30 Hz, H2′), 8.26 (1H, d, J = 2.30 Hz, H4′), 7.61 (1H, t, J = 7.82 Hz, H4), 7.27 (1H, d, J = 7.35 Hz, H3), 6.67 (1H, d, J = 8.21 Hz, H5), 6.60 (1H, d, J = 15.96 Hz, H7), 6.40 (1H, dt, J = 15.90 and 6.90 Hz, H8), 4.04 (3H, s, OMe), 4.02 (3H, s, OMe), 2.26 (2H, q, J = 7.17 Hz, CH_2), 1.50 (2H, quintet, J = 7.41 Hz, CH_2), 1.40–1.26 (6H, m, $(CH_2)_3$), 0.90 (3H, t, J = 6.82 Hz, H14); **^{13}C NMR** (100 MHz, $CDCl_3$) δ_C 164.1, 161.4, 152.9, 143.7, 139.5 (C4), 134.7, 133.0, 128.7, 123.7, 121.2, 112.4 (C3), 109.3 (C5), 54.0 (OMe), 53.6 (OMe), 33.9, 32.1, 29.7, 29.3, 23.0 and 14.5 (C14); $\boldsymbol{m/z}$ (ESI^+) 857.28 (100 %), 579.18 (78 %), 327.21 ($[M+H]^+$, 22 %); **HRMS** (ESI^+) found 327.2059 ($[M+H]^+$, $C_{20}H_{27}N_2O_2$ requires 327.2067).

6,6′-dimethoxy-5′-octyl-2,3′-bipyridine 150

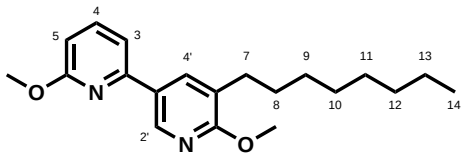

150

A solution of (E)-6,6′-dimethoxy-5′-(oct-1-en-1-yl)-2,3′-bipyridine **149** (100 mg, 0.31 mmol, 1.0 eq.) and palladium on carbon (about 15 mg) in EtOAc (5 mL) was stirred under a hydrogen atmosphere for 30 m. The mixture was filtered through celite and concentrated under reduced pressure to afford

6,6′-dimethoxy-5′-octyl-2,3′-bipyridine **150** (98 mg, 0.30 mmol, 97 %) as a clear oil; $\mathbf{R_f}$ 0.26 (10:1 P.E.:Et_2O); $\boldsymbol{\nu_{max}}$ (thin film) / cm^{-1} 2926, 2361, 2342, 1578, 1465, 1412, 1385, 1254, 1026, 800, 669; ^{1}**H NMR** (400 MHz, $CDCl_3$) δ_H 8.68 (1H, d, J = 2.31 Hz, H2′), 8.02 (1H, dd, J = 2.39 and 0.59 Hz, H4′), 7.60 (1H, td, J = 7.82 and 0.57 Hz, H4), 7.25 (1H, d, J = 7.39 Hz, H3), 6.66 (1H, d, J = 8.21 Hz, H5), 4.02 (3H, d, J = 0.61 Hz, OMe), 4.01 (3H, d, J = 0.58 Hz, OMe), 2.62 (2H, t, J = 7.72 Hz, H7), 1.63 (2H, quintet, J = 7.39 Hz, H13), 1.41–1.21 (10H, m, $(CH_2)_5$), 0.88 (3H, t, J = 6.85 Hz, H14); ^{13}**C NMR** (100 MHz, $CDCl_3$) δ_C 163.9, 162.8, 152.9, 142.8, 139.3 (C4), 136.0, 128.3, 125.1, 112.1 (C3), 109.0 (C5), 53.7 (OMe), 53.3 (OMe), 32.1, 30.1, 29.63, 29.59, 29.4, 29.2, 22.8, 14.3 (C14); $\boldsymbol{m/z}$ (ESI^+) 413.29 (100 %), 329.24 ($[M+H]^+$, 87 %); **HRMS** (ESI^+) found 329.2221 ($[M+H]^+$, $C_{20}H_{29}N_2O_2$ requires 329.2224).

5′-octyl-[2,3′-bipyridine]-6,6′(1H,1′H)-dione 151

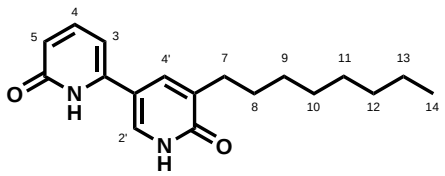

151

A solution of 6,6′-dimethoxy-5′-octyl-2,3′-bipyridine **150** (30 mg, 0.091 mmol, 1.0 eq.), HBr (48 %, 1.0 mL) and AcOH (0.5 mL) was stirred in a vial at 120 °C for two hours. After cooling to r.t. the solution was quenched with aqueous NaOH. The solids were isolated by sinter filtration and dried over P_2O_5 under reduced pressure to afford 5′-octyl-[2,3′-bipyridine]-6,6′(1H,1′H)-dione **151** (15 mg, 0.05 mmol, 55 %) as an off-white powder; $\mathbf{R_f}$ 0.13 (10:1 EtOAc:MeOH); $\boldsymbol{\nu_{max}}$ (thin film) / cm^{-1} 2923, 2852, 1683, 1648, 1614, 1562, 1472, 1381, 1271, 1160, 1004, 877, 786, 719, 695, 667; ^{1}**H NMR** (500 MHz, DMSO) δ_H 7.81 (1H, d, J = 2.60 Hz, H4′), 7.71 (1H, s, H2′), 7.50 (1H, dd, J = 8.79 and 7.23 Hz, H4), 6.65 (1H, d, J = 7.31 Hz, H3), 6.30 (1H, d, J = 8.74 Hz, H5), 2.41 (2H, t, J = 7.64 Hz, H7), 1.53 (2H, dt, J = 14.34 and 7.15 Hz, H8), 1.29–1.25 (10H, m, H8–H12), 0.86 (3H, t, J = 6.95 Hz, H14); ^{13}**C NMR** (125 MHz, DMSO) δ_C 163.1 (C6), 161.9 (C6′), 146.1, 141.0 (C4), 135.0 (C2′), 134.0, 132.6, 131.8 (C4′), 112.4, 104.2 (C3), 31.3, 29.9, 28.92, 28.87, 28.7, 27.8, 22.1 and 14.0 (C14); $\boldsymbol{m/z}$ (ESI^-) 331.08 (100 %), 299.20 (92 %, $[M-H]^-$); **HRMS** (ESI^+) found 323.1723 ($[M+Na]^+$, $C_{18}H_{24}N_2O_2Na$ requires 323.1730).

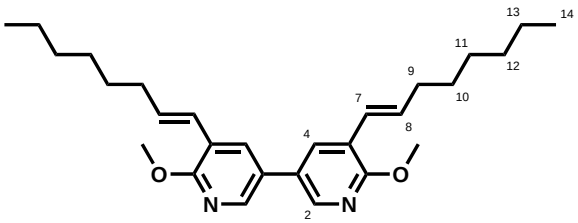

152

6,6′-dimethoxy-5,5′-di((E)-oct-1-en-1-yl)-3,3′-bipyridine 152

A solution of (E)-(6-methoxy-5-(oct-1-en-1-yl)pyridin-3-yl)boronic acid **148** (160 mg, 0.61 mmol, 1.0 eq.), (E)-5-bromo-2-methoxy-3-(oct-1-en-1-yl)pyridine **145** (292 mg, 0.97 mmol, 1.6 eq.), tetrakis-(triphenylphosphine)palladium (18 mg, 0.0153 mmol, 0.025 eq.), Na_2CO_3 (1.04 mmol, 0.52 mL of 2 M solution, 1.7 eq.), EtOH (0.26 mL) and toluene (10 mL) was degassed for 10 m and then stirred at 110 °C for 16 h. After cooling to room temperature, the mixture was concentrated under reduced pressure and purified by flash chromatography (9:1 P.E.:EtOAc mobile phase) to afford 6,6′-dimethoxy-5,5′-di((E)-oct-1-en-1-yl)-3,3′-bipyridine **152** (106 mg, 0.24 mmol, 40 %); ^{1}**H NMR** (400 MHz, $CDCl_3$) δ_H 8.16 (2H, d, J = 2.36 Hz, H2), 7.75 (2H, d, J = 2.38 Hz, H4), 6.58 (2H, d, J = 16.03 Hz, H7), 6.36 (2H, dt, J = 15.91 and 6.91 Hz, H8), 4.01 (6H, s, OMe), 2.25 (4H, m, H9), 1.53–1.43 (4H, m, CH_2), 1.40–1.21 (12H, m, $(CH_2)_3$), 0.89 (6H, t, J = 6.70 Hz, H14).

6,6′-dimethoxy-5,5′-dioctyl-3,3′-bipyridine 154

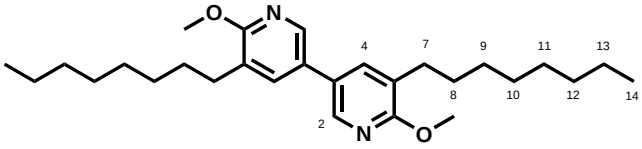

154

A solution of 6,6′-dimethoxy-5,5′-di((E)-oct-1-en-1-yl)-3,3′-bipyridine **322** (41 mg, 0.094 mmol, 1.0 eq) and palladium on carbon in EtOAc (5 mL) was stirred under a hydrogen atmosphere for 30 m. The solution was filtered through celite and concentrated under reduced pressure to afford 6,6′-dimethoxy-5,5′-dioctyl-3,3′-bipyridine **154** (38 mg, 0.086 mmol, 92 %) as a clear oil; $\mathbf{R_f}$ 0.14 (10:1 P.E.:Et_2O); $\boldsymbol{\nu_{max}}$ (thin film) / cm^{-1} 2924, 2855, 2361, 2341, 1735, 1603, 1463, 1407, 1372, 1297, 1248, 1175, 1023, 900, 782; ^{1}**H NMR** (500 MHz, $CDCl_3$) δ_H 8.15 (2H, d, J = 2.41 Hz, H2), 7.51 (2H, d, J = 2.35 Hz, H4), 3.99 (6H, s, OMe), 2.60 (4H, t, J = 7.75 Hz, H7), 1.64–1.58 (4H, m, CH_2), 1.36–1.24 (20H, m, $(CH_2)_5$), 0.88 (6H, t, J = 6.94 Hz, H14); ^{13}**C NMR** (125 MHz, $CDCl_3$)

δ_C 161.8, 141.6 (C2), 136.4 (C4), 127.3, 125.6, 84.6, 32.0, 30.0, 29.64, 29.58, 29.4, 29.2, 22.8 and 14.3 (C14); ***m/z*** (ESI$^+$) 485.34 (100 %), 441.38 (72 %, [M+H]$^+$); **HRMS** (ESI$^+$) found 441.3466 ([M+H]$^+$, $C_{28}H_{45}N_2O_2$ requires 441.3476).

5,5′-dioctyl-[3,3′-bipyridine]-6,6′(1H,1′H)-dione 153

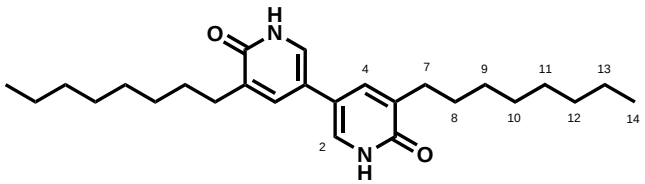

153

A solution of 6,6′-dimethoxy-5,5′-dioctyl-3,3′-bipyridine **154** (30 mg, 0.07 mmol, 1.0 eq.), NaI (42 mg, 0.28 mmol, 4.0 eq.), TMSCl (36μ L, 0.28 mmol, 4.0 eq.) and MeCN (1 mL) was stirred at r.t. for 30 m. The MeCN was removed under reduced pressure to afford 5,5′-dioctyl-[3,3′-bipyridine]-6,6′(1H,1′H)-dione **153** (27 mg, 0.066 mmol, 94 %); ^{1}**H NMR** (400 MHz, $CDCl_3$) δ_H 8.65 (2H, s, H4), 8.29 (2H, s, H2), 2.79 (4H, m, CH_2), 1.66 (4H, m, CH_2), 1.43–1.18 (20H, m, $(CH_2)_5$), 0.86 (6H, m, CH_3).

(E)-5-(6,6′-dimethoxy-[2,3′-bipyridin]-5′-yl)pent-3-en-1-ol 165

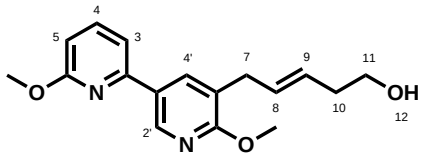

165

A solution of 5′-allyl-6,6′-dimethoxy-2,3′-bipyridine **323** (62 mg, 0.24 mmol, 1.0 eq.), butenol (0.10 mL, 1.21 mmol, 5.0 eq.) and DCM (0.1 mL) was degassed for 5 m. Grubbs II catalyst (4 mg, 0.0048 mmol, 0.02 eq.) was added and the solution stirred at room temperature for 24 h. The crude reaction mixture was evaporated under reduced pressure and purified by flash chromatography (1:1 P.E.:Et_2O mobile phase) to afford (E)-5-(6,6′-dimethoxy-[2,3′-bipyridin]-5′-yl)pent-3-en-1-ol **165** (21 mg, 0.07 mmol, 29 %) as an off-white semisolid; $\mathbf{R_f}$ 0.50 (100 % Et_2O); $\boldsymbol{\nu_{max}}$ (thin film) / cm^{-1} 3375, 2947, 1578, 1466, 1412, 1383, 1331, 1254, 1154, 1024, 973, 845, 800, 734; ^{1}**H NMR** (500 MHz, $CDCl_3$) δ_H 8.70 (1H, d, J = 2.37 Hz, H2′), 8.04 (1H, d, J = 2.21 Hz, H4′), 7.60 (1H, t, J = 7.85 Hz, H4), 7.24 (1H, m, H3), 6.66 (1H, d, J = 8.19 Hz, H5), 5.78–5.71 (1H, m, CH), 5.61–5.49 (1H, m, CH), 4.01 (6H, m, MeO), 3.71 (0.2H, q, J = 6.04 Hz, CH_2), 3.65 (0.8H, q, J = 5.99 Hz,

CH_2), 3.44 (0.2H, d, J = 7.32 Hz, CH_2), 3.37 (0.8H, d, J = 6.62 Hz, CH_2), 2.47 (0.2H, q, J = 6.68 Hz, CH_2), 2.32 (0.8H, q, J = 6.45 Hz, CH_2), 1.61 (0.2H, t, J = 5.66 Hz, OH), 1.50 (0.8H, t, J = 5.73 Hz, OH); **^{13}C NMR** (125 MHz, $CDCl_3$) δ_C 163.9, 162.5, 152.7, 143.3, 139.4 (C4), 136.2, 130.7, 128.5, 128.3, 123.0, 112.1 (C3), 109.1 (C5), 62.0, 53.8 (OMe), 53.4 (OMe), 36.1 and 33.2; ***m/z*** (ESI$^+$) 323.13 (100 %, $[M+Na]^+$), 623.35 (17 %, $[2M+Na]^+$); **HRMS** (ESI$^+$) found 323.1357 ($[M+Na]^+$, $C_{17}H_{20}N_2O_3Na$ requires 323.1366).

5-(6,6′-dimethoxy-[2,3′-bipyridin]-5′-yl)pentan-1-ol 166

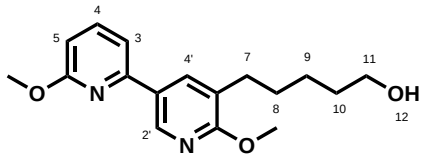

166

A solution of (E)-5-(6,6′-dimethoxy-[2,3′-bipyridin]-5′-yl)pent-3-en-1-ol **165** (35 mg, 0.117 mmol, 1.0 eq.), Pd/C (30 mg), and EtOAc (4 mL) was stirred at room temperature under an atmosphere of H_2 for 20 m. The solution was then filtered through an inch of silica and the filtrate concentrated under reduced pressure to afford 5-(6,6′-dimethoxy-[2,3′-bipyridin]-5′-yl)pentan-1-ol **166** (31 mg, 0.103 mmol, 88 %) as an oil; $\mathbf{R_f}$ 0.38 (1:1 EtOAc:P.E.); $\boldsymbol{\nu_{max}}$ (thin film) / cm^{-1} 3395, 2941, 1578, 1465, 1412, 1384, 1330, 1253, 1169, 1025 and 800; **^{1}H NMR** (500 MHz, $CDCl_3$) δ_H 8.68 (1H, d, J = 2.36 Hz, H2′), 8.02 (1H, d, J = 2.43 Hz, H4′), 7.60 (1H, dd, J = 8.19 and 7.51 Hz, H4), 7.25 (1H, d, J = 7.65 Hz, H3), 6.66 (1H, d, J = 8.19 Hz, H5), 4.01 (3H, s, OMe), 4.00 (3H, s, OMe), 3.66 (2H, t, J = 6.55 Hz, H11), 2.65 (2H, t, J = 7.68 Hz, H7), 1.70–1.60 (4H, m, $(CH_2)_2$), 1.48–1.42 (2H, m, CH_2); **^{13}C NMR** (125 MHz, $CDCl_3$) δ_C 164.0, 162.7, 152.8, 142.8, 139.4 (C4), 136.2, 128.4, 124.9, 112.2 (C3), 109.0 (C5), 63.1, 53.8 (OMe), 53.4 (OMe), 32.7, 30.1, 29.0 and 25.7; ***m/z*** (ESI$^+$) 303.14 ($[M+H]^+$, 100%); **HRMS** (ESI$^+$) found 303.1707 ($C_{17}H_{23}N_2O_3$ requires 303.1703).

5′-(5-hydroxypentyl)-[2,3′-bipyridine]-6,6′(1H,1′H)-dione 167

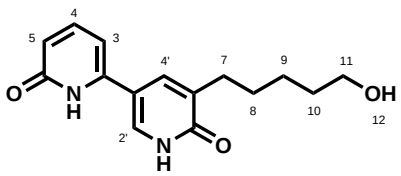

167

A solution of 5-(6,6′-dimethoxy-[2,3′-bipyridin]-5′-yl)pentan-1-ol **166** (20 mg, 0.066 mmol, 1.0 eq.), NaI (40 mg, 0.264 mmol, 4.0 eq.), TMSCl (29 mg, 0.264 mmol, 4.0 eq.) and MeCN (0.5 mL) was stirred at 40 °C for 1 h. After cooling to room temperature the mixture was filtered through cotton wool and concentrated under reduced pressure to afford 5′-(5-hydroxypentyl)-[2,3′-bipyridine]-6,6′-(1H,1′H)-dione **167** (16 mg, 0.058 mmol, 86 %); $\mathbf{R_f}$ 0.32 (20:1 EtOAc:MeOH); ^{1}**H NMR** (500 MHz, DMSO) δ_H 7.79 (1H, d, J = 2.77 Hz, H4′), 7.69 (1H, s, H2′), 7.51 (1H, dd, J = 8.83 and 7.25 Hz, H4), 7.61 (1H, d, J = 7.11 Hz, H3), 6.32 (1H, d, J = 8.84 Hz, H5), 3.37 (2H, t, J = 6.55 Hz, H11), 2.43 (2H, t, J = 7.55 Hz, H7), 1.55–1.25 (6H, m, $(CH_2)_3$); ^{13}**C NMR** (125 MHz, DMSO) δ_C 163.4 (C6), 162.6 (C6′), 151.3, 140.5, 135.5, 132.7, 131.5, 119.5, 111.4, 108.4, 61.0, 32.6, 30.3, 28.1 and 25.6.

5′-(5-((tert-butyldimethylsilyl)oxy)pentyl)-6,6′-dimethoxy-2,3′-bipyridine 168

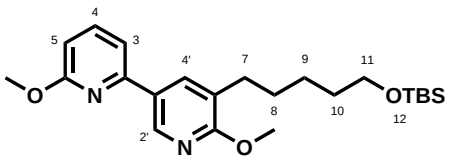

168

To a solution of 5-(6,6′-dimethoxy-[2,3′-bipyridin]-5′-yl)pentan-1-ol **166** (16 mg, 0.053 mmol, 1.0 eq.), imidazole (9 mg, 0.133 mmol, 2.5 eq.), and DCM (1 mL) at 0 °C was added *tert*-butyldimethylchlorosilane (10 mg, 0.064 mmol, 1.2 eq.). The solution was stirred at room temperature for 1 h. Aqueous ammonium chloride was added and the mixture extracted with DCM (3 × 10 mL). The combined organic phases were concentrated under reduced pressure and filtered through an inch of silica in a sinter funnel to afford 5′-(5-((tert-butyldimethylsilyl)oxy)pentyl)-6,6′-dimethoxy-2,3′-bipyridine **168** (20 mg, 0.048 mmol, 92 %); $\mathbf{R_f}$ 0.25 (10:1 P.E.:Et_2O); ^{1}**H NMR** (500 MHz, $CDCl_3$) δ_H 8.68 (1H, d, J = 2.34 Hz, ArH), 8.02 (1H, d, J = 2.24 Hz, ArH), 7.61 (1H, m, J = 7.80 Hz, ArH), 7.25 (1H, d, J = 7.43 Hz, ArH), 6.66 (1H, d, J = 8.21 Hz, ArH), 4.01 (3H, s, OMe), 4.00 (3H, s, OMe), 3.66 (2H, t, J = 6.62 Hz, CH_2), 2.63 (2H, m, CH_2), 1.75–1.54 (4H, m, $(CH_2)_2$), 1.49–1.39 (2H, m, CH_2), 0.88 (9H, s, $SiC(CH_3)_3$), 0.04 (6H, s, $Si(CH_3)_2$); ^{13}**C NMR** (125 MHz, $CDCl_3$) δ_C 164.0, 162.7, 152.8, 142.9, 139.4, 136.2, 128.3, 124.8, 112.2, 109.0, 63.0, 53.7, 53.4, 32.7, 30.1, 29.0, 26.1, 25.8, 25.7 and -3.4; ***m/z*** (ESI$^+$) 417.24 ([M+H]$^+$, 100 %); **HRMS** (ESI$^+$) found 417.2551 ($C_{23}H_{37}N_2O_3Si$, ([M+H]$^+$) requires 417.2568).

(but-3-en-1-yloxy)(tert-butyl)dimethylsilane 159

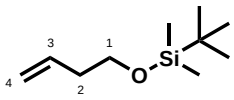

159

To a solution of butenol **161** (3.0 mL, 34.92 mmol, 1.0 eq.), imidazole (5.936 g, 87.29 mmol, 2.5 eq.), and DCM (90 mL) at 0 °C was added *tert*-butyldimethylchlorosilane (6.327 g, 41.90 mmol, 1.2 eq.). The solution was stirred at room temperature for 1 h. Aqueous ammonium chloride was added and the mixture extracted with DCM (3 × 20 mL). The combined organic phases were concentrated under reduced pressure and filtered through an inch of silica in a sinter funnel to afford (but-3-en-1-yloxy)(tert-butyl)dimethylsilane **159** (3.251 g, 17.48 mmol, 50 %); **^{1}H NMR** (400 MHz, $CDCl_3$) δ_H 5.87–5.76 (1H, m, H3), 5.11–5.00 (2H, m, H4), 3.66 (2H, t, J = 6.82 Hz, H1), 2.28 (2H, qt, J = 6.81 and 1.32 Hz, H2), 0.89 (9H, s, $SiC(CH_3)_3$), 0.05 (6H, s, $Si(CH_3)_2$). Data agrees with literature.[234]

(E)-5-bromo-3-(5-((tert-butyldimethylsilyl)oxy)pent-2-en-1-yl)-2-methoxypyridine 160

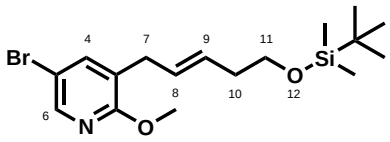

160

A solution of 3-allyl-5-bromo-2-methoxypyridine **130** (75 mg, 0.33 mmol, 1.0 eq.), (but-3-en-1-yloxy)-(tert-butyl)dimethylsilane **159** (306 mg, 1.65 mmol, 5.0 eq.) and DCM (0.25 mL) was degassed for 5 m. Grubbs II catalyst (6 mg, 0.0066 mmol, 0.02 eq.) was added and the solution stirred at room temperature for 16 h. The crude reaction mixture was evaporated under reduced pressure and purified by flash chromatography (5:1 P.E.:EtOAc mobile phase) to afford (E)-5-bromo-3-(5-((tert-butyldimethylsilyl)oxy)pent-2-en-1-yl)-2-methoxypyridine **160** (40 mg, 0.104 mmol, 32 %) as an oil; $\boldsymbol{\nu_{max}}$ (thin film) / cm^{-1} 2954, 2929, 2857, 1570, 1466, 1414, 1389, 1303, 1252, 1099, 1020, 836 and 776; **^{1}H NMR** (500 MHz, $CDCl_3$) δ_H 8.04 (1H, dd, J = 8.35 and 2.29 Hz, ArH), 7.47 (1H, dd, J = 8.23 and 2.21 Hz, ArH), 5.60–5.49 (2H, m, H8 and H9), 3.92 (3H, s, OMe), 3.66–3.58 (2H, m, CH_2), 3.29 (0.5H, d, J = 6.53 Hz, CH_2), 3.23 (1.5H, d, J = 6.17 Hz, CH_2), 2.34 (0.5H, q, J = 6.70 Hz, CH_2), 2.27 (1.5H, q, J = 6.52 Hz, CH_2), 0.88 (9H, s, $SiC(CH_3)_3$), 0.04 (6H, s, $Si(CH_3)_2$); **^{13}C NMR** (125 MHz, $CDCl_3$) δ_C 160.9, 145.0, 139.9, 130.0, 128.8, 128.0, 117.3, 111.8, 63.4, 53.8, 36.5, 26.1, 18.5 and -5.1.

(E)-5-(5-bromo-2-methoxypyridin-3-yl)pent-3-en-1-ol 162

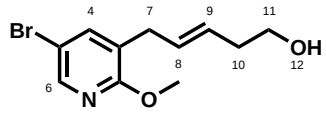

162

A solution of 3-allyl-5-bromo-2-methoxypyridine **130** (42 mg, 0.18 mmol, 1.0 eq.), butenol (79 μL, 0.92 mmol, 5.0 eq.) and DCM (0.25 mL) was degassed for 5 m. Grubbs II catalyst (3 mg, 0.0036 mmol, 0.02 eq.) was added and the solution stirred at room temperature for 16 h. The crude reaction mixture was evaporated under reduced pressure and purified by flash chromatography (3:1 P.E.:EtOAc mobile phase) to afford (E)-5-(5-bromo-2-methoxypyridin-3-yl)pent-3-en-1-ol **162** (13 mg, 0.048 mmol, 26 %) as an oil; $\mathbf{R_f}$ 0.29 (2:1 P.E.:EtOAc); ^{1}**H NMR** (500 MHz, $CDCl_3$) δ_H 8.05 (1H, d, J = 2.30 Hz, ArH), 7.47 (1H, d, J = 2.41 Hz, ArH), 5.69–5.47 (2H, m, H8 and H9), 3.92 (3H, s, OMe), 3.69 (0.4H, t, J = 6.41 Hz, CH_2), 3.66 (1.6H, t, J = 6.30 Hz, CH_2), 3.33 (0.4H, d, J = 6.71 Hz, CH_2), 3.26 (1.6H, d, J = 6.70 Hz, CH_2), 2.41 (0.4H, q, J = 6.59 Hz, CH_2), 2.31 (1.6H, q, J = 6.60 Hz, CH_2), 1.88 (1H, s, OH); ^{13}**C NMR** (125 MHz, $CDCl_3$) δ_C 160.9, 145.0, 140.0, 129.6, 129.1, 125.5, 111.8, 62.0, 53.9, 36.0 and 32.8.

(E)-methyl 4-(5-bromo-2-methoxypyridin-3-yl)but-2-enoate 164

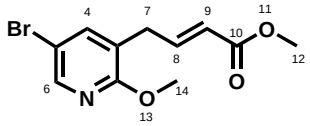

164

A solution of 3-allyl-5-bromo-2-methoxypyridine **130** (47 mg, 0.21 mmol, 1.0 eq.), methyl acrylate (57 μL, 0.63 mmol, 3.0 eq.) and Grubbs(II) catalyst (4 mg, 4.2 μmol, 0.02 eq.) in DCM (0.5 mL) was stirred in a vial for 24 h. The mixture was concentrated under reduced pressure and purified by flash chromatography (5:1 P.E.:Et_2O mobile phase) to afford (E)-methyl 4-(5-bromo-2-methoxypyridin-3-yl)but-2-enoate **164** (25 mg, 0.087 mmol, 42 %) as an off-white solid; $\mathbf{R_f}$ 0.40 (4:1 P.E.:Et_2O); **mp** 58.7–60.6 °C; $\boldsymbol{\nu_{max}}$ (thin film) / cm^{-1} 2949, 1722, 1656, 1574, 1466, 1435, 1419, 1391, 1335, 1296, 1273, 1249, 1209, 1178, 1140, 1058, 1018, 994, 908, 786; ^{1}**H NMR** (400 MHz, $CDCl_3$) δ_H 8.09 (1H, d, J = 2.39 Hz, ArH), 7.45 (1H, d, J = 2.40 Hz, ArH), 7.02 (1H, dt, J = 15.61 and 6.84 Hz, H8), 5.83 (1H, dd, J = 15.61 and 1.47 Hz, H9), 3.92 (3H, s, OMe), 3.73 (3H, s, OMe), 3.43 (2H, d, J = 6.82 Hz, H7); ^{13}**C NMR** (100 MHz, $CDCl_3$) δ_C 166.8, 160.9, 145.9, 145.0, 140.5, 122.9, 122.7,

111.7, 54.0, 51.7 and 32.4; ***m/z*** (ESI$^+$) 308.00 ([M+Na]$^+$, 100%), 286.04 ([M+H]$^+$, 22 %); **HRMS** (ESI$^+$) found 307.9881 ($C_{11}H_{12}BrNNaO_3$ requires 307.9893).

3-(5-bromo-2-methoxypyridin-3-yl)propan-1-ol 155

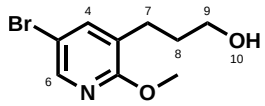

155

A solution of 3-allyl-5-bromo-2-methoxypyridine **130** (500 mg, 2.19 mmol, 1.0 eq.) and borane dimethyl sulfide complex (0.37 mL, 3.70 mmol, 1.7 eq.) was stirred at room temperature in THF (5 mL) for 60 m. Then, aqueous sodium hydroxide (1.1 mL, 3.0 M, 1.5 eq.) and hydrogen peroxide (1.0 mL, 4.5 eq.) were added, and the solution stirred at room temperature for 2 h. The solution was quenched with brine and extracted with Et_2O (3 × 15 mL). The combined organic phases were concentrated under reduced pressure and purified by flash chromatography (100 % Et_2O mobile phase) to afford 3-(5-bromo-2-methoxypyridin-3-yl)propan-1-ol **155** (227 mg, 0.92 mmol, 42 %) as an oil; $\mathbf{R_f}$ 0.26 (1:1 Et_2O:P.E.); $\boldsymbol{\nu_{max}}$ (thin film) / cm^{-1} 3347, 2949, 1569, 1466, 1415, 1392, 1308, 1248, 1186, 1020, 899 and 645; ^{1}**H NMR** (500 MHz, $CDCl_3$) δ_H 8.05 (1H, d, J = 2.50 Hz, ArH), 7.50 (1H, d, J = 2.29 Hz, ArH), 3.93 (3H, s, OMe), 3.65 (2H, t, J = 6.28 Hz, CH_2), 2.64 (2H, t, J = 7.54 Hz, CH_2), 1.87–1.81 (2H, m, CH_2), 1.58 (1H, s, OH); ^{13}**C NMR** (125 MHz, $CDCl_3$) δ_C 161.1, 144.9, 140.4, 126.5, 111.9, 62.0, 53.9, 31.9 and 26.0; ***m/z*** (ESI$^+$) 248.01 ([M+H]$^+$, 100%); **HRMS** (ESI$^+$) found 248.0125 ($C_9H_13BrNO_2$ requires 248.0104).

3-(3-(benzyloxy)propyl)-5-bromo-2-methoxypyridine 156

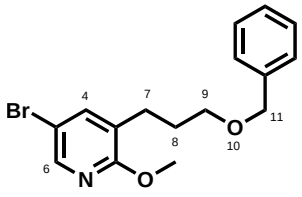

156

To a stirred solution of sodium hydride (26 mg, 1.10 mmol, 1.2 eq.) in dry THF (1 mL) was added a solution of 3-(5-bromo-2-methoxypyridin-3-yl)propan-1-ol **155** (225 mg, 0.91 mmol, 1.0 eq.) in dry THF (4 mL) over a period of five minutes. The mixture was stirred for 30 m before adding benzyl bromide (0.13 mL, 1.10 mmol, 1.2 eq.) over a period of two minutes. The mixture was heated to

reflux temperature and stirred for 14 hours. It was cooled to room temperature, quenched with water (20 mL), and extracted with Et_2O (3 × 20 mL), concentrated under reduced pressure, and purified by flash chromatography (5:1 P.E.:Et_2O mobile phase) to afford 3-(3-(benzyloxy)propyl)-5-bromo-2-methoxypyridine **156** (127 mg, 0.38 mmol, 41 %) as a clear oil; $\mathbf{R_f}$ 0.3 (5:1 P.E.:Et_2O); $\boldsymbol{\nu_{max}}$ (thin film) / cm^{-1} 2948, 2857, 1720, 1569, 1465, 1415, 1392, 1307, 1248, 1195, 1103, 1021, 900, 737, 698, 645; ^{1}**H NMR** (400 MHz, $CDCl_3$) δ_H 8.05 (1H, d, J = 2.24 Hz, ArH), 7.47 (1H, d, J = 2.01 Hz, ArH), 7.39–7.28 (5H, m, PhH), 4.51 (2H, s, OCH_2Ph), 3.92 (3H, s, OMe), 3.49 (2H, t, J = 6.24 Hz, CH_2), 2.65 (2H, t, J = 7.62 Hz, CH_2), 1.90 (2H, quintet, J = 7.21 Hz, CH_2); ^{13}**C NMR** (100 MHz, $CDCl_3$) δ_C 161.2, 144.7, 140.2, 138.6, 128.5, 127.8, 127.7, 126.7, 111.7, 73.1, 69.5, 53.7, 28.7 and 26.6; $\boldsymbol{m/z}$ (ESI^+) 413.29 (100%), 358.07 ([M+Na]$^+$, 47 %), 336.09 ([M+H]$^+$, 29 %), **HRMS** (ESI^+) found 336.0594 ($C_{16}H_{19}BrNO_2$ requires 336.0594).

3-(3-(benzyloxy)propyl)-5-bromopyridin-2(1H)-one 158

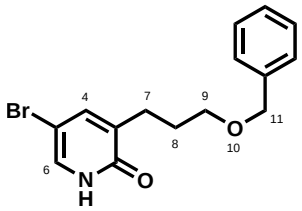

158

A solution of 3-(3-(benzyloxy)propyl)-5-bromo-2-methoxypyridine **156** (25 mg, 0.074 mmol, 1.0 eq.), NaI (45 mg, 0.30 mmol, 4.0 eq.), TMSCl (39 μL, 0.30 mmol, 4.0 eq.) and MeCN (1 mL) was stirred at room temperature for 45 m. After cooling to room temperature the mixture was concentrated under reduced pressure to afford 3-(3-(benzyloxy)propyl)-5-bromopyridin-2(1H)-one **158** (16 mg, 0.50 mmol, 66 %); ^{1}**H NMR** (400 MHz, $CDCl_3$) δ_H 7.40–7.21 (7H, m, H4 and H6 and C_6H_5), 3.50 (2H, t, J = 5.75 Hz, CH_2), 2.88–2.78 (2H, m, CH_2), 1.96–1.89 (2H, m, CH_2), 4.56 (2H, s, CH_2).

2-(benzyloxy)pyridine 176

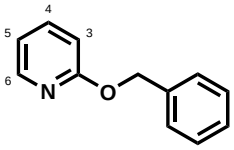

176

To a solution of 2-bromopyridine **177** (0.18 mL, 1.90 mmol, 1.0 eq.) and 60 % NaH in oil (192 mg, 4.80 mmol, 2.5 eq.) in THF (10 mL) at 0 ℃ was added phenylmethanol (0.39 mL, 3.80 mmol, 2.0 eq.). The mixture was stirred at 80 ℃ for 16 h, then concentrated under reduced pressure and purified by flash chromatography (5:1 P.E.:EtOAc mobile phase) to afford 2-(benzyloxy)pyridine **176** (323 mg, 1.75 mmol, 92 %); **^{1}H NMR** (400 MHz, $CDCl_3$) δ_H 8.18 (1H, dd, J = 5.10 and 1.91 Hz, ArH), 7.59 (1H, m, ArH), 7.47 (2H, d, J = 7.35 Hz, ArH), 7.38 (2H, m, ArH), 7.32 (1H, m, ArH), 6.89 (1H, dd, J = 5.12 and 0.85 Hz, ArH), 6.81 (1H, d, J = 8.36 Hz, ArH), 5.38 (2H, s, O$CH_2C_6H_5$). Data agrees with literature.[235]

3,5-dibromopyridin-2(1H)-one 180

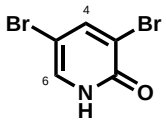

180

To a solution of pyridin-2(1H)-one **178** (500 mg, 5.26 mmol, 1.0 eq.) in MeCN (25 mL) was added NBS (1.9 g, 10.67 mmol, 2.0 eq.). The mixture was stirred in the dark at r.t. for 24 h, then concentrated under reduced pressure. The residue was dissolved in DCM and washed with water (3 × 30 mL) to afford 3,5-dibromopyridin-2(1H)-one **180** (620 mg, 2.45 mmol, 47 %); **^{1}H NMR** (400 MHz, $CDCl_3$) δ_H 7.94 (1H, d, J = 2.56 Hz, ArH), 7.58 (1H, d, J = 2.55 Hz, ArH). Data agrees with literature.[97]

2-(benzyloxy)-3,5-dibromopyridine 175

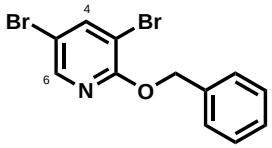

175

A solution of 3,5-dibromopyridin-2(1H)-one **180** (510 mg, 2.02 mmol, 1.0 eq.), benzyl bromide (0.3 mL, 2.42 mmol, 1.2 eq.) and silver carbonate (374 mg, 1.35 mmol, 0.66 eq.) in EtOAc (4 mL) was stirred in the dark at 40 ℃ for 16 h. After cooling to room temperature the mixture was concentrated under reduced pressure and purified by flash chromatography (5:1 P.E.:EtOAc mobile phase) to afford 2-(benzyloxy)-3,5-dibromopyridine **175** (580 mg, 1.69 mmol, 84 %) as a white solid;

^{1}H NMR (400 MHz, $CDCl_3$) δ_H 8.14 (1H, d, J = 2.19 Hz, ArH), 7.94 (1H, d, J = 2.20 Hz, ArH), 7.50–7.46 (2H, m, ArH), 7.41–7.36 (2H, m, ArH), 7.35–7.30 (1H, m, ArH), 5.43 (2H, s, OCH_2C$_6$H$_5$).

3-allyl-2-(benzyloxy)-5-bromopyridine 181

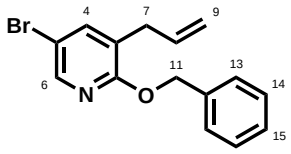

181

To a solution of 2-(benzyloxy)-3,5-dibromopyridine **175** (810 mg, 2.36 mmol, 1.0 eq) in dry Et_2O (20 mL) at −78 °C was added *n*-butyllithium (1.13 mL, 2.5 M, 2.83 mmol, 1.2 eq.). The temperature was raised to -30 °C before the addition of CuI (46 mg, 0.24 mmol, 0.1 eq.) and allyl bromide (0.51 mL, 5.90 mmol, 2.5 eq.). The solution was then raised to room temperature and stirred for 1 hour. The solution was then quenched with water (40 mL) and extracted with Et_2O (3 × 10 mL), and purified by flash chromatography (20:1 P.E.:Et_2O) to afford 3-allyl-2-(benzyloxy)-5-bromopyridine **181** (620 mg, 2.04 mmol, 86 %) as a clear oil; $\mathbf{R_f}$ 0.25 (20:1 P.E.:Et_2O); $\boldsymbol{\nu_{max}}$ (thin film) / cm^{-1} 3033, 2944, 1640, 1579, 1497, 1432, 1397, 1361, 1318, 1246, 1159, 1138, 996, 919, 853, 734, 697; **^{1}H NMR** (400 MHz, $CDCl_3$) δ_H 8.09 (1H, d, J = 2.44 Hz, ArH), 7.53 (1H, d, J = 2.45 Hz, ArH), 7.47–7.31 (5H, m, OCH$_2$$C_6H_5$), 5.95 (1H, ddt, J = 16.9, 10.2 and 6.7 Hz, CH$_2$$CH$=CH$_2$), 5.39 (2H, s, O$CH_2$), 5.17–5.10 (2H, m, CH$_2$CH=$CH_2$), 3.37 (2H, d, J = 6.75 Hz, CH_2CH=CH$_2$); **^{13}C NMR** (100 MHz, $CDCl_3$) δ_C 160.3, 145.0, 140.2, 137.4, 134.7, 128.5, 127.9, 127.7, 125.2, 117.5, 112.0, 67.9 and 33.8; $\boldsymbol{m/z}$ (ESI$^+$) 413.30 (100 %), 326.04 (61 %), 304.06 ([M+H]$^+$, 24 %); **HRMS** (ESI$^+$) found 304.0328 ($C_{15}H_{15}BrNO$ [M+H]$^+$ requires 304.0332).

(5-allyl-6-(benzyloxy)pyridin-3-yl)boronic acid 182

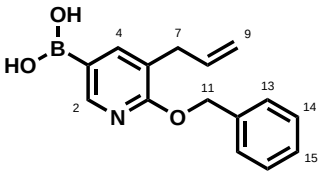

182

To a solution of 3-allyl-2-(benzyloxy)-5-bromopyridine **181** (150 mg, 0.49 mmol, 1.0 eq.) in dry Et_2O (3 mL) at −78 °C was added *n*-butyllithium (0.28 mL, 2.5 M, 0.69 mmol, 1.4 eq.). The solution was stirred for 10 min before the addition of an excess of triisopropyl borate (0.23 mL, 0.98 mmol,

2 eq.). The solution was then raised to room temperature and stirred for 1 hour. It was then quenched with water (10 mL) and stirred for a further hour. The Et_2O was removed under reduced pressure and the remaining aqueous phase taken to neutral pH with 1 M HCl. It was then extracted with Et_2O (3 × 10 mL), and purified by flash chromatography (100 % Et_2O) to afford (5-allyl-6-(benzyloxy)pyridin-3-yl)boronic acid **182** (50 mg, 0.19 mmol, 39 %) as a white solid; $\mathbf{R_f}$ 0.30 (100 % Et_2O); **mp** 145.5–149.7 °C; $\boldsymbol{\nu_{max}}$ (KBr disc) / cm^{-1} 3376, 1639, 1604, 1573, 1498, 1476, 1417, 1348, 1251, 1214, 1197, 1143, 1057, 1005, 904, 844, 742, 709, 679, 608; **^{1}H NMR** (400 MHz, $(CD_3)_2CO$) δ_H 8.50 (1H, d, J = 1.94 Hz, ArH), 7.92 (1H, d, J = 1.95 Hz, ArH), 7.51–7.27 (5H, m, $OCH_2C_6H_5$), 6.06–5.96 (1H, m, $CH_2CH{=}CH_2$), 5.45 (2H, s, OCH_2), 5.11–5.02 (2H, m, $CH_2CH{=}CH_2$), 3.38 (2H, d, J = 6.68 Hz, $CH_2CH{=}CH_2$); **^{13}C NMR** (100 MHz, $(CD_3)_2CO$) δ_C 163.6, 156.6, 152.1, 144.4, 138.9, 136.9, 129.1, 128.45, 128.37, 122.3, 116.4, 67.9 and 34.6; $\boldsymbol{m/z}$ (ESI^-) 519.23 (100 %), 268.12 ($[M\text{-}H]^-$, 59 %); **HRMS** (ESI^+) found 292.1109 ($C_{15}H_{16}BNNaO_3$ $[M{+}Na]^+$ requires 292.1118).

2,6-dibromopyridin-3-amine 173

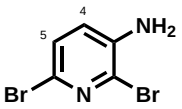

173

To a solution of pyridin-3-amine **170** (5.0 g, 53.0 mmol, 1.0 eq.) in MeCN (200 mL) at 0 °C was added NBS (18.85 g, 106 mmol, 2.0 eq.). The mixture was stirred at room temperature for 16 h, then concentrated under reduced pressure and purified by flash chromatography (100 % DCM mobile phase) followed by recrystallisation from pure DCM to afford 2,6-dibromopyridin-3-amine **173** (4.24 g, 16.83 mmol, 32 %); **^{1}H NMR** (400 MHz, $CDCl_3$) δ_H 7.21 (1H, d, J = 8.21 Hz, ArH), 6.90 (1H, d, J = 8.15 Hz, ArH), 4.13 (2H, s, NH_2). Data agrees with literature.[236]

2,6-dibromopyridin-3-amine 183

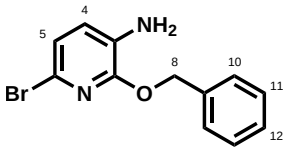

183

To a solution of 2,6-dibromopyridin-3-amine **173** (200 mg, 0.79 mmol, 1.0 eq.) and NaH (80 mg of 60 % dispersion in oil, 1.98 mmol, 2.5 eq.) in THF (5 mL) at 0 °C was added benzyl alcohol (81 μL, 0.79 mmol, 1.0 eq.). The mixture was stirred at reflux temperature for 16 h, then quenched with aqueous ammonium chloride and extracted (3 × 10 mL) with DCM. The organic phase was concentrated under reduced pressure and purified by flash chromatography (100 % DCM mobile phase) to afford 2,6-dibromopyridin-3-amine **183** (30 mg, 0.11 mmol, 14 %); ^{1}**H NMR** (400 MHz, $CDCl_3$) δ_H 7.47 (2H, m, H10), 7.42–7.31 (3H, m, H11 and H12), 6.89 (1H, d, J = 7.85 Hz, ArH), 6.78 (1H, d, J = 7.86 Hz, ArH), 5.39 (2H, s, H8), 3.78 (2H, s, NH_2).

N-(2-(benzyloxy)-6-bromopyridin-3-yl)benzamide 184

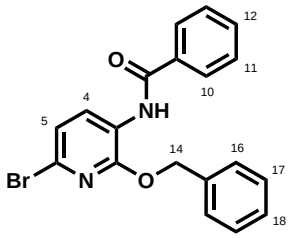

184

To a solution of benzyl alcohol **179** (0.12 mL, 1.17 mmol, 1.0 eq) and NaH (70 mg, 2.93 mmol, 2.5 eq.) in THF (10 mL) was added N-(2,6-dibromopyridin-3-yl)benzamide **186** (415 mg, 1.17 mmol, 1.0 eq.). The mixture was stirred for 16 h at reflux temperature, then quenched with aqueous ammonium chloride. The aqueous phase was isolated and extracted with DCM (2 × 10 mL). The combined organic phases were dried ($MgSO_4$) and concentrated *in vacuo*. Purification by flash column chromatography (3:1 P.E.:Et_2O) afforded N-(2-(benzyloxy)-6-bromopyridin-3-yl)benzamide **184** (261 mg, 0.71 mmol, 61 %) as white flakes; $\mathbf{R_f}$ 0.33 (3:1 P.E.:Et_2O); $\boldsymbol{\nu_{max}}$ (KBr disc) / cm^{-1} 3312, 1648, 1592, 1520, 1489, 1462, 1427, 1396, 1361, 1256, 1220, 1132, 1116, 1094, 1019, 912, 825, 728, 709, 692; ^{1}**H NMR** (400 MHz, $CDCl_3$) δ_H 8.68 (1H, d, J = 8.21 Hz, ArH), 8.34 (1H, s, NH), 7.83–7.80 (2H, m, ArH), 7.58–7.35 (8H, m, ArH), 7.15 (1H, dd, J = 8.21 and 0.45 Hz, ArH), 5.50 (2H, s, CH_2); ^{13}**C NMR** (100 MHz, $CDCl_3$) δ_C 165.7, 152.1, 136.2, 134.3, 132.4, 130.5, 129.14, 129.06, 128.8, 128.6, 128.5, 127.1, 122.2, 121.2 and 69.3; $\boldsymbol{m/z}$ (ESI$^+$) 405.06 ([M+Na]$^+$, 100 %), 407.05 (94 %), 383.08 ([M+H]$^+$, 30 %); **HRMS** (ESI$^+$) found 407.0186 ($C_{19}H_{15}BrN_2NaO_2$ [M+Na]$^+$ requires 407.0189).

N-(2,6-dibromopyridin-3-yl)benzamide 186

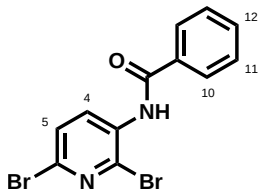

186

A solution of 2,6-dibromopyridin-3-amine **173** (500 mg, 1.98 mmol, 1.0 eq), benzoyl chloride **185** (0.35 mL, 2.97 mmol, 1.5 eq.) and triethylamine (0.41 mL, 2.97 mmol, 1.5 eq.) in DCM (10 mL) was stirred at room temperature under an inert atmosphere for 1.5 h. The reaction mixture was quenched with water, the phases separated, and the aqueous phase extracted with DCM (2 × 10 mL). The combined organic phases were dried ($MgSO_4$) and concentrated *in vacuo*. Purification by flash column chromatography (3:1 P.E.:Et_2O) and recrystallization from 3:1 P.E.:Et_2O afforded N-(2,6-dibromopyridin-3-yl)benzamide **186** (510 mg, 1.43 mmol, 72 %) as white flakes; **mp** 112.0–113.4 °C; $\mathbf{R_f}$ 0.26 (3:1 P.E.:Et_2O); $\boldsymbol{\nu_{max}}$ (KBr disc) / cm^{-1} 3406, 3097, 1686, 1599, 1577, 1559, 1513, 1485, 1413, 1343, 1293, 1259, 1229, 1125, 1092, 1050, 836, 721, 698, 533; ^{1}**H NMR** (400 MHz, $CDCl_3$) δ_H 8.74 (1H, d, J = 8.52 Hz, ArH), 8.42 (1H, s, NH), 7.92–7.89 (2H, m, H10), 7.63–7.59 (1H, m, H12), 7.55–7.51 (2H, m, H11), 7.47 (1H, d, J = 8.50 Hz, ArH); ^{13}**C NMR** (100 MHz, $CDCl_3$) δ_C 165.5, 133.6, 133.5, 133.3, 132.9, 131.5, 130.7, 129.2, 128.0 and 127.2; $\boldsymbol{m/z}$ (ESI^+) 354.88 ($[M+H]^+$, 100 %), 352.89 (72 %), 356.90 (63 %); **HRMS** (ESI^-) found 354.8914 ($C_{12}H_9Br_2N_2O$ $[M+H]^-$ requires 354.8911).

N-(5′-allyl-6,6′-bis(benzyloxy)-[2,3′-bipyridin]-5-yl)benzamide 187

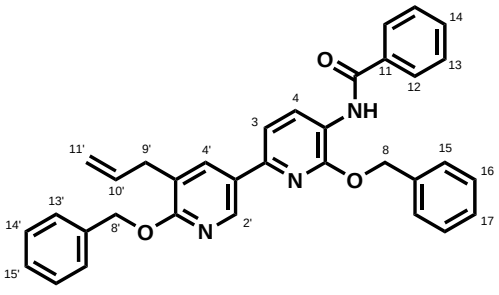

187

A solution of (5-allyl-6-(benzyloxy)pyridin-3-yl)boronic acid **182** (50 mg, 0.19 mmol, 1.7 eq.), N-(2-(benzyloxy)-6-bromopyridin-3-yl)benzamide **184** (40 mg, 0.11 mmol, 1.0 eq.), tetrakis(triphenylphosphine)palladium (6 mg, 0.005 mmol, 0.025 eq.), ethanol (0.05 mL), sodium carbonate (0.1 mL, 2 M solution, 1.7 eq.), and toluene (2 mL) was degassed for 10 m, then stirred in a sealed vial at

80 °C for 16 h. After cooling to room temperature the mixture was concentrated under reduced pressure, and purified by flash chromatography (1:1 P.E.:Et_2O mobile phase) to afford N-(5′-allyl-6,6′-bis(benzyloxy)-[2,3′-bipyridin]-5-yl)benzamide **187** (36 mg, 0.068 mmol, 63 %) as a white powder; $\mathbf{R_f}$ 0.19 (2:1 P.E.:Et_2O); **mp** 140.8–142.8 °C; $\boldsymbol{\nu_{max}}$ (thin film) / cm^{-1} 3438, 3032, 2361, 2341, 1679, 1603, 1523, 1494, 1474, 1448, 1422, 1360, 1302, 1246, 1154, 1128, 1101, 1078, 1001, 915, 827, 793, 734, 696 and 634; ^{1}**H NMR** (500 MHz, $CDCl_3$) δ_H 8.84 (1H, d, J = 8.13 Hz, H3), 8.71 (1H, d, J = 2.39 Hz, H2′), 8.51 (1H, s, NH), 8.02 (1H, d, J = 2.40 Hz, H4′), 7.88–7.86 (2H, m, H12 or H13), 7.58–7.55 (1H, m, H14), 7.53–7.48 (6H, m, ArH includes H12 or H13); 7.43–7.31 (7H, m, ArH includes H4); 6.05 (1H, ddt, J = 16.95, 10.18 and 6.72 Hz, H10′), 5.63 (2H, s, CH_2), 5.49 (2H, s, CH_2), 5.19–5.14 (2H, m, H11′), 3.47 (2H, d, J = 6.66 Hz, H9′); ^{13}**C NMR** (125 MHz, $CDCl_3$) δ_C 165.6, 161.6, 152.3, 146.2, 142.9 (C2′), 137.8, 137.2, 136.0, 135.7, 134.7, 132.2 (C14), 129.0, 128.8, 128.5, 128.3, 128.1, 127.8, 127.7, 127.6, 127.1, 122.8, 121.7, 116.8 (C11′), 113.1 (C4), 68.2, 67.8 and 34.2 (C9′); $\boldsymbol{m/z}$ (ESI$^+$) 550.21 (100 %, $[M+Na]^+$), 528.23 (27 %, $[M+H]^+$); **HRMS** (ESI$^+$) found 550.2104 ($[M+Na]^+$, $C_{34}H_{29}N_3O_3Na$ requires 550.2101).

N-(6,6′-bis(benzyloxy)-5′-(3-hydroxypropyl)-[2,3′-bipyridin]-5-yl)benzamide 188

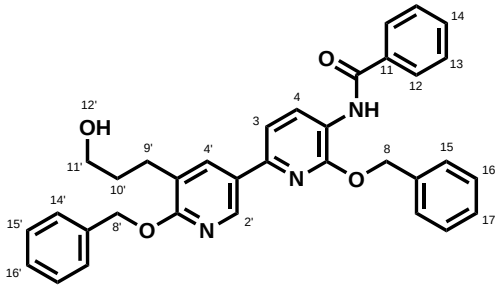

188

To a solution of N-(5′-allyl-6,6′-bis(benzyloxy)-[2,3′-bipyridin]-5-yl)benzamide **187** (36 mg, 0.068 mmol, 1.0 eq.), sodium hydroxide (0.034 mL, 3 M solution, 1.5 eq.), hydrogen peroxide (0.031 mL, 35 % solution, 4.5 eq.), and dry THF (1 mL) was added dropwise borane-dimethyl sulfide complex (8 μL, 10 M solution, 1.2 eq.). The mixture was stirred at r.t. for 2 h, filtered through celite, and concentrated under reduced pressure to afford alcohol N-(6,6′-bis(benzyloxy)-5′-(3-hydroxypropyl)-[2,3′-bipyridin]-5-yl)benzamide **188** (35 mg, 0.064 mmol, 94 %) as a beige solid; $\mathbf{R_f}$ 0.37 (100 % Et_2O); **mp** 143.5–147.2 °C; $\boldsymbol{\nu_{max}}$ (thin film) / cm^{-1} 3734, 3432, 2933, 2361, 2341, 1675, 1602, 1522, 1474, 1426, 1359, 1304, 1246, 1102, 1001, 827, 735 and 696; ^{1}**H NMR** (500 MHz, $CDCl_3$) δ_H 8.84 (1H, d, J = 8.14 Hz, H3), 8.69 (1H, d, J = 2.39 Hz, H2′), 8.51 (1H, s, NH), 8.01 (1H, d, J = 2.39 Hz, H4′), 7.88–7.86 (2H, m, H12 or H13), 7.58–7.55 (1H, m, H14), 7.53–7.48 (6H, m, ArH includes H12

or H13); 7.43–7.31 (7H, m, ArH includes H4); 5.63 (2H, s, CH_2), 5.48 (2H, s, CH_2), 3.67 (2H, t, J = 6.27 Hz, H11′), 2.80 (2H, t, J = 7.45 Hz, H9′), 1.96–1.91 (2H, m, H10′), 1.64 (1H, s, OH); **^{13}C NMR** (125 MHz, $CDCl_3$) δ_C 165.6, 161.8, 152.3, 146.2, 142.8 (C2′), 137.7, 137.6, 137.2, 136.3 (C4′), 134.6, 132.2, 129.0, 128.8, 128.6, 128.4, 128.3, 128.1, 128.0, 127.9, 127.81, 127.78, 127.66, 127.1, 124.1, 121.7, 113.1, 68.3, 68.0, 67.95, 67.5, 66.0, 62.0 (H11′), 32.4 (H10′) and 26.2 (H9′); ***m/z*** (ESI$^+$) 546.23 (100 %, $[M+H]^+$, 568.22 (77 %, $[M+Na]^+$), **HRMS** (ESI$^-$) found 568.2215 ($[M+Na]^+$, $C_{34}H_{31}N_3O_4Na$ requires 568.2207).

N-(6,6′-bis(benzyloxy)-5′-(3-((tert-butyldiphenylsilyl)oxy)propyl)-[2,3′-bipyridin]-5-yl)benzamide 189

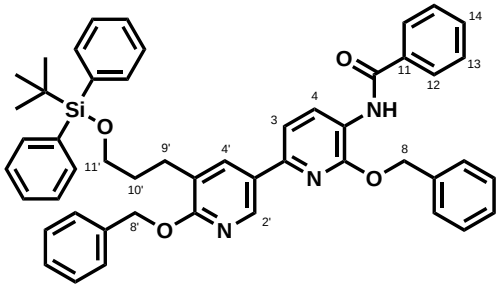

189

A solution of N-(6,6′-bis(benzyloxy)-5′-(3-hydroxypropyl)-[2,3′-bipyridin]-5-yl)benzamide **188** (35 mg, 0.064 mmol, 1.0 eq.), tert-butyldiphenylsilylchloride (27 μL, 0.10 mmol, 1.5 eq.), imidazole (13 mg, 0.19 mmol, 3.0 eq.), dimethylaminopyridine (4 mg, 0.032 mmol, 0.5 eq.), and DCM (0.5 mL) was stirred in a sealed vial at r.t. for 16 h. Aqueous sodium bicarbonate was added, and the mixture extracted with DCM (3 x 5 mL). The combined organic phases were concentrated under reduced pressure and purified with flash chromatography (100 % DCM mobile phase) to afford N-(6,6′-bis(benzyloxy)-5′-(3-((tert-butyldiphenylsilyl)oxy)propyl)-[2,3′-bipyridin]-5-yl)benzamide **189** (32 mg, 0.041 mmol, 64 %) as a yellow oily solid; $\mathbf{R_f}$ 0.22 (2:1 P.E.:Et_2O); $\boldsymbol{\nu_{max}}$ (thin film) / cm^{-1} 2930, 2857, 2360, 2342, 1677, 1602, 1520, 1472, 1427, 1359, 1303, 1244, 1200, 1104, 1000, 897, 824, 734, 699 and 613; **^{1}H NMR** (500 MHz, $CDCl_3$) δ_H 8.85 (1H, d, J = 8.16 Hz, H3), 8.71 (1H, d, J = 2.38 Hz, H2′), 8.52 (1H, s, NH), 8.01 (1H, d, J = 2.37 Hz, H4′), 7.88 (2H, m, H12 or H13), 7.68–7.66 (4H, m, ArH), 7.58–7.55 (1H, m, H14), 7.53–7.48 (7H, m, ArH includes H12 or H13); 7.43–7.29 (12H, m, ArH includes H4); 5.62 (2H, s, CH_2), 5.48 (2H, s, CH_2), 3.75 (2H, t, J = 6.15 Hz, H11′), 2.84 (2H, t, J = 7.62 Hz, H9′), 1.99–1.93 (2H, m, H10′), 1.07 (9H, s, $(CH_3)_3$); **^{13}C NMR** (125 MHz, $CDCl_3$) δ_C 165.6, 161.9, 152.3, 146.4, 142.6 (C2′), 137.8, 137.2, 136.1 (C4′), 135.7,

134.7, 134.1, 132.2, 129.7, 129.0, 128.8, 128.5, 128.3, 128.15, 128.07, 127.75, 127.70, 127.64, 127.59, 127.1, 124.5, 121.6, 113.1, 68.2, 67.7, 66.0, 63.4 (C11′), 31.9 (C10′), 30.5, 27.1, 27.0, 26.7, 19.4 and 15.4; ***m/z*** (ESI$^+$) 784.37 (100 %, [M+H]$^+$, 806.35 (99 %, [M+Na]$^+$); **HRMS** (ESI$^+$) found 806.3371 ([M+Na]$^+$, $C_{50}H_{49}N_3O_4SiNa$ requires 806.3385).

N-(5′-(3-((tert-butyldiphenylsilyl)oxy)propyl)-6,6′-dioxo-1,1′,6,6′-tetrahydro-[2,3′-bipyridin]-5-yl)benzamide 190

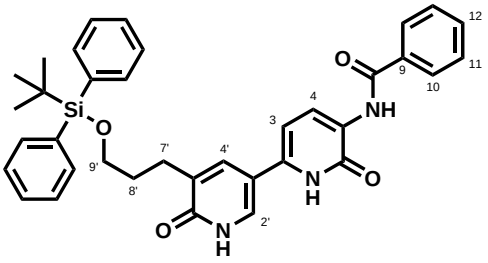

190

A solution of N-(6,6′-bis(benzyloxy)-5′-(3-((tert-butyldiphenylsilyl)oxy)propyl)-[2,3′-bipyridin]-5-yl)-benzamide **189** (32 mg, 0.041 mmol, 1.0 eq.) and palladium on carbon (about 10 mg) in EtOAc (4 mL) and MeOH (2 mL) was stirred under a hydrogen atmosphere for 2 h. The mixture was filtered through celite and concentrated under reduced pressure to afford N-(5′-(3-((tert-butyldiphenylsilyl)-oxy)propyl)-6,6′-dioxo-1,1′,6,6′-tetrahydro-[2,3′-bipyridin]-5-yl)benzamide **190** (19 mg, 0.031 mmol, 77 %); $\mathbf{R_f}$ 0.15 (30:1 Et_2O:MeOH); **mp** > 250 °C; $\boldsymbol{\nu_{max}}$ (thin film) / cm^{-1} 3258, 2928, 2856, 2360, 2342, 1642, 1523, 1471, 1428, 1254, 1110, 1026, 823 and 704; ^{1}**H NMR** (500 MHz, $(CD_3)_2CO$) δ_H 8.28 (1H, d, J = 7.71 Hz, ArH), 7.93 (2H, m, ArH), 7.76 (1H, m, ArH), 7.65–7.33 (15H, m, ArH), 3.67 (2H, t, J = 6.29 Hz, CH_2), 2.53 (2H, m, CH_2), 1.85 (2H, m, CH_2), 0.99 (9H, s, $(CH_3)_3$); ^{13}**C NMR** (125 MHz, $(CD_3)_2CO$) δ_C 164.8, 161.8, 135.4, 135.3, 135.2, 135.1, 134.5, 134.0, 133.3, 132.1, 129.9, 128.9, 127.9, 127.7, 127.2, 65.0, 63.2, 55.0, 30.5, 26.8, 26.7, 26.5, 18.9 and 15.2; ***m/z*** (ESI$^-$) 602.22 (100 %, [M-H]$^-$); **HRMS** (ESI$^-$) found 602.2456 ([M-H]$^-$, $C_{36}H_{36}N_3O_4Si$ requires 602.2481).

6-chloro-N-(pyridin-2-yl)nicotinamide 200

A mixture of 6-chloronicotinoyl choride **197** (309 mg, 1.77 mmol, 1.0 eq.), 2-aminopyridine **83** (165 mg, 1.77 mmol, 1.0 eq.), triethylamine (0.48 mL, 3.54 mmol, 2.0 eq.), and DCM (8 mL) was stirred for 3 h at r.t. and then quenched with aqueous sodium bicarbonate (30 mL). The solution

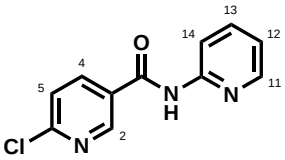

200

was extracted with DCM (3 × 30 mL) and the combined organic phases concentrated under reduced pressure and purified by flash chromatography (100 % Et_2O mobile phase) to afford 6-chloro-N-(pyridin-2-yl)nicotinamide **200** (233 mg, 1.00 mmol, 57 %); $\mathbf{R_f}$ 0.15 (1:1 Et_2O:P.E.); **mp** 160.0–162.9 °C; $\boldsymbol{\nu_{max}}$ (thin film) / cm^{-1} 3372, 3049, 1666, 1580, 1544, 1474, 1436, 1366, 1301, 1145, 1105, 1023, 993, 839, 773, 756 and 629; ^{1}**H NMR** (400 MHz, $CDCl_3$) δ_H 8.93 (1H, d, J = 2.48 Hz, ArH), 8.43 (1H, s, NH), 8.34 (2H, m, 2 × ArH), 8.20 (1H, dd, J = 8.31 and 2.56 Hz, ArH), 7.80 (1H, m, ArH), 7.50 (1H, d, J = 8.31 Hz, ArH), 7.14 (1H, dd, J = 7.34 and 4.98 Hz, ArH); ^{13}**C NMR** (100 MHz, $CDCl_3$) δ_C 163.3, 155.1, 151.2, 148.9, 147.6, 139.1, 138.1, 129.1, 124.6, 120.7 and 115.0; $\boldsymbol{m/z}$ (ESI^+) 234.03 ($[M+H]^+$, 100 %); **HRMS** (ESI^+) found 234.0421 ($C_11H_9ClN_3O$ requires 234.0429).

6-oxo-1,6-dihydropyridine-3-carbonyl chloride 193

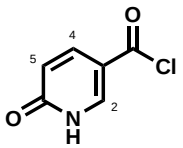

193

A mixture of 6-oxo-1,6-dihydropyridine-3-carboxylic acid **195** (50 mg, 0.36 mmol, 1.0 eq.) and thionyl chloride **196** (3 mL) was stirred at 90 °C for 3 h. After cooling to room temperature the solution was concentrated under reduced pressure, dissolved in DCM, and filtered through a sinter filter. The filtrate was concentrated under reduced pressure to afford 6-oxo-1,6-dihydropyridine-3-carbonyl chloride **193** (53 mg, 0.34 mmol, 93 %); ^{1}**H NMR** (400 MHz, $CDCl_3$) δ_H 8.43 (1H, d, J = 2.57 Hz, ArH), 8.00 (1H, dd, J = 9.73 and 2.63 Hz, ArH), 6.63 (1H, d, J = 9.76 Hz, ArH).

methyl 6-methoxynicotinate 202

A mixture of 6-chloronicotinic acid **199** (200 mg, 1.27 mmol, 1.0 eq.), H_2SO_4 (0.5 mL), and MeOH (4 mL) was stirred at 65 °C for 16 h. After cooling to room temperature the solution was quenched with aqueous sodium bicarbonate and extracted into DCM (3 × 20 mL). The combined organic

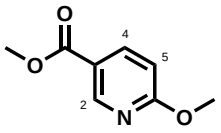

202

phases were concentrated under reduced pressure to afford methyl 6-methoxynicotinate **202** (178 mg, 1.07 mmol, 84 %); ^{1}**H NMR** (400 MHz, $CDCl_3$) δ_H 8.83 (1H, d, J = 2.38 Hz, ArH), 8.15 (1H, dd, J = 2.39 and 8.69 Hz, ArH), 6.76 (1H, dd, J = 0.68 and 8.71 Hz, ArH), 4.00 (3H, s, OMe), 3.91 (3H, s, OMe). Data agrees with literature.[237]

6-methoxynicotinic acid 201

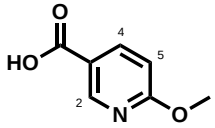

201

A mixture of 6-methoxynicotinate **202** (178 mg, 1.07 mmol, 1.0 eq.), MeOH (2.5 mL), 1 M NaOH (2.5 mL) and THF (2.5 mL) was stirred at 50 °C for 30 m. After cooling to room temperature the solution was concentrated under reduced pressure. H_2O and 1 M HCl were added, and the mixture was extracted into EtOAc (3 × 20 mL). The combined organic phases were concentrated under reduced pressure to afford 6-methoxynicotinic acid **201** (155 mg, 1.01 mmol, 95 %); ^{1}**H NMR** (400 MHz, $CDCl_3$) δ_H 8.91 (1H, d, J = 2.39 Hz, ArH), 8.19 (1H, dd, J = 2.39 and 8.72 Hz, ArH), 6.80 (1H, d, J = 8.69 Hz, ArH), 4.02 (3H, s, OMe). Data agrees with literature.[238]

6-methoxy-N-(pyridin-2-yl)nicotinamide 198

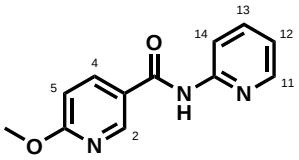

198

A mixture of 6-methoxynicotinic acid **201** (1.0 g, 6.6 mmol, 1.0 eq.), 2-aminopyridine **83** (620 mg, 6.6 mmol, 1.0 eq.), DCC (1.36 g, 6.6 mmol, 1.0 eq.) and DMAP (160 mg, 1.32 mmol, 0.2 eq.) in DCM (20 mL) was stirred for 7 hours and then quenched with aqueous sodium bicarbonate (50 mL). The solution was extracted with Et_2O (3 × 50 mL) and the combined organic phases added to 1 M HCl

(150 mL). The aqueous phase was washed with DCM (3 × 50 mL) and then the pH increased to neutral with aqueous sodium bicarbonate. The aqueous phase was extracted with Et_2O (3 × 50 mL) and the combined organic phases concentrated under reduced pressure and purified by flash chromatography (100 % Et_2O mobile phase) to afford 6-methoxy-N-(pyridin-2-yl)nicotinamide **198** (559 mg, 2.44 mmol, 37 %) as a white solid; $\mathbf{R_f}$ 0.48 (100 % Et_2O); **mp** 143.8–145.7 °C; $\boldsymbol{\nu_{max}}$ (KBr disc) / cm^{-1} 3232, 1670, 1581, 1544, 1497, 1439, 1375, 1295, 1157, 1131, 1112, 1023, 993, 891, 834, 786, 737, 720, 659, 609; ^{1}**H NMR** (400 MHz, $CDCl_3$) δ_H 9.07 (1H, s, NH), 8.76 (1H, d, J = 2.44 Hz, ArH), 8.35 (1H, d, J = 8.40 Hz, ArH), 8.17 (1H, dd, J = 4.91 and 0.90 Hz, ArH), 8.10 (1H, dd, J = 8.70 and 2.55 Hz, ArH), 7.75–7.71 (1H, m, H13), 7.05–7.02 (1H, m, H12), 6.79 (1H, d, J = 8.70 Hz, ArH), 3.98 (3H, s, OMe); ^{13}**C NMR** (100 MHz, $CDCl_3$) δ_C 166.5, 164.3, 151.7, 147.9, 147.3, 138.7, 137.9, 123.6, 120.1, 114.6, 111.2 and 54.2; $\boldsymbol{m/z}$ (ESI^+) 624.38 (100 %), 252.08 ($[M+Na]^+$, 84 %), 230.11 ($[M+H]^+$, 40 %); **HRMS** (ESI^+) found 230.0922 ($C_12H_12N_3O_2$ requires 230.0924).

6-oxo-N-(pyridin-2-yl)-1,6-dihydropyridine-3-carboxamide 194

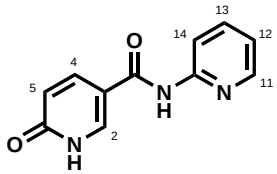

194

A solution of 6-methoxy-N-(pyridin-2-yl)nicotinamide **198** (40 mg, 0.175 mmol, 1.0 eq) and BBr_3 (1 M in DCM) was stirred at 40 °C for 16 h. After cooling to r.t., the solution was placed in an ice-bath and quenched slowly with water. The solution was then concentrated under reduced pressure. To the solid residue was added water and the suspension filtered through a sinter. The solid filtrand was collected and dried over phosphorus pentoxide under vacuum to afford 6-oxo-N-(pyridin-2-yl)-1,6-dihydropyridine-3-carboxamide **194** (18 mg, 0.077 mmol, 48 %) as a dark solid; $\mathbf{R_f}$ 0.42 (10:1 EtOAc:MeOH); **mp** > 300 °C; $\boldsymbol{\nu_{max}}$ (thin film) / cm^{-1} 3413, 1978, 1657, 1607, 1582, 1539, 1430, 1308, 1264, 1128, 1004, 836 and 777; ^{1}**H NMR** (500 MHz, DMSO) δ_H 10.52 (1H, s, NH), 8.35 (1H, ddd, J = 4.84, 1.89 and 0.82 Hz, H11), 8.32–8.31 (1H, m, H2), 8.10 (1H, d, J = 8.39 Hz, H14), 7.95 (1H, dd, J = 9.54 and 2.75 Hz, H5), 7.79 (1H, ddd, J = 8.38, 7.34 and 1.92 Hz, H13), 7.12 (1H, ddd, J = 7.28, 4.88 and 0.91 Hz, H12), 6.30 (1H, d, J = 9.54 Hz, H4); ^{13}**C NMR** (125 MHz, DMSO) δ_C 163.6, 152.4, 147.9 (C11), 140.7 (H2), 139.0 (H5), 138.1 (H13), 119.5 (C12), 118.2 (C4), 114.6 (C14), 111.7 and 79.2; $\boldsymbol{m/z}$ (ESI^-) 148.96 (100 %), 214.07 (57 %); **HRMS** (ESI^-) found 214.0617 ($[M-H]^-$, $C_{11}H_8N_3O_2$ requires 214.0622).

N-(4,6-dimethylpyridin-2-yl)-6-methoxynicotinamide 204

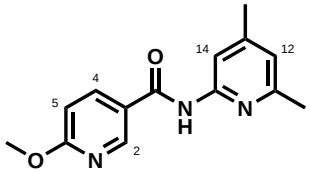

204

A mixture of 6-methoxynicotinic acid **201** (533 mg, 3.48 mmol, 1.0 eq.), 4,6-dimethylpyridin-2-amine **203** (430 mg, 3.48 mmol, 1.0 eq.), DCC (728 mg, 3.48 mmol, 1.0 eq.) and DMAP (86 mg, 0.71 mmol, 0.2 eq.) in DCM (12 mL) was stirred for 3 hours and then quenched with aqueous sodium bicarbonate (30 mL). The solution was extracted with DCM (3 × 30 mL) and the combined organic phases added to 1 M HCl (100 mL). The aqueous phase was washed with DCM (3 × 50 mL) and then the pH increased to neutral with aqueous sodium bicarbonate. The aqueous phase was extracted with DCM (3 × 30 mL) and the combined organic phases concentrated under reduced pressure and purified by flash chromatography (100 % EtOAc mobile phase) to afford N-(4,6-dimethylpyridin-2-yl)-6-methoxynicotinamide **204** (90 mg, 0.35 mmol, 10 %) as an off-white solid; $\mathbf{R_f}$ 0.55 (100 % Et_2O); **mp** 85.1–86.2 °C; $\boldsymbol{\nu_{max}}$ (KBr disc) / cm^{-1} 2950, 1674, 1604, 1573, 1494, 1425, 1372, 1279, 1222, 1160, 1117, 1017, 969, 887, 843, 776, 717, 631, 614, 526; ^{1}**H NMR** (400 MHz, $CDCl_3$) δ_H 8.75 (1H, d, J = 2.29 Hz, ArH), 8.46 (1H, s, NH), 8.09 (1H, dd, J = 8.68 and 2.46 Hz, ArH), 8.00 (1H, s, ArH), 6.81 (1H, d, J = 8.70 Hz, ArH), 6.77 (1H, s, ArH), 4.00 (3H, s, OMe), 2.41 (3H, s, CH_3), 2.35 (3H, s, CH_3); ^{13}**C NMR** (100 MHz, $CDCl_3$) δ_C 166.5, 163.9, 156.6, 150.8, 150.4, 147.2, 137.7, 123.6, 120.9, 111.9, 111.1, 54.2, 23.9 and 21.5; $\boldsymbol{m/z}$ (ESI^+) 537.22 ($[2M+Na]^+$, 100%), 280.11 ($[M+Na]^+$, 93 %), 258.13 ($[M+H]^+$, 71 %); **HRMS** (ESI^+) found 258.1235 ($C_{14}H_{16}N_3O_2$ requires 258.1237).

N-(4,6-dimethylpyridin-2-yl)-6-oxo-1,6-dihydropyridine-3-carboxamide 205

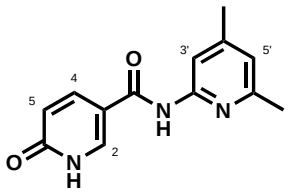

205

A solution of N-(4,6-dimethylpyridin-2-yl)-6-methoxynicotinamide **204** (72 mg, 0.28 mmol, 1.0 eq.) and BBr_3 (1 M in DCM) was stirred at 40 °C for 16 hours. After cooling to r.t., the solution was placed in an ice-bath and quenched slowly with water. The solution was then concentrated under reduced pressure. To the solid residue was added water and the solids removed by filtering through a sinter. The aqueous filtrate was washed with DCM (2 x 10 mL), concentrated under reduced pressure and dried over phosphorus pentoxide under vacuum to afford N-(4,6-dimethylpyridin-2-yl)-6-oxo-1,6-dihydropyridine-3-carboxamide **205** (60 mg, 0.25 mmol, 88 %) as light orange flakes; $\mathbf{R_f}$ 0.33 (10:1 EtOAc:MeOH); **mp** > 300 °C; $\boldsymbol{\nu_{max}}$ (thin film) / cm^{-1} 3188, 2361, 2342, 1648, 1418, 1194, 914 and 640; ^{1}**H NMR** (500 MHz, MeOD) δ_H 8.47 (1H, d, J = 2.63 Hz, H2), 8.16 (1H, dd, J = 9.69 and 2.76 Hz, H4), 7.51 (1H, s, ArH), 7.38 (1H, s, ArH), 6.61 (1H, d, J = 9.65 Hz, H5), 2.72 (1H, s, CH_3), 2.59 (1H, s, CH_3); ^{13}**C NMR** (125 MHz, MeOD) δ_C 167.3, 165.3, 162.4, 150.1, 149.0, 141.4 (C2), 140.6 (C4), 123.5, 120.8 (C5), 114.9, 113.0, 22.4 and 19.8; $\boldsymbol{m/z}$ (ESI^-) 148.96 (100 %), 242.11 (17 %, $[M-H]^-$); **HRMS** (ESI^-) found 242.0937 ($[M-H]^-$, $C_{13}H_{12}N_3O_2$ requires 242.0935).

N-(3-aminophenyl)cinnamamide 214

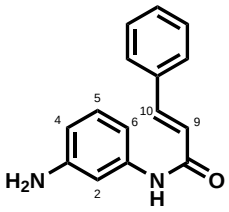

214

To a solution of benzene-1,3-diamine **215** (194 mg, 1.80 mmol, 3.0 eq.) in DCM (1 mL) was added a solution of cinnamoyl chloride **89** (100 mg, 0.60 mmol, 1.0 eq.) in DCM (3 mL). The mixture was stirred at room temperature for 30 m, then 1 M sodium hydroxide was added, and the solution extracted with EtOAc (3 × 15 mL). The combined organic phases were concentrated under reduced pressure and purified by flash chromatography (100 % EtOAc mobile phase) to afford N-(3-aminophenyl)cinnamamide **214** (104 mg, 0.44 mmol, 73 %); ^{1}**H NMR** (400 MHz, $CDCl_3$) δ_H 8.62 (1H, s, NH), 7.71 (1H, d, J = 15.60 Hz, C10), 7.36 (2H, m, ArH), 7.30–7.20 (4H, m, ArH), 7.08–6.96 (2H, m, ArH), 6.69 (1H, d, J = 15.60 Hz, C9), 6.39 (1H, d, J = 7.62 Hz, ArH), 3.64 (2H, s, NH_2). Data agrees with literature.[239]

benzyl (3-aminophenyl)carbamate 217

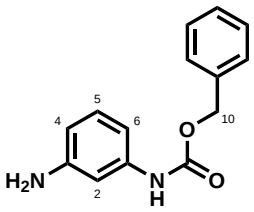

217

To a solution of benzene-1,3-diamine **215** (1.0 g, 9.26 mmol, 1.0 eq.) and DIPEA (1.61 mL, 9.26 mmol, 1.0 eq.) in DCM (15 mL) at 0 °C was added dropwise benzyl chloroformate **216** (1.32 mL, 9.26 mmol, 1.0 eq.). The solution was stirred at room temperature for 2 h, then aqueous sodium bicarbonate was added, and the solution extracted with DCM (3 × 20 mL). The combined organic phases were concentrated under reduced pressure and purified by flash chromatography (100 % Et_2O mobile phase) to afford benzyl (3-aminophenyl)carbamate **217** (1.247 g, 5.15 mmol, 56 %); $\mathbf{R_f}$ 0.12 (1:1 P.E.:Et_2O); $\boldsymbol{\nu_{max}}$ (thin film) / cm^{-1} 3327, 2927, 1718, 1611, 1547, 1498, 1455, 1321, 1227, 1055, 766, 746 and 695; ^{1}**H NMR** (400 MHz, $CDCl_3$) δ_H 7.42–7.32 (5H, m, C_6H_5), 7.05 (1H, t, J = 7.97 Hz, H5), 6.93 (1H, s, NH), 6.89 (1H, s, H2), 6.64 (1H, dd, J = 8.03 and 1.59 Hz, H4 or H6), 6.38 (1H, ddd, J = 7.95, 2.11 and 0.77 Hz, H4 or H6), 5.18 (2H, s, H10), 3.69 (2H, s, NH_2); ^{13}**C NMR** (100 MHz, $CDCl_3$) δ_C 153.4, 147.3, 138.9, 136.2, 129.8, 128.6, 128.4, 128.3, 110.4, 108.8, 105.3 and 66.9; $\boldsymbol{m/z}$ (ESI^+) 243.10 ($[M+H]^+$, 100 %); **HRMS** (ESI^+) found 243.1127 ($C_{14}H_{15}N_2O_2$, $[M+H]^+$ requires 243.1128).

(E)-benzyl (3-cinnamamidophenyl)carbamate 218

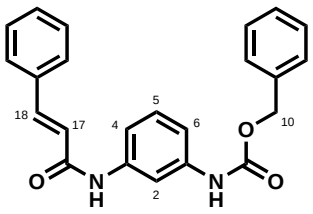

218

A solution of benzyl (3-aminophenyl)carbamate **217** (1.0 g, 4.13 mmol, 1.0 eq.), cinnamoyl chloride **89** (690 mg, 4.13 mmol, 1.0 eq.) and DCM (20 mL) was stirred at room temperature for 16 h. Aqueous sodium bicarbonate was added, and the solution extracted with DCM (3 × 30 mL). The combined organic phases were concentrated under reduced pressure and purified by flash chromatography (100 % Et_2O mobile phase) to afford (E)-benzyl (3-cinnamamidophenyl)carbamate **218** (1.458 g, 3.92 mmol, 95 %); $\mathbf{R_f}$ 0.29 (2:1 Et_2O:P.E.); $\boldsymbol{\nu_{max}}$ (thin film) / cm^{-1} 3304, 2361, 1706,

1665, 1607, 1541, 1491, 1450, 1424, 1340, 1218, 1171, 1066, 975, 862, 763, 738, 696 and 618; **^{1}H NMR** (400 MHz, $CDCl_3$) δ_H 7.79 (1H, s, NH), 7.73 (1H, d, J = 15.52 Hz, H18), 7.59 (1H, s, NH), 7.53–7.47 (2H, m, ArH), 7.42–7.30 (8H, m, ArH), 7.28–7.22 (2H, m, ArH), 7.18–7.13 (1H, m, ArH), 6.84 (1H, s, ArH), 6.52 (1H, d, J = 15.51 Hz, H17), 5.19 (2H, s, H10).

N-(3-aminophenyl)acetamide 221

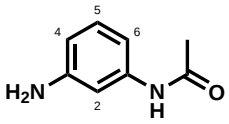

221

To a solution of benzene-1,3-diamine **215** (1.0 g, 9.26 mmol, 1.0 eq.) in DCM (15 mL) at was added dropwise acetic anhydride **220** (0.88 mL, 9.26 mmol, 1.0 eq.). The solution was stirred at room temperature for 1 h, then aqueous sodium bicarbonate was added, and the solution extracted with DCM (3 × 20 mL). The combined organic phases were concentrated under reduced pressure and purified by flash chromatography (100 % EtOAc mobile phase) to afford N-(3-aminophenyl)acetamide **221** (357 mg, 2.38 mmol, 26 %); **^{1}H NMR** (400 MHz, $CDCl_3$) δ_H 7.40 (1H, s, NH), 7.13 (1H, s, H2), 7.06 (1H, t, J = 7.96 Hz, H5), 6.66 (1H, d, J = 7.95 Hz, H4 or H6), 6.41 (1H, d, J = 8.01 Hz, H4 or H6), 3.70 (2H, s, NH_2), 2.15 (3H, s, CH_3). Data agrees with literature.[240]

N-(3-acetamidophenyl)cinnamamide 222

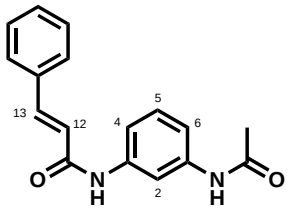

222

A solution of N-(3-aminophenyl)acetamide **221** (168 mg, 1.12 mmol, 1.0 eq.) and cinnamoyl chloride **89** (281 mg, 1.68 mmol, 1.5 eq.) and DCM (5 mL) was stirred at room temperature for 16 h. Aqueous sodium bicarbonate was added, and the solution extracted with DCM (3 × 10 mL). The combined organic phases were concentrated under reduced pressure and purified by flash chromatography (100 % EtOAc mobile phase) to afford N-(3-acetamidophenyl)cinnamamide **222** (74 mg, 0.26 mmol, 24 %); **^{1}H NMR** (400 MHz, $CDCl_3$) δ_H 7.92 (1H, s, NH), 7.75 (1H, d, J = 15.51 Hz, H13), 7.55

(2H, m, ArH), 7.45–7.37 (5H, m, ArH), 7.29 (2H, m, ArH), 6.53 (1H, d, J = 15.54 Hz, H12), 2.19 (3H, s, CH_3).

(E)-3-ethoxyacryloyl chloride 224

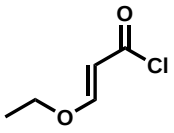

224

To a solution of oxalyl chloride **226** (2.0 mL, 23.62 mmol, 1.5 eq.) at 0 °C was added dropwise ethoxyethene **225** (1.5 mL, 15.75 mmol, 1.0 eq.). The mixture was stirred at 0 °C for 2 h then at r.t. for 16 h. Excess oxalyl chloride was removed by vacuum distillation and the residue stirred at 120 °C for 30 m. The product was purified and isolated by vacuum distillation to afford (E)-3-ethoxyacryloyl chloride **224** (1170 mg, 8.66 mmol, 55 %); **^{1}H NMR** (400 MHz, $CDCl_3$) δ_H 7.79 (1H, d, J = 12.10 Hz, CH), 5.51 (1H, d, J = 12.11 Hz, CH), 4.05 (2H, q, J = 7.07 Hz, CH_2), 1.40 (3H, t, J = 7.08 Hz, CH_3). Data agrees with literature.[161]

N-(3-aminophenyl)-3-chloropropanamide 230

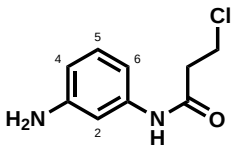

230

To a solution of benzene-1,3-diamine **215** (4.50 g, 41.88 mmol, 4.0 eq.) at 0 °C in DCM (3 mL) was added dropwise 3-chloropropanoyl chloride **228** (1.0 mL, 10.47 mmol, 1.0 eq.) in DCM (6 mL). The mixture was stirred at r.t. for 1 h, then aqueous sodium bicarbonate was added and the solution extracted with DCM (3 × 15 mL). The combined organic phases were concentrated under reduced pressure and purified by flash chromatography (100 % EtOAc mobile phase) to afford N-(3-aminophenyl)-3-chloropropanamide **230** (834 mg, 4.19 mmol, 40 %); **^{1}H NMR** (400 MHz, $CDCl_3$) δ_H 7.16 (1H, s, NH), 7.08 (1H, t, J = 7.99 Hz, H5), 6.67 (1H, d, J = 7.98 Hz, ArH), 6.47 (1H, d, J = 8.01 Hz, ArH), 3.87 (2H, t, J = 6.44 Hz, CH_2), 2.78 (2H, t, J = 6.42 Hz, CH_2).

N-(2-oxo-1,2-dihydroquinolin-7-yl)acetamide 223

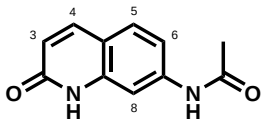

223

A solution of 7-bromoquinolin-2(1H)-one **70** and 5-bromoquinolin-2(1H)-one **90** isomer mixture (3:2 mixture of 7-br:5-br) (250 mg total, 1.13 mmol, 1.0 eq.), CuI (44 mg, 0.24 mmol, 0.2 eq.), DMEDA (34 μL, 0.24 mmol, 0.2 eq.), K_2CO_3 (312 mg, 2.26 mmol, 2.0 eq.), acetamide (800 mg, 13.56 mmol, 12.0 eq.), and NMP (3.0 mL) was stirred at 150 °C for 16 h. After cooling to room temperature water was added and the solution extracted with EtOAc (8 × 10 mL). The combined organic phases were washed with water and concentrated under reduced pressure to afford N-(2-oxo-1,2-dihydroquinolin-7-yl)acetamide **223** (85 mg of 7-isomer, 0.70 mmol, 62 % from pure 7-br isomer); ^{1}**H NMR** (400 MHz, $CDCl_3$) δ_H 7.77 (1H, d, J = 9.52 Hz, ArH), 7.49 (1H, d, J = 8.37 Hz, ArH), 7.44 (1H, d, J = 1.82 Hz, ArH), 7.19 (1H, dd, J = 8.38 and 1.93 Hz, ArH), 6.69 (1H, d, J = 9.39 Hz, ArH), 1.73 (3H, s, CH_3).

4,6-diamino-2-bromonicotinonitrile 237

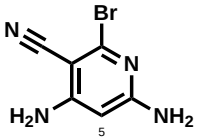

237

A solution of *tert*-butyl bromide (3.4 mL, 30.30 mmol, 2.0 eq.), triphenylphosphine (7.94 g, 30.30 mmol, 2.0 eq.), and tetrabutylammonium bromide (1.56 g, 4.85 mmol, 0.32 eq.) was stirred at reflux temperature (85 °C) for 90 m, after which time the HBr-phosphonium salt had formed in the flask. Glass tubing was fixed to the top of the condenser and directed into a second flask containing malononitrile (1.0 g, 15.15 mmol, 1.0 eq.) and toluene (20 mL) at 0 °C. A plastic tube exhaust from the second flask was directed through a container of water to quench the HBr gas. To the HBr-phosphonium salt in the first flask was added *m*-xylene (15 mL) and the mixture stirred at reflux temperature (150 °C) for 6 h while a nitrogen stream from the vacuum line was sent through the solution in the first flask, directing the evolving HBr gas through the glass tube and through the solution in the second flask. The malononitrile and toluene mixture was stirred at 0 °C for 1 h, then room temperature for 5 h, during which time HBr gas continued to be evolved. The glass tube was removed and the malononitrile solution stirred for a further 16 h at room temperature

under argon, and then for 2 h at reflux temperature (120 °C). After cooling to room temperature the solid was collected by filtration, washed with aqueous sodium hydroxide, and dried under vacuum over P_2O_5 to afford 4,6-diamino-2-bromonicotinonitrile **237** (645 mg, 3.03 mmol, 40 %); $\mathbf{R_f}$ 0.19 (1:1 EtOAc:P.E.); **mp** > 250 °C; $\boldsymbol{\nu_{max}}$ (thin film) / cm^{-1} 3344, 3189, 2361, 2342, 1690, 1622, 1575, 1476, 1392, 1273, 1151, 1025, 1000 and 823; ^{1}**H NMR** (500 MHz, $(CD_3)_2SO$) δ_H 6.92 (2H, s, NH_2), 6.62 (2H, s, NH_2), 5.60 (1H, s, H5); ^{13}**C NMR** (125 MHz, $(CD_3)_2SO$) δ_C 165.1, 161.3, 158.0, 154.4, 116.8 and 87.2; **HRMS** (FI^+) found 211.9691 (M^+, $C_6H_5BrN_4$ requires 211.9698). Data agrees with literature.[165]

4,6-diaminonicotinonitrile 238

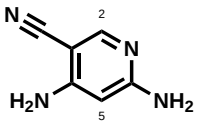

238

A solution of 4,6-diamino-2-bromonicotinonitrile **237** (100 mg, 0.47 mmol, 1.0 eq.), KOAc (46 mg, 0.47 mmol, 1.0 eq.), Pd/C (27 mg), THF (1.0 mL) and MeOH (0.5 mL) was stirred under an atmosphere of H_2 at 4.5 bar for 10 days at r.t.. The solution was filtered through celite then concentrated under reduced pressure to afford 4,6-diaminonicotinonitrile **238** (63 mg, 0.47 mmol, 100 % by NMR) as a light pink/brown powder; $\mathbf{R_f}$ 0.30 (100 % EtOAc); **mp** 156.6–159.9 °C; ^{1}**H NMR** (500 MHz, $CDCl_3$) δ_H 8.06 (1H, s, H2), 5.69 (1H, s, H5); ^{13}**C NMR** (125 MHz, $CDCl_3$) δ_C 167.9, 132.5, 131.1, 129.0, 89.8 and 66.4; **HRMS** (FI^+) found 134.0589 (M^+, $C_6H_6N_4$ requires 134.0592). Data agrees with literature.[165]

tert-butyl pyridin-2-ylcarbamate 245

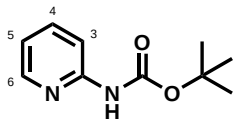

245

A mixture of 2-aminopyridine **83** (1.0 g, 10.64 mmol, 1.0 eq.), di-*tert*-butyl-dicarbonate (3.48 g, 15.96 mmol, 1.5 eq.), and *tert*-butyl alcohol (40 mL) was stirred at 30 °C for 6 hours. The solution was then concentrated under reduced pressure, water added, and the solution extracted with DCM (3 × 50 mL). The combined organic phases were concentrated under reduced pressure and purified

by flash chromatography (100 % Et_2O mobile phase) to afford tert-butyl pyridin-2-ylcarbamate **245** (1.86 g, 9.59 mmol, 90 %); ^{1}**H NMR** (400 MHz, $CDCl_3$) δ_H 8.24 (1H, d, J = 4.89 Hz, H6), 7.93 (1H, d, J = 8.46 Hz, H3), 7.65 (1H, dd, J = 1.93 and 8.42 Hz, ArH), 6.94 (1H, ddd, J = 1.02, 4.95 and 7.26 Hz, ArH), 1.53 (9H, s, $(CH_3)_3$). Data agrees with literature.[241]

tert-butyl (3-bromopyridin-2-yl)carbamate 248

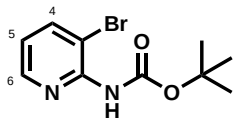

248

A mixture of 2-amino-3-bromopyridine **247** (500 mg, 2.89 mmol, 1.0 eq.), di-*tert*-butyl-dicarbonate (1.26 g, 5.78 mmol, 2.0 eq.), and *tert*-butyl alcohol (15 mL) was stirred at 70 °C for 4 hours. The solution was then concentrated under reduced pressure, water added, and the solution extracted with DCM (3 × 20 mL). The combined organic phases were concentrated under reduced pressure and purified by recrystallization from Et_2O, DCM and P.E. to afford tert-butyl (3-bromopyridin-2-yl)carbamate **248** (453 mg, 1.66 mmol, 57 %); $\mathbf{R_f}$ 0.21 (1:1 Et_2O:P.E.); $\boldsymbol{\nu_{max}}$ (thin film) / cm^{-1} 2978, 2361, 1722, 1578, 1497, 1442, 1392, 1367, 1251, 1148, 1076, 1051, 1027, 843, 791 and 670; ^{1}**H NMR** (400 MHz, $CDCl_3$) δ_H 8.38 (1H, d, J = 4.70 Hz, H6), 7.78 (1H, d, J = 7.88 Hz, H4), 7.29 (1H, s, NH_2), 6.85 (1H, dd, J = 7.78 and 4.81 Hz, H5), 1.51 (9H, s, $(CH_3)_3$); ^{13}**C NMR** (100 MHz, $CDCl_3$) δ_C 150.7, 148.7, 147.5, 141.0, 119.8, 109.4, 81.6 and 28.3; $\boldsymbol{m/z}$ (ESI^-) 255.23 (100 %), 271.01 (65 %, $[M\text{-}H]^-$); **HRMS** (ESI^+) found 295.0053 ($[M+Na]^+$, $C_{10}H_{13}BrN_2ON_2Na$ requires 295.0053). Data agrees with literature.[242]

3-(4,4,5,5-tetramethyl-1,3,2-dioxaborolan-2-yl)pyridin-2-amine 213

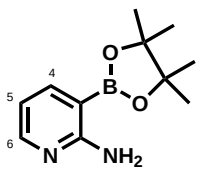

213

A vial containing 1,4-dioxane (2 mL) was degassed for 20 m. 2-amino-3-bromopyridine **247** (100 mg, 0.58 mmol, 1.0 eq.), $Pd(dppf)_2Cl_2$ (24 mg, 0.03 mmol, 0.05 eq.), KOAc (86 mg, 0.88 mmol, 1.5 eq.), and bis(pinacolato)diboron (224 mg, 0.88 mmol, 1.5 eq.) were added, and the solution was stirred

at 80 °C for 16 h. After cooling to room temperature the solution was filtered through celite and concentrated under reduced pressure to afford 3-(4,4,5,5-tetramethyl-1,3,2-dioxaborolan-2-yl)pyridin-2-amine **213** (102 mg, 0.46 mmol, 80 % by NMR); ^{1}**H NMR** (400 MHz, $CDCl_3$) δ_H 8.10 (1H, dd, J = 5.04 and 2.05 Hz, H6), 7.85 (1H, dd, J = 7.17 and 2.05 Hz, H4), 6.57 (1H, dd, J = 7.19 and 4.97 Hz, H5), 5.56 (2H, s, NH_2), 1.34 (12H, s, $(CH_3)_4$).

(2-aminopyridin-3-yl)boronic acid 251

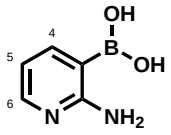

251

A vial containing 1,4-dioxane (2 mL) was degassed for 20 m. Pd_2dba_3 (26 mg, 0.03 mmol, 0.05 eq.) and PCy_3 (22 mg, 0.08 mmol, 0.14 eq.) were added, and the solution stirred for 20 m. 2-amino-3-bromopyridine **247** (100 mg, 0.58 mmol, 1.0 eq.), KOAc (86 mg, 0.88 mmol, 1.5 eq.), and bis-(pinacolato)diboron (224 mg, 0.88 mmol, 1.5 eq.) were added, and the solution was stirred at 80 °C for 16 h. After cooling to room temperature the solution was concentrated under reduced pressure and purified by flash chromatography (3:1 EtOAc:MeOH mobile phase) to afford (2-aminopyridin-3-yl)boronic acid **324** (5 mg, 0.036 mmol, 6 %) as a semi-solid; $\boldsymbol{\nu_{max}}$ (thin film) / cm^{-1} 3326, 1613, 1574, 1442, 1254, 1120, 996, 772 and 697; ^{1}**H NMR** (500 MHz, $CDCl_3$) δ_H 8.11 (1H, s, H6), 7.40 (1H, dd, J = 7.25 Hz, H4), 6.78 (1H, m, H5), 4.76 (2H, s, NH_2 or $B(OH)_2$), 3.25 (2H, s, NH_2 or $B(OH)_2$); ^{13}**C NMR** (125 MHz, $CDCl_3$) δ_C 155.8, 147.9, 139.6, 117.2 and 114.6.

benzyl (6-bromopyridin-2-yl)carbamate 253

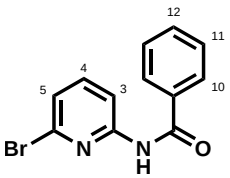

253

To a solution of 2-amino-6-bromopyridine **82** (2.0 g, 11.56 mmol, 1.0 eq.) in DCM (20 mL) was added benzoyl chloride **185** (2.0 mL, 17.36 mmol, 1.5 eq.) and pyridine (1.4 mL, 17.36 mmol, 1.5 eq.). The solution was stirred for 20 m, then water (40 mL) was added and the organic phase isolated. The

aqueous phase was extracted with DCM (3 × 20 mL) and the combined organic phases washed with water (3 × 40 mL) then concentrated under reduced pressure. The product was recrystallized from hot P.E./Et_2O to afford benzyl (6-bromopyridin-2-yl)carbamate **253** (1.663 g, 6.00 mmol, 52 %) as two types of crystals (with identical NMR spectra): clear prisms and white needles; $\mathbf{R_f}$ 0.29 (3:1 P.E.:Et_2O); **mp** (prisms) 83.3–86.1 °C; **mp** (needles) 88.1–89.6 °C; $\boldsymbol{\nu_{max}}$ (KBr disc) / cm^{-1} 3417, 1676, 1563, 1520, 1491, 1432, 1387, 1322, 1296, 1260, 1235, 1156, 1139, 1097, 1072, 787, 707, 684, 614, 567; ^{1}**H NMR** (400 MHz, $CDCl_3$) δ_H 8.64 (1H, s, NH), 8.32 (1H, dd, J = 8.18 and 0.60 Hz, H3 or H5), 7.89–7.86 (2H, m, ArH), 7.58–7.51 (2H, m, ArH), 7.48–7.43 (2H, m, ArH), 7.20 (1H, dd, J = 7.71 and 0.67 Hz, H3 or H5); ^{13}**C NMR** (100 MHz, $CDCl_3$) δ_C 165.6, 151.6, 140.7, 139.3, 133.7, 132.6, 128.9, 127.3, 123.7 and 112.6; $\boldsymbol{m/z}$ (ESI^+) 298.99 ($[M+Na]^+$, 100 %), 277.03 ($[M+H]^+$, 21 %); **HRMS** (ESI^+) found 298.9787 ($C_{12}H_9BrN_2NaO$ $[M+Na]^+$ requires 298.9790).

N-(2′-amino-[2,3′-bipyridin]-6-yl)benzamide 256

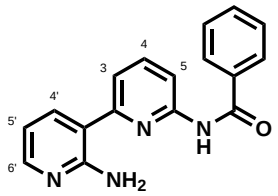

256

A solution of 3-(4,4,5,5-tetramethyl-1,3,2-dioxaborolan-2-yl)pyridin-2-amine **213** (64 mg, 0.29 mmol, 1.0 eq.), benzyl (6-bromopyridin-2-yl)carbamate **253** (80 mg, 0.29 mmol, 1.0 eq.), tetrakis(triphenylphosphine)palladium (17 mg, 0.015 mmol, 0.05 eq.), K_2CO_3 (60 mg, 0.44 mmol, 1.5 eq.), DME (0.5 mL), and H_2O (0.5 mL) was stirred at 100 °C for 16 h. After cooling to room temperature the mixture was concentrated under reduced pressure and purified by flash chromatography (100 % EtOAc mobile phase) to afford N-(2′-amino-[2,3′-bipyridin]-6-yl)benzamide **256** (23 mg, 0.08 mmol, 27 %) as a semisolid; $\mathbf{R_f}$ 0.38 (100 % EtOAc); ^{1}**H NMR** (500 MHz, $CDCl_3$) δ_H 8.85 (1H, s, NH), 8.27 (1H, d, J = 8.21 Hz, ArH), 8.01 (1H, d, J = 5.04 Hz, ArH), 7.95 (1H, d, J = 7.27 Hz, ArH), 7.84 (1H, m, ArH), 7.69–7.40 (6H, m, ArH), 6.75 (2H, s, NH_2), 6.72 (1H, dd, J = 7.57 and 5.05 Hz, ArH); ^{13}**C NMR** (125 MHz, $CDCl_3$) δ_C 139.7, 137.8, 132.5, 132.3, 132.2, 132.09, 132.07, 129.0, 128.7, 128.6, 127.5, 127.4, 118.3, 113.5 and 112.6; $\boldsymbol{m/z}$ (ESI^+) 297.22 (100 %), 291.12 ($[M+H]^+$, 98 %); **HRMS** (ESI^+) found 291.1238 ($C_{17}H_{15}N_4O$, $[M+H]^+$ requires 291.1240).

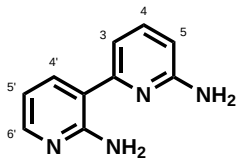

257

[2,3′-bipyridine]-2′,6-diamine 257

A solution of 3-(4,4,5,5-tetramethyl-1,3,2-dioxaborolan-2-yl)pyridin-2-amine **213** (128 mg, 0.58 mmol, 1.0 eq.), 2-amino-6-bromopyridine **82** (100 mg, 0.58 mmol, 1.0 eq.), tetrakis(triphenylphos -phine)-palladium (34 mg, 0.029 mmol, 0.05 eq.), K_2CO_3 (120 mg, 0.88 mmol, 1.5 eq.), DME (1.0 mL), and H_2O (1.0 mL) was stirred at 100 °C for 16 h. After cooling to room temperature the mixture was concentrated under reduced pressure and purified by flash chromatography (100 % EtOAc mobile phase) to afford [2,3′-bipyridine]-2′,6-diamine **257** (54 mg, 0.29 mmol, 50 %); $\mathbf{R_f}$ 0.43 (10:1 EtOAc:MeOH); $\boldsymbol{\nu_{max}}$ (thin film) / cm^{-1} 3328, 1604, 1564, 1445, 1248, 1178, 988 and 782; ^{1}**H NMR** (400 MHz, $CDCl_3$) δ_H 7.87 (1H, d, J = 5.32 Hz, H6′), 7.81 (1H, dd, J = 7.59 and 1.74 Hz, H4′), 7.49 (1H, t, J = 8.00 Hz, H4), 6.94 (1H, d, J = 7.60 Hz, ArH), 6.63 (1H, dd, J = 7.58 and 5.37 Hz, H5′), 6.43 (1H, d, J = 8.17 Hz, ArH); ^{13}**C NMR** (100 MHz, $CDCl_3$) δ_C 157.2, 157.1, 155.4, 146.9, 138.8, 137.3, 117.8, 113.1, 112.2 and 106.8; $\boldsymbol{m/z}$ (ESI^+) 187.07 ($[M+H]^+$, 100 %); **HRMS** (ESI^+) found 187.0978 ($C_{10}H_{11}N_4$ $[M+H]^+$ requires 187.0978).

benzyl (6-bromopyridin-2-yl)carbamate 243

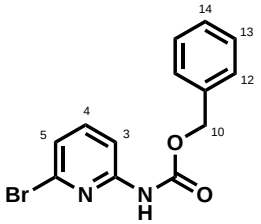

243

To a solution of 2-amino-6-bromopyridine **82** (500 mg, 2.89 mmol, 1.0 eq.) in DCM (8 mL) was added benzyl chloroformate **216** (1.03 mL, 7.23 mmol, 2.5 eq.) and pyridine (0.36 mL, 4.34 mmol, 1.5 eq.). The solution was stirred for 16 h, then water (20 mL) was added. The organic phase was isolated and the aqueous phase extracted with DCM (3 × 10 mL). The combined organic phases were washed with water (3 × 20 mL) then concentrated under reduced pressure. The product was recrystallized from hot P.E./Et_2O to afford benzyl (6-bromopyridin-2-yl)carbamate **243** (700 mg,

2.28 mmol, 79 %) as clear block-like crystals; $\mathbf{R_f}$ 0.42 (3:1 P.E.:Et_2O); **mp** 100.0–101.6 °C; $\boldsymbol{\nu_{max}}$ (KBr disc) / cm^{-1} 3355, 2361, 1733, 1588, 1568, 1526, 1435, 1395, 1374, 1255, 1203, 1158, 1133, 1049, 982, 872, 793, 757, 702, 659; ^{1}**H NMR** (400 MHz, $CDCl_3$) δ_H 7.94 (1H, d, J = 8.20 Hz, H3 or H5), 7.64 (1H, s, NH), 7.50 (1H, t, J = 7.96 Hz, H4), 7.39–7.31 (5H, m, ArH), 7.14 (1H, d, J = 7.69 Hz, H3 or H5), 5.22 (2H, s, CH_2); ^{13}**C NMR** (100 MHz, $CDCl_3$) δ_C 152.7, 151.6, 140.5, 139.4, 135.7, 128.7, 128.5, 128.2, 122.8, 110.8 and 67.4; $\boldsymbol{m/z}$ (ESI^+) 329.01 ($[M+Na]^+$, 100 %); **HRMS** (ESI^+) found 328.9901 ($C_{13}H_{11}BrN_2NaO_2$ $[M+Na]^+$ requires 328.9896).

benzyl (2′-amino-[2,3′-bipyridin]-6-yl)carbamate 6

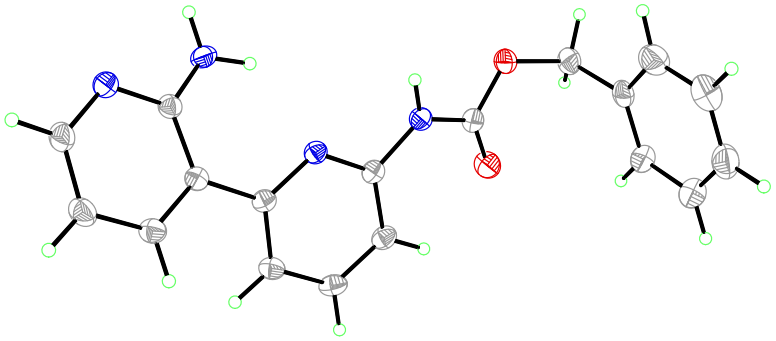

Crystal structure of **6**. Thermal ellipsoids drawn at 50 % probability. The minor component of the disordered benzyl group is omitted for clarity.

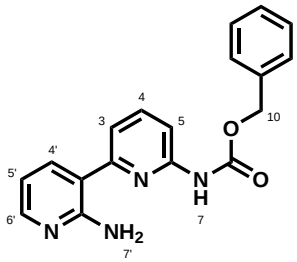

6

A solution of 3-(4,4,5,5-tetramethyl-1,3,2-dioxaborolan-2-yl)pyridin-2-amine **213** (79 mg, 0.36 mmol, 0.62 eq.), benzyl (6-bromopyridin-2-yl)carbamate **243** (178 mg, 0.58 mmol, 1.0 eq.), $Pd(PPh_3)_4$ (34 mg, 0.029 mmol, 0.05 eq.), K_2CO_3 (120 mg, 0.88 mmol, 1.5 eq.), H_2O (1.0 mL), and DME (1.0 mL) was degassed for 10 m, then stirred at 100 °C for 16 h. After cooling to room temperature the solution was concentrated under reduced pressure and purified by flash chromatography (100 % EtOAc mobile phase) to afford benzyl (2′-amino-[2,3′-bipyridin]-6-yl)carbamate **6** (83 mg, 0.26 mmol, 72 %); $\mathbf{R_f}$ 0.19 (1:1 EtOAc:P.E.); **mp** 156.6–159.7 °C; $\boldsymbol{\nu_{max}}$ (thin film) / cm^{-1} 2925, 1735, 1604, 1560, 1446, 1218, 1091, 768, 743 and 698; ^{1}**H NMR** (500 MHz, $CDCl_3$) δ_H 8.95 (1H, s, H7), 8.08 (1H, dd, J = 1.78 and 4.94 Hz, H6′), 7.93 (1H, d, J = 8.32 Hz, H5), 7.77 (1H, t, J = 8.03 Hz, H4), 7.71

(1H, dd, J = 1.77 and 7.59 Hz, H4′), 7.45–7.34 (5H, m, Ph), 7.28 (1H, dd, J = 0.62 and 7.73 Hz, H3), 6.64 (1H, dd, J = 4.94 and 7.57 Hz, H5′), 6.35 (2H, s, H7′), 5.27 (2H, s, H10); **^{13}C NMR** (125 MHz, $CDCl_3$) δ_C 157.4 (C2′), 155.9 (C2), 153.4 (C8), 150.8 (C6), 149.0 (C6′), 139.7 (C4), 137.5 (C4′), 135.9, 128.80, 128.79, 128.6, 128.5, 117.3 (C3), 113.7 (C5′), 110.6 (C5) and 67.4 (C10); ***m/z*** (ESI^+) 321.12 (100 %, $[M+H]^+$); **HRMS** (ESI^+) found 321.1337 ($[M+H]^+$, $C_{18}H_{17}N_4O_2$ requires 321.1346).

1,3-dimethylpyrimidine-2,4(1H,3H)-dione 263

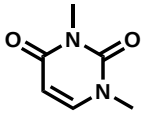

263

To a solution of uracil **265** (16.6 g, 148 mmol, 1.0 eq.), K_2CO_3 (81.8 g, 593 mmol, 4.0 eq.) and acetone (100 mL) was added methyl iodide (37 mL, 593 mmol, 4.0 eq.). The solution was stirred at r.t. for 48 h, then subjected to reduced pressure to remove excess methyl iodide. With acetone still remaining, the solution was filtered through a sinter and the solid filtrand washed with DCM. The filtrate was concentrated under reduced pressure to afford 1,3-dimethylpyrimidine-2,4(1H,3H)-dione **263** (20.54 g, 147 mmol, 99 %); **^{1}H NMR** (400 MHz, $CDCl_3$) δ_H 7.12 (1H, d, J = 7.83 Hz, CH), 5.71 (1H, d, J = 7.84 Hz, CH), 3.38 (3H, s, CH_3), 3.32 (3H, s, CH_3). Data agrees with literature.[187]

2-aminopyrimidin-4(3H)-one 262

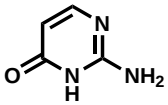

262

A solution of 1,3-dimethylpyrimidine-2,4(1H,3H)-dione **263** (17.31 g, 124 mmol, 1.0 eq.), guanidine hydrochloride **264** (35.60 g, 371 mmol, 3.0 eq.) and K^{t}OBu powder (41.53 g, 371 mmol, 3.0 eq.) and MeOH (150 mL) was stirred at 75 ℃ for 72 h. Solids were removed by sinter filtration, and the organic MeOH filtrate transferred to a separatory funnel. Et_2 was added, and the funnel shaken to mix the Et_2O and MeOH. An oily crash appeared at the bottom of the funnel and was separated from the Et_2O and MeOH layer. The oily crash was concentrated under reduced pressure to afford 2-aminopyrimidin-4(3H)-one **262** (13.72 g, 124 mmol, 100 %); $\mathbf{R_f}$ 0.50 (5:1 EtOAc:MeOH); **^{1}H NMR** (400 MHz, D_2O) δ_H 7.60 (1H, d, J = 6.15 Hz, ArH), 5.73 (1H, d, J = 6.15 Hz, ArH); ***m/z*** (ESI^+)

250.96 (100 %), 112.03 ([M+H]$^+$, 44 %); **HRMS** (ESI$^+$) found 112.0503 ($C_4H_6N_3O$, ([M+H]$^+$) requires 112.0505). Data agrees with literature.[243]

4-bromopyrimidin-2-amine 260

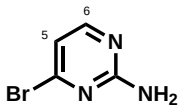

260

A mixture of isocytosine **262** (100 mg, 0.90 mmol, 1.0 eq.) and $POBr_3$ (260 mg, 0.90 mmol, 1.0 eq.) was stirred at 135 °C for 6 h. The flask was cooled to 0 °C, and water was slowly added to the mixture. Acetone was also added to help to dissolve the solids. The solution was stirred at r.t. for 30 m, then the acteone was removed under reduced pressure. The remaining aqueous solution was adjusted to pH 16 with aqueous NaOH, then placed in continuous liquid/liquid extraction apparatus. It was extracted for 16 h with EtOAc, which was concentrated under reduced pressure to afford 4-bromopyrimidin-2-amine **260** (105 mg, 0.60 mmol, 67 %); $\mathbf{R_f}$ 0.28 (100 % EtOAc); **mp** > 250 °C; ^{1}**H NMR** (500 MHz, $CDCl_3$) δ_H 8.04 (1H, d, J = 5.19 Hz, ArH), 6.81 (1H, d, J = 5.04 Hz, ArH), 5.29 (2H, s, NH_2); ^{13}**C NMR** (125 MHz, $CDCl_3$) δ_C 161.7, 157.9, 152.2 and 114.3; ***m/z*** (ESI$^+$) 173.96 ([M+H]$^+$, 100 %); **HRMS** (ESI$^+$) found 173.9669 ($C_4H_5BrN_3$, ([M+H]$^+$) requires 173.9661).

2-amino-6-methylpyrimidin-4(3H)-one 266

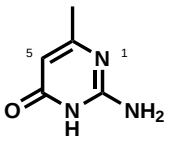

266

A mixture of guanidine hydrochloride **264** (3.04 g, 31.7 mmol, 2.0 eq.), ethyl acetoacetate (2.0 mL, 15.8 mmol, 1.0 eq.), sodium methoxide (3.42 g, 63.4 mmol, 4.0 eq.), and ethanol (40 mL) was stirred at 90 °C for 16 hours. The solution was then concentrated under reduced pressure, 1 M aqueous sodium hydroxide added, and the aqueous solution washed with EtOAc (3 × 20 mL). The aqueous phase was concentrated reduced pressure, then a little water added, and the mixture filtered through a sinter filter. The filtrand was concentrated under reduced pressure, a little water added again, and sinter-filtered again. The filtrand was concentrated under reduced pressure and vacuum-dried

over P_2O_5 to afford 2-amino-6-methylpyrimidin-4(3H)-one **266** (0.57 g, 4.56 mmol, 29 %); $\mathbf{R_f}$ 0.31 (5:1 Et_2O:MeOH); $\boldsymbol{\nu_{max}}$ (thin film) / cm^{-1} 3351, 1739, 1660, 1528, 1473, 1371, 1217, 828, 767, 651 and 608; ^{1}**H NMR** (400 MHz, CD_3OD) δ_H 5.61 (1H, d, J = 0.67 Hz, H5), 7.82 (3H, d, J = 0.67 Hz, CH_3); ***m/z*** (ESI^+) 126.04 ($[M+H]^+$, 100 %); **HRMS** (ESI^+) found 126.0666 ($C_5H_8N_3O$, ($[M+H]^+$) requires 126.0662). Data agrees with literature.[188,244]

3-((trimethylsilyl)ethynyl)pyridin-2-amine 275

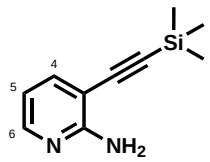

275

A solution of 2-amino-3-bromopyridine **247** (2.0 g, 11.56 mmol, 1.0 eq.), $Pd(OAc)_2$ (52 mg, 0.23 mmol, 0.02 eq.), Et_3N (6.0 mL), PPh_3 (121 mg, 0.46 mmol, 0.04 eq.), and DMF (25 mL) was degassed for 15 m. Trimethylsilylacetylene **274** (2.8 mL, 19.65 mmol, 1.7 eq.) was added, and the mixture stirred for 24 h at 50 °C. After cooling to room temperature saturated ammonium chloride was added, and the solution extracted with EtOAc (3 × 30 mL). The combined organic phases were concentrated under reduced pressure and purified by flash chromatography (2:1 P.E.:EtOAc mobile phase) to afford 3-((trimethylsilyl)ethynyl)pyridin-2-amine **275** (1.52 g, 7.98 mmol, 69 %); ^{1}**H NMR** (400 MHz, $CDCl_3$) δ_H 7.98 (1H, dd, J = 5.05 and 1.79 Hz, H6), 7.50 (1H, dd, J = 7.46 and 1.85 Hz, H4), 6.55 (1H, dd, J = 7.47 and 5.05 Hz, H5), 5.20 (2H, s, NH_2), 0.24 (9H, s, $Si(CH_3)_3$); ^{13}**C NMR** (100 MHz, $CDCl_3$) δ_C 159.4, 148.2, 140.2, 113.3, 103.0, 101.1, 100.4, 0.07 ($Si(CH_3)_3$). Data agrees with literature.[245]

3-ethynylpyridin-2-amine 276

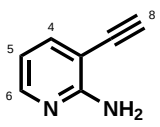

276

A solution of 3-((trimethylsilyl)ethynyl)pyridin-2-amine **275** (1.386 g, 7.29 mmol, 1.0 eq.), K_2CO_3 (2.01 g, 14.58 mmol, 2.0 eq.), and MeOH (15 mL) was stirred at room temperature for 2 h. The mixture was concentrated under reduced pressure and filtered through celite to afford 3-ethynyl

-pyridin-2-amine **276** (851 mg, 7.21 mmol, 99 %); ^{1}**H NMR** (400 MHz, $CDCl_3$) δ_H 8.01 (1H, dd, J = 5.04 and 1.80 Hz, H6), 7.56 (1H, dd, J = 7.50 and 1.87 Hz, H4), 6.60 (1H, dd, J = 7.50 and 5.02 Hz, H5), 3.32 (1H, s, H8). Data agrees with literature.[246]

tert-butyl (3-ethynylpyridin-2-yl)carbamate 277

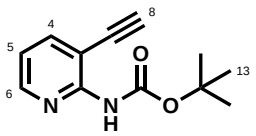

277

A solution of 3-ethynylpyridin-2-amine **276** (507 mg, 2.93 mmol, 1.0 eq.), di-tert-butyl dicarbonate (1.92 g, 8.79 mmol, 3.0 eq.), and tert-butanol (20 mL) was stirred at 40 °C for 16 h. After cooling to room temperature the solution was concentrated under reduced pressure and purified by flash chromatography (3:1 P.E.:EtOAc mobile phase) to afford tert-butyl (3-ethynylpyridin-2-yl)-carbamate **277** (630 mg, 2.31 mmol, 79 %) as beige powdery crystals; $\mathbf{R_f}$ 0.16 (1:1 P.E.:Et_2O); **mp** > 270 °C; $\boldsymbol{\nu_{max}}$ (thin film) / cm^{-1} 3264, 3193, 2983, 2361, 2341, 1724, 1589, 1522, 1450, 1391, 1366, 1278, 1245, 1165, 1079, 1045, 814, 768 and 669; ^{1}**H NMR** (500 MHz, $CDCl_3$) δ_H 8.44 (1H, dd, J = 4.93 and 1.89 Hz, H6), 7.73 (1H, dd, J = 7.60 and 1.90 Hz, H4), 7.51 (1H, s, NH), 6.95 (1H, dd, J = 7.64 and 4.95 Hz, H5), 3.55 (1H, s, CH), 1.55 (9H, s, $C(CH_3)_3$); ^{13}**C NMR** (125 MHz, $CDCl_3$) δ_C 152.8, 150.6, 148.8 (C6), 141.0 (C4), 117.8 (C5), 106.8, 85.7 (C8), 81.5, 78.0 and 28.4 (C13); $\boldsymbol{m/z}$ (ESI^+) 460.17 (100 %), 241.08 (78 %, $[M+Na]^+$); **HRMS** (ESI^+) found 241.0952 ($C_{12}H_{14}N_2O_2Na$ ($[M+Na]^+$) requires 241.0947).

1-(2-aminopyridin-3-yl)oct-1-yn-3-ol 280

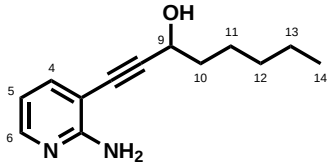

280

A solution of 2-amino-3-bromo pyridine **247** (2.0 g, 11.56 mmol, 1.0 eq.), oct-1-yn-3-ol **279** (2.53 mL, 17.34 mmol, 1.5 eq.), copper iodide (220 mg, 1.16 mmol, 0.1 eq.), tetrakis(triphenylphosphine)-palladium (668 mg, 0.58 mmol, 0.05 eq.) and triethylamine (50 mL) was degassed for 15 m, then stirred at 50 °C for 16 h in a flask sealed with a subaseal. After cooling to room temperature the

solution was concentrated under reduced pressure and purified by flash chromatography (100 % EtOAc mobile phase) to afford 1-(2-aminopyridin-3-yl)oct-1-yn-3-ol **280** (2.039 g, 9.35 mmol, 81 %) as dark red-brown powdery flakes; $\mathbf{R_f}$ 0.39 (100% EtOAc); **mp** 58.0–61.5 °C; $\boldsymbol{\nu_{max}}$ (thin film) / cm^{-1} 3734, 3475, 3343, 3184, 2954, 2930, 2859, 2361, 2342, 1614, 1572, 1456, 1378, 1335, 1273, 1221, 1121, 1028, 911, 788, 766, 725 and 669; ^{1}**H NMR** (400 MHz, $CDCl_3$) δ_H 7.99 (1H, d, J = 3.07 Hz, H6), 7.47 (1H, dd, J = 7.49 and 1.56 Hz, H4), 6.58 (1H, dd, J = 7.43 and 5.06 Hz, H5), 5.05 (2H, s, NH_2), 4.62 (1H, t, J = 6.64 Hz, H9), 1.87–1.73 (2H, m, H10), 1.54–1.47 (2H, m, H11), 1.33 (4H, m, H12 and H13), 0.90 (3H, m, H14); ^{13}**C NMR** (100 MHz, $CDCl_3$) δ_C 159.0, 147.9, 140.4, 113.5, 102.9, 97.2, 79.9, 62.9, 38.0, 31.6, 25.2, 22.7 and 14.1 (C14); $\boldsymbol{m/z}$ (ESI^+) 219.14 (100 %, $[M+H]^+$), 497.23 (76 %), 241.13 (58 %, $[M+Na]^+$); **HRMS** (ESI^+) found 219.1500 ($[M+H]^+$, $C_{13}H_{19}N_2O$ requires 219.1492).

1-(2-aminopyridin-3-yl)oct-1-yn-3-one 281

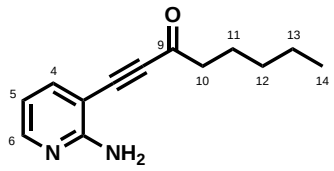

281

A solution of 1-(2-aminopyridin-3-yl)oct-1-yn-3-ol **280** (120 mg, 0.55 mmol, 1.0 eq.), DMP (257 mg, 0.61 mmol, 1.1 eq.), and sodium bicarbonate (44 mg, 0.52 mmol, 0.95 eq.) in DCM (5 mL) was stirred at room temperature for 16 h. A 1:1 mixture of aqueous saturated $NaHCO_3$:$Na_2S_2O_3$ was added, and the solution extracted with DCM (3 × 10 mL). The combined organic phases were concentrated under reduced pressure and purified by flash chromatography (1:1 P.E.:Et_2O mobile phase) to afford 1-(2-aminopyridin-3-yl)oct-1-yn-3-one **281** (76 mg, 0.35 mmol, 64 %) as dark red-brown powdery flakes; $\mathbf{R_f}$ 0.19 (2:1 Et_2O:P.E.); $\boldsymbol{\nu_{max}}$ (thin film) / cm^{-1} 3166, 2929, 2361, 2342, 2178, 1661, 1609, 1561, 1453, 1297, 1230, 1125, 1073 and 766; ^{1}**H NMR** (400 MHz, $CDCl_3$) δ_H 8.09 (1H, d, J = 4.91 Hz, H6), 7.59 (1H, d, J = 7.58 Hz, H4), 6.60 (1H, dd, J = 7.21 and 5.33 Hz, H5), 5.50 (2H, s, NH_2), 2.62 (2H, t, J = 7.43 Hz, H10), 1.70 (2H, quintet, J = 7.02 Hz, H11), 1.34–1.26 (4H, m, H12 and H13), 0.87 (3H, t, J = 6.37 Hz, H14); ^{13}**C NMR** (100 MHz, $CDCl_3$) δ_C 187.7 (C9), 160.3, 150.9, 142.3, 113.5, 99.1, 94.3, 86.5, 45.4, 31.2, 23.9, 22.4 and 13.9 (C14); $\boldsymbol{m/z}$ (ESI^-) 215.12 (100 %, $[M-H]^-$); **HRMS** (ESI^+) found 239.1152 ($[M+Na]^+$, $C_{13}H_{16}N_2ONa$ requires 239.1155).

tert-butyl (3-(3-oxooct-1-yn-1-yl)pyridin-2-yl)carbamate 282

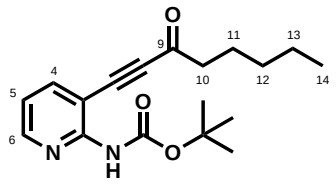

282

A solution of 1-(2-aminopyridin-3-yl)oct-1-yn-3-one **281** (341 mg, 1.58 mmol, 1.0 eq.), di-*tert*-butyl dicarbonate (689 mg, 3.16 mmol, 2.0 eq.), Et_3N (0.44 mL, 3.16 mmol, 2.0 eq.), and DMAP (39 mg, 0.32 mmol, 0.2 eq.) in DCM (20 mL) was stirred at room temperature for 16 h. Water was added and the solution extracted with DCM (3 × 20 mL). The combined organic phases were concentrated under reduced pressure and purified by flash chromatography (1:1 P.E.:Et_2O mobile phase) to afford tert-butyl (3-(3-oxooct-1-yn-1-yl)pyridin-2-yl)carbamate **282** (211 mg, 0.67 mmol, 42 %) as an oil; $\mathbf{R_f}$ 0.25 (2:1 P.E.:Et_2O); $\boldsymbol{\nu_{max}}$ (thin film) / cm^{-1} 2979, 1796, 1759, 1457, 1430, 1369, 1243, 1143, 1118, 1097, 850, 777 and 733; ^{1}**H NMR** (400 MHz, $CDCl_3$) δ_H 8.43 (1H, dd, J = 4.87 and 1.83 Hz, H6), 7.79 (1H, dd, J = 7.74 and 1.83 Hz, H4), 7.23 (1H, d, J = 4.85 Hz, H5), 5.79 (1H, t, J = 7.75 Hz, NH), 2.14 (2H, m, H10), 1.53 (9H, s, $C(CH_3)_3$), 1.48–1.27 (6H, m, H11, H12, and H13), 0.89 (3H, m, H14); ^{13}**C NMR** (100 MHz, $CDCl_3$) δ_C 150.2, 147.9, 140.4, 131.1, 129.6, 122.5, 118.3, 90.4, 83.5, 82.9, 30.5, 27.7, 27.6, 25.8, 22.2 and 13.8 (C14).

4-ethoxy-2-pentyl-1,8-naphthyridine 285

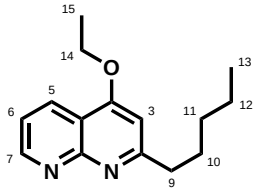

285

A solution of 1-(2-aminopyridin-3-yl)oct-1-yn-3-one **281** (69 mg, 0.32 mmol, 1.0 eq.), guanidine hydrochloride **264** (61 mg, 0.64 mmol, 2.0 eq.), sodium methoxide (69 mg, 1.28 mmol, 4.0 eq.) and ethanol (3 mL) was stirred at reflux temperature for 16 h. The mixture was concentrated under reduced pressure and purified by flash chromatography (100 % EtOAc mobile phase) to afford 4-ethoxy-2-pentyl-1,8-naphthyridine **285** (10 mg, 0.041 mmol, 13 %) as a brown semisolid; $\mathbf{R_f}$ 0.37 (100 % EtOAc); $\boldsymbol{\nu_{max}}$ (thin film) / cm^{-1} 2955, 2929, 2859, 2361, 2342, 1607, 1597, 1556, 1503, 1474, 1456, 1409, 1379, 1365, 1329, 1252, 1210, 1151, 1109, 1090, 1022, 983, 915, 866, 820, 789, 669

and 612; **^{1}H NMR** (500 MHz, $CDCl_3$) δ_H 9.02 (1H, s, H7), 8.52 (1H, d, J = 7.93 Hz, H5), 7.37 (1H, s, H6), 6.67 (1H, s, H3), 4.27 (2H, q, J = 7.00 Hz, H14), 2.95 (2H, t, J = 7.84 Hz, H9), 1.87 (2H, dt, J = 14.88 and 7.40 Hz, H10), 1.57 (3H, t, J = 7.00 Hz, H15), 1.42–1.33 (4H, m, H11 and H12), 0.90 (3H, t, J = 7.06 Hz, H13); **^{13}C NMR** (125 MHz, $CDCl_3$) δ_C 168.0, 162.1, 157.1, 153.3 (C7), 131.6 (C5), 120.3 (C6), 114.7, 101.5 (C3), 64.6 (C14), 40.2 (C9), 31.9, 29.4, 22.7, 14.6 and 14.2 (C13); ***m/z*** (ESI^+) 267.13 (100 %, $[M+Na]^+$), 245.15 (88 %, $[M+H]^+$); **HRMS** (ESI^+) found 245.1647 ($C_{15}H_{21}N_2O$ ($[M+H]^+$) requires 245.1648).

4-(2-aminopyridin-3-yl)-6-pentylpyrimidin-2-amine 284

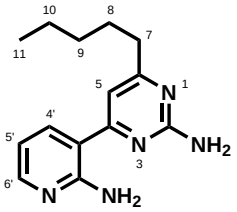

284

A solution of 1-(2-aminopyridin-3-yl)oct-1-yn-3-one **281** (100 mg, 0.46 mmol, 1.0 eq.), guanidine hydrochloride **264** (88 mg, 0.92 mmol, 2.0 eq.), potassium carbonate (254 mg, 1.84 mmol, 4.0 eq.) and toluene (3 mL) were stirred at reflux temperature for 16 h. After cooling to room temperature the solution was filtered through celite and concentrated under reduced pressure to afford 4-(2-aminopyridin-3-yl)-6-pentylpyrimidin-2-amine **284** (69 mg, 0.27 mmol, 58 %) as a brown solid; $\mathbf{R_f}$ 0.22 (100 % EtOAc); $\boldsymbol{\nu_{max}}$ (thin film) / cm^{-1} 3309, 2927, 2361, 2342, 1697, 1639, 1543, 1496, 1454, 1362, 1286, 1158, 1028, 798, 732 and 698; **^{1}H NMR** (500 MHz, $CDCl_3$) δ_H 8.13 (1H, d, J = 4.67 Hz, H6′), 7.86 (1H, dd, J = 7.72 and 1.01 Hz, H4′), 6.84 (1H, s, H5), 6.71 (2H, s, NH_2'), 6.68 (1H, dd, J = 7.56 and 4.65 Hz, H5′), 5.00 (2H, s, NH_2), 2.60 (2H, dd, J = 8.62 and 7.07 Hz, H7), 1.73–1.67 (2H, m, H8), 1.39–1.31 (4H, m, H9 and H10), 0.91–0.88 (3H, m, H11); **^{13}C NMR** (125 MHz, $CDCl_3$) δ_C 172.9, 165.4, 162.1, 157.9, 150.6 (C6′), 137.3 (C4′), 114.3 (C5′), 113.4 (C5), 107.4, 38.4 (C7), 31.8 (C9 or C10), 28.8 (C8), 22.7 (C9 or C10) and 14.1 (C11); ***m/z*** (ESI^+) 258.16 (100 %, $[M+H]^+$); **HRMS** (ESI^+) found 258.1715 ($C_{14}H_{20}N_5$ requires 258.1713).

1-(3-(2-amino-6-pentylpyrimidin-4-yl)pyridin-2-yl)-3-phenylurea 287

A solution of 4-(2-aminopyridin-3-yl)-6-pentylpyrimidin-2-amine **284** (15 mg, 0.058 mmol, 1.0 eq.), phenyl isocyanate **268** (7 mg, 0.058 mmol, 1.0 eq.) and 1,4-dioxane (1 mL) was stirred at room temperature for 24 h. The solution was concentrated under reduced pressure and the residue purified

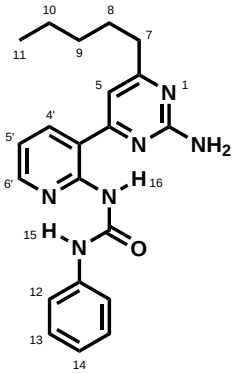

287

by flash chromatography (100 % EtOAc mobile phase) to afford 1-(3-(2-amino-6-pentylpyrimidin-4-yl)pyridin-2-yl)-3-phenylurea **287** (5 mg, 0.13 mmol, 23 %) as a yellow semisolid; $\mathbf{R_f}$ 0.24 (1:1 P.E.:Et_2O); $\boldsymbol{\nu_{max}}$ (thin film) / cm^{-1} 3316, 3154, 2954, 2926, 2857, 2361, 1660, 1592, 1543, 1509, 1498, 1466, 1446, 1348, 1324, 1233, 1179, 1080, 1019, 899, 829, 788, 753, 707, 689 and 614; ^{1}**H NMR** (500 MHz, $CDCl_3$) δ_H 12.04 (1H, s, H15), 11.94 (1H, s, H2′), 8.34 (1H, dd, J = 4.91 and 1.78 Hz, H6′), 8.12 (1H, dd, J = 7.94 and 1.76 Hz, H4′), 7.62 (1H, dd, J = 8.61 and 1.08 Hz, H12), 7.34 (1H, dd, J = 8.46 and 7.47 Hz, H13), 7.08 (1H, tt, J = 7.40 and 1.06 Hz, H14), 7.03 (1H, dd, J = 7.81 and 4.91 Hz, H5′), 6.88 (1H, s, H5), 5.49 (2H, s, NH_2), 2.63 (2H, dd, J = 8.61 and 7.05 Hz, H7), 1.75–1.69 (2H, m, H8), 1.38–1.33 (4H, m, H9 and H10), 0.93–0.90 (3H, m, H11); ^{13}**C NMR** (125 MHz, $CDCl_3$) δ_C 174.0, 163.0, 161.9, 153.1, 152.0, 147.8 (C6′), 138.8, 138.0, 129.1 (C13), 123.5 (C14), 120.4 (C12), 116.8, 116.6, 107.1 (C5), 38.5 (C7), 31.7 (C9 or C10), 28.7 (C8), 22.6 (C9 or C10) and 14.1 (C11); $\boldsymbol{m/z}$ (ESI^+) 775.39 (100 %), 377.20 (96 %, $[M+H]^+$); **HRMS** (ESI^+) found 399.1901 ($C_{21}H_{24}N_6ONa$ requires 399.1904).

tert-butyl (3-(2-amino-6-pentylpyrimidin-4-yl)pyridin-2-yl)carbamate 283

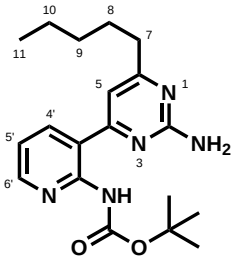

283

A solution of 4-(2-aminopyridin-3-yl)-6-pentylpyrimidin-2-amine **284** (40 mg, 0.16 mmol, 1.0 eq.), di-*tert*-butyl dicarbonate (102 mg, 0.47 mmol, 3.0 eq.) and tert-butanol (3 mL) was stirred at 30 °C for

16 h. The solution was concentrated under reduced pressure and purified by flash chromatography (100 % EtOAc mobile phase) to afford tert-butyl (3-(2-amino-6-pentylpyrimidin-4-yl)pyridin-2-yl)-carbamate **283** (34 mg, 0.095 mmol, 61 %) as a pale beige powder; $\mathbf{R_f}$ 0.21 (100% Et_2O); **mp** 152.7–153.9 °C; $\boldsymbol{\nu_{max}}$ (thin film) / cm^{-1} 3315, 3169, 2929, 2360, 1716, 1663, 1596, 1567, 1462, 1364, 1280, 1246, 1171, 873 and 742; ^{1}**H NMR** (500 MHz, $CDCl_3$) δ_H 11.46 (1H, s, NH), 8.54 (1H, dd, J = 4.79 and 1.85 Hz, H6′), 7.99 (1H, dd, J = 7.86 and 1.85 Hz, H4′), 7.03 (1H, dd, J = 7.80 and 4.80 Hz, H5′), 6.89 (1H, s, H5), 5.09 (2H, s, NH_2), 2.65–2.62 (2H, m, H7), 1.75–1.69 (2H, m, H8), 1.54 (9H, s, $(CH_3)_3$), 1.37 (4H, dq, J = 7.27 and 3.62 Hz, H9 and H10), 0.93–0.90 (3H, m, H11); ^{13}**C NMR** (125 MHz, $CDCl_3$) δ_C 174.0, 164.1, 161.7, 151.3, 151.2, 150.6, 137.3 (C4′), 118.5, 117.8, 108.1 (C5), 80.5, 38.5 (C7), 31.7, 28.8, 28.5, 22.6 and 14.1 (C11); $\boldsymbol{m/z}$ (ESI^+) 737.38 (100 %), 380.20 (49 %, $[M+Na]^+$); **HRMS** (ESI^+) found 380.2065 ($[M+Na]^+$, $C_{19}H_{27}N_5O_2Na$ requires 380.2057).

tert-butyl (3-(2-amino-6-pentylpyrimidin-4-yl)pyridin-2-yl)(benzylcarbamoyl)carbamate 289

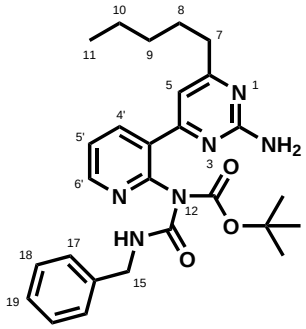

289

A solution of tert-butyl (3-(2-amino-6-pentylpyrimidin-4-yl)pyridin-2-yl)carbamate **283** (20 mg, 0.056 mmol, 1.0 eq.), benzyl isocyanate **259** (21 μL, 0.17 mmol, 3.0 eq.), sodium hydride (2 mg (60 % disp.), 0.056 mmol, 1.0 eq.), and THF (1 mL) was stirred at room temperature for 16 h. The solution was concentrated under reduced pressure and purified by flash chromatography (100 % EtOAc mobile phase) to afford tert-butyl (3-(2-amino-6-pentylpyrimidin-4-yl)pyridin-2-yl)(benzylcarba-moyl)carbamate **289** (6 mg, 0.012 mmol, 22 %); ^{1}**H NMR** (400 MHz, $CDCl_3$) δ_H 8.92 (1H, t, J = 5.80 Hz, NH), 8.56 (1H, dd, J = 4.78 and 1.56 Hz, H6′), 8.02 (1H, dd, J = 7.68 and 1.68 Hz, H4′), 7.37 (1H, dd, J = 7.67 and 4.77 Hz, H5′), 7.34–7.17 (5H, m, C_6H_5), 6.66 (1H, s, H5), 5.21 (2H, s, NH_2), 4.93 (2H, s, H15), 2.51 (2H, t, J = 7.77 Hz, H7), 1.61 (2H, m, H8), 1.17 (9H, s, $(CH_3)_3$), 1.34–1.23 (4H, m, H9 and H10), 0.90–0.85 (3H, m, H11); $\boldsymbol{m/z}$ (ESI^+) 981.54 (100 %), 491.26 (90 %, $[M+H]^+$); **HRMS** (ESI^+) found 513.2585 ($[M+Na]^+$, $C_{27}H_{34}N_6O_3Na$ requires 513.2585).

1,3-dibenzylurea 294

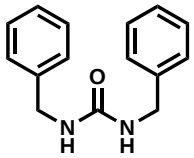

294

To a solution of benzyl amine **291** (1.0 mL, 9.53 mmol, 1.0 eq.) in dry THF (5 mL) at 0 ℃ was added carbonyldiimidazole (1.70 g, 10.48 mmol, 1.1 eq.). The mixture was stirred at r.t. for 7 h, then guanidine hydrochloride (3.62 g, 38.12 mmol, 4.0 eq.) was added, and the mixture stirred at r.t. for 16 h. The mixture was concentrated under reduced pressure, water added, and the solution taken to neutral pH with 1 M HCl. The solids were removed by sinter filtration and dried under reduced pressure over P_2O_5 to afford 1,3-dibenzylurea **294** (370 mg, 2.29 mmol, 24 %) as a white solid; **mp** 162.2–164.4 ℃; ^{1}**H NMR** (400 MHz, $CDCl_3$) δ_H 7.33–7.22 (10H, m, $(C_6H_5)_2$), 4.83 (2H, m, NH × 2), 4.34 (2H, s, CH_2), 4.32 (2H, s, CH_2). Data agrees with literature.[247]

guanidine-benzylurea 290 and guanidine-bis-benzylurea 295

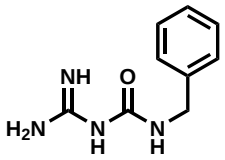

290

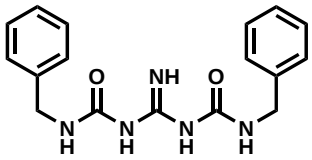

295

To a solution of guanidine hydrochloride **264** (2.33 g, 24.3 mmol, 10.0 eq.), sodium hydride (195 mg (60 % disp.), 4.86 mmol, 2.0 eq.) and MeCN (20 mL) at 0 ℃ was added dropwise benzyl isocyanate **259** (0.30 mL, 2.43 mmol, 1.0 eq.). The mixture was stirred for 16 h at room temperature, water added, and the MeCN removed under reduced pressure, whereupon a white crash formed in the aqueous solution. This was filtered off and vacuum dried over P_2O_5 to afford guanidine-bis-benzylurea **295** (390 mg, 1.20 mmol, 49 %) as a white solid; $\mathbf{R_f}$ 0.15 (1:1 P.E.:EtOAc); $\boldsymbol{\nu_{max}}$ (thin film) / cm^{-1} 3301, 2924, 1638, 1495, 1286, 1158 and 698; ^{1}**H NMR** (400 MHz, $CDCl_3$) δ_H 7.32–7.18 (10H, m, $(C_6H_5)_2$), 4.29 (4H, s, $(CH_2)_2$); ^{13}**C NMR** (100 MHz, $CDCl_3$) δ_C 158.5, 128.84, 128.78, 127.6, 127.5, 127.4 and 44.8; ***m/z*** (ESI^+) 326.14 ($[M+H]^+$, 100 %); **HRMS** (ESI^+) found 326.1612 ($C_{17}H_{20}N_5O_2$ requires 326.1612).

The aqueous filtrate was extracted with DCM (5 × 20 mL) and EtOAc (3 × 20 mL), and the combined organic phases concentrated under reduced pressure to afford guanidine-benzylurea **290**

(173 mg, 0.90 mmol, 37 %) as a yellow oil; $\mathbf{R_f}$ 0.15 (2:1 Et_2O:P.E.); $\boldsymbol{\nu_{max}}$ (thin film) / cm^{-1} 3327, 2188, 1597, 1494, 1453, 1293, 1028, 909, 797, 729 and 697; ^{1}**H NMR** (400 MHz, $CDCl_3$) δ_H 7.26–7.12 (5H, m, C_6H_5), 4.22 (2H, s, CH_2); ^{13}**C NMR** (100 MHz, $CDCl_3$) δ_C 139.2, 128.7, 128.6, 127.3, 127.12, 127.07 and 44.3; $\boldsymbol{m/z}$ (ESI^+) 326.14 (100 %), 193.09 ($[M+H]^+$, 50%); **HRMS** (ESI^+) found 193.1083 ($C_9H_{13}N_4O$ requires 193.1083).

1-(4-(2-aminopyridin-3-yl)-6-pentylpyrimidin-2-yl)-3-benzylurea 5

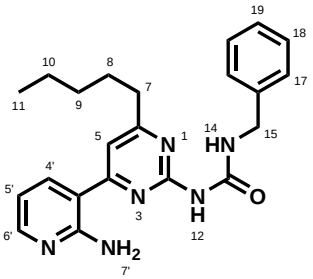

5

A solution of 1-(2-aminopyridin-3-yl)oct-1-yn-3-one **281** (160 mg, 0.74 mmol, 1.0 eq.), guanidine-bis-benzylurea **295** (481 mg, 1.48 mmol, 2.0 eq.) and K_2CO_3 (408 mg, 2.96 mmol, 4.0 eq.) in toluene (5 mL) was stirred at 120 ℃ for 16 h. After cooling to r.t. the mixture was concentrated under reduced pressure and purified by flash chromatography (1:1 Et_2O:MeCN mobile phase) to afford 1-(4-(2-aminopyridin-3-yl)-6-pentylpyrimidin-2-yl)-3-benzylurea **5** (39 mg, 0.10 mmol, 14 %) as a yellow/brown solid; $\mathbf{R_f}$ 0.23 (2:1 EtOAc:P.E.); $\boldsymbol{\nu_{max}}$ (thin film) / cm^{-1} 2923, 1682, 1577, 1525, 1262, 1019, 799, 699 and 634; ^{1}**H NMR** (500 MHz, $CDCl_3$) δ_H 9.74 (1H, t, J = 4.49 Hz, H14), 9.29 (1H, s, H12), 8.17 (1H, dd, J = 1.73 and 4.75 Hz, H6′), 7.91 (1H, dd, J = 1.65 and 7.84 Hz, H4′), 7.41–7.27 (5H, m, Ph), 7.06 (1H, s, H5), 6.79 (2H, s, H7′), 6.67 (1H, dd, J = 4.76 and 7.77 Hz, H5′), 4.63 (2H, d, J = 5.41 Hz, H15), 2.63 (2H, t, J = 7.70 Hz, H7), 1.62–1.56 (2H, m, H8), 1.24 (4H, m, H9 and H10), 0.85 (3H, t, J = 7.04 Hz, H11); ^{13}**C NMR** (125 MHz, $CDCl_3$) δ_C 170.8, 165.7, 158.1, 157.4, 155.5, 151.5 (C6′), 138.7, 137.4 (C4′), 128.8, 127.6, 127.5 (C19), 113.1, 112.8, 109.4 (C5), 44.3 (C15), 37.8 (C7), 31.4, 28.2 (C8), 22.5 and 14.1 (C11); $\boldsymbol{m/z}$ (ESI^+) 391.23 (100 %, $[M+H]^+$), 803.46 (57 %, $[M+Na]^+$); **HRMS** (ESI^+) found 391.2246 ($C_{22}H_{27}N_6O$ ($[M+H]^+$) requires 391.2241).

9 Appendix A

9.1 Binding Data

This section contains tables of the data acquired during the ^{1}H NMR binding experiments between Units A and B, and Units A′ and B.

Table 9.1 Binding data (multiple NMR tubes) for binding between A′ (guest) and B (host).

Conc. of A′ in mM ([A′] / mM)	Conc. of B in mM ([B] / mM)	A′H7 shift relative to A′H7 shift with zero B ($\Delta\delta_{A'H7}$)	A′H7′ shift relative to A′H7′ shift with zero B ($\Delta\delta_{A'H7'}$)
1.22	0	Doesn't show	0
1.22	0.12	Doesn't show	0.64
1.22	0.3	Doesn't show	1.45
1.22	0.61	Doesn't show	1.83
1.22	0.85	Doesn't show	3.23
1.22	1.03	Doesn't show	4.34
1.22	1.22	Doesn't show	5.7
1.22	1.83	Doesn't show	9.52
1.22	2.43	Doesn't show	10.87
1.22	4.83	Doesn't show	21.96
1.22	9.73	Doesn't show	31.54
1.22	14.67	Doesn't show	47.22

Table 9.2 Binding data (multiple NMR tubes) for binding between B (guest) and A′ (host).

Conc. of B in mM ([B] / mM)	Conc. of A′ in mM ([A′] / mM)	BH7 shift relative to BH7 shift with zero A′ ($\Delta\delta_{BH7}$)	BH7′ shift relative to BH7′ shift with zero A′ ($\Delta\delta_{BH7'}$)
1.22	0	0	0
1.22	0.12	−1.09	−5.11
1.22	0.3	1.09	−2.3
1.22	0.61	3.46	Doesn't show
1.22	0.85	3.76	Doesn't show
1.22	1.03	4.35	Doesn't show
1.22	1.22	7.71	Doesn't show
1.22	1.83	10.08	Doesn't show
1.22	2.43	12.26	Doesn't show
1.22	4.83	24.02	Doesn't show
1.22	9.73	41.23	Doesn't show
1.22	14.67	59.22	Doesn't show

Table 9.3 Binding data (multiple NMR tubes) for binding between A (guest) and B (host).

Conc. of A in mM ([A] / mM)	Conc. of B in mM ([B] / mM)	AH12 shift relative to AH12 shift with zero B ($\Delta\delta_{\mathrm{AH12}}$)	AH7′ shift relative to AH7′ shift with zero B ($\Delta\delta_{\mathrm{AH7'}}$)
1.22	0	0	0
1.22	0.12	−9.88	0.9
1.22	0.3	1.08	7.4
1.22	0.61	13.26	16.06
1.22	1.03	23.82	28.33
1.22	1.22	34.85	35.73
1.22	1.83	48.01	45.11
1.22	4.83	108.84	104.29
1.22	9.73	269.81	195.27
1.22	14.67	303.93	264.05
1.22	29.2	523.63	385.27

Table 9.4 Binding data (multiple NMR tubes) for binding between B (guest) and A (host).

Conc. of B in mM ([B] / mM)	Conc. of A in mM ([A] / mM)	BH7 shift relative to BH7 shift with zero A ($\Delta\delta_{BH7}$)	BH7′ shift relative to BH7′ shift with zero A ($\Delta\delta_{BH7'}$)
1.22	0	0	0
1.22	0.12	6.48	7.91
1.22	0.3	14.44	18.89
1.22	0.61	29.22	38.5
1.22	0.85	35.61	45.92
1.22	1.03	44.6	55.36
1.22	1.22	53.16	66.68
1.22	1.83	78.57	98.38
1.22	2.43	97.58	122.97
1.22	4.83		186.32
1.22	9.73	227.93	287.41
1.22	14.67	304.17	389.44

Table 9.5 Binding data (single NMR tube) for binding between A′ (guest) and B (host).

Conc. of A′ in mM ([A′] / mM)	Conc. of B in mM ([B] / mM)	A′H7 shift relative to A′H7 shift with zero B ($\Delta\delta_{A'H7}$)	A′H7′ shift relative to A′H7′ shift with zero B ($\Delta\delta_{A'H7'}$)
2.8	0	0	0
2.8	0.28	0.38	1.03
2.8	0.48	4.73	2.93
2.8	0.84	6.05	3.98
2.8	0.92	8.95	5.68
2.8	1.26	9.80	7.00
2.8	1.37	13.20	8.43
2.8	1.65	16.70	10.13
2.8	1.82	16.70	10.98
2.8	2.13	19.85	12.5
2.8	2.27	21.18	13.65
2.8	2.74	26.89	16.2
2.8	3.72	31.23	20.28
2.8	5.82	46.73	29.23
2.8	9.94	68.78	43.73
2.8	16.35	104.18	64.18
2.8	29.68	143.18	90.15
2.8	35.00	170.73	107.83
2.8	44.74	189.60	118.78
2.8	48.36	210.73	130.53

Table 9.6 Binding data (single NMR tube) for binding between B (guest) and A′ (host).

Conc. of B in mM ([B] / mM)	Conc. of A′ in mM ([A′] / mM)	BH7 shift relative to BH7 shift with zero A′ ($\Delta\delta_{BH7}$)	BH7′ shift relative to BH7′ shift with zero A′ ($\Delta\delta_{BH7'}$)
4.25	0	0	0
4.25	0.68	−11.96	−6.51
4.25	1.40	Doesn't show	−2.87
4.25	1.79	Doesn't show	−2.30
4.25	2.17	−3.32	−0.23
4.25	2.51	0.14	2.21
4.25	2.81	0.54	2.91
4.25	3.06	2.64	4.89
4.25	3.27	5.97	6.75
4.25	3.70	6.44	7.92
4.25	4.08	9.29	9.85
4.25	4.38	10.04	10.65
4.25	4.63	12.48	12.45
4.25	5.23	14.58	14.77
4.25	6.46	21.36	19.81
4.25	8.93	30.11	28.39
4.25	13.69	49.51	45.08
4.25	19.85	73.82	66.35
4.25	31.11	112.45	Doesn't show
4.25	48.11	Doesn't show	137.76
4.25	64.13	194.09	165.19
4.25	80.62	219.35	184.63
4.25	86.45	Doesn't show	201.77
4.25	91.29	256.53	213.21

Table 9.7 Binding data (single NMR tube) for binding between A (guest) and B (host).

Conc. of A in mM ([A] / mM)	Conc. of B in mM ([B] / mM)	AH12 shift relative to AH12 shift with zero B ($\Delta\delta_{AH12}$)	AH7′ shift relative to AH7′ shift with zero B ($\Delta\delta_{AH7'}$)
3.68	0	0	0
3.68	0.18	5.78	4.85
3.68	0.44	15.60	11.10
3.68	0.66	21.73	15.98
3.68	0.99	31.20	22.85
3.68	1.36	36.03	29.08
3.68	1.66	45.65	35.50
3.68	1.84	50.75	40.83
3.68	2.39	56.50	45.05
3.68	2.61	64.35	49.70
3.68	3.13	68.53	56.08
3.68	3.46	79.73	Doesn't show
3.68	3.64	84.78	Doesn't show
3.68	4.12	94.58	Doesn't show
3.68	4.67	100.68	Doesn't show
3.68	5.81	118.93	94.73
3.68	7.07	Doesn't show	124.45
3.68	9.53	189.05	161.1
3.68	17.66	276.08	246.40
3.68	31.35	401.88	Doesn't show
3.68	52.00	517.35	Doesn't show
3.68	68.89	601.85	502.88
3.68	75.44	648.83	536.13

Table 9.8 Binding data (single NMR tube) for binding between B (guest) and A (host).

Conc. of B in mM ([B] / mM)	Conc. of A in mM ([A] / mM)	BH7 shift relative to BH7 shift with zero A ($\Delta\delta_{BH7}$)	BH7′ shift relative to BH7′ shift with zero A ($\Delta\delta_{BH7'}$)
3.83	0	0	0
3.83	0.15	−29.16	−19.46
3.83	0.27	−37.19	−26.03
3.83	0.50	−27.03	−20.19
3.83	0.80	−17.55	−13.37
3.83	0.88	−7.72	−5.4
3.83	1.07	4.21	3.13
3.83	1.23	12.81	10.52
3.83	1.42	24.04	17.32
3.83	1.49	30.19	24.74
3.83	1.65	42.12	32.13
3.83	1.80	47.74	38.10
3.83	1.95	59.09	46.30
3.83	2.60	105.71	85.35
3.83	3.26	114.92	91.23
3.83	3.60	120.34	96.53
3.83	3.94	126.31	Doesn't show
3.83	5.32	170.57	136.27
3.83	6.32	215.30	173.74
3.83	9.12	294.31	227.68
3.83	13.06	367.89	297.52
3.83	21.98	471.18	379.94
3.83	28.27	527.78	423.43
3.83	31.18	573.06	459.29
3.83	34.97	595.70	475.12

9.2 Job Plot Data

This section contains tables of the data acquired for the Job Plots for Units A, A′, and B.

Table 9.9 Data recorded for the Job plots - Binding between A and B.

Total conc. of A + B ([A + B])	Conc. of A ([A])	Conc. of B ([B])	H12 (on A) shift relative to H12 on pure A at 9.78 mM ($\Delta\delta_{AH12}$)	H7′ (on A) shift relative to H7′ on pure A at 9.78 mM ($\Delta\delta_{AH7'}$)	H7′ (on B) shift relative to H7′ on pure B at 9.78 mM ($\Delta\delta_{BH7'}$)	H7 (on B) shift relative to H7 on pure B at 9.78 mM ($\Delta\delta_{BH7}$)	Conc. A × AH12 shift ([A]$\Delta\delta_{AH12}$)	Conc. A × AH7′ shift ([A]$\Delta\delta_{AH7'}$)	Conc. B × BH7′ shift ([B]$\Delta\delta_{BH7'}$)	Conc. B × BH7 shift ([B]$\Delta\delta_{BH7}$)	Mole Fraction of A (X_A)	Mole Fraction of B (X_B)
9.78	9.78	0	0	0			0	0	0	0	1	0
9.78	7.82	1.96	−19.1	21.5	211.4	188	−149.362	168.13	414.344	368.48	0.80	0.20
9.78	6.45	3.52	−62.4	40.9	177.1	167.5	−402.48	263.805	623.392	589.6	0.66	0.36
9.78	4.89	4.89	−105.5	56.7	142.2	146.2	−515.895	277.263	695.358	714.918	0.5	0.5
9.78	3.52	6.45	−150.1	74.1	104.5	124.7	−528.352	260.832	674.025	804.315	0.36	0.66
9.78	1.96	7.82	−207.4	87.1	63.7	96.5	−406.504	170.716	498.134	754.63	0.20	0.80
9.78	0	9.78			0	0	0	0	0	0	0	1

Table 9.10 Data recorded for the Job plots - Binding between A′ and B.

Total conc. of A′ + B ([A′+B])	Conc. of A′ ([A′])	Conc. of B ([B])	H7 (on A′) shift relative to H7 on pure A′ at 9.78 mM ($\Delta\delta_{\mathrm{A'H7}}$)	H7′ (on A′) shift relative to H7′ on pure A′ at 9.78 mM ($\Delta\delta_{\mathrm{A'H7'}}$)	H7′ (on B) shift relative to H7′ on pure B at 9.78 mM ($\Delta\delta_{\mathrm{BH7'}}$)	H7 (on B) shift relative to H7 on pure B at 9.78 mM ($\Delta\delta_{\mathrm{BH7}}$)	Conc. A′ × A′H7 shift ($[\mathrm{A'}]\Delta\delta_{\mathrm{A'H7}}$)	Conc. A′ × A′H7′ shift ($[\mathrm{A'}]\Delta\delta_{\mathrm{A'H7'}}$)	Conc. B × BH7′ shift ($[\mathrm{B}]\Delta\delta_{\mathrm{BH7'}}$)	Conc. B × BH7 shift ($[\mathrm{B}]\Delta\delta_{\mathrm{BH7}}$)	Mole Fraction of A′ ($X_{\mathrm{A'}}$)	Mole Fraction of B (X_{B})
9.78	9.78	0	0	0			0	0	0	0	1	0
9.78	7.82	1.96	76.7	7.5	25.9		599.794	58.65	50.764	0	0.80	0.20
9.78	6.45	3.52	53	9.9	21.6	−36.5	341.85	63.855	76.032	−128.48	0.66	0.36
9.78	4.89	4.89	34.3	16.8	19.8	7.5	167.727	82.152	96.822	36.675	0.5	0.5
9.78	3.52	6.45	15.3	19.8	16.6	21.4	53.856	69.696	107.07	138.03	0.36	0.66
9.78	1.96	7.82	−8.6	24.5	13.1	41.7	−16.856	48.02	102.442	326.094	0.20	0.80
9.78	0	9.78			0	0	0	0	0	0	0	1

10 Appendix B

10.1 Crystallographic Data

Crystallographic data for Unit A **6**, referred to as sample '6420'.

Table 1. Crystal data and structure refinement for 6420.

Identification code	6420	
Empirical formula	C18 H16 N4 O2	
Formula weight	320.35	
Temperature	150 K	
Wavelength	1.54180 Å	
Crystal system	Orthorhombic	
Space group	P b c a	
Unit cell dimensions	a = 13.7831(1) Å	α= 90°.
	b = 9.1462(1) Å	β= 90°.
	c = 24.5389(3) Å	γ= 90°.
Volume	3093.45(6) $Å^3$	
Z	8	
Density (calculated)	1.376 Mg/m^3	
Absorption coefficient	0.757 mm^{-1}	
F(000)	1344.000	
Crystal size	0.220 x 0.100 x 0.020 mm^3	
Theta range for data collection	4.825 to 76.905°.	
Index ranges	-17<=h<=17, -11<=k<=11, -30<=l<=30	
Reflections collected	62469	
Independent reflections	3252 [R(int) = 0.036]	
Completeness to theta = 75.367°	100.0 %	
Absorption correction	Semi-empirical from equivalents	
Max. and min. transmission	0.98 and 0.77	
Refinement method	Full-matrix least-squares on F^2	
Data / restraints / parameters	3241 / 256 / 272	
Goodness-of-fit on F^2	0.9774	
Final R indices [I>2sigma(I)]	R1 = 0.0313, wR2 = 0.0784	
R indices (all data)	R1 = 0.0342, wR2 = 0.0810	
Largest diff. peak and hole	0.21 and -0.22 $e.Å^{-3}$	

Table 2. Atomic coordinates (x 10^4) and equivalent isotropic displacement parameters ($Å^2$x 10^3) for 6420. U(eq) is defined as one third of the trace of the orthogonalized U^{ij} tensor.

	x	y	z	U(eq)
N(1)	8041(1)	5388(1)	4990(1)	20
C(2)	7891(1)	6354(1)	4582(1)	19
C(3)	6961(1)	6842(1)	4449(1)	23
C(4)	6182(1)	6363(1)	4759(1)	25
C(5)	6327(1)	5391(1)	5181(1)	24
C(6)	7276(1)	4915(1)	5276(1)	20
N(11)	10393(1)	6576(1)	3939(1)	26
C(12)	9616(1)	6054(1)	4208(1)	21
C(13)	8751(1)	6887(1)	4277(1)	20
C(14)	8726(1)	8250(1)	4029(1)	24
C(15)	9509(1)	8764(1)	3730(1)	28
C(16)	10322(1)	7896(1)	3702(1)	28
N(17)	9678(1)	4643(1)	4382(1)	27
N(18)	7524(1)	3923(1)	5688(1)	22
C(19)	6896(1)	3060(1)	5970(1)	22
O(20)	6024(1)	2998(1)	5918(1)	30
O(21)	7406(1)	2236(1)	6326(1)	27
C(22)	6838(1)	1525(1)	6751(1)	28
C(23)	6683(5)	2611(13)	7201(4)	32
C(24)	7438(7)	3010(13)	7538(4)	32
C(25)	7311(9)	4079(10)	7934(3)	40
C(26)	6418(10)	4731(8)	7998(3)	40
C(27)	5655(8)	4333(9)	7674(4)	45
C(28)	5786(6)	3282(13)	7272(5)	42
C(123)	6558(4)	2625(9)	7182(3)	25
C(124)	7239(5)	3126(10)	7555(3)	39
C(125)	6996(7)	4191(7)	7933(2)	42
C(126)	6074(8)	4762(6)	7940(2)	41
C(127)	5389(6)	4281(7)	7575(3)	41
C(128)	5630(4)	3212(9)	7197(3)	32

Table 3. Bond lengths [Å] and angles [°] for 6420.

N(1)-C(2)	1.3515(12)	C(23)-C(24)	1.379(4)
N(1)-C(6)	1.3384(12)	C(23)-C(28)	1.391(4)
C(2)-C(3)	1.3958(12)	C(24)-C(25)	1.389(4)
C(2)-C(13)	1.4835(12)	C(24)-H(241)	0.966
C(3)-C(4)	1.3867(13)	C(25)-C(26)	1.377(4)
C(3)-H(31)	0.953	C(25)-H(251)	0.944
C(4)-C(5)	1.3803(14)	C(26)-C(27)	1.366(4)
C(4)-H(41)	0.961	C(26)-H(261)	0.959
C(5)-C(6)	1.3985(13)	C(27)-C(28)	1.390(5)
C(5)-H(51)	0.938	C(27)-H(271)	0.947
C(6)-N(18)	1.4008(12)	C(28)-H(281)	0.956
N(11)-C(12)	1.3465(12)	C(123)-C(124)	1.387(4)
N(11)-C(16)	1.3431(13)	C(123)-C(128)	1.389(3)
C(12)-C(13)	1.4247(13)	C(124)-C(125)	1.388(4)
C(12)-N(17)	1.3618(12)	C(124)-H(1241)	0.971
C(13)-C(14)	1.3875(13)	C(125)-C(126)	1.374(3)
C(14)-C(15)	1.3878(14)	C(125)-H(1251)	0.945
C(14)-H(141)	0.954	C(126)-C(127)	1.374(3)
C(15)-C(16)	1.3760(15)	C(126)-H(1261)	0.961
C(15)-H(151)	0.966	C(127)-C(128)	1.388(3)
C(16)-H(161)	0.970	C(127)-H(1271)	0.963
N(17)-H(171)	0.885	C(128)-H(1281)	0.974
N(17)-H(172)	0.895		
N(18)-C(19)	1.3601(12)	C(2)-N(1)-C(6)	118.68(8)
N(18)-H(181)	0.882	N(1)-C(2)-C(3)	121.50(8)
C(19)-O(20)	1.2103(12)	N(1)-C(2)-C(13)	117.79(8)
C(19)-O(21)	1.3511(12)	C(3)-C(2)-C(13)	120.71(8)
O(21)-C(22)	1.4571(11)	C(2)-C(3)-C(4)	118.80(9)
C(22)-C(23)	1.500(4)	C(2)-C(3)-H(31)	121.3
C(22)-H(221)	0.976	C(4)-C(3)-H(31)	119.9
C(22)-H(222)	0.993	C(3)-C(4)-C(5)	120.23(9)
C(22)-C(123)	1.510(3)	C(3)-C(4)-H(41)	120.6
C(22)-H(223)	0.980	C(5)-C(4)-H(41)	119.2
C(22)-H(224)	0.993	C(4)-C(5)-C(6)	117.44(9)

C(4)-C(5)-H(51)	121.1	H(221)-C(22)-H(222)	110.5
C(6)-C(5)-H(51)	121.5	O(21)-C(22)-C(123)	110.0(4)
C(5)-C(6)-N(1)	123.28(9)	O(21)-C(22)-H(223)	104.4
C(5)-C(6)-N(18)	123.34(8)	C(123)-C(22)-H(223)	110.1
N(1)-C(6)-N(18)	113.36(8)	O(21)-C(22)-H(224)	110.5
C(12)-N(11)-C(16)	118.20(9)	C(123)-C(22)-H(224)	111.8
N(11)-C(12)-C(13)	122.37(9)	H(223)-C(22)-H(224)	109.8
N(11)-C(12)-N(17)	116.05(8)	C(22)-C(23)-C(24)	120.62(6)
C(13)-C(12)-N(17)	121.46(8)	C(22)-C(23)-C(28)	120.71(6)
C(2)-C(13)-C(12)	123.56(8)	C(24)-C(23)-C(28)	118.61(6)
C(2)-C(13)-C(14)	119.76(8)	C(23)-C(24)-C(25)	120.68(6)
C(12)-C(13)-C(14)	116.65(9)	C(23)-C(24)-H(241)	118.1
C(13)-C(14)-C(15)	121.16(9)	C(25)-C(24)-H(241)	121.1
C(13)-C(14)-H(141)	119.6	C(24)-C(25)-C(26)	119.85(6)
C(15)-C(14)-H(141)	119.2	C(24)-C(25)-H(251)	119.7
C(14)-C(15)-C(16)	117.66(9)	C(26)-C(25)-H(251)	120.5
C(14)-C(15)-H(151)	121.5	C(25)-C(26)-C(27)	120.40(6)
C(16)-C(15)-H(151)	120.8	C(25)-C(26)-H(261)	119.3
C(15)-C(16)-N(11)	123.84(9)	C(27)-C(26)-H(261)	120.3
C(15)-C(16)-H(161)	119.6	C(26)-C(27)-C(28)	119.80(6)
N(11)-C(16)-H(161)	116.6	C(26)-C(27)-H(271)	120.0
C(12)-N(17)-H(171)	118.2	C(28)-C(27)-H(271)	120.2
C(12)-N(17)-H(172)	116.4	C(23)-C(28)-C(27)	120.63(6)
H(171)-N(17)-H(172)	116.1	C(23)-C(28)-H(281)	118.9
C(6)-N(18)-C(19)	126.00(8)	C(27)-C(28)-H(281)	120.5
C(6)-N(18)-H(181)	117.7	C(22)-C(123)-C(124)	120.60(6)
C(19)-N(18)-H(181)	116.2	C(22)-C(123)-C(128)	120.70(6)
N(18)-C(19)-O(20)	127.27(9)	C(124)-C(123)-C(128)	118.61(5)
N(18)-C(19)-O(21)	108.74(8)	C(123)-C(124)-C(125)	120.69(6)
O(20)-C(19)-O(21)	123.99(9)	C(123)-C(124)-H(1241)	119.3
C(19)-O(21)-C(22)	115.60(7)	C(125)-C(124)-H(1241)	119.9
O(21)-C(22)-C(23)	107.9(6)	C(124)-C(125)-C(126)	119.83(6)
O(21)-C(22)-H(221)	106.0	C(124)-C(125)-H(1251)	121.2
C(23)-C(22)-H(221)	111.1	C(126)-C(125)-H(1251)	119.0
O(21)-C(22)-H(222)	110.2	C(125)-C(126)-C(127)	120.40(6)
C(23)-C(22)-H(222)	111.1	C(125)-C(126)-H(1261)	119.9

C(127)-C(126)-H(1261)	119.7	C(123)-C(128)-C(127)	120.64(6)
C(126)-C(127)-C(128)	119.83(6)	C(123)-C(128)-H(1281)	119.2
C(126)-C(127)-H(1271)	120.4	C(127)-C(128)-H(1281)	120.1
C(128)-C(127)-H(1271)	119.8		

Symmetry transformations used to generate equivalent atoms:

Table 4. Anisotropic displacement parameters ($Å^2 x\ 10^3$) for 6420. The anisotropic displacement factor exponent takes the form: $-2\pi^2[\ h^2\ a^{*2}U^{11} + ... + 2\ h\ k\ a^*\ b^*\ U^{12}\ ]$

	U^{11}	U^{22}	U^{33}	U^{23}	U^{13}	U^{12}
N(1)	18(1)	19(1)	21(1)	0(1)	1(1)	-1(1)
C(2)	20(1)	16(1)	22(1)	-2(1)	0(1)	0(1)
C(3)	22(1)	19(1)	27(1)	1(1)	-2(1)	1(1)
C(4)	18(1)	22(1)	34(1)	-1(1)	-1(1)	2(1)
C(5)	18(1)	24(1)	29(1)	-1(1)	3(1)	-1(1)
C(6)	21(1)	19(1)	21(1)	-3(1)	1(1)	-1(1)
N(11)	20(1)	29(1)	27(1)	5(1)	1(1)	0(1)
C(12)	20(1)	23(1)	20(1)	1(1)	-1(1)	-1(1)
C(13)	20(1)	20(1)	20(1)	-1(1)	-2(1)	-1(1)
C(14)	23(1)	21(1)	28(1)	1(1)	-1(1)	1(1)
C(15)	29(1)	24(1)	31(1)	8(1)	-1(1)	-3(1)
C(16)	23(1)	32(1)	29(1)	8(1)	2(1)	-4(1)
N(17)	21(1)	24(1)	36(1)	7(1)	7(1)	5(1)
N(18)	18(1)	25(1)	23(1)	3(1)	1(1)	-1(1)
C(19)	23(1)	22(1)	21(1)	-1(1)	2(1)	-1(1)
O(20)	21(1)	35(1)	34(1)	8(1)	0(1)	-6(1)
O(21)	24(1)	30(1)	26(1)	8(1)	4(1)	1(1)
C(22)	32(1)	25(1)	28(1)	7(1)	6(1)	-3(1)
C(23)	36(2)	30(2)	29(2)	11(2)	7(2)	1(2)
C(24)	39(2)	32(2)	25(2)	3(2)	-3(2)	-1(2)
C(25)	53(4)	37(2)	28(2)	1(1)	-4(2)	-7(3)
C(26)	57(4)	35(2)	28(2)	-1(2)	5(3)	-3(2)
C(27)	45(3)	48(2)	41(3)	-3(2)	7(2)	6(2)
C(28)	43(2)	48(2)	36(3)	5(2)	2(2)	-4(2)
C(123)	31(1)	24(2)	21(2)	6(1)	4(1)	-3(1)
C(124)	41(2)	39(2)	37(2)	8(1)	-1(2)	2(2)
C(125)	51(3)	44(2)	32(1)	4(1)	-5(2)	-4(2)
C(126)	56(3)	37(1)	29(2)	4(1)	8(2)	4(2)
C(127)	45(2)	45(2)	33(2)	2(1)	8(2)	11(2)
C(128)	32(2)	36(2)	29(2)	1(1)	6(1)	4(1)

Table 5. Hydrogen coordinates (x 10^4) and isotropic displacement parameters (Å^{2}x 10^3) for 6420.

	x	y	z	U(eq)
H(31)	6856	7497	4153	27
H(41)	5537	6709	4685	28
H(51)	5808	5071	5398	26
H(141)	8163	8849	4067	26
H(151)	9497	9717	3560	33
H(161)	10891	8242	3507	32
H(241)	8065	2568	7477	44
H(251)	7833	4334	8164	45
H(261)	6335	5466	8273	46
H(271)	5044	4792	7718	51
H(281)	5257	2991	7045	40
H(1241)	7878	2678	7564	41
H(1251)	7453	4528	8191	48
H(1261)	5903	5492	8205	44
H(1271)	4742	4677	7581	45
H(1281)	5155	2900	6926	41
H(181)	8144	3821	5768	27
H(171)	10251	4207	4369	34
H(172)	9293	4392	4659	32
H(221)	7226	699	6876	33
H(222)	6209	1181	6601	33
H(223)	7278	792	6905	32
H(224)	6261	1035	6592	33

Table 6. Hydrogen bonds for 6420 [Å and °].

D-H...A	d(D-H)	d(H...A)	d(D...A)	<(DHA)
C(16)-H(161)...O(21)#1	0.970	2.423	3.134(7)	129.82
N(18)-H(181)...N(11)#1	0.882	2.171	3.048(7)	172.45
N(17)-H(171)...O(20)#2	0.885	2.386	3.133(7)	142.15
N(17)-H(172)...N(1)	0.895	2.113	2.790(7)	131.82

Symmetry transformations used to generate equivalent atoms:

#1 -x+2,-y+1,-z+1 #2 x+1/2,-y+1/2,-z+1

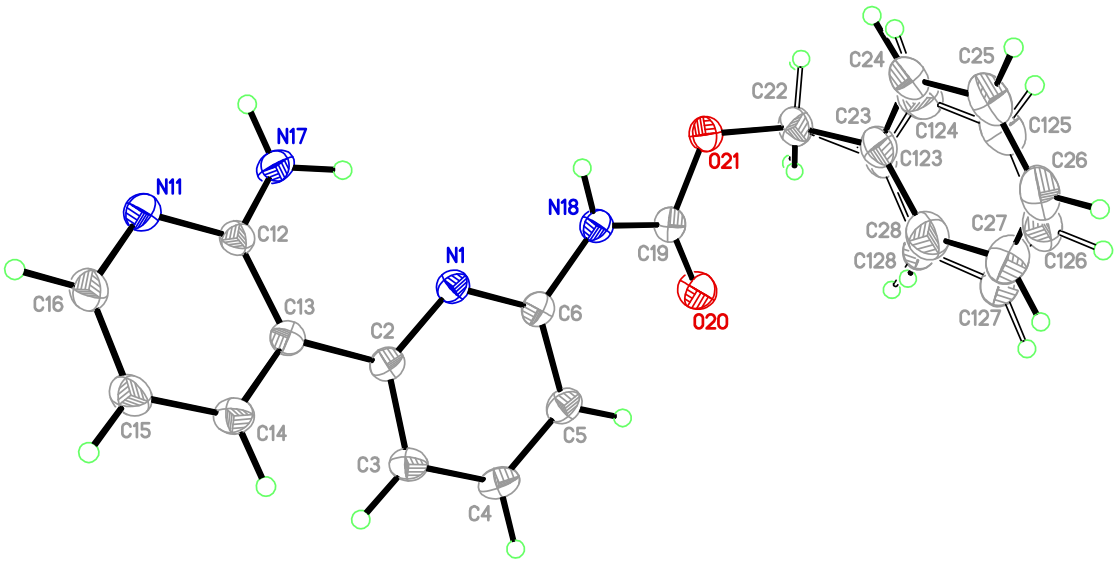

11 Appendix C

11.1 Experimental Data

11.1.1 Boronic acid synthesis

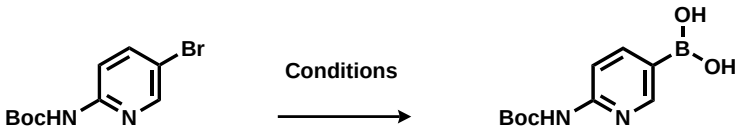

76 **75**

Scheme 11.1 Synthesis of boronic acid **75**.

Bromide **76** was converted to the corresponding boronic acid **75** (Scheme 11.1). Initial experiments were based on related literature examples:[101,248] *n*-BuLi was added to a solution of the starting material in THF at −78 °C, followed by the addition of triisopropyl borate. The reaction mixture was quenched with 1 M HCl before extraction into EtOAc.

The initial experiments failed to produce any product. A model reaction to convert bromobenzene into phenyl boronic acid using the same procedure was a success, suggesting that experimental error was not the cause of the problem, and that a different procedure would be necessary for our particular substrate **76**.

There were a number of possible reasons for the reaction not working: bromine-lithium exchange may not have been taking place; the borate may not be trapping the carbanion; the borate may form but later be lost by protodeboronation during work-up; or the product may form but not be isolated correctly during work-up. It was possible to rule out the two former cases due to the model reaction experiment which produced phenyl boronic acid.

None of the crude reaction ^{1}H NMR spectra showed the presence of starting material, which implied that full lithiation had indeed taken place. However, in the NMR spectra of both the crude and purified product were compounds corresponding to protonation at the 5-position, suggesting

that protonation had taken place either on the lithiated intermediate or the borylated compound (protodeboronation).

The amphoteric nature of pyridine boronic acids can cause difficulties with their isolation. An extensive survey of the literature yielded a procedure which involved a novel work-up,[231] and successfully delivered some of the desired boronic acid. Following the same initial reaction conditions (adding *n*-BuLi at −78 °C followed by the borate), the reaction was quenched with water and stirred for 20 min. Before addition of the water, the boron would be in the form of a tetravalent borate species, $[ArB(O^iPr)_3]^-$. Following water addition the pH was measured at 14, still very basic, and the boron is hydrolyzed to the tetravalent acid, $[ArB(OH)_3]^-$. The negatively-charged borate species $[ArB(OH)_3]^-$ enters the aqueous phase, which was separated and washed with more Et_2O to remove any neutral organic compounds still present, such as the protodeboronated pyridine. The aqueous phase was then carefully acidified to pH 6. The desired compound precipitated from solution at around pH 8. It is at this pH that the negatively-charged borate species $[ArB(OH)_3]^-$ becomes the neutral $ArB(OH)_2$, causing it to precipitate from aqueous solution (the pyridine, with a pK_a of around 5, also remains neutral at pH 8). The product was subsequently isolated by filtration and dried under vacuum over P_2O_5.

Following a series of experiments which focussed on the work-up (Table 11.1), the production of boronic acid **75** was optimised. The solvent in all cases is Et_2O and the reaction is always quenched with water, although the number of equivalents of *n*-BuLi is varied. There were initial difficulties in the isolation of the product, with little or no precipitate appearing during acidification. It was also important not to acidify too much, thereby protonating the pyridine and sending the product into the aqueous phase. In the end, it was discovered that isolating the aqueous phase and then removing all traces of Et_2O under vacuum resulted in a much cleaner precipitate (although the yield could not be improved beyond 32 %).

Table 11.1 Optimising the work-up of boronic acid **75**.

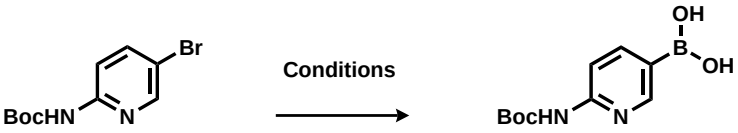

76 **75**

n-BuLi eq.	Stir following H_2O quench	Procedure	Acidify aq. phase with	Procedure	Result
3.0	16 h	Extract Et_2O with H_2O, separate aq. phases	48 % HBr to pH 5	Extract with EtOAc, concentrate	Nothing in extraction
3.0	25 min	Separate aq. phase, wash with Et_2O	1 M HCl to pH 5	Extract with EtOAc, concentrate	Nothing in extraction. SM found in Et_2O phase
3.0	30 min	Remove Et_2O under vacuum, wash with Et_2O	1 M HCl to pH 7	Isolate precipitate (trace amount)	SM found in Et_2O phase
3.0	20 min	Add a lot of H_2O		Extract with Et_2O, concentrate	Nothing in extraction
4.5	16 h	Separate aq. phase, wash with Et_2O	1 M HCl to pH 7		Nothing precipitates
4.5	16 h	Remove Et_2O under vacuum, wash with Et_2O	48 % HBr to pH 6		Trace precipitate
4.5	1 h	Remove Et_2O under vacuum, stir for further 2 h	48 % HBr to pH 6	Product precipitates, isolated by filtration	23 % yield
4.0	15 min	Separate aq. phase and subject to vacuum again	1 M HCl to pH 7	Product precipitates, nice white solid, isolated by filtration	25 % yield
4.0	15 min	Remove Et_2O under vacuum, wash with Et_2O, and subject aq. phase to vacuum again	1 M HCl to pH 7	Product precipitates, nice white solid, isolated by filtration	32 % yield

11.1.2 Attempted methoxypyridine deprotection

Table 11.2 Attempts at the deprotection of methoxypyridine **198**.

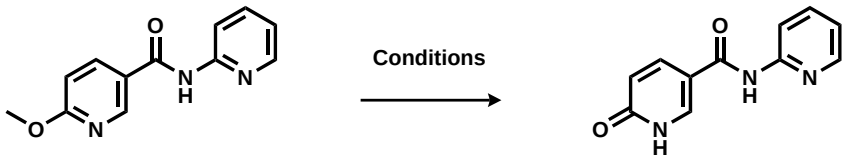

198 **194**

	Reagents	Temp.	Time	Yield	Comments
1	HBr, AcOH	r.t.	4 h	0 %	Pure starting material returned.
2	HBr, AcOH	70 °C	2 h	0 %	Pure starting material returned.
3	HBr, AcOH	120 °C	45 min	0 %	Amide bond cleaved, 2-aminopyridine isolated.
4	HBr, AcOH	95 °C	45 min	0 %	Amide bond cleaved, 2-aminopyridine isolated.
5	TMSCl, NaI	r.t.	16 h	0 %	Amide oxygen silylated.
6	TMSCl, NaI	70 °C	16 h	34 %	Successful.
7	TMSCl, NaI	40 °C	16 h	39 %	Successful.
8	BBr_3, DCM	r.t.	16 h	0 %	No product isolated.
9	BBr_3, DCM	70 °C	16 h	31 %	Successful. Cleaner product than TMSCl conditions.
10	BBr_3, DCM	40 °C	16 h	48 %	Successful. Cleaner product than TMSCl conditions.

11.1.3 Attempted aminoquinolone synthesis

Table 11.3 Attempted cyclisations to synthesise aminoquinolone **210**.

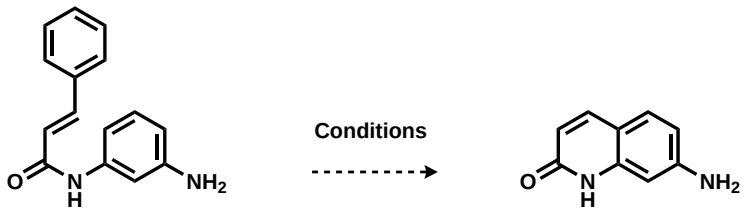

214 **210**

	Reagents	Temp.	Time	Yield	Comments
1	$AlCl_3$, THF	reflux	16 h	0 %	Returned pure starting material.
2	$AlCl_3$, dioxane, NaOAc	reflux	16 h	0 %	Returned pure starting material.
3	$AlCl_3$, toluene	reflux	16 h	0 %	Returned pure starting material.
4	$AlCl_3$, toluene, NaOAc	reflux	16 h	0 %	Returned pure starting material.
5	$AlCl_3$, dioxane	reflux	16 h	0 %	Some SM, mainly unidentifiable products.
6	$AlCl_3$ (neat)	Initiated by heat-gun, reflux	16 h	0 %	Unidentifiable products.
7	$AlCl_3$, 1,2-dichlorobenzene	130 °C	16 h	0 %	No SM, but only unidentifiable products.
8	$AlCl_3$, 1,2-dichlorobenzene	150 °C	16 h	0 %	No SM, but only unidentifiable products.
9	$AlCl_3$, 1,2-dichlorobenzene	170 °C	16 h	0 %	No SM, but only unidentifiable products.
10	$AlCl_3$, 1,2-dichlorobenzene	130 °C	30 min	0 %	No SM, only unidentifiable products.

11.1.4 Attempted pyridine debromination

Table 11.4 Attempts at the debromination of pyridine **237**.

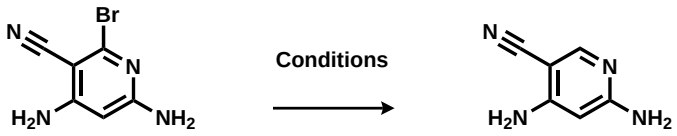

237 **238**

	Reagents	Temp.	Time	Yield	Comments
1	DIBAL, toluene	−78 °C	16 h	0 %	No product recovered.
2	*n*-BuLi, THF	−78 °C	1 h	0 %	No product recovered.
3	Cs_2CO_3, $Pd(PPh_3)_4$, and EtOH	reflux	16 h	0 %	No product recovered.
4	Bu_3SnH, AIBN	reflux	16 h	0 %	No product recovered.
5	Bu_3SnH, $Pd(PPh_3)_4$, EtOH	reflux	16 h	0 %	No product recovered.
6	Bu_3SnH, $Pd(OAc)_2$, EtOH	reflux	16 h	0 %	No product recovered.
7	Zinc dust, 1 M HCl, DMF	r.t.	16 h	0 %	No product recovered.
8	Zinc dust, 1 M HCl, EtOH	r.t.	48 h	0 %	No product recovered.
9	H_2, 4.5 bar, Pd/C, KOAc, THF, MeOH	r.t.	10 days	100 % by NMR	Product isolated in good yield.

Bibliography

[1] Nicolaou, K. C.; Sorensen, E. J. *Classics in Total Synthesis: Targets, Strategies, Methods*; Wiley VCH, 1996.

[2] Crimmins, M. T.; Zuccarello, J. L.; Ellis, J. M.; McDougall, P. J.; Haile, P. A.; Parrish, J. D.; Emmitte, K. A. *Org. Lett.* **2009**, *12*, 489–492.

[3] Prins, L. J.; Reinhoudt, D. N.; Timmerman, P. *Angew. Chem., Int. Ed.* **2001**, *40*, 2382–2426.

[4] Nernst, W. *Z. Phys. Chem.* **1892**, *8*, 110.

[5] Werner, A. *Leibigs Ann. Chem.* **1902**, *322*, 261.

[6] Latimer, W. M.; Rodebush, W. H. *J. Am. Chem. Soc.* **1920**, *42*, 1419–1433.

[7] Bernal, J. D.; Megaw, H. D. *R. Soc. Lond. Proc. Ser. A* **1935**, *151*, 384–420.

[8] Huggins, M. L. *J. Org Chem.* **1936**, *1*, 407–456.

[9] Moran, S.; Ren, R. X. F.; Rumney, S.; Kool, E. T. *J. Am. Chem. Soc.* **1997**, *119*, 2056–2057.

[10] Davis, A. M.; Teague, S. J. *Angew. Chem., Int. Ed.* **1999**, *38*, 736–749.

[11] Hunter, C. A. *Angew. Chem., Int. Ed.* **2004**, *43*, 5310–5324.

[12] Whitesides, G. M.; Simanek, E. E.; Mathais, J. P.; Seto, C. T.; Chin, D.; Mammen, M.; Gordon, D. M. *Acc. Chem. Res.* **1995**, *28*, 37–44.

[13] Wilson, A. J. *Soft Matter* **2007**, *3*, 409–425.

[14] Ariga, K.; Hill, J. P.; Lee, M. V.; Vinu, A.; Charvet, R.; Acharya, S. *Sci. Technol. Adv. Mater.* **2008**, *9*, 014109.

[15] Kyogoku, Y.; Lord, R. C.; Rich, A. *Biochim. Biophys. Acta* **1969**, *179*, 10–17.

[16] Hamilton, A. D.; Engen, D. V. *J. Am. Chem. Soc.* **1987**, *109*, 5035–5036.

[17] Jorgensen, W. L.; Pranata, J. *J. Am. Chem. Soc.* **1990**, *112*, 2008–2010.

[18] Pranata, J.; G.Wierschke, S.; Jorgensen, W. L. *J. Am. Chem. Soc.* **1991**, *113*, 2810–2819.

[19] Sartorius, J.; Schneider, H.-J. *Chem.–Eur. J.* **1996**, *2*, 1446–1452.

[20] Zimmerman, S. C.; Murray, T. J. *Tetrahedron Lett.* **1994**, *35*, 4077–4080.

[21] Zimmerman, S. C.; Murray, T. J. *Philos. Trans. R. Soc. London, A* **1993**, *345*, 49–56.

[22] Murray, T. J.; Zimmerman, S. C. *J. Am. Chem. Soc.* **1992**, *114*, 4010–4011.

[23] Griffin, R. J.; Lowe, P. R. *J. Chem. Soc., Perkin Trans. I* **1992**, 1811–1819.

[24] Beijer, F. H.; Kooijman, H.; Spek, A. L.; Sijbesma, R. P.; Meijer, E. W. *Angew. Chem., Int. Ed.* **1998**, *37*, 75–78.

[25] Lüning, U.; Kühl, C. *Tetrahedron Lett.* **1998**, *39*, 5735–5738.

[26] Sijbesma, R. P.; Beijer, F. H.; Brunsveld, L.; Folmer, B. J. B.; Hirschberg, J. H. K. K.; Lange, R. F. M.; Lowe, J. K. L.; Meijer, E. W. *Science* **1997**, *278*, 1601–1604.

[27] Park, T.; Zimmerman, S. C.; Nakashima, S. *J. Am. Chem. Soc.* **2005**, *127*, 6520–6521.

[28] Corbin, P. S.; Zimmerman, S. C. *J. Am. Chem. Soc.* **1998**, *120*, 9710–9711.

[29] Blight, B. A.; Hunter, C. A.; Leigh, D. A.; McNab, H.; Thomson, P. I. T. *Nat. Chem.* **2011**, *3*, 244–248.

[30] Benner, S. A. *Acc. Chem. Res.* **2004**, *37*, 784–797.

[31] Ge, Y.; Lilienthal, R. R.; Smith, D. K. *J. Am. Chem. Soc.* **1996**, *118*, 3976–3977.

[32] Bu, J. J.; Lilienthal, N. D.; Woods, J. E.; Nohrden, C. E.; Hoang, K. T.; Truong, D.; Smith, D. K. *J. Am. Chem. Soc.* **2005**, *127*, 6423–6429.

[33] Tucker, J. H. R.; Collinson, S. R. *Chem. Soc. Rev.* **2002**, *31*, 147–156.

[34] Breinlinger, E.; Niemz, A.; Rotello, V. M. *J. Am. Chem. Soc.* **1995**, *117*, 5379–5380.

[35] Legrand, Y.-M.; Gray, M.; Cooke, G.; Rotello, V. M. *J. Am. Chem. Soc.* **2003**, *125*, 15789–15795.

[36] Cooke, G.; Rotello, V. M. *Chem. Soc. Rev.* **2002**, *31*, 275–286.

[37] Herder, M.; Pätzel, M.; Grubert, L.; Hecht, S. *Chem. Commun.* **2011**, *47*, 460–462.

[38] Blight, B. A.; Camara-Campos, A.; Djurdjevic, S.; Kaller, M.; Leigh, D. A.; McMillan, F. M.; McNab, H.; Slawin, A. M. Z. *J. Am. Chem. Soc.* **2009**, *131*, 14116–14122.

[39] Li, Y.; Park, T.; Quansah, J. K.; Zimmerman, S. C. *J. Am. Chem. Soc.* **2011**, *133*, 17118–17121.

[40] Bialecki, J. B.; Yuan, L.-H.; Gong, B. *Tetrahedron* **2007**, *63*, 5460–5469.

[41] Zeng, H.; Miller, R. S.; Flowers II, R. A.; Gong, B. *J. Am. Chem. Soc.* **2000**, *122*, 2635–2644.

[42] Corbin, P. S.; Zimmerman, S. C. *J. Am. Chem. Soc.* **2000**, *122*, 3779–3780.

[43] Chang, S.-K.; Hamilton, A. D. *J. Am. Chem. Soc.* **1988**, *110*, 1318–1319.

[44] Safont-Sempere, M. M.; Fernández, G.; Würthner, F. *Chem. Rev.* **2011**, *111*, 5784–5814.

[45] Wu, A.; Isaacs, L. *J. Am. Chem. Soc.* **2003**, *125*, 4831–4835.

[46] Saha, M. L.; Schmittel, M. *Org. Biomol. Chem.* **2012**, *10*, 4651–4684.

[47] Elemans, J. A. A. W.; Lei, S.; De Feyter, S. *Angew. Chem. Int. Ed.* **2009**, *48*, 7298–7332.

[48] Kramer, R.; Lehn, J. M.; Marquis-Rigault, A. *Proc. Natl. Acad. Sci. USA* **1993**, *90*, 5394–5398.

[49] Chu, W.-J.; an C.-F. Chen, J. C.; Yang, Y.; Shuai, Z. *J. Org. Chem.* **2012**, *77*, 7815–7822.

[50] Jiang, W.; Winkler, H. D. F.; Schalley, C. A. *J. Am. Chem. Soc.* **2008**, *130*, 13852–13853.

[51] Taylor, P. N.; Anderson, H. N. *J. Am. Chem. Soc.* **1999**, *121*, 11538–11545.

[52] Jolliffe, K. A.; Timmerman, P.; Reinhoudt, D. N. *Angew. Chem. Int. Ed.* **1999**, *38*, 933–937.

[53] Timmerman, P.; Vreekamp, R. H.; Hulst, R.; Verboom, W.; Reinhoudt, D. N.; Rissanen, K.; Udachin, K. A.; Ripmeester, J. *Chem.–Eur. J.* **1997**, *3*, 1823–1832.

[54] Pinalli, R.; Cristini, V.; Sottili, V.; Geremia, S.; Campagnolo, M.; Caneschi, A.; Dalcanale, E. *J. Am. Chem. Soc.* **2004**, *126*, 6516–6517.

[55] Caulder, D. L.; Raymond, K. N. *Angew. Chem., Int. Ed.* **1997**, *36*, 1440–1442.

[56] Zheng, Y.-R.; Northrop, B. H.; Yang, H.-B.; Zhao, L.; Stang, P. J. *J. Org. Chem.* **2009**, *74*, 3554–3557.

[57] De, S.; Mahata, K.; Schmittel, M. *Chem. Soc. Rev.* **2010**, *39*, 1555–1575.

[58] Mahata, K.; Schmittel, M. *J. Am. Chem. Soc.* **2009**, *131*, 16544–16554.

[59] Mahata, K.; Saha, M. L.; Schmittel, M. *J. Am. Chem. Soc.* **2010**, *132*, 15933–15935.

[60] Smulders, M. M. J.; Jiménez, A.; Nitschke, J. R. *Angew. Chem., Int. Ed.* **2012**, *51*, 6681–6685.

[61] Ghadiri, M. R.; Granja, J. R.; Milligan, R. A.; McRee, D. E.; Khazanovich, N. *Nature* **1993**, *366*, 324–327.

[62] Baumeister, B.; Matile, S. *Chem. Commun.* **2000**, 913–914.

[63] Ajami, D.; Hou, J.-L.; Dale, T. J.; Barrett, E.; J. Rebek, J. *Proc. Natl. Acad. Sci. USA* **2009**, *106*, 10430–10434.

[64] MacGillivray, L. R.; Atwood, J. L. *Nature* **1997**, *389*, 469–472.

[65] Zimmerman, S. C.; Duerr, B. F. *Chem. Commun.* **1992**, *57*, 2215–2217.

[66] Mascal, M.; Hext, N. M.; Warmuth, R.; Moore, M. H.; Turkenburg, J. P. *Angew. Chem. Int. Ed.* **1996**, *35*, 2204–2206.

[67] Huck, W. T. S.; Hulst, R.; Timmerman, P.; van Veggel, F. C. J. M.; Reinhoudt, D. N. *Angew. Chem. Int. Ed.* **1997**, *36*, 1006–1008.

[68] Bruns, C. J.; Stoddart, J. F. *Nat. Nanotech.* **2013**, *8*, 9–10.

[69] Berná, J.; Leigh, D. A.; Lubomska, M.; Mendoza, S. M.; Pérez, E. M.; Rudolf, P.; Teobaldi, G.; Zerbetto, F. *Nat. Materials* **2005**, *4*, 704–710.

[70] Fahrenbach, A. C.; Sampath, S.; Late, D. J.; Barnes, J. C.; Kleinman, S. L.; Valley, N.; Hartlieb, K. J.; Liu, Z.; Dravid, V. P.; Schatz, G. C.; Duyne, R. P. V.; Stoddart, J. F. *ACS Nano.* **2012**, *6*, 9964–9971.

[71] Wallace, K. J.; Belcher, W. J.; Turner, D. R.; Syed, K. F.; Steed, J. W. *J. Am. Chem. Soc.* **2003**, *125*, 9699–9715.

[72] Ciesielski, A.; Samorì, P. *Nanoscale* **2011**, *3*, 1397–1410.

[73] Clever, G. H.; Tashiro, S.; Shionoya, M. *Angew. Chem. Int. Ed.* **2009**, *48*, 7010–7012.

[74] Clever, G. H.; Kawamura, W.; Tashiro, S.; Shiro, M.; Shionoya, M. *Angew. Chem. Int. Ed.* **2012**, *51*, 2606–2609.

[75] Olenyuk, B.; Whiteford, J. A.; Fechtenkötter, A.; Stang, P. J. *Nature* **1999**, *398*, 796–799.

[76] Ghosh, K.; Hu, J.; White, H. S.; Stang, P. J. *J. Am. Chem. Soc.* **2009**, *131*, 6695–6697.

[77] Argent, S. P.; Adams, H.; Riis-Johannessen, T.; Jeffery, J. C.; Harding, L. P.; Ward, M. D. *J. Am. Chem. Soc.* **2006**, *128*, 72–73.

[78] Al-Rasbi, N. K.; Tidmarsh, I. S.; Argent, S. P.; Adams, H.; Harding, L. P.; Ward, M. D. *J. Am. Chem. Soc.* **2008**, *130*, 11641–11649.

[79] Fujita, D.; Takahashi, A.; Sato, S.; Fujita, M. *J. Am. Chem. Soc.* **2011**, *133*, 13317–13319.

[80] Moulton, B.; Lu, J.; Mondal, A.; Zaworotko, M. J. *Chem. Commun.* **2001**, 863–864.

[81] Goodman, R. P.; Schaap, I. A. T.; Tardin, C. F.; Erben, C. M.; Berry, R. M.; Schmidt, C. F.; Turberfield, A. J. *Science* **2005**, *310*, 1661–1664.

[82] Chen, J.; Seeman, N. C. *Nature* **1991**, *350*, 631–633.

[83] Rothemund, P. K. W. *Nature* **2006**, *440*, 297–302.

[84] Bai, X.-C.; Martin, T. G.; Scheres, S. H. W.; Dietz, H. *Proc. Natl. Acad. Sci. USA* **2012**, *109*, 20012–20017.

[85] Gellman, S. H. *Acc. Chem. Res.* **1998**, *31*, 173–180.

[86] Goodman, C. M.; Choi, S.; Shandler, S.; DeGrado, W. F. *Nat. Chem. Biol.* **2007**, *3*, 252–262.

[87] Horne, W. S.; Gellman, S. H. *Acc. Chem. Res.* **2008**, *41*, 1399–1408.

[88] Brunsveld, L.; Folmer, B. J. B.; Meijer, E. W.; Sijbesma, R. P. *Chem. Rev.* **2001**, *101*, 4071–4079.

[89] Beijer, F. H.; Sijbesma, R. P.; Kooijman, H.; Spek, A. L.; Meijer, E. W. *J. Am. Chem. Soc.* **1998**, *120*, 6761–6769.

[90] Hirschberg, J. H. K. K.; Beijer, F. H.; van Aert, H. A.; Magusin, P. C. M. M.; Sijbesma, R. P.; Meijer, E. W. *Macromolecules* **1999**, *32*, 2696–2705.

[91] Zhao, X.; Wang, X.-Z.; Jiang, X.-K.; Chen, Y.-Q.; Li, Z.-T.; Chen, G.-J. *J. Am. Chem. Soc.* **2003**, *125*, 15128–15139.

[92] Ligthart, G. B. W. L.; Ohkawa, H.; Sijbesma, R. P.; Meijer, E. W. *J. Am. Chem. Soc.* **2005**, *127*, 810–811.

[93] Sijbesma, R. P.; Meijer, E. W. *Chem. Commun.* **2003**, 5–16.

[94] McGhee, A. M.; Kilner, C.; Wilson, A. J. *Chem. Commun.* **2008**, 344–346.

[95] Brammer, S.; Lüning, U.; Kühl, C. *Eur. J. Org. Chem.* **2002**, 4054–4062.

[96] Miyaura, N.; Suzuki, A. *Chem. Rev.* **1995**, *95*, 2457–2483.

[97] Cañibano, V.; Rodríguez, J. F.; Santos, M.; Sanz-Tejedor, M. A.; Carreño, M. C.; González, G.; García-Ruano, J. L. *Synthesis* **2001**, 2175–2179.

[98] Kelly, T. A.; McNeil, D. W. *Tetrahedron Lett.* **1994**, *35*, 9003–9006.

[99] Jung, K.-Y.; Kim, S.-K.; Gao, Z.-G.; Gross, A. S.; Melman, N.; Jacobson, K. A.; Kim, Y.-C. *Bioorg. Med. Chem.* **2004**, *12*, 613–623.

[100] Ilhan, F.; Galow, T. H.; Gray, M.; Clavier, G.; Rotello, V. M. *J. Am. Chem. Soc.* **2000**, *122*, 5895–5896.

[101] Jónsson, S.; Odille, F. G. J.; Norrby, P.-O.; Wärnmark, K. *Org. Biomol. Chem.* **2006**, *4*, 1927–1948.

[102] Doebner, O.; v. Miller, W. *Chem. Ber.* **1884**, *17*, 1712–1721.

[103] Denmark, S. E.; Venkatraman, S. *J. Org. Chem.* **2006**, *71*, 1668–1676.

[104] Becker, M. R. et al. *Bioorg. Med. Chem. Lett.* **1999**, *9*, 2753–2758.

[105] Breault, G.; Eyermann, C. J.; Geng, B.; Morningstar, M.; Reck, F. *Compounds for the treatment of multi-drug resistant bacterial infections*; 2006; Patent number WO2006134378.

[106] Warner, P.; Barker, A. J.; Jackman, A. L.; Burrows, K. D.; Roberts, N.; Bishop, J. A. M.; O′Connor, B. M.; ; Hughes, L. R. *J. Med. Chem.* **1992**, *35*, 2761–2768.

[107] Singh, B.; Lesher, G. Y.; Brundage, R. P. *Synthesis* **1991**, 894–896.

[108] Negoro, N. et al. *J. Med. Chem.* **2012**, *55*, 1538–1552.

[109] Inglis, S.; Jones, R.; Fritz, D.; Stojkoski, C.; Booker, G.; Pyke, S. *Org. Biomol. Chem.* **2005**, 2543–2557.

[110] Watanabe, T.; Kikuchi, E.; Tamura, W.; Akita, Y.; Tsutsui, M.; Ohta, A. *Heterocycles* **1980**, *14*, 287–290.

[111] White, J. D.; Hansen, J. D. *J. Am. Chem. Soc.* **2002**, *124*, 4950–4951.

[112] Brenner, E.; Baldwin, R. M.; Tamagnan, G. *Tetrahedron Lett.* **2004**, *45*, 3607–3610.

[113] Morgentin, R.; Jung, F.; Lamorlette, M.; Maudet, M.; Ménard, M.; Plé, P.; Pasquet, G.; Renaud, F. *Tetrahedron* **2009**, *65*, 757–764.

[114] Loubinoux, B.; Sinnes, J.-L.; O′Sullivan, A. C.; Winkler, T. *Tetrahedron* **1995**, *51*, 3549–3558.

[115] Conda-Sheridan, M.; Marler, L.; Park, E.-J.; Kondratyuk, T. P.; Jermihov, K.; Mesecar, A. D.; Pezzuto, J. M.; Asolkar, R. N.; Fenical, W.; Cushman, M. *J. Med. Chem.* **2010**, *53*, 8688–8699.

[116] Jackson, M.; Mantsch, H. H. *Biochim. Biophys. Acta* **1991**, *1078*, 231–235.

[117] Arakawaa, T.; Kitab, Y.; Timasheffc, S. N. *Biophys. Chem.* **2007**, *131*, 62–70.

[118] Tsukamoto, I.; Koshio, H.; Kuramochi, T.; Saitoh, C.; Yanai-Inamura, H.; Kitada-Nozawa, C.; Yamamoto, E.; Yatsu, T.; Shimada, Y.; Sakamoto, S.; Tsukamoto, S. *Bioorg. Med. Chem.* **2009**, *17*, 3130–3141.

[119] Struk, Ł.; Sośnicki, J. G. *Synthesis* **2012**, 735–746.

[120] Bargar, T. M.; Dulworth, J. K.; Kenny, M. T.; Massad, R.; Daniel, J. K.; Wilson, T.; Sargent, R. N. *J. Med. Chem.* **1986**, *29*, 1590–1595.

[121] Snieckus, V. *Chem. Rev.* **1990**, *90*, 879–933.

[122] Schlosser, M. *Angew. Chem., Int. Ed.* **2005**, *44*, 376–393.

[123] Nakamura, E.; Mori, S. *Angew. Chem., Int. Ed.* **2000**, *39*, 3750–3771.

[124] Hong, Y.-R.; Gorman, C. B. *J. Org. Chem.* **2003**, *68*, 9019–9025.

[125] Noël, S.; Pinel, C.; Djakovitch, L. *Org. Biomol. Chem.* **2006**, *4*, 3760–3762.

[126] Taylor, E. C.; Liu, B. *J. Org. Chem.* **2003**, *68*, 9938–9947.

[127] Lucet, D.; Sabelle, S.; Kostelitz, O.; Gall, T. L.; Mioskowski, C. *Eur. J. Org. Chem.* **1999**, *1999*, 2583–2591.

[128] Browder, C. C.; Marmsäter, F. P.; West, F. G. *Org. Lett.* **2001**, *3*, 3303–3035.

[129] Schelkun, R. M.; Yuen, P.; Wustrow, D. J.; Kinsora, J.; Su, T.-Z.; Vartanian, M. G. *Bioorg. Med. Chem. Lett.* **2006**, *16*, 2329–2332.

[130] Takács, D.; Nagy, I.; Bombicz, P.; Egyed, O.; Jemnitz, K.; Riedl, Z.; Molnár, J.; Amaral, L.; Hajós, G. *Bioorg. Med. Chem.* **2012**, *20*, 4258–4270.

[131] Das, B.; Shinde, D. B.; Kanth, B. S.; Kamle, A.; Kumar, C. G. *Eur. J. Med. Chem.* **2011**, *46*, 3124–3129.

[132] Ayala, L.; Lucero, C. G.; Romero, J. A. C.; Tabacco, S. A.; Woerpel, K. A. *J. Am. Chem. Soc.* **2003**, *125*, 15521–15528.

[133] Adamczyk, M.; Johnson, D. D.; Reddy, R. E. *Angew. Chem., Int. Ed.* **1999**, *38*, 3537–3539.

[134] Bode, J. W.; Carreira, E. M. *J. Org. Chem.* **2001**, *66*, 6410–6424.

[135] Nguyen, S. T.; Grubbs, R. H.; Ziller, J. W. *J. Am. Chem. Soc.* **1993**, *115*, 9858–9859.

[136] Schwab, P.; Grubbs, R. H.; Ziller, J. W. *J. Am. Chem. Soc.* **1996**, *118*, 100–110.

[137] Bahde, R. J.; Rychnovsky, S. D. *Org. Lett.* **2008**, *10*, 4017–4020.

[138] Krafft, M. E.; Haxell, T. F. N. *J. Am. Chem. Soc.* **2005**, *127*, 10168–10169.

[139] Majumdar, K. C.; Mondal, S. *Tetrahedron Lett.* **2007**, *48*, 6951–6953.

[140] Tee, O. S.; Paventi, M. *J. Am. Chem. Soc.* **1982**, *104*, 4142–4146.

[141] Shiao, M.-J.; Tarng, K.-Y. *Heterocycles* **1990**, *31*, 819–824.

[142] Heo, J.-N.; Song, Y. S.; Kim, B. T. *Tetrahedron Lett.* **2005**, *46*, 4621–4625.

[143] Parlow, J. J.; Kurumbail, R. G.; Stegeman, R. A.; Stevens, A. M.; Stallings, W. C.; South, M. S. *J. Med. Chem.* **2003**, *46*, 4696–4701.

[144] Zou, M.-F.; Cao, J.; Rodriguez, A. L.; Conn, P. J.; Newman, A. H. *Bioorg. Med. Chem. Lett.* **2011**, *21*, 2650–2654.

[145] Raghavan, B.; Balasubramanian, R.; Steele, J. C.; Sackett, D. L.; Fecik, R. A. *J. Med. Chem.* **2008**, *51*, 1530–1533.

[146] Gardinier, K. M.; Khoury, R. G.; Lehn, J.-M. *Chem.–Eur. J.* **2000**, *6*, 4124–4131.

[147] Frister, H.; Kemper, K.; Boos, K.-S.; Schlimme, E. *Liebigs Ann. Chem.* **1985**, *1985*, 510–516.

[148] Tie, C.; Gallucci, J. C.; Parquette, J. R. *J. Am. Chem. Soc.* **2006**, *128*, 1162–1171.

[149] Dyatkin, A. B.; Gong, Y.; Miskowski, T. A.; Kimball, E. S.; Prouty, S. M.; Fisher, M. C.; Santulli, R. J.; Schneider, C. R.; Wallace, N. H.; Hornby, P. J.; Diamond, C.; Kinney, W. A.; Maryanoff, B. E.; Damiano, B. P.; He, W. *Bioorg. Med. Chem.* **2005**, *13*, 6693–6702.

[150] Sambrook, M. R.; Beer, P. D.; Wisner, J. A.; Paul, R. L.; Cowley, A. R.; Szemes, F.; Drew, M. G. B. *J. Am. Chem. Soc.* **2005**, *127*, 2292–2302.

[151] Zou, H.; Zhanga, L.; Ouyanga, J.; Giulianottib, M. A.; Yua, Y. *Eur. J. Med. Chem.* **2011**, *46*, 5970–5977.

[152] Gaeta, A.; Molina-Holgado, F.; Kong, X. L.; Salvage, S.; Fakih, S.; Francis, P. T.; Williams, R. J.; Hider, R. C. *Bioorg. Med. Chem.* **2011**, *19*, 1285–1297.

[153] Barluenga, J.; Álvarez-Gutiérrez, J.; Ballesteros, A.; González, J. *Angew. Chem., Int. Ed.* **2007**, *46*, 1281–1283.

[154] Moenius, T.; Troxler, T.; Masero, R. *J. Label. Compd. Radiopharm.* **2007**, *50*, 613–615.

[155] Keegstra, M. A.; Peters, T. H. A.; Brandsma, L. *Tetrahedron* **1992**, *48*, 3633–3652.

[156] Kvita, V.; Sauter, H.; Rihs, G. *Helv. Chim. Acta* **1991**, *74*, 407–416.

[157] Keenan, M. et al. *J. Med. Chem.* **2012**, *55*, 4189–4202.

[158] Ohsawa, F.; Morishita, K.; Yamada, S.; Makishima, M.; Kakuta, H. *Med. Chem. Lett.* **2010**, *1*, 521–525.

[159] Kumar, S.; Johansson, H.; Kanda, T.; Engman, L.; Müller, T.; Jonsson, M.; Pedulli, G. F.; Petrucci, S.; Valgimigli, L. *Org. Lett.* **2008**, *10*, 4895–4898.

[160] Geneste, H.; Hesse, M. *Tetrahedron* **1998**, *54*, 15199–15214.

[161] Fernández, F.; García-Mera, X.; Morales, M.; Rodríguez-Borges, J. E. *Synthesis* **2001**, 239–242.

[162] Jamieson, C. et al. *Bioorg. Med. Chem. Lett.* **2010**, *20*, 6072–6075.

[163] Kalvinsh, I.; Kauss, V.; Trifanova, D.; Zemribo, R.; Danysz, W.; Henrich, M.; Parsons, C. G. R.; Weil, T. *Cyclic and acyclic propenones for treating CNS disorders*; 2006; US Patent number US2006074083(A1).

[164] Palani, A.; Rao, A. U.; Chen, X.; Shao, N.; Huang, Y. R.; Aslanian, R. G. *Bicyclic heterocyclic derivatives and methods of use thereof*; 2010; US Patent number WO2010071819(A1).

[165] Barvian, M. R.; Denny, W. A.; Dobrusin, E. M.; Hamby, J. M.; Showalter, H. D. H.; Thompson, A. M.; Winters, R. T.; Wu, Z. *Naphthyridinones for inhibiting protein tyrosine kinase and cell cycle kinase mediated cellular proliferation*; 2000; US Patent number US6150359.

[166] Johnson, S. J.; Choi, C.; Fay, L. K.; Favor, D. A.; Repine, J. T.; White, A. D.; Akunne, H. C.; Fitzgerald, L.; Nicholls, K.; Snyder, B. J.; Whetzel, S. Z.; Zhang, L.; Serpa, K. A. *Bioorg. Med. Chem. Lett.* **2011**, *21*, 2621–2625.

[167] Wang, X.; Schlosser, M. *Synthesis* **1994**, 479.

[168] de M. Muñoz, J.; Alcázar, J.; de la Hoz, A.; Díaz-Ortiz, A. *Tetrahedron Lett.* **2011**, *52*, 6058–6060.

[169] Hardouin, C.; Kelso, M. J.; Romero, F. A.; Rayl, T. J.; Leung, D.; Hwang, I.; Cravatt, B. F.; Boger, D. L. *J. Med. Chem.* **2007**, *50*, 3359–3368.

[170] Molander, G. A.; Dehmel, F. *J. Am. Chem. Soc.* **2004**, *126*, 10313–10318.

[171] Yasuike, S.; Kiharada, T.; Tsuchiya, T.; Kurita, J. *Chem. Pharm. Bull.* **2003**, *51*, 1283–1288.

[172] Song, Z. J. et al. *J. Org. Chem.* **1999**, *64*, 9658–9667.

[173] Chen, J.; Zhang, Y.; Yang, L.; Zhang, X.; Liu, J.; Li, L.; Zhang, H. *Tetrahedron* **2007**, *63*, 4266–4270.

[174] Krasavin, M.; Shkavrov, S.; Kravchenko, D. *Synth. Commun.* **2006**, *36*, 181–186.

[175] Wissner, A.; Hamann, P. R.; Nilakantan, R.; Greenberger, L. M.; Ye, F.; Rapuano, T. A.; Loganzo, F. *Bioorg. Med. Chem. Lett.* **2004**, *14*, 1411–1416.

[176] Koolman, H.; Heinrich, T.; Reggelin, M. *Synthesis* **2010**, 3152–3162.

[177] Wang, L.; Cui, X.; Zhu, Z.; Wu, Y.; Li, J.; Wu, Y. *Eur. J. Org. Chem.* **2012**, 595–603.

[178] Kim, J.; Hong, S.; Hong, S. *Bioorg. Med. Chem. Lett.* **2011**, *21*, 6977–6981.

[179] Augeri, D. J.; Tarver Jr., J. E.; Qinghong, F.; Voronkov, M. V.; Hackley, D.; Mertzman, M. E.; Carlsen, M. *Aryl pyridines and methods of their use*; 2007; US Patent number US2007032501.

[180] Golding, D. R. V.; Senear, A. E. *J. Org. Chem.* **1947**, *12*, 293–294.

[181] Tedeschi, D. H.; Pennsauken, N. J. *Compositions and methods for producing tranquilizing activity*; 1967; US Patent number US3303095.

[182] Gotor, V.; Quirós, M.; Liz, R. *Tetrahedron* **1997**, *53*, 6421–6432.

[183] Roblin Jr., R. O.; Williams, J. H.; Winnek, P. S.; English, J. P. *J. Am. Chem. Soc.* **1940**, *62*, 2002–2005.

[184] Tibiletti, F.; Simonetti, M.; Nicholas, K. M.; Palmisano, G.; Parravicini, M.; Imbesi, F.; Tollari, S.; Penoni, A. *Tetrahedron* **2010**, *66*, 1280–1288.

[185] Watanabe, K. A.; Su, T. L.; Pankiewicz, K. W.; Harada, K. *Heterocycles* **1984**, *21*, 289–307.

[186] Chu, C. K.; Fox, J. J.; Hirota, K.; Reichman, U.; Watanabe, K. A. *Pyrimidine to pyrimidine transformation process*; 1979; US Patent number US4171429(A).

[187] Vega, E.; Rood, G. A.; de Waard, E. R.; Pandit, U. K. *Tetrahedron* **1991**, *47*, 4361–4368.

[188] Botta, M.; Angelis, F. D.; Finizia, G.; Gambacorta, A.; Nicoletti, R. *Synth. Commun.* **1985**, *15*, 27–34.

[189] Custelcean, R.; Craciun, L. *Tetrahedron* **2000**, *56*, 5067–5075.

[190] Braker, W.; Pribyl, E. J.; Sheehan, J. T.; Spitzmiller, E. R.; Lott, W. A. *J. Am. Chem. Soc.* **1947**, *69*, 3072–3078.

[191] Wierenga, W.; Skulnick, H. I.; Stringfellow, D. A.; Weed, S. D.; Renis, H. E.; Eidson, E. E. *J. Med. Chem.* **1980**, *23*, 237–239.

[192] Karpov, A. S.; Merkul, E.; Rominger, F.; Müller, T. J. J. *Angew. Chem., Int. Ed.* **2005**, *44*, 6951–6956.

[193] Bannwarth, P.; Valleix, A.; Grée, D.; Grée, R. *J. Org. Chem.* **2009**, *74*, 4646–4649.

[194] Johns, B. A.; Gudmundsson, K. S.; Turner, E. M.; Allen, S. H.; Jung, D. K.; Sexton, C. J.; Boyd, F. L.; Peel, M. R. *Tetrahedron* **2003**, *59*, 9001–9011.

[195] Haddach, M.; Pastor, R.; Riess, J. G. *J. Fluorine. Chem.* **1991**, *51*, 197–205.

[196] Masayuki, M. *Pyridine derivative containing ((phosphonooxy)methyl)pyridinium ring, and antifungal agent containing these derivatives*; 2010; US Patent number US2010331282.

[197] Shintani, R.; Hayashi, T. *Org. Lett.* **2005**, *7*, 2071–2073.

[198] Zhou, C.; Dubrovsky, A. V.; Larock, R. C. *J. Org. Chem.* **2006**, *71*, 1626–1632.

[199] Eagon, S.; DeLieto, C.; McDonald, W. J.; Haddenham, D.; Saavedra, J.; Kim, J.; Singaram, B. *J. Org. Chem.* **2010**, *75*, 7717–7725.

[200] Hamed, O.; Henry, P. M.; Becker, D. P. *Tetrahedron Lett.* **2010**, *51*, 3514–3517.

[201] Das, B.; Nagendra, S.; Reddy, C. R. *Tetrahedron: Asymmetry* **2011**, *22*, 1249–1254.

[202] Tietze, L. F.; Gericke, K. M.; Singidi, R. R. *Angew. Chem., Int. Ed.* **2006**, *45*, 6990–6993.

[203] Takamura, H.; Abe, T.; Nishiuma, N.; Fujiwara, R.; Tsukeshiba, T.; Kadota, I. *Tetrahedron* **2012**, *68*, 2245–2260.

[204] Hayashi, Y.; Shoji, M.; Yamaguchi, J.; Sato, K.; Yamaguchi, S.; Mukaiyama, T.; Sakai, K.; Asami, Y.; Kakeya, H.; Osada, H. *J. Am. Chem. Soc.* **2002**, *124*, 12078–12079.

[205] Radi, M.; Contemori, L.; Castagnolo, D.; Spinosa, R.; Esté, J. A.; Massa, S.; Botta, M. *Org. Lett.* **2007**, *9*, 3157–3160.

[206] Yan, J.; Garzan, A.; Narayan, R. S.; Vasileiou, C.; Borhan, B. *Chem.–Eur. J.* **2010**, *16*, 13749–13756.

[207] Siu, T.; Liang, J.; Arruda, J.; Li, Y.; Jones, R. E.; Defeo-Jones, D.; Barnett, S. F.; Robinson, R. G. *Bioorg. Med. Chem. Lett.* **2008**, *18*, 4186–4190.

[208] Tetsuhashi, M.; Ishikawa, M.; Hashimoto, M.; Hashimoto, Y.; Aoyama, H. *Bioorg. Med. Chem.* **2010**, *18*, 5323–5338.

[209] Kleeman, H.-W.; Brendel, J.; Schwark, J.-R.; Weichert, A.; Lang, H.-J.; Albus, U.; Scholz, W. *Substituted benzyloxycarbonylguanidines, a process for their preparation, their use as a medicament or diagnostic, and a medicament containing them*; 1998; US Patent number US5753710.

[210] Fielding, L. *Tetrahedron* **2000**, *56*, 6151–6170.

[211] Fielding, L. *Prog. Nucl. Magn. Reson. Spectrosc.* **2007**, *51*, 219–242.

[212] Job, P. *Ann. Chim. (Paris, Fr.)* **1928**, *9*, 113–203.

[213] Sahai, R.; Loper, G. L.; Lin, S. H.; Eyring, H. *Proc. Natl. Acad. Sci. USA* **1974**, *71*, 1499–1503.

[214] Gil, V. M. S.; Oliveira, N. C. *J. Chem. Educ.* **1990**, 473–478.

[215] Pellizzaro, M. L.; McGhee, A. M.; Renton, L. C.; Nix, M. G.; Fisher, J.; Turnbull, W. B.; Wilson, A. J. *Chem.–Eur. J.* **2011**, *17*, 14508–14517.

[216] Pellizzaro, M. L.; Barrett, S. A.; Fisher, J.; Wilson, A. J. *Org. Biomol. Chem.* **2012**, *10*, 4899–4906.

[217] Eliadou, K.; Yannakopoulou, K.; Rontoyianni, A.; Mavridis, I. M. *Carbohyd. Res.* **2002**, *337*, 1387–1395.

[218] Loontiens, F. G.; Regenfuss, P.; Zechel, A.; Dumortier, L.; Clegg, R. M. *Biochemistry* **1990**, *29*, 9029–9039.

[219] O'Mahoney, J.; Molinelli, A.; Nolan, K.; Smyth, M. R.; Mizaikoff, B. *Biosens. Bioelectron.* **2005**, *20*, 1884–1893.

[220] Zouvelekis, D.; Yannakopoulou, K.; Mavridis, I. M.; Antoniadou-Vyza, E. *Carbohyd. Res.* **2002**, *337*, 1387–1395.

[221] Rether, C.; Sicking, W.; Boese, R.; Schmuck, C. *Beilstein J. Org. Chem.* **2010**, *6*.

[222] Camara-Campos, A.; Hunter, C. A.; Tomas, S. *Proc. Natl. Acad. Sci. USA* **2006**, *103*, 3034–3038.

[223] Chai, C.; Armarego, W. L. F. *Purification of Laboratory Chemicals*; Butterworth-Heinemann, 2009.

[224] Lu, G.; Franzén, R.; Zhang, Q.; Xu, Y. *Tetrahedron Lett.* **2005**, *46*, 4255–4259.

[225] Legoabe, L.; Kruger, J.; Petzer, A.; Bergh, J. J.; Petzer, J. P. *Eur. J. Med. Chem.* **2011**, *46*, 5162–5174.

[226] Broch, S.; Anizon, F.; Moreau, P. *Synthesis* **2008**, 2039–2044.

[227] Kiyoto, T.; Tanaka, T.; Tsutsui, Y.; Ando, J.; Motono, M.; Kawaguchi, Y.; Noguchi, T.; Ushiki, Y.; Ushiyama, F.; Urabe, H. *Novel nitrogenated heterocyclic compound and salt thereof*; 2008; European Patent number EP1900732(A1).

[228] Hazeldine, S. T.; Polin, L.; Kushner, J.; White, K.; Bouregeois, N. M.; Crantz, B.; Palomino, E.; Corbett, T. H.; Horwitz, J. P. *J. Med. Chem.* **2002**, *45*, 3130–3137.

[229] Karramkam, M.; Dollé, F.; Valette, H.; Besret, L.; Bramoullé, Y.; Hinnen, F.; Vaufrey, F.; Franklin, C.; Bourg, S.; Coulon, C.; Ottaviani, M.; Delaforge, M.; Loc'H, C.; Bottlaender, M.; Crouzel, C. *Bioorg. Med. Chem.* **2002**, *10*, 2611–2623.

[230] Palmgren, A.; Larsson, A. L. E.; Bäckvall, J.-E. *J. Org. Chem.* **1999**, *64*, 836–842.

[231] Parry, P. R.; Wang, C.; Batsanov, A. S.; Bryce, M. R.; Tarbit, B. *J. Org. Chem.* **2002**, *67*, 7541–7543.

[232] Burstein, C.; Lehmann, C. W.; Glorius, F. *Tetrahedron* **2005**, *61*, 6207–6217.

[233] Liu, C.; Han, N.; Song, X.; Qiu, J. *Eur. J. Org. Chem.* **2010**, 5548–5551.

[234] Gieseler, M. T.; Kalesse, M. *Org. Lett.* **2011**, *13*, 2430–2432.

[235] Lanni, E. L.; Bosscher, M. A.; Ooms, B. D.; Shandro, C. A.; Ellsworth, B. A.; Anderson, C. E. *J. Org. Chem.* **2008**, *73*, 6425–6428.

[236] Delgado, O.; Müller, H. M.; Bach, T. *Eur. J. Org. Chem.* **2008**, *14*, 2322–2339.

[237] Yamano, K.; Shirahama, H. *Tetrahedron* **1992**, *48*, 1457–1464.

[238] Dainter, R. S.; Suschitzky, H.; Wakefield, B. J.; Hughes, N.; Nelson, A. J. *J. Chem. Soc., Perkin Trans.* **1988**, *1*, 227–233.

[239] Yamada, A.; Tomishima, M.; Hayashida, H.; Imanishi, M.; Spears, G. W.; Ito, K.; Takahashi, F.; Miyake, H. *Novel Amide Compounds*; 2002; European Patent number EP1264820.

[240] dos Santos, C. M. G.; McCabe, T.; Watson, G. W.; Kruger, P. E.; Gunnlaugsson, T. *J. Org. Chem.* **2008**, *73*, 9235–9244.

[241] Krein, D. M.; Lowary, T. L. *J. Org. Chem.* **2002**, *67*, 4965–4967.

[242] Thansandote, P.; Hulcoop, D. G.; Langer, M.; Lautens, M. *J. Org. Chem.* **2009**, *74*, 1673–1678.

[243] Saladino, R.; Neri, V.; Crestini, C.; Costanzo, G.; Graciotti, M.; Mauro, E. D. *J. Am. Chem. Soc.* **2008**, *130*, 15512–15518.

[244] Suver, M.; Žinić, B.; Portada, T.; Bzowska, A.; Glavaš-Obrovac, L. *Croat. Chem. Acta* **2008**, *81*, 147–156.

[245] Nair, R. N.; Lee, P. J.; Rheingold, A. L.; Grotjahn, D. B. *Chem.–Eur. J.* **2010**, *16*, 7992–7995.

[246] Sakai, N.; Tamura, K.; Shimamura, K.; Ikeda, R.; Konakahara, T. *Org. Lett.* **2012**, *14*, 836–839.

[247] Wang, H.-M.; Li, H.-X.; Yu, X.-Y.; Ren, Z.-G.; Lang, J.-P. *Tetrahedron* **2011**, *67*, 1530–1535.

[248] Mewshaw, R. E.; R. J. Edsall, J.; Yang, C.; Manas, E. S.; Xu, Z. B.; Henderson, R. A.; J. C. Keith, J.; Harris, H. A. *J. Med. Chem.* **2005**, *48*, 3953–3979.